Proceedings of the Third ICFA Mini-Workshop on High Intensity, High Brightness Hadron Accelerators

May 7-9, 1997, Brookhaven National Laboratory

BNL-64754
Informal Report

Proceedings of the Third ICFA Mini-Workshop on High Intensity, High Brightness Hadron Accelerators

T. Roser, et. al.

May 7-9, 1997

AGS Department

Brookhaven National Laboratory
Associated Universities, Inc.
Upton, Long Island, New York 11973

Under Contract No. DE-AC02-76CH00016 with the

UNITED STATES DEPARTMENT OF ENERGY

DISCLAIMER

Portions of this document may be illegible in electronic image products. Images are produced from the best available original document.

Preface

The 3rd mini-workshop on high intensity, high brightness hadron accelerators was held at Brookhaven National Laboratory on May 7-9, 1997 and had about 30 participants.

The workshop focussed on rf and longitudinal dynamics issues relevant to intense and/or bright hadron synchrotrons. A plenary session was followed by four sessions on particular topics. This document contains copies of the viewgraphs used as well as summaries written by the session chairs.

M. Blaskiewicz
Scientific Secretary

Contents

Plenary Session

T. Roser

During the plenary session summary and status talks from the four organizing laboratories (BNL, CERN, FNAL, and KEK) and also from LANL were presented.

Mike Brennan reported on the various high intensity and high brightness efforts at BNL. In preparation for RHIC operation the AGS needs to produce very bright Gold beams with 10^9 ions per bunch and a bunch area of $0.2\,eVs/u$. The present performance has reached already 0.4×10^9 ions per bunch with a bunch area of $0.6\,eVs/u$. This intensity was achieved by merging 8 bunches into one which is most effectively done early in the acceleration cycle.

High intensity proton beams are accelerated in the Booster and AGS. With second harmonic cavities more than 2×10^{13} protons on two bunches each with a bunch area of about $1.5\,eVs$ were accelerated in the Booster. The beak performance is very sensitive to the relative phase of the first and second harmonic rf system. Four Booster beam batches are accumulated in the AGS for a maximum intensity of 6×10^{13} protons. Stability during accumulation can only be achieved by diluting the bunches to about $4\,eVs$ using a high frequency cavity.

To avoid excessive blow-up and also to allow for the accumulation of more than four Booster batches a Barrier bucket system is being developed. With such isolated sine waves gaps in the debunched beam can be manipulated in such a way as to stack successive loads from the Booster. So far with two $12\,kV$ cavities an intensity of 3×10^{13} protons was achieved by stacking six Booster loads. The development goal is to build $80\,kV$ cavities to produce $250\,ns$ long sine waves.

The development and upgrade plans for the CERN PS and PS Booster in the LHC era were presented by Roland Garoby. With only one bunch accelerated per Booster ring two Booster loads can be accumulated in the PS. Before extraction to the SPS the beam will be debunched and rebunched into 84 bunches with a new $140\,MHz$ rf system. Each bunch will have to contain 10^{11} protons in a bunch area of $0.3\,eVs$. The goal is to send nominal LHC beam to the SPS in 1998.

The status and plans for high intensity beams at FNAL was summarized by David Wildman. The next Tevatron collider run will make use of the new Main Injector with increased production and stacking rate for antiprotons. High proton intensity will also be required for the long baseline neutrino experiment and in the future for even higher Tevatron luminosity. Presently longitudinal coupled bunch instabilities driven by higher order modes of the rf cavities in the Booster, Main Ring, and Tevatron are limiting intensity unless a number of active and passive dampers are used. A permanent magnet $8\,GeV$ Recycler ring has recently been made part of the Main Injector project. This ring will be used to store and cool anti-protons both remaining from the previous store and directly from the Antiproton Accumulator ring. Wide band ferrite loaded barrier cavities with a peak voltage of $2\,kV$ will be used to manipulate the antiprotons in the Recycler.

Chihiro Ohmori reported on the plans for the Japanese Hadron Facility. It will consist of a $200\,MeV$ Linac, a $3\,GeV$ Booster accelerating 5×10^{13} protons at $25\,Hz$ and a $50\,GeV$ Main ring accelerating 2×10^{14} protons. The Main ring lattice will be transition-free. A development program is underway to use Finemet (Fine-Crystal High μ Metal) in the main ring cavities. This material has high permeability, a low Q factor ($Q < 1$) and performs well even for large rf fields. These cavities will be used for acceleration as well as Barrier Cavities.

Arch Thiessen gave an overview of the LANSCE PSR status and upgrade plans. The intensity at $800\,MeV$ is limited to 4×10^{13} protons by a fast transverse instability which is believed to be caused by electrons. Clearing gaps in the beam help suppress this instability and an upgrade of the rf system including a second harmonic system is underway to improve the situation. Potential well distortion from space charge is typically overcome by using much larger rf gap voltage. Alternatively the vacuum pipe impedance could be modified to cancel the space charge effects. A test is planned this year at the PSR of such an impedance tuner.

Workshop on High Intensity-High Brightness Beams: RF Issues

BOOSTER/AGS/RHIC

J. M. Brennan

- **High Brightness for RHIC** — J. Rose - stability; E. Onillon - Beam control
- **High Intensity Protons** — M. Blaskiewicz - NSNS
- **Barrier Cavity, Development** — M. Yoshi

3

Issues for Discussion

- **Phase modulation for emittance blow-up**
- **Higher brightness for...e.g. g-2 experiment**
- **Very high brightness for a proton driver**
- **More accumulation for higher average current**

  ➨ **Barrier Cavities**

High Brightness for RHIC
($^{179}Au^{+79}$, γ=12)

I. Specifications

Bunch Intensity = 10^9 ions
Longitudinal Emittance = 0.2 eVs/u

II. Performance to date (Jan. 97)

Bunch Intensity = 0.4 x 10^9 ions
Longitudinal Emittance = 0.6 eVs/u

III. Operating Mode

Bunch merging, 2 x 2 x 2
Accumulation in AGS at 430 MeV/c/u
Motivations

Gold Acceleration at the AGS

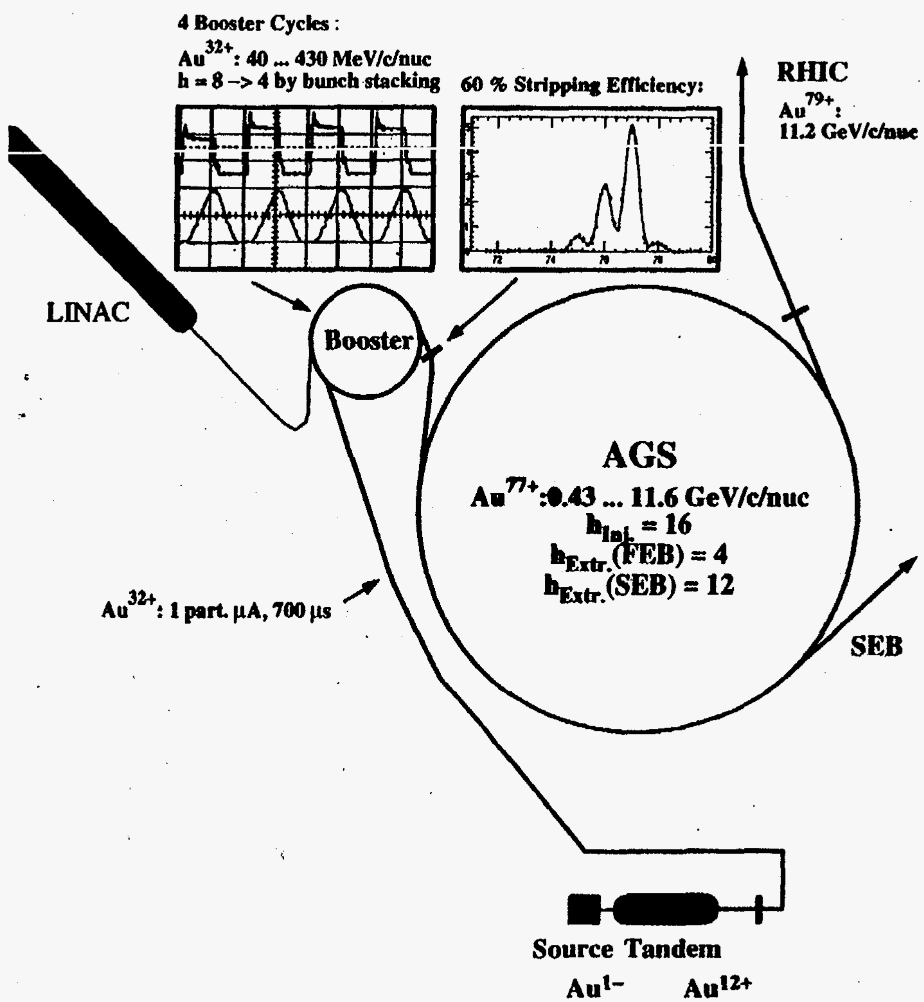

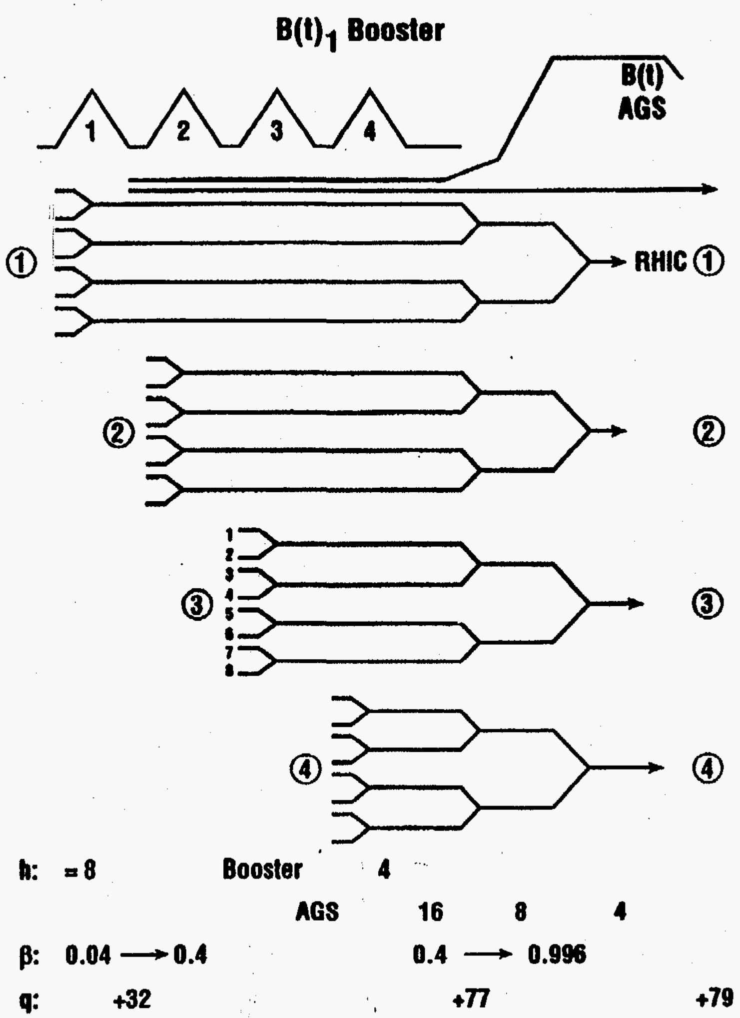

1. luminosity formula

$$L = 3/2\ f_{rev}\ B\ (\beta\gamma)\ N_B^2 / \epsilon_N\ \beta^*$$

→intensity per bunch is paramount

2. transverse emittance must be low

3. longitudinal emittance is not in the formula,
   i. chromatic non-linearities at transition, →growth
   ii. leakage into adjacent buckets at re-bucketing to 197 MHZ
   d. filling time, IBS at low energy, blows up longitudinal emittance

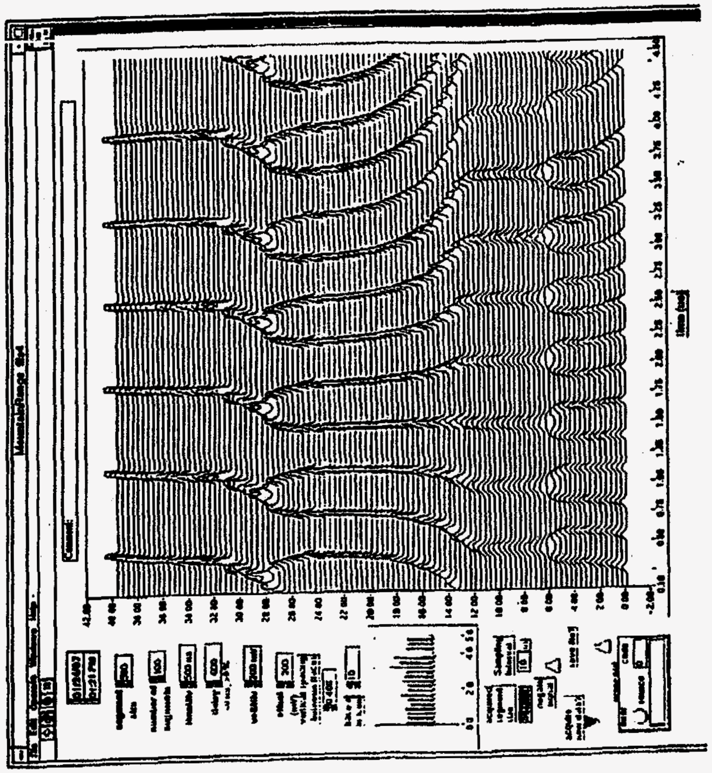

8

Acceleration in the AGS

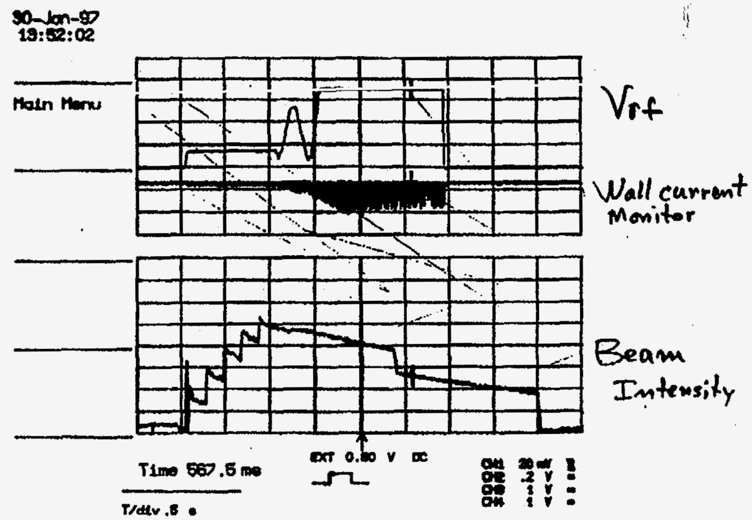

- The loss rate was a surprise!
- Same rate with rf on or off.
- Vacuum?
  - a. not predicted
  - b. capture? Au^{+77}
  - c. problem for RHIC? Au^{+79}

Longitudinal Emittance After Three Bunch Mergings

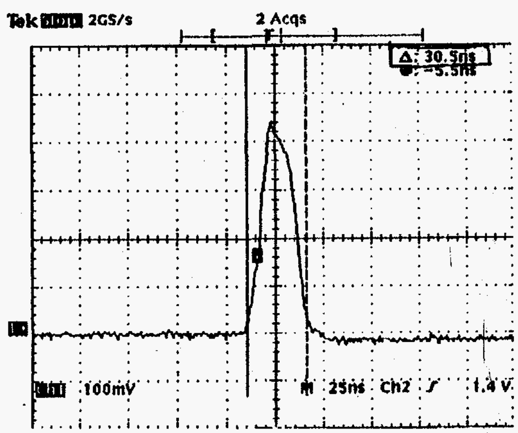

$V_{rf} = 220$ kV
$\dot{B} = 0$, $h = 8$
$l = 28$ ns
$\Rightarrow \epsilon = 0.60$ eVs/u

The Booster Emittance is Small Enough.

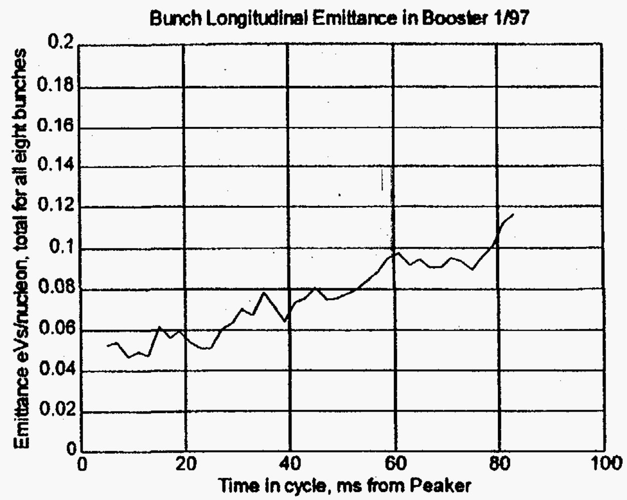

- If we put all the Booster beam into one RHIC bunch we still have a factor of two head room.
- There is 100% growth in the Booster

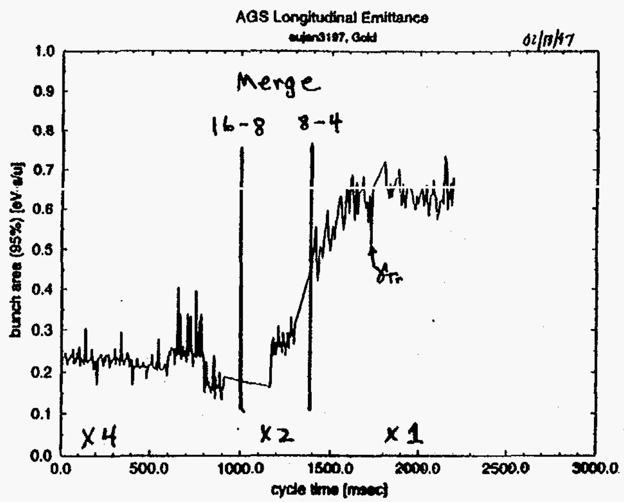

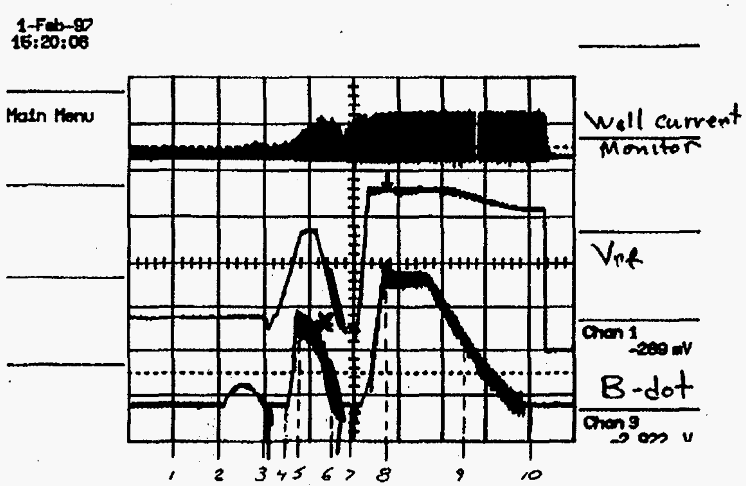

* $\delta\left(\frac{\dot{B}}{V_{rf}}\right)$ is Large + fast !

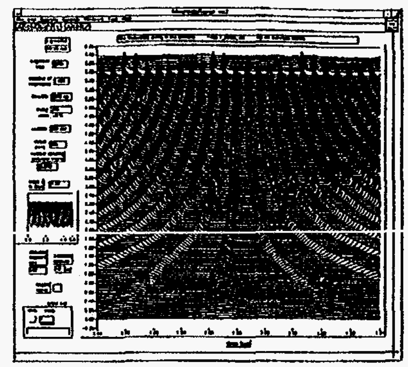

Booster Cycle

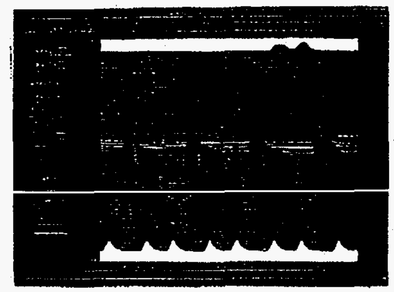

$h = 8 \rightarrow 4 \quad \Delta T \cong 100\mu s$

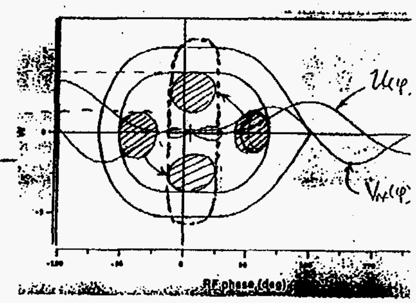

Merge in Double rf

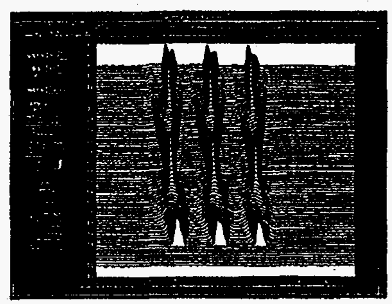

In AGS, after +32 → +77 Stripping

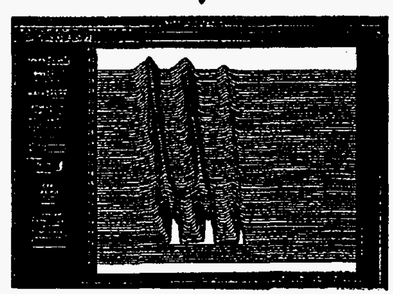

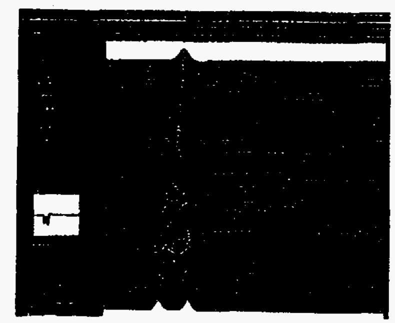

Mismatch at AGS Injection

- Momentum Error
- Bucket shape mismatch, need more Vrf for ΔE
- New batch perturbs old batch via phase loop
- Batch-by-batch phase Loop, bunch shape damper

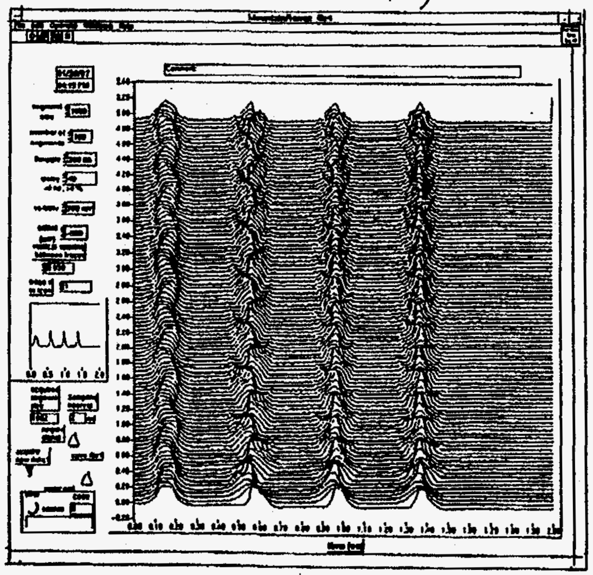

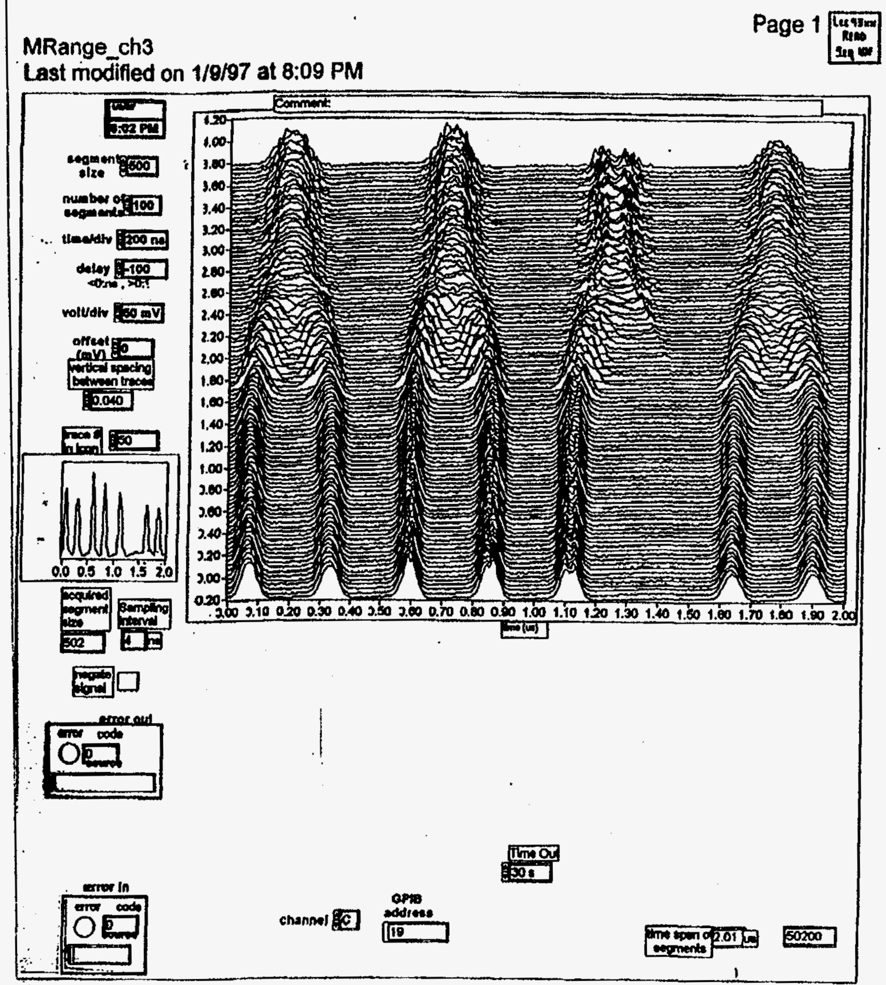

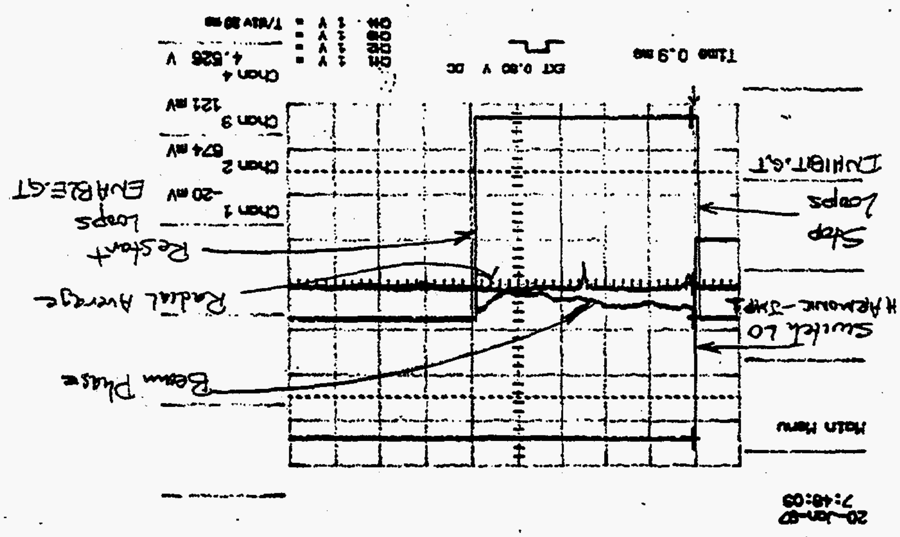

With odd number of bunches phase of h=8 is not equal to phase of h=16. This causes ~~transient~~ (glitch) in phase loop during 16→8 merge.

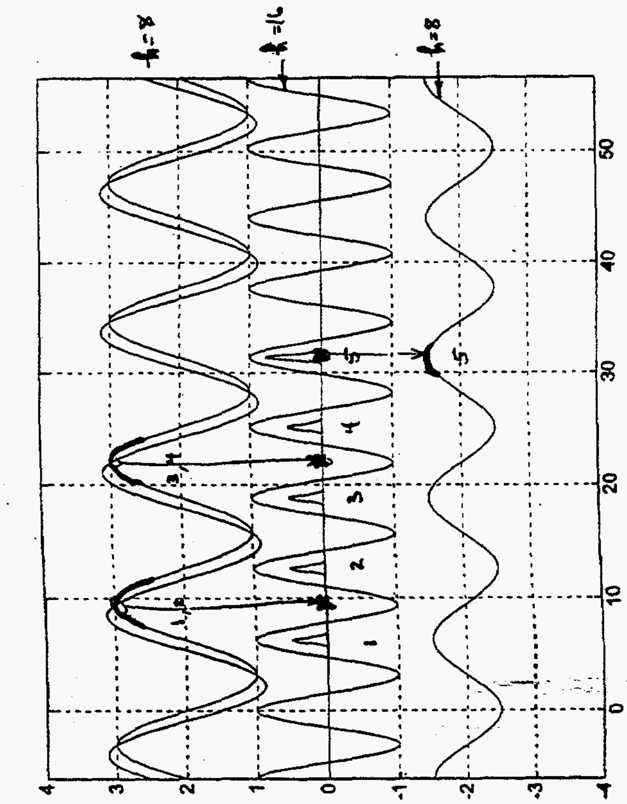

MountainRange_jmb
Last modified on 1/20/97 at 6:34 AM

Page 1

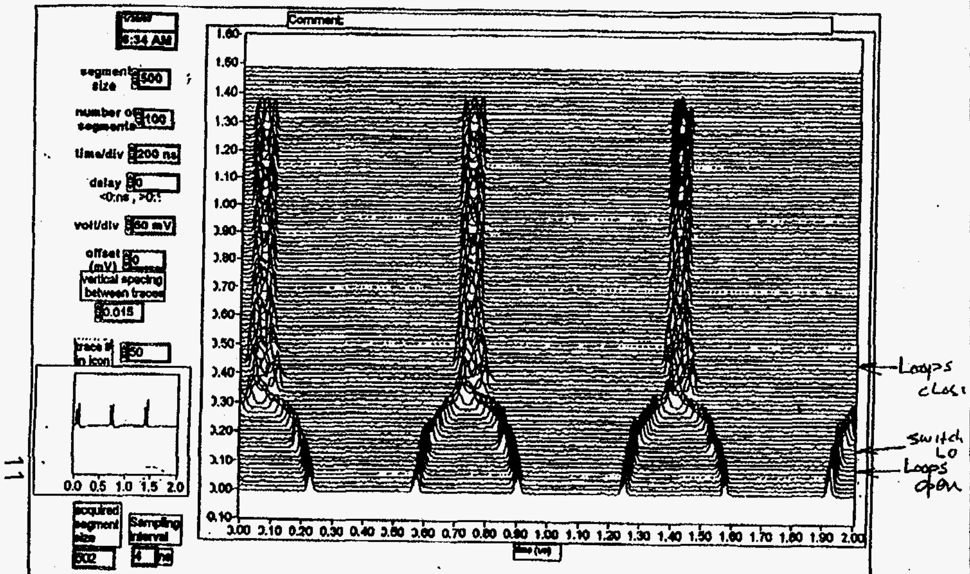

At top energy ($\gamma = 12$) $^{197}Au^{+77}$ when the bunch area is small compared to the bucket area the merge $h=8 \rightarrow h=4$ causes much emittance growth.

2048 turns per trace $\qquad$ $T_{rev} = 2.7\mu s$

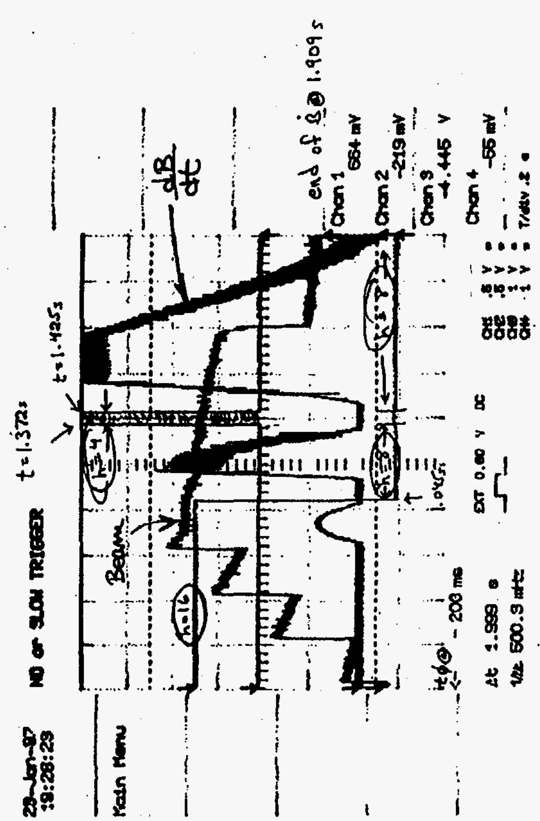

Issues for Discussion

- Preserving the phase feedback during merge
- "Vacuum loss"?
- Using larger emittance in RHIC
- Bunch stability in RHIC
- RF Noise during 10 hour store

Booster
(200 Mev to 1.9 GeV, 2 x 10^{13}ppp)

I. Parameters

1. Frequency range: 1.6 to 2.8 MHz, h=2
2. Voltage: 2 x 45 kV, h=2
   2 x 15 kV, h=4
3. Beam Current: 8 - 10 Amps, rf
4. Power: h=2 2 x 120 kW to beam
   2 x 60 kW to ferrite
   2 x 120 kW tetrodes

II. Current transformer plot

III. Second harmonic

1. Bucket area
2. Bunching factor

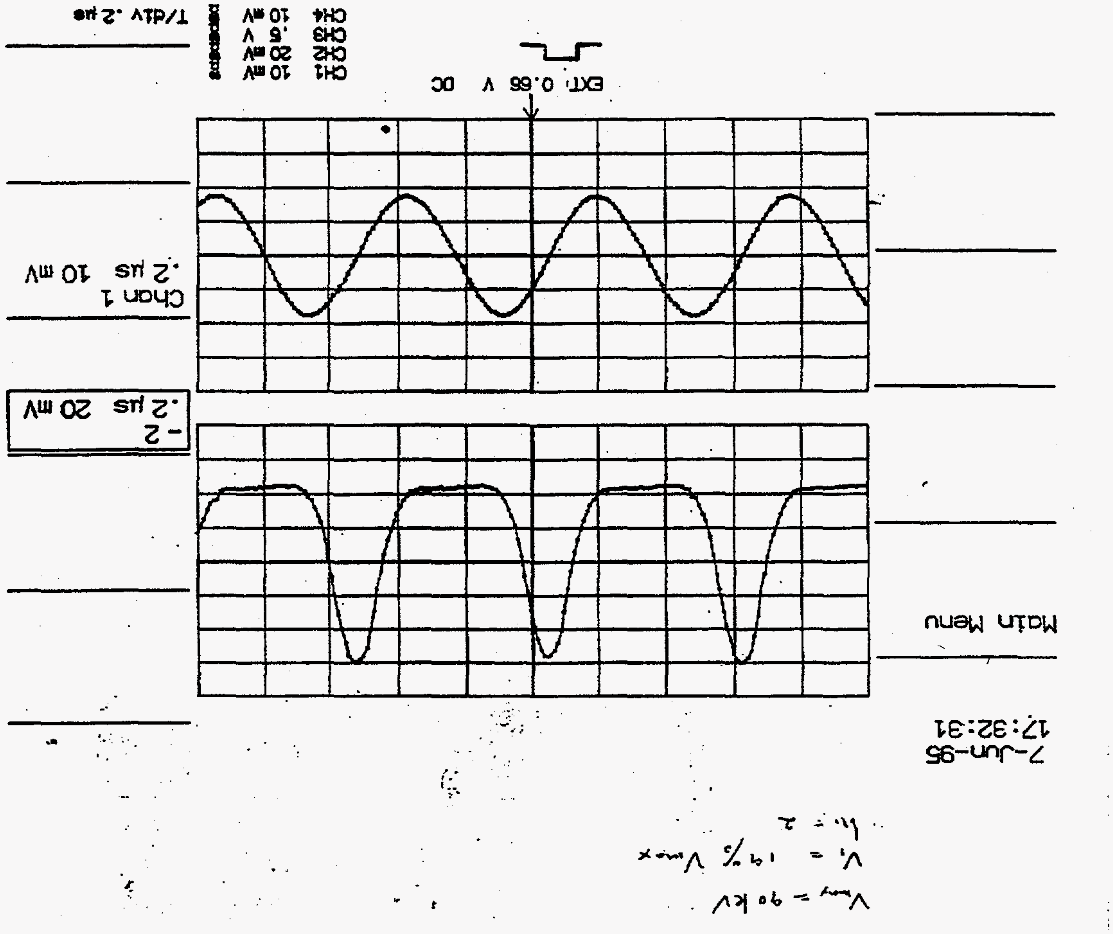
CH1 10 mV
CH2 20 mV
CH3 .5 V
CH4 10 mV
T/div .2 µs
EXT 0.66 V DC
Chan 1 .2 µs 10 mV
-2 .2 µs 20 mV
Main Menu
7-Jun-95
17:32:31
V_max = 90 kV
V_1 = 19% V_max
h = 2

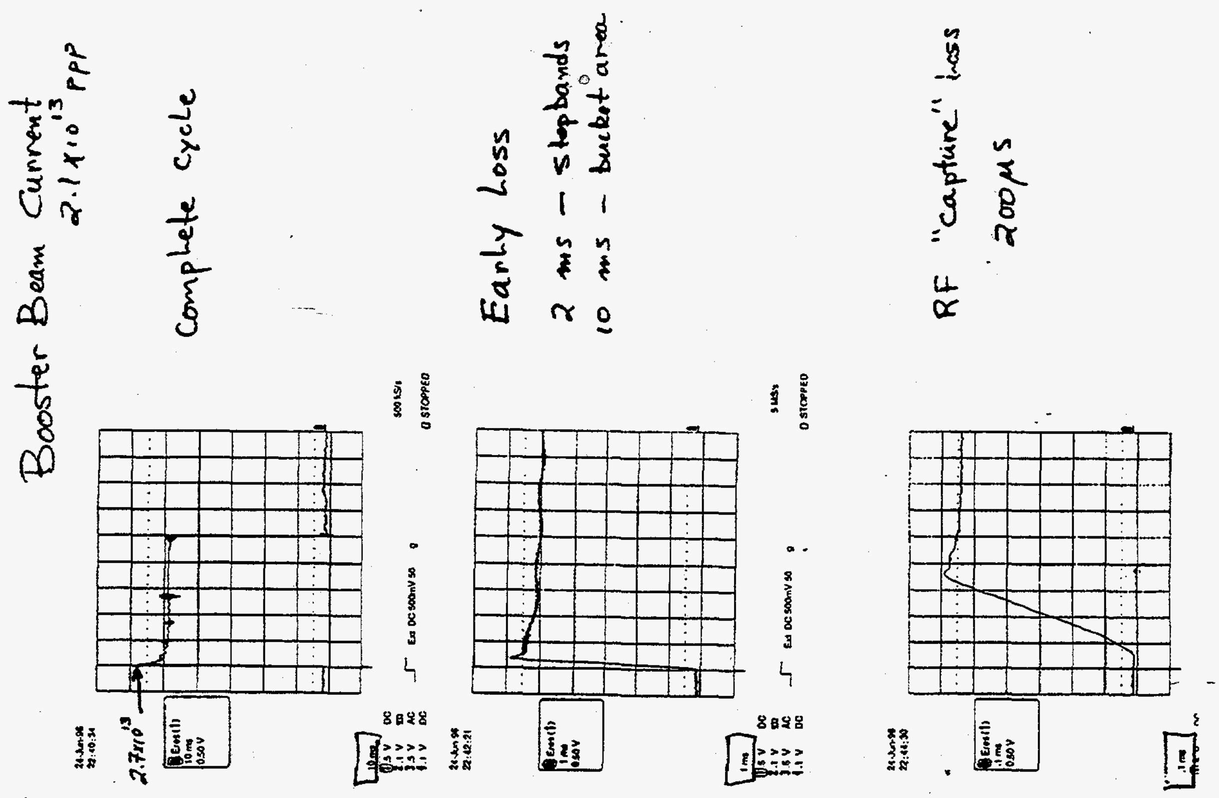
Booster Beam Current
2.1x10^13 ppp
Complete cycle
Early Loss
2 ms — stopbands
10 ms — bucket area
RF "capture" loss
200 µs
2.7x10^13

$V_{max} = 40$ kV
$V_1 = 19\% V_{max}$
$V_2 = 9.1\% V_{max}$
$h_1 = 2$
$h_2 = 4$

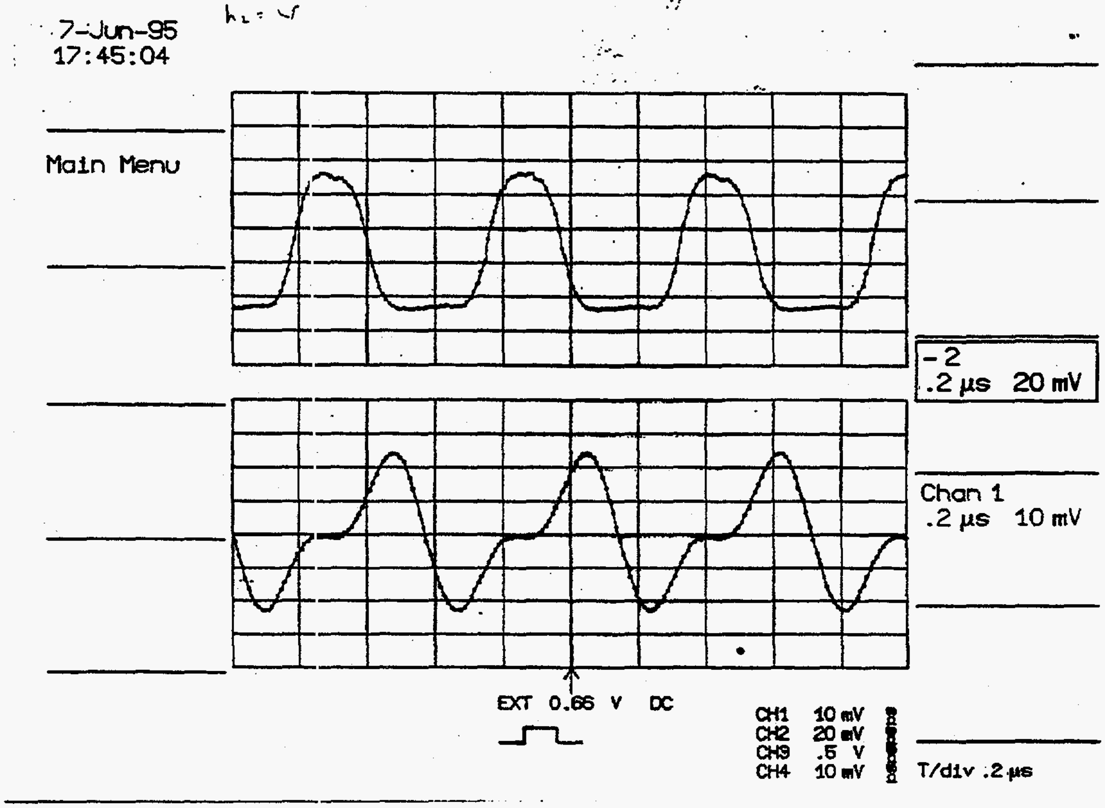

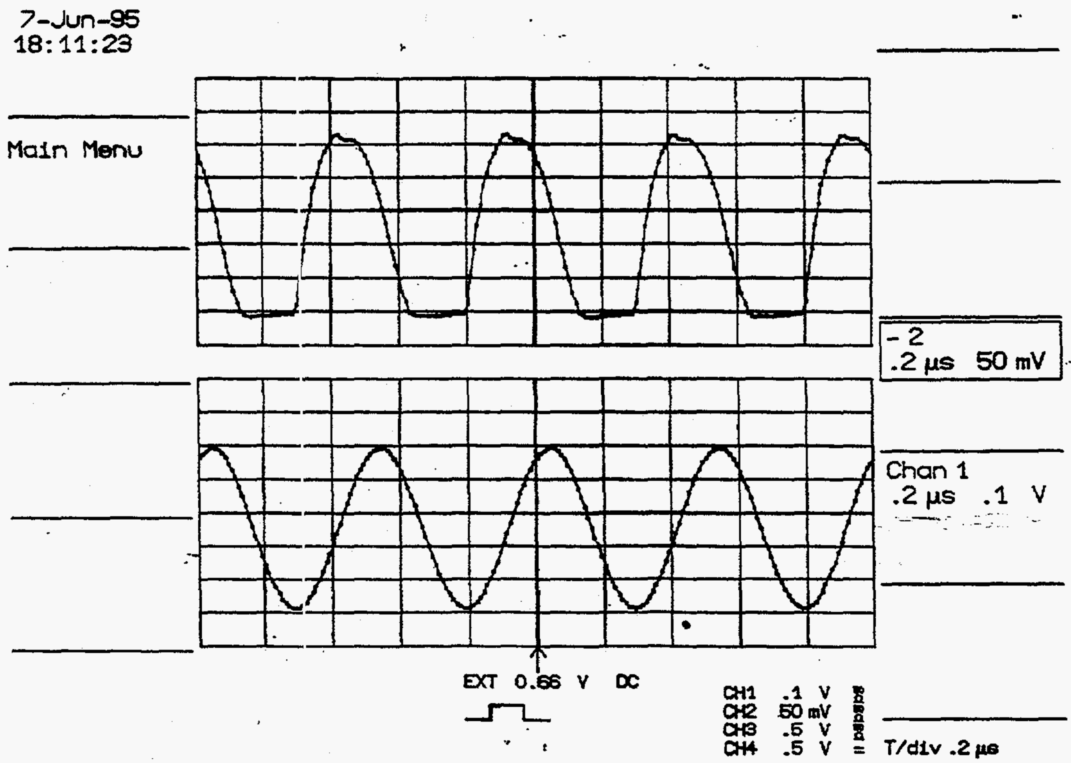

20 TP

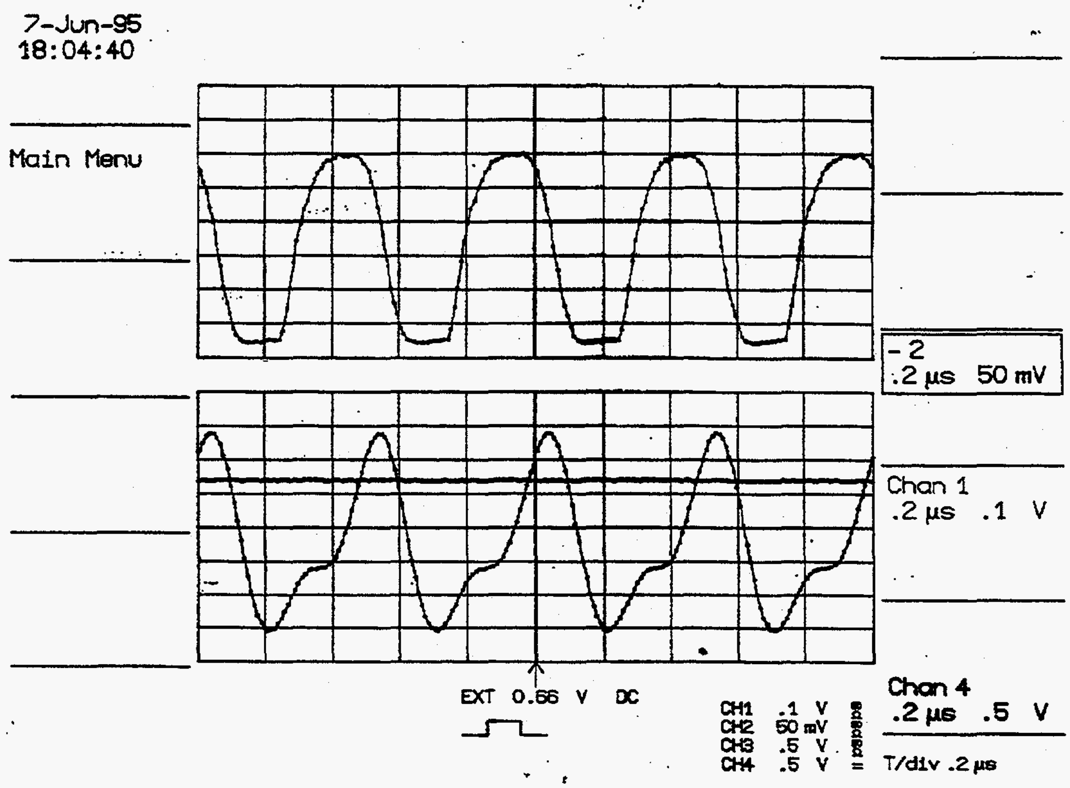

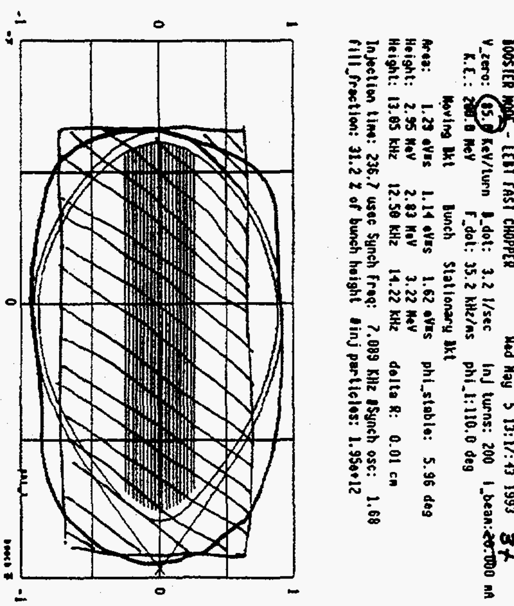

Figure 4. Longitudinal phase space: "dilute" population of 20 turns injected over the period of 200 turns.

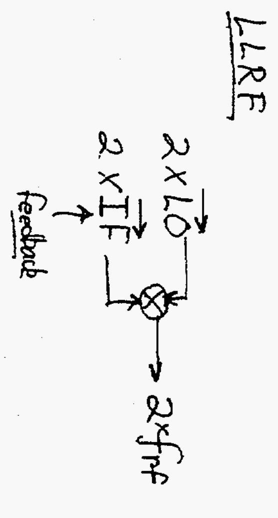

Issues for Discussion

- Near Beam-loading limit
  1. Rf feedback
  2. Feedforward compensation
  3. Low-level drive feedback

- Optimize use of second harmonic
  1. Programing the phase h=4/h=2
  2. Stability in double rf bucket

AGS
(1.9 GeV to 23 GeV, 6 x 10^{13}ppp)

I. Parameters

1. Frequency range: 2.8 to 2.9 MHz, h=8
2. Voltage: 10 x 40 kV (4 gaps each)
3. Beam Current: 5 to 7 Amps, rf
4. Power: 10 x 60 kW to beam
10 x 50 kW to ferrite
10 x 190 kW in tetrode

II. Description of cycle

1. Four batches, 450 ms accumulation
2. Low voltage at injection, transition, and de-bunching for slow spill
3. Power booster at key points
4. Emittance blow-up via "VHF", 93 MHz

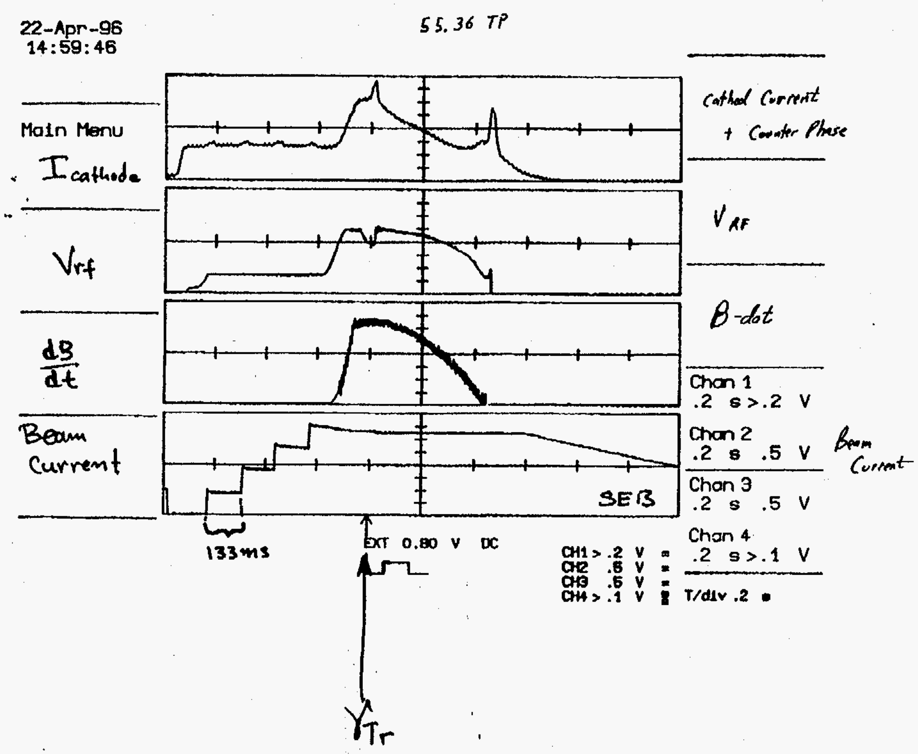
22-Apr-96
14:59:46
55.36 TP
Main Menu
I cathode
Vrf
dB/dt
Beam Current
Cathod Current + Counter Phase
V RF
B-dot
Beam Current
Chan 1 .2 s >.2 V
Chan 2 .2 s .5 V
Chan 3 .2 s .5 V
Chan 4 .2 s >.1 V
SEB
133 ms
EXT 0.80 V DC
CH1 > .2 V
CH2 .5 V
CH3 .5 V
CH4 > .1 V
T/div .2
γTr

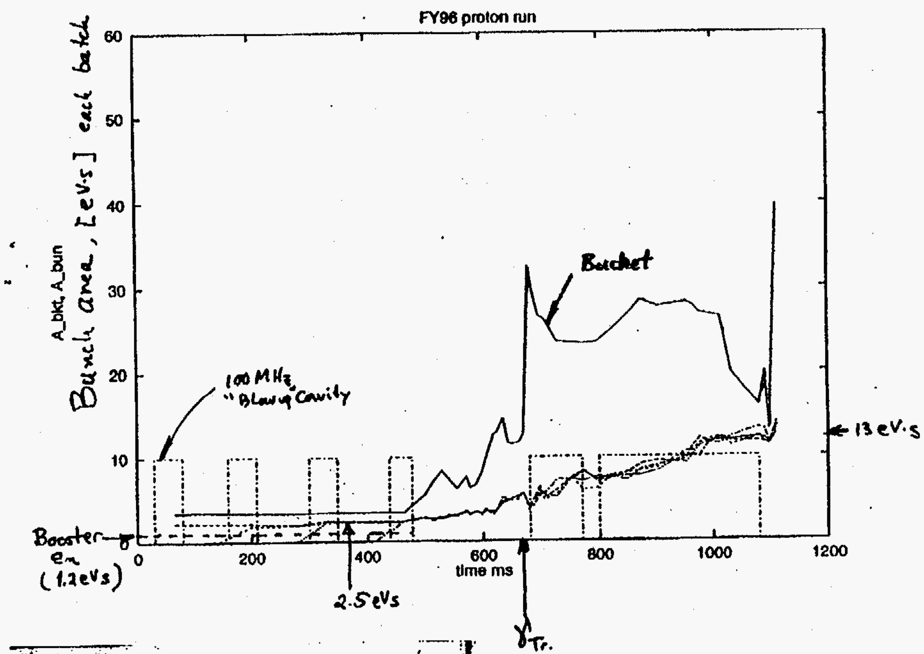
FY96 proton run
A_bkt, A_bun
Bunch area, [eV·s] each batch
time ms
Bucket
100 MHz "Blowup Cavity"
Booster εn (1.2eVs)
2.5eVs
γTr.
13 eV·s

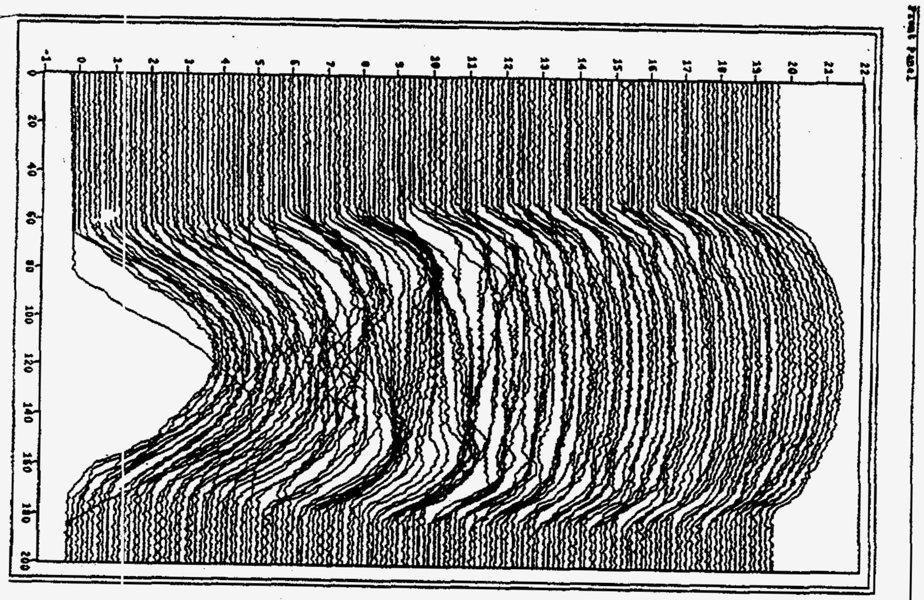

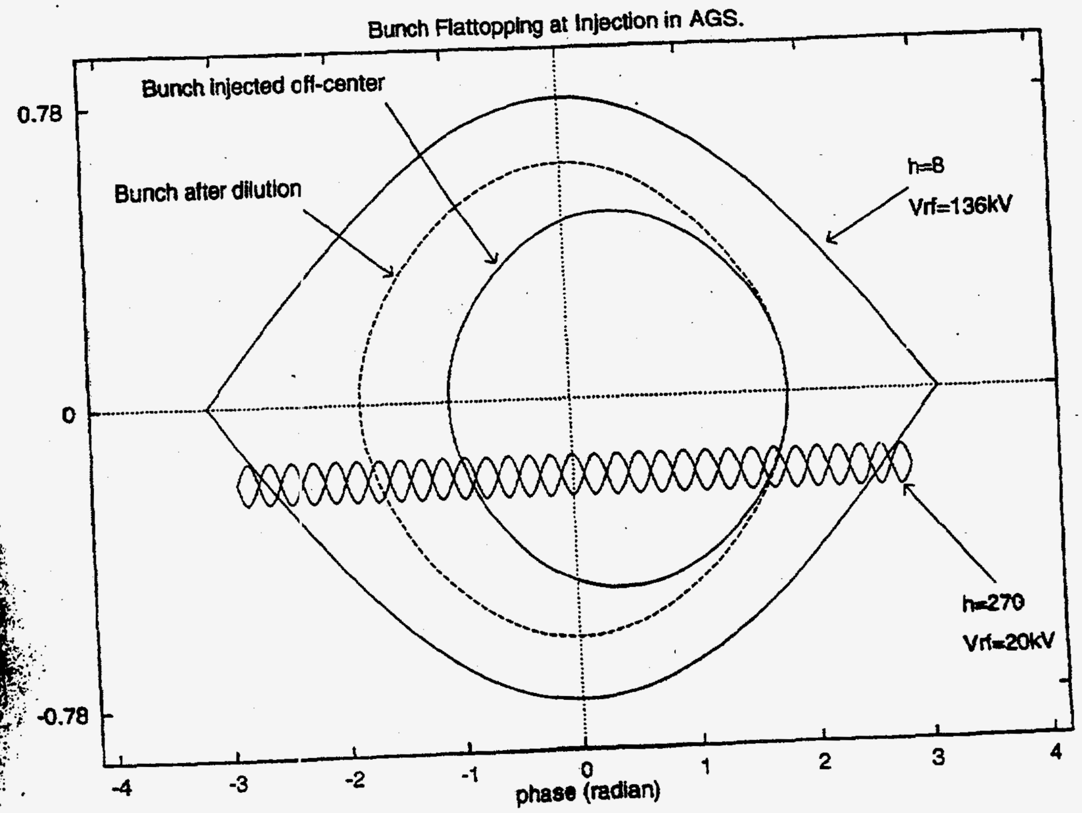
Bunch Flattopping at Injection in AGS.
Bunch injected off-center
Bunch after dilution
h=8
Vrf=136kV
h=270
Vrf=20kV
0.78
0
-0.78
-4
-3
-2
-1
0
1
2
3
4
phase (radian)

Barrier Cavity Development

I. Motivation

1. Slow loss during accumulation, AGS
2. Accumulate more than 4 loads
3. Prospects for a dedicated accumulator

II. Our approach

1. Isolated sine waves
2. High-Q cavities
3. Two cavities, two barriers

III. Development goals

1. 80 kV per cavity
2. 250 ns sine wave, 3 µs rep. rate

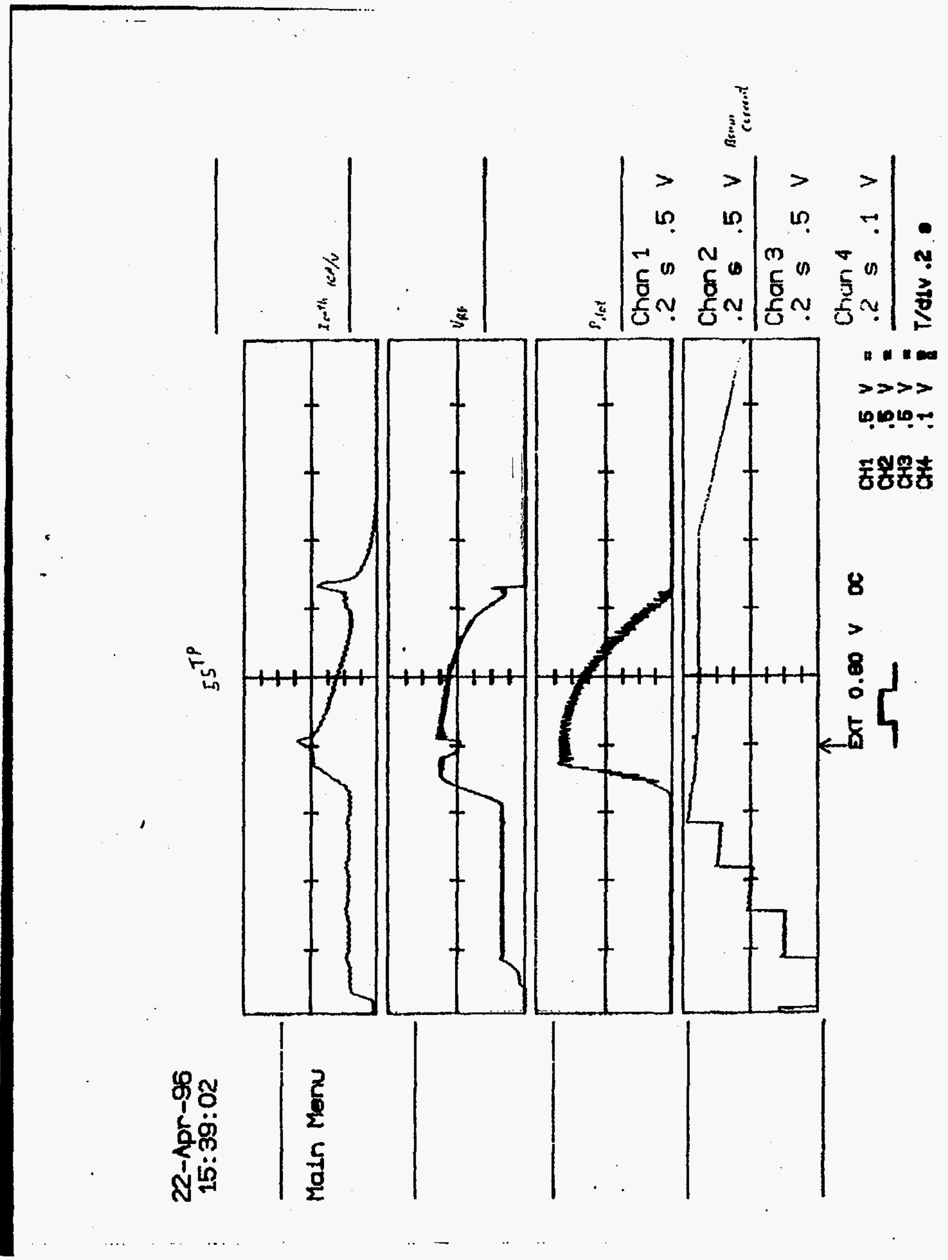

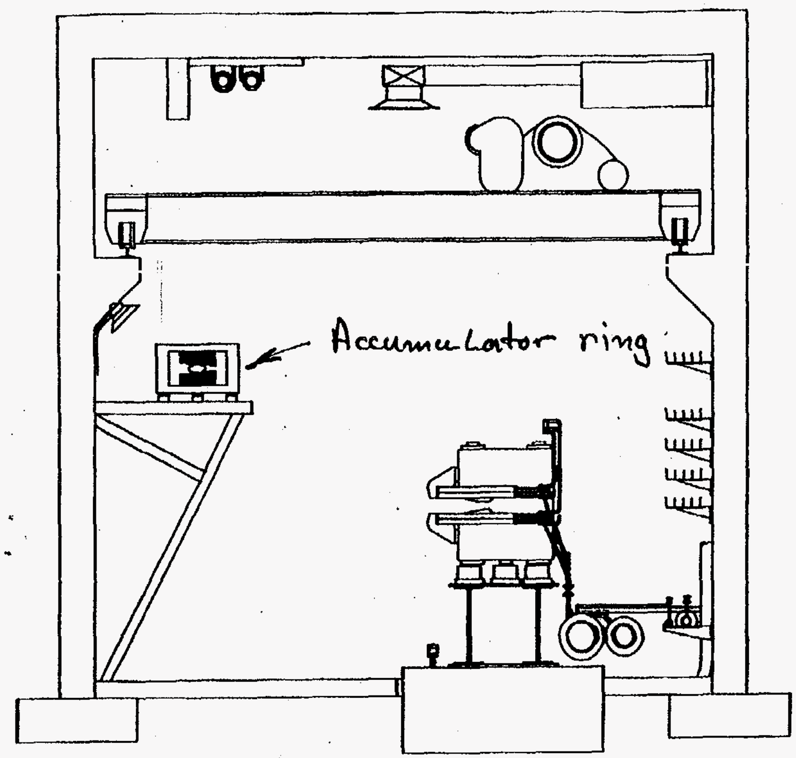

An accumulator could be added to the AGS tunnel

AGS WITH ACCUMULATOR RING

SLOW EXTRACTED BEAM:

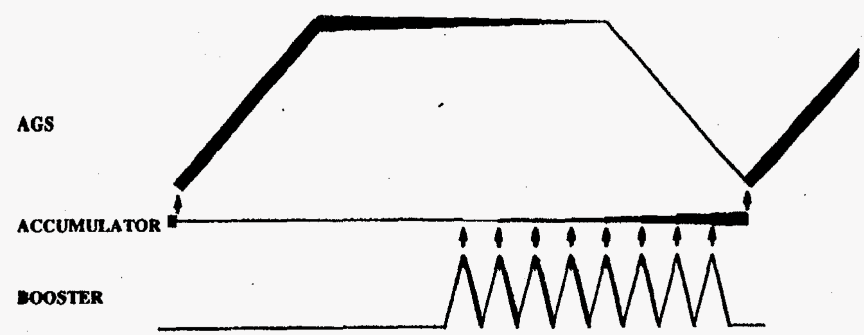

FAST EXTRACTED BEAM:

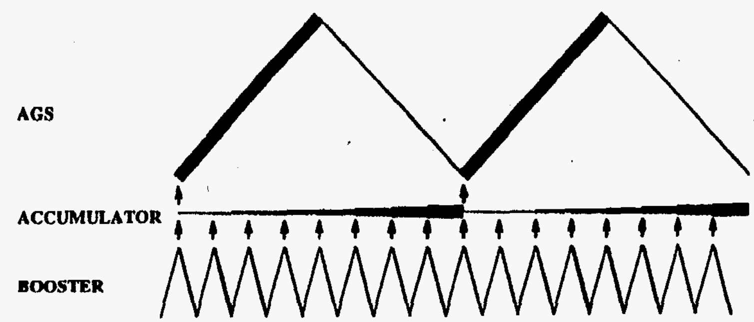

Time Domain Stacking with Barrier Bucket Cavity

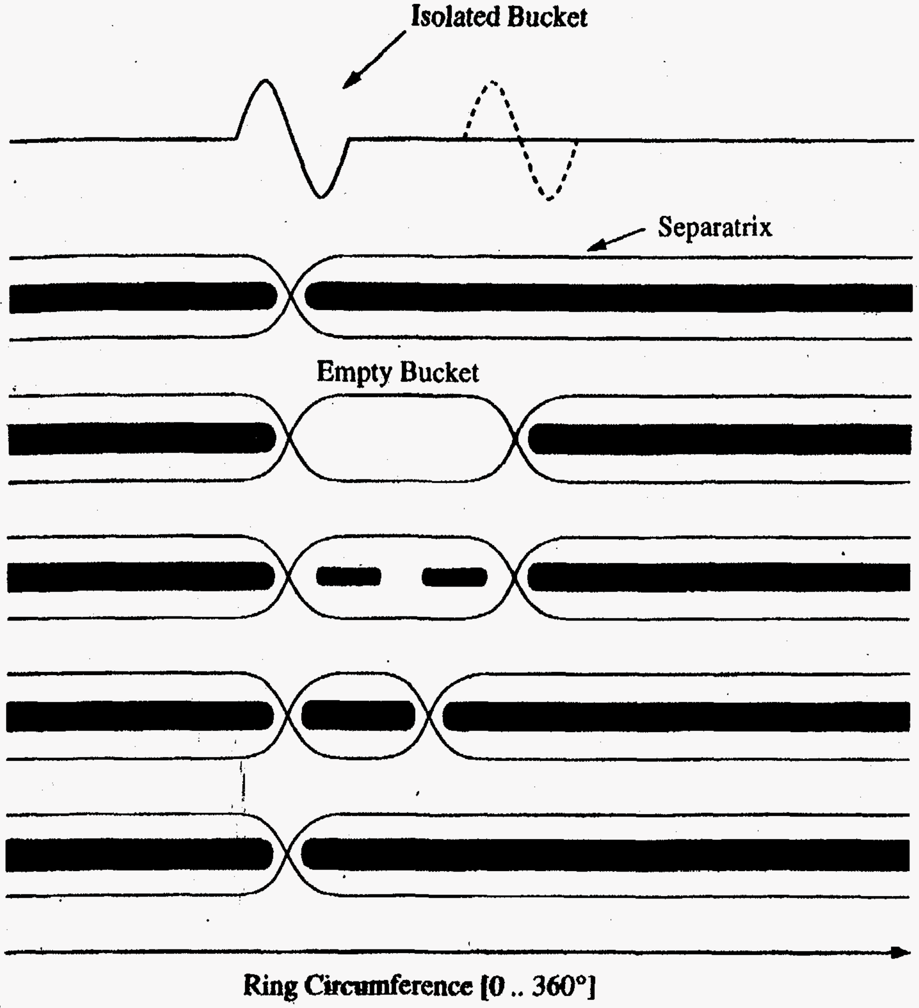

$$I(t) = \frac{V}{R} + C\frac{dV}{dt} + \frac{1}{\mathcal{L}}\int^{t} V(t')\,dt'$$

$$V(t) = V_0 \sin\omega t \qquad 0 < \omega t < 2\pi$$

$$I(t) = \frac{V_0}{R}\sin\omega t + \frac{V_0}{\omega\mathcal{L}} + V_0\cos\omega t\left(\omega C - \frac{1}{\omega\mathcal{L}}\right)$$

RF Waveform for Barrier Bucket (below transition)

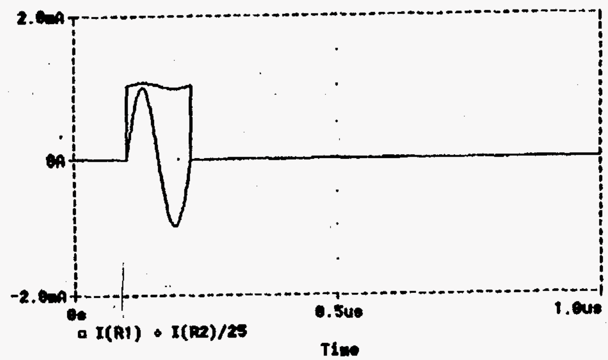

Cavity Voltage and Current for Q = 25

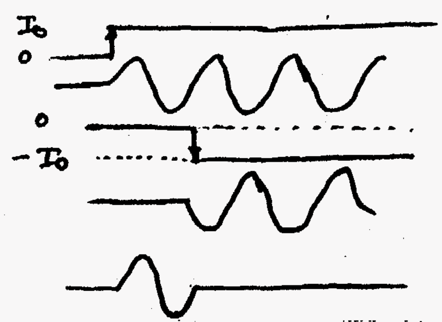

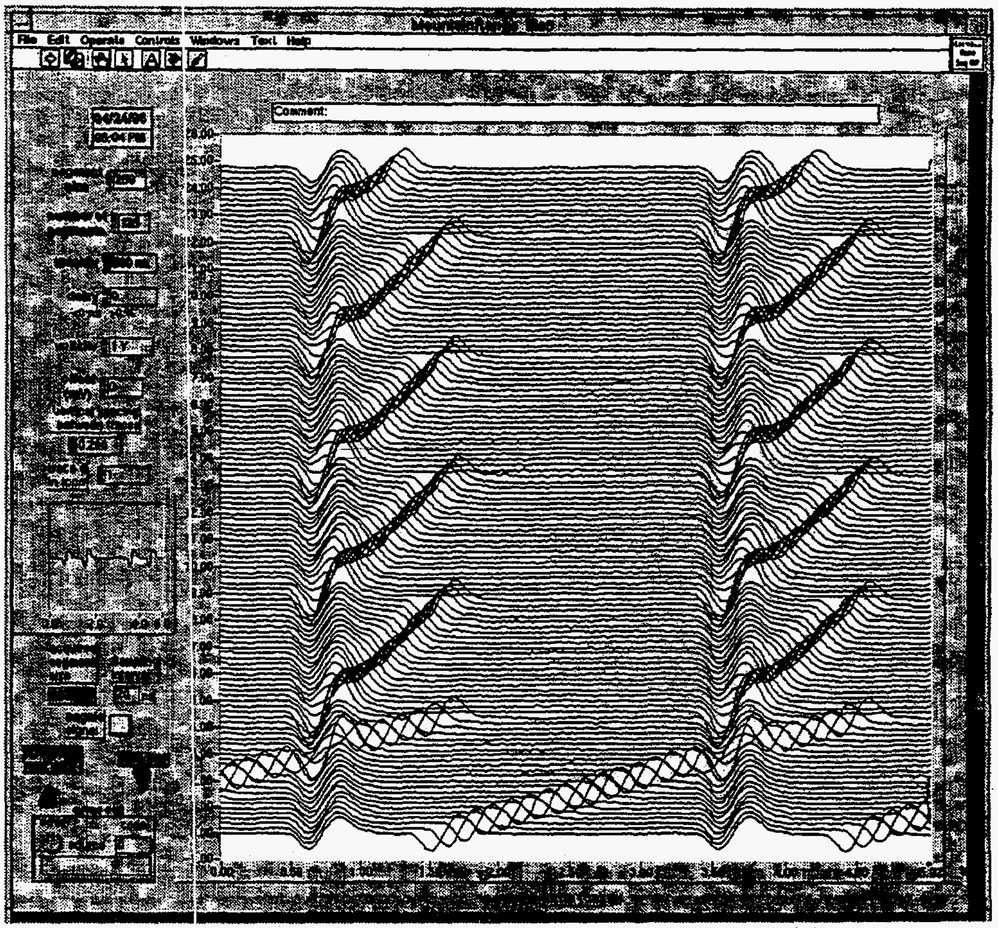
File Edit Operate Controls Windows Text Help
Comment:

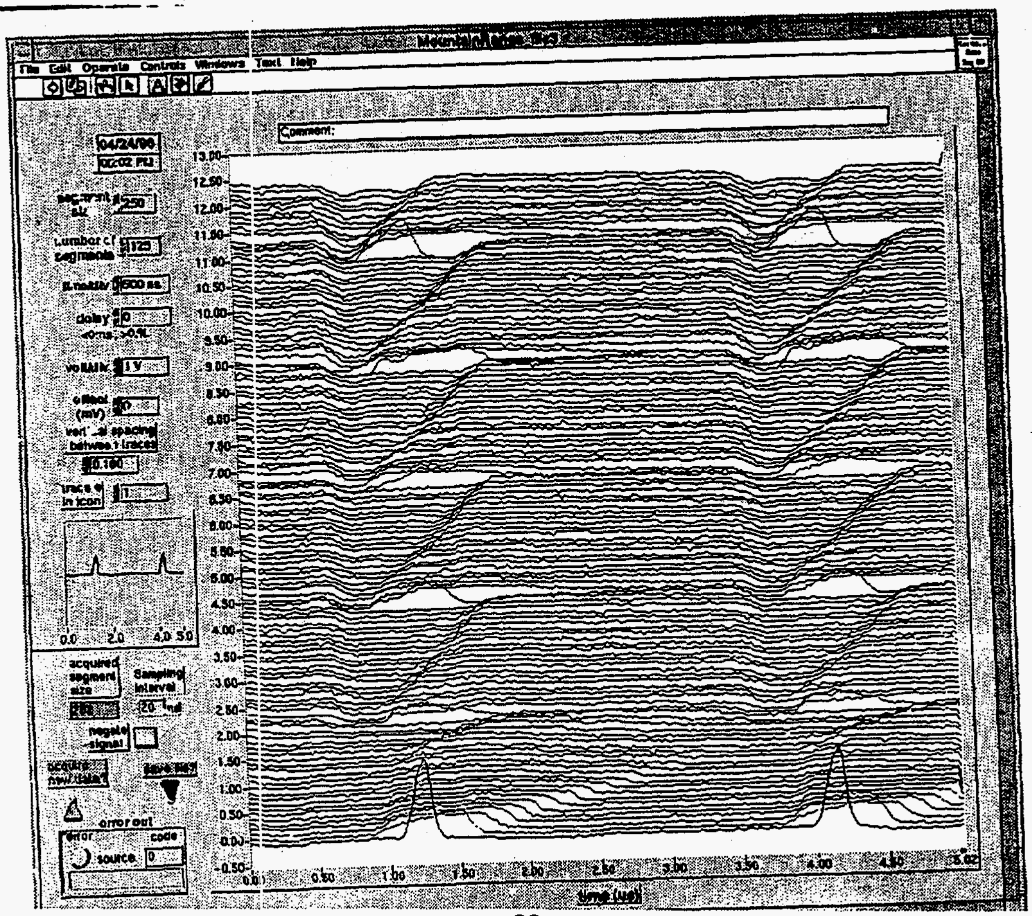
File Edit Operate Controls Windows Text Help
Comment:
04/24/96
error out
code
source
Sampling interval
acquired segment size
0.0 2.0 4.0 5.0

Barrier Buckets (12kV each)

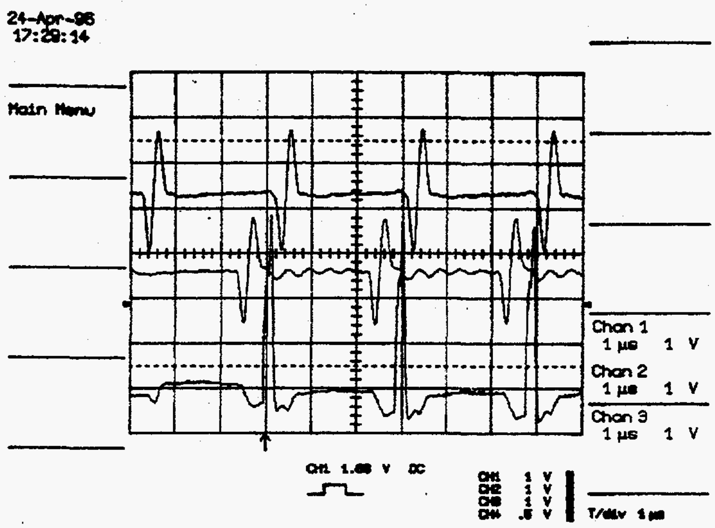

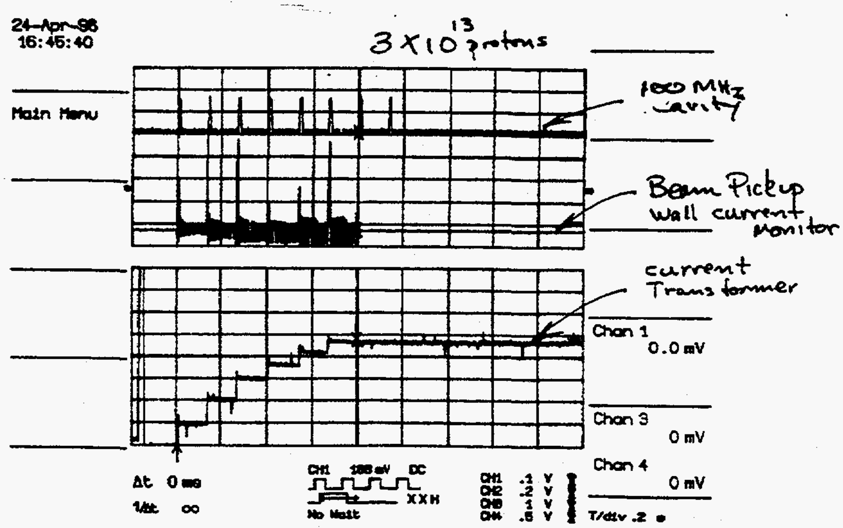

25

05/06/97
R. Garoby

STATUS OF THE CERN PS INJECTOR COMPLEX IN VIEW OF LHC

References:

- Beams in the PS Complex during the LHC era, CERN/PS 93-08 (DI) - Revised –
- Proceedings of the 3rd International Workshop on High Brightness Beams for Large Hadron Colliders (LHC96), Montreux, Switzerland, 13-18 October 1996 (to be published as a special issue of Particle Accelerators):
    1. The PS Booster as Pre-Injector for LHC, K. Schindl
    2. The PS in the LHC injection chain, R. Cappi
    3. Bunched beam longitudinal instabilities in the PSB, F. Pedersen
    4. Longitudinal limitations in the PS complex for the generation of the LHC proton beam, R. Garoby
    5. Microwave instability and impedance measurement in the SPS, E. Chapochnikova, T. Linnecar
    6. And plenty more ….

05/06/97
R. Garoby

1. INTRODUCTION

The big picture …

The Injectors' complex

This talk analyzes issues in the PS complex

2. REMINDER

The injectors' chain for protons

Conclusion no. 1: the transverse emittance budget is tight

Operations in the longitudinal phase plane

Conclusion no. 2: the longitudinal emittance budget is also tight

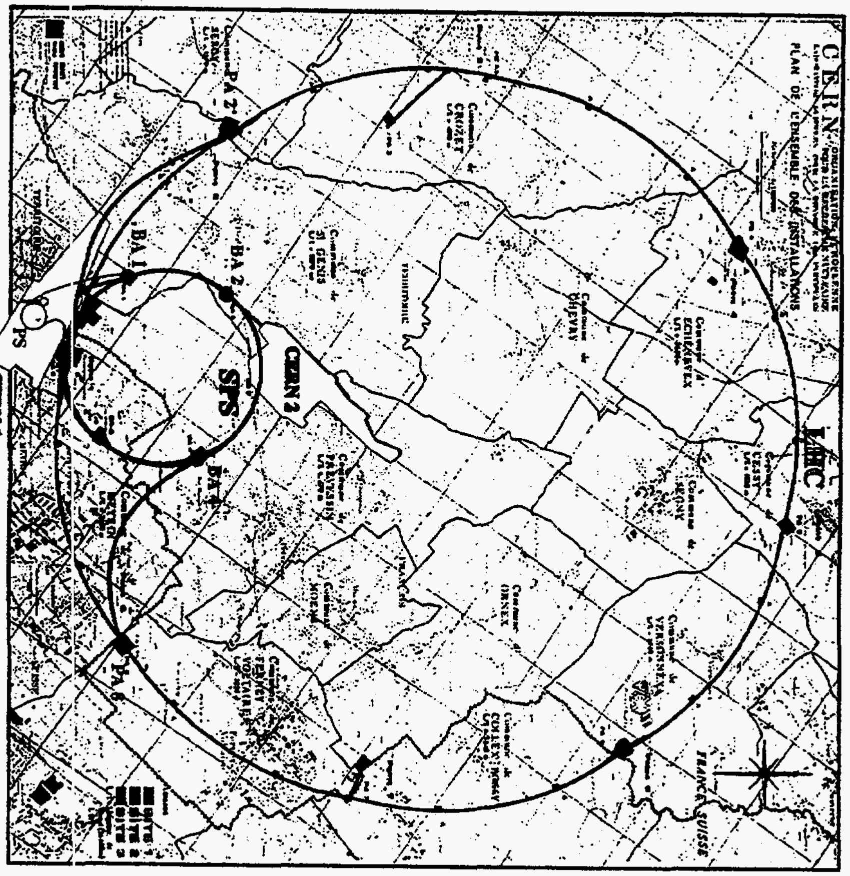

The LHC injection complex

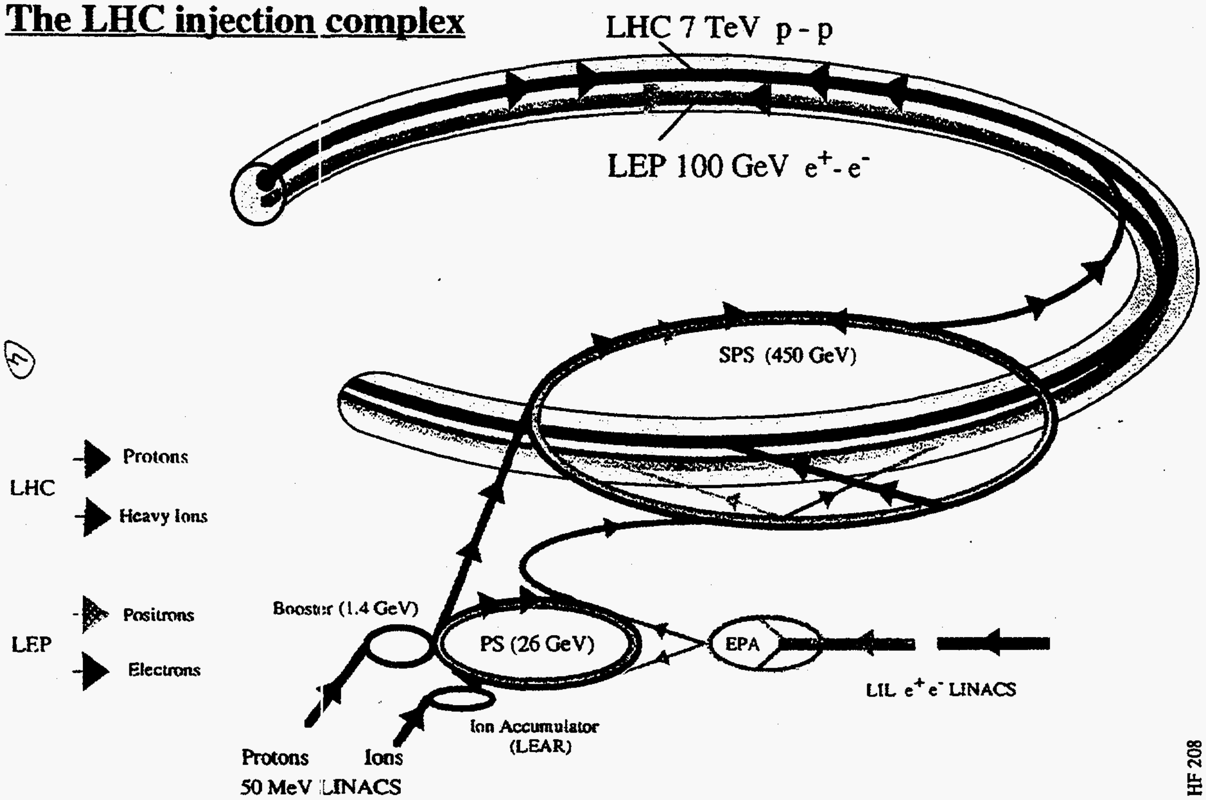

HF 208

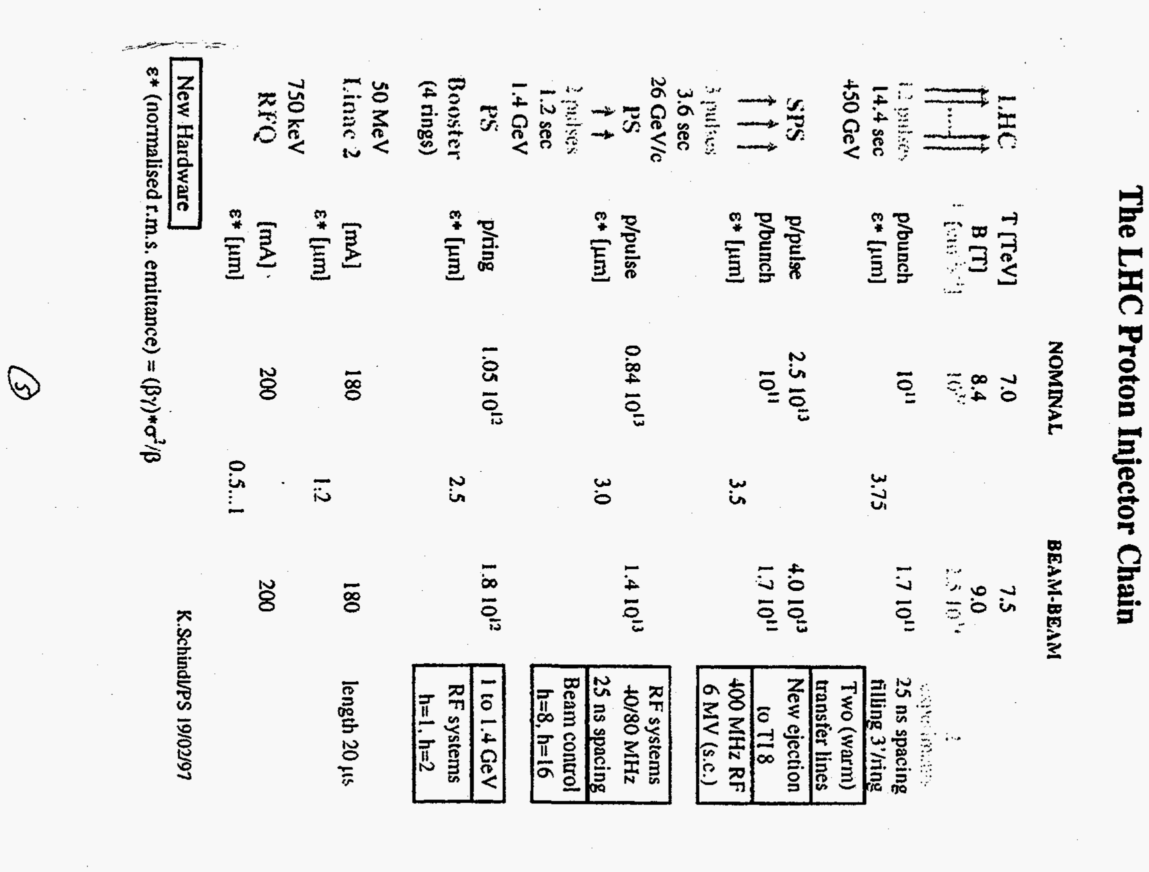

LHC96 - October 96
R. Garoby

LONGITUDINAL LIMITATIONS OF THE PS FOR THE LHC PROTON BEAM

1. NOMINAL OPERATING SCHEME ([1, 2] and R. Cappi at LHC96)

Id.	DESCRIPTION	COMMENT
1	1 bunch / ring in the PSB, reduction of peak line density with second harmonic cavity	~ OK (under test)
2	Controlled blow-up of longitudinal emittance during acceleration in the PSB: aim for hollow particle distribution	~ OK (under test)
3	Bunch to bucket transfer PSB to PS of 2 PSB batches	OK
4	Bunch splitting in the PS (8 ➡ 16 bunches) at low energy	OK
5	Controlled longitudinal blow-ups during PS flat-tops	OK
6	Acceleration up to 26 GeV	OK
7	Debunching (h=16) & rebunching (h=84)	MARGINAL
8	Fast ejection	MARGINAL

1

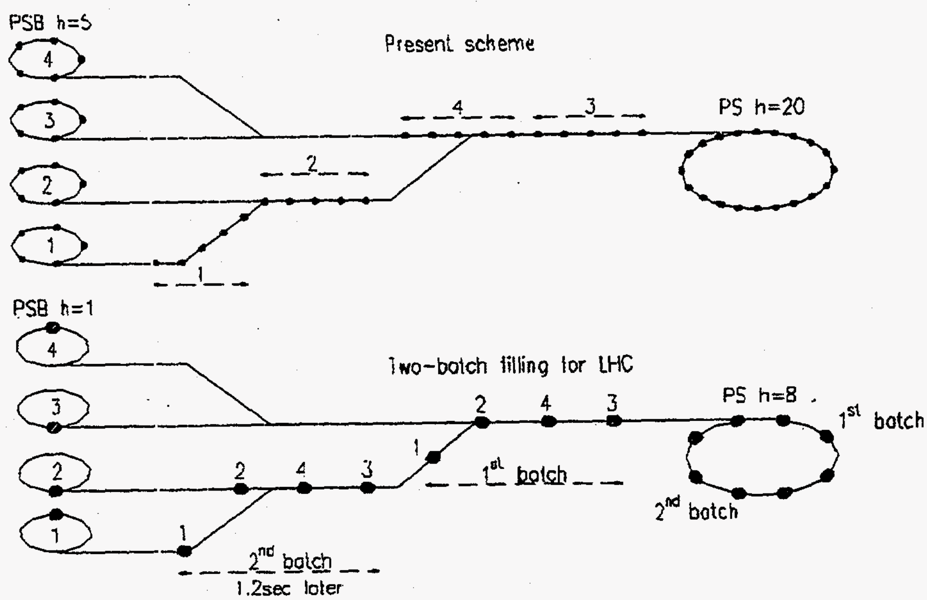

2. DELICATE PROCESSES (items 1, 2, 7 and 8)

2.1 Dual harmonic operation in the PSB (1)

- **Lots of experience with h=5 & 10 in the PSB since > 10 years**
- **Thoughts and experiments with h=1 & 2 presented by F. Pedersen at this workshop**

2.2 Blow-up during acceleration in the PSB (2)

- **The defocusing h=2 spoils the "normal" operation of the blow-up process. Understood after the test in 12/93 but experimental demonstration is still to be done. (Presented at EPAC94 [3])**

2.3 Debunching (h=16) and rebunching (h=84) at 26 GeV in the PS

- **Tight longitudinal emittance budget (following figures from low intensity simulation):**
  - **Total initial beam emittance (h=16): 16 eVs**
  - **Emittance of debunched beam: 26 eVs**
  - **Emittance of compressed bunches: 30 eVs**
- **Bunch dimensions (lb, Dp) marginally satisfying for capture and stability in SPS, although with an already very large voltage for the PS**
- **Non-adiabatic beam gymnastics prior to ejection (=> phase and energy drift of the beam w.r.t. reference)**

2.4 Fast ejection at 26 GeV from the PS

- **Kicker rise-time longer than distance between bunches:**
  - **3 bunches will be lost in the PS extraction system,**
  - **1 (2 ?) bunch(es) will be incorrectly deflected and will end up with a tail at large transverse amplitudes**

BUNCH CHARACTERISTICS AT INJECTION INTO SPS (26 GEV)

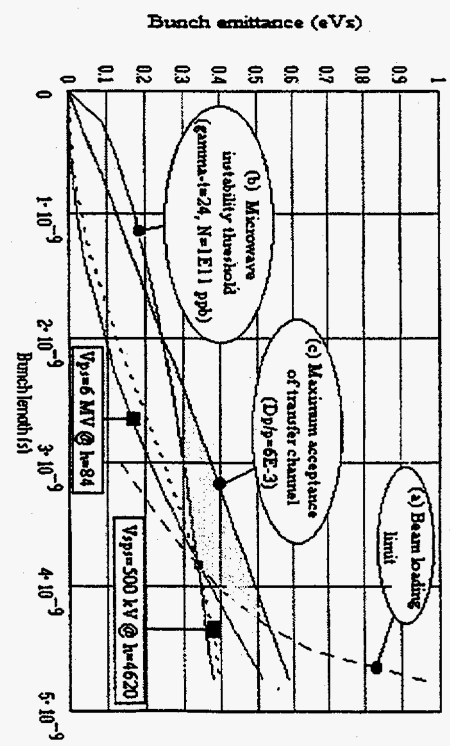

6/5/97
R. Garoby

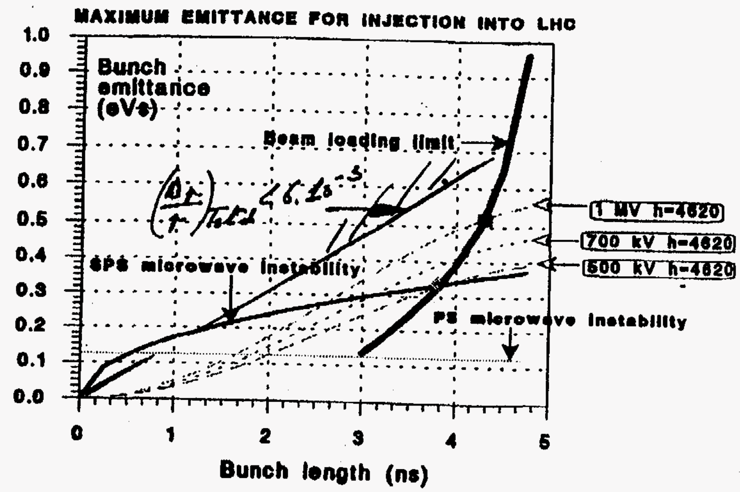

Figure 1 : Bunch parameters

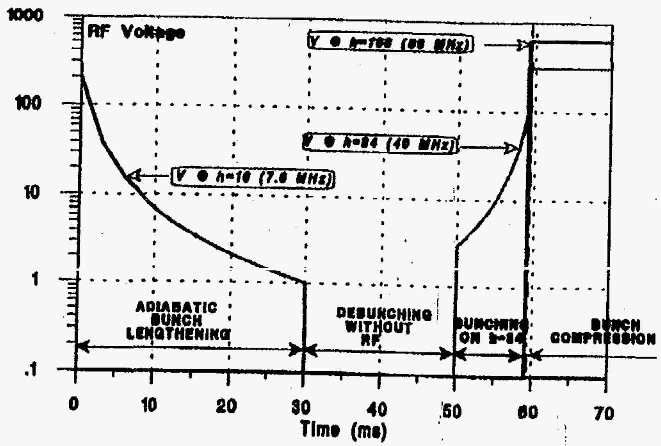

Figure 2 : Voltage programmes

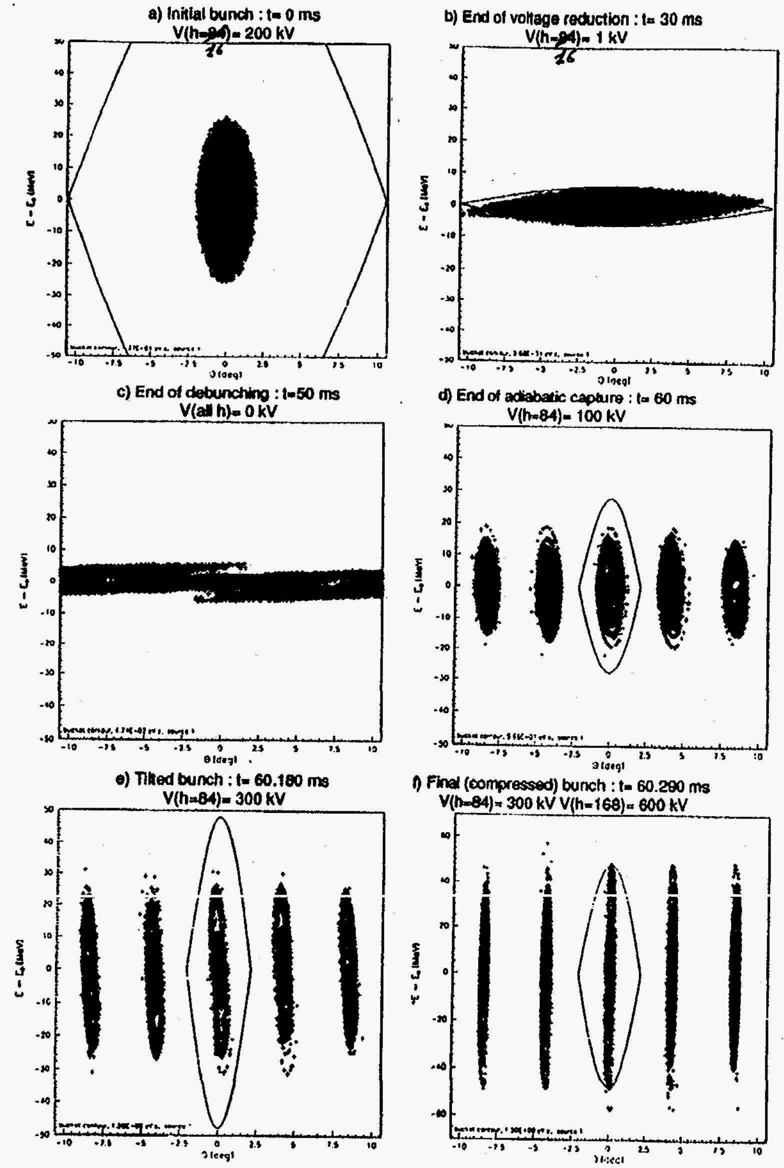

Figure 3 : Results of longitudinal tracking

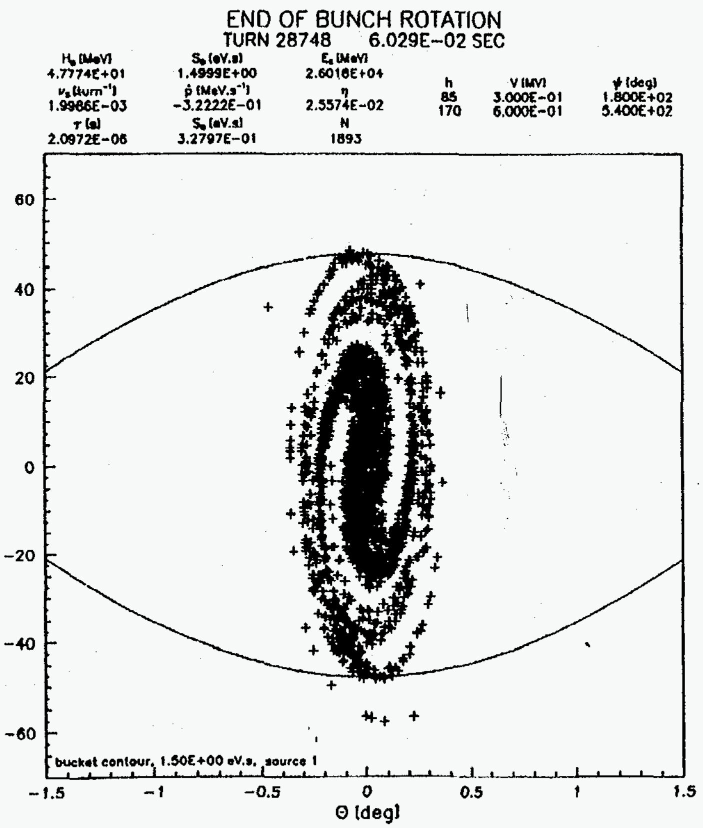

3. RECENT RESULTS

3.1 Hardware

- Prototype 40 MHz system for the PS ("C40"):
  - built and ready on time for first installation in the PS (week 40 / 1996)
  - Nominal performance achieved {V range: 3 to 300 kV pulsed, V rise-time < 20 μs, Closed loop bandwidth: ~ 400 kHz, Gap short-circuit active, H.O.M. dampers installed}

- Prototype 0.6 – 1.8 MHz system for the PSB ("C02"):
  - built and tested on bench in 1996
  - Nominal performance achieved {V range: up to 8 kV CW, Open loop gain of fast feedback: ~ 20 dB}
  - installed on ring 3 during the 96 winter shut-down

- 1.2 – 3.6 MHz systems for the PSB ("C04"):
  - operationally available (modification of present C08 systems)

bulletin

Semaine du lundi 21 avril — no 17/97 — Week Monday 21 April

Le synchrotron à protons du CERN apprend de nouveaux tours

Lorsque le LHC produira des collisions entre ses premiers faisceaux de protons en 2005, ceux-ci auront été préaccélérés dans le PS et le SPS exactement comme les faisceaux d'électrons et de positons du LEP aujourd'hui. Mais auparavant, il faudra encore beaucoup de travail, et pour être prêt à temps il faut commencer dès maintenant. Le LHC fonctionnera avec une fréquence de répétition des paquets de 40 MHz, ce qui revient à dire que les paquets de particules qui circuleront dans la machine ne seront espacés que de 25 milliardièmes de seconde (nanosecondes, ns). C'est beaucoup plus rapproché que les paquets du LEP, et c'est un chiffre qui a été choisi pour fournir aux expériences un maximum de données sans surcharger leurs systèmes d'acquisition de données. Mais c'est également un chiffre qui signifie que le PS, qui est déjà la machine la plus habile au monde à jongler avec les particules, devra ajouter de nouveaux tours à son répertoire.

Dans la chaîne des accélérateurs qui préparent les faisceaux pour le LHC, le PS est le meilleur endroit pour grouper les particules en paquets courts et intenses. On emploiera pour cela de nouvelles cavités radiofréquence (RF), semblables à celles qui servent à accélérer les particules. La différence est qu'elle serviront uniquement au groupage. Lorsque le PS aura fini d'accélérer les faisceaux de protons pour le LHC, une cavité à 40 MHz se mettra en service et comprimera les paquets en appliquant un brusque changement de tension. Les paquets seront alors devenus si courts qu'il ne leur faudra

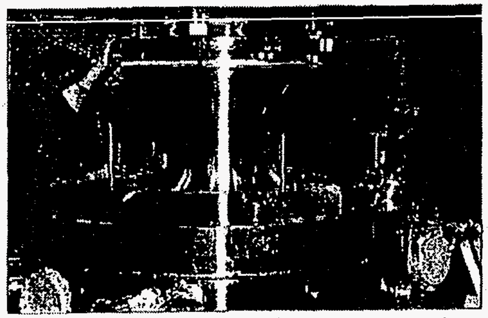

▲ *A delicate operation during the assembly of the new 40 MHz cavity as the mushroom-shaped electrode is carefully inserted.*
Une opération délicate lors de l'assemblage de la nouvelle cavité à 40 MHz: l'électrode, en forme de champignon, est insérée prudemment.

▼ *Cette nouvelle cavité est installée au PS. L'amplificateur qui alimente la cavité est clairement visible au premier plan.*
The new 40 MHz cavity installed in the PS. The amplifier powering the cavity can clearly be seen in the foreground.

CERN's Proton Synchrotron learns new tricks

When the LHC collides its first proton beams in 2005, they will have been pre-accelerated through the PS and SPS just like LEP's electron and positron beams today. But before that can happen, there's much work to be done, and in order to be ready on time, it has to start now. The LHC will operate at a bunch repetition frequency of 40 MHz, or to put it another way, the bunches of particles travelling around the machine will be just 25 billionths of a second (nanoseconds, ns) apart. That's a lot closer together than LEP's bunches, and it is a figure which has been chosen to provide the experiments with as much data as possible without overloading their data acquisition systems. But it's also a figure which means that the PS, already the world's most versatile particle juggler, will have to add new tricks to its repertoire.

The PS is the best place in the chain of accelerators preparing beams for the LHC to group the particles together into short intense bunches. The way this will work is by using new radio frequency, RF, cavities similar to the ones used for accelerating particles. The difference is that these ones will be used just for bunching. When the PS has finished accelerating the proton beams for the LHC, a 40 MHz cavity will switch on and squeeze the bunches together by applying a rapid change in voltage. This will make the bunches so short that they will only take 10 ns to pass any given point. But that is still not quite short enough because the SPS will operate

(19)

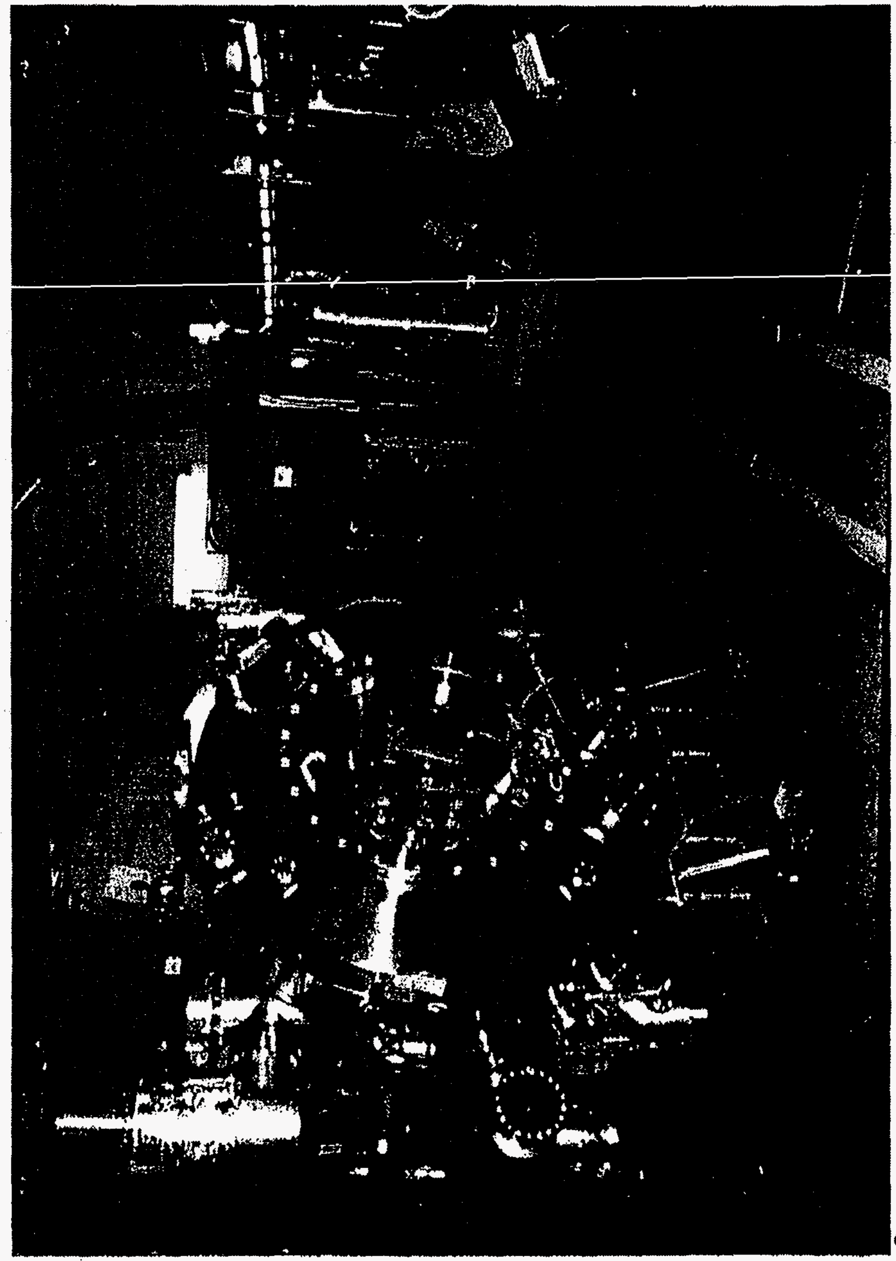

(20)

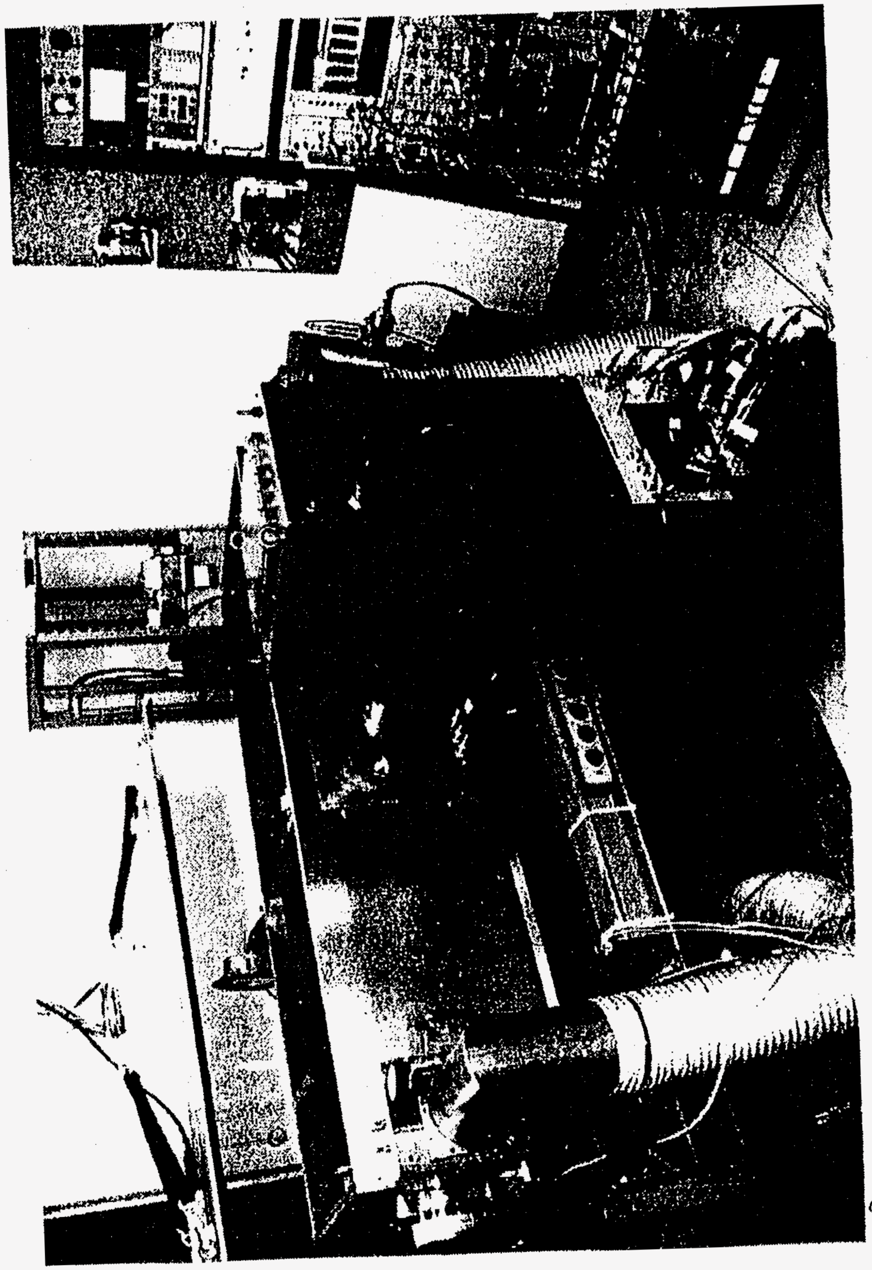

(17)

3.2 Beam experiments

- Rebunching at 40 MHz in the PS (12/96):
  - no problem has been observed on any of the PS beam with the short-circuit open {neither with leptons (HOM) nor with high intensity protons}. Multi-pactor at low field was very helpful (but unreliable over the long term).
  - Debunching (h=20) / rebunching (h=83) could be achieved up to 10^{13} ppp and provided bunches of quasi-nominal emittance (~ 0.4 eVs , 9 ns)
  - Nominal voltage range measured on the beam

- Single bunch compression in the PS (4/97):
  - a single bunch of 1.5 10^{11} ppp was accelerated on h=20 without blow-up up to 26 GeV, and synchronized to SPS revolution frequency
  - bunch to bucket transfer into h=84 worked OK
  - bunch compression -> 5.1 ns (adiabatic) & 3.8 ns (non-adiabatic)

- Acceleration with h=1 in the PSB (ring 3):
  - successful demonstration test (4/97) with ~ 2 10^{12} ppp and check of ppm compatibility

(18)

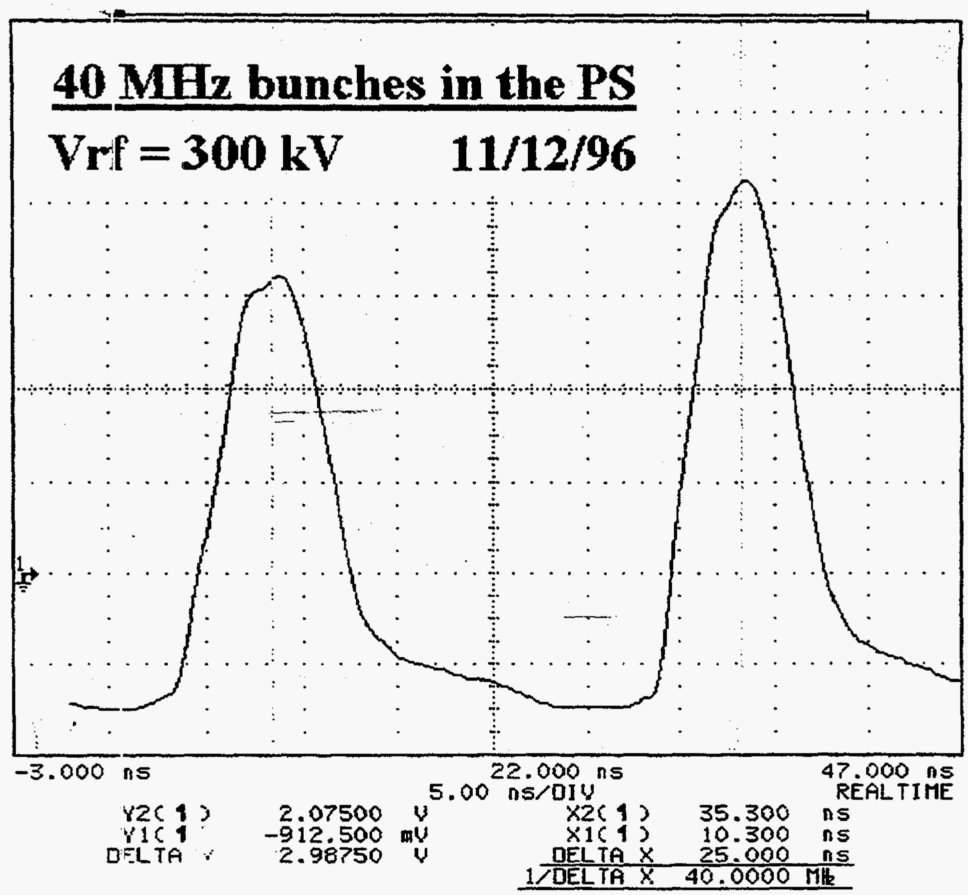
40 MHz bunches in the PS
Vrf = 300 kV 11/12/96
-3.000 ns
22.000 ns
5.00 ns/DIV
47.000 ns
REALTIME
Y2(1) 2.07500 V
Y1(1 -912.500 mV
DELTA Y 2.98750 V
X2(1) 35.300 ns
X1(1) 10.300 ns
DELTA X 25.000 ns
1/DELTA X 40.0000 MHz

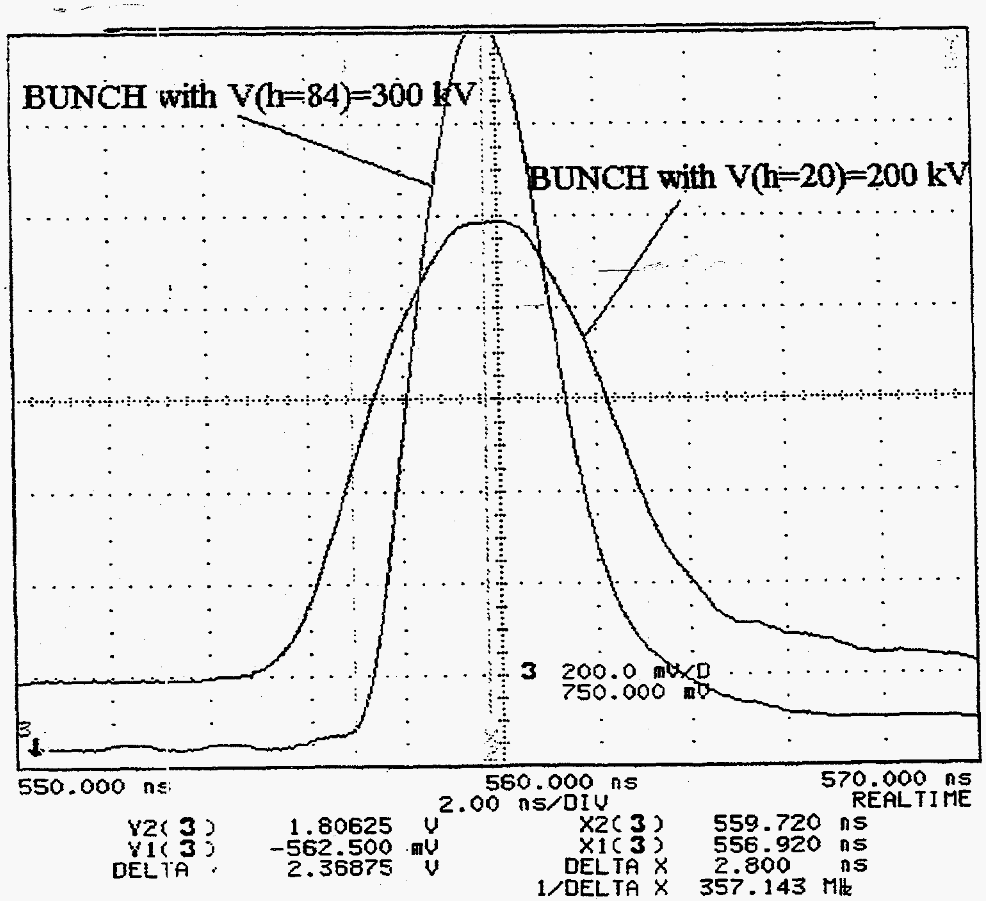
BUNCH with V(h=84)=300 kV
BUNCH with V(h=20)=200 kV
3 200.0 mV/D
750.000 mV
550.000 ns
560.000 ns
2.00 ns/DIV
570.000 ns
REALTIME
Y2(3) 1.80625 V
Y1(3) -562.500 mV
DELTA Y 2.36875 V
X2(3) 559.720 ns
X1(3) 556.920 ns
DELTA X 2.800 ns
1/DELTA X 357.143 MHz

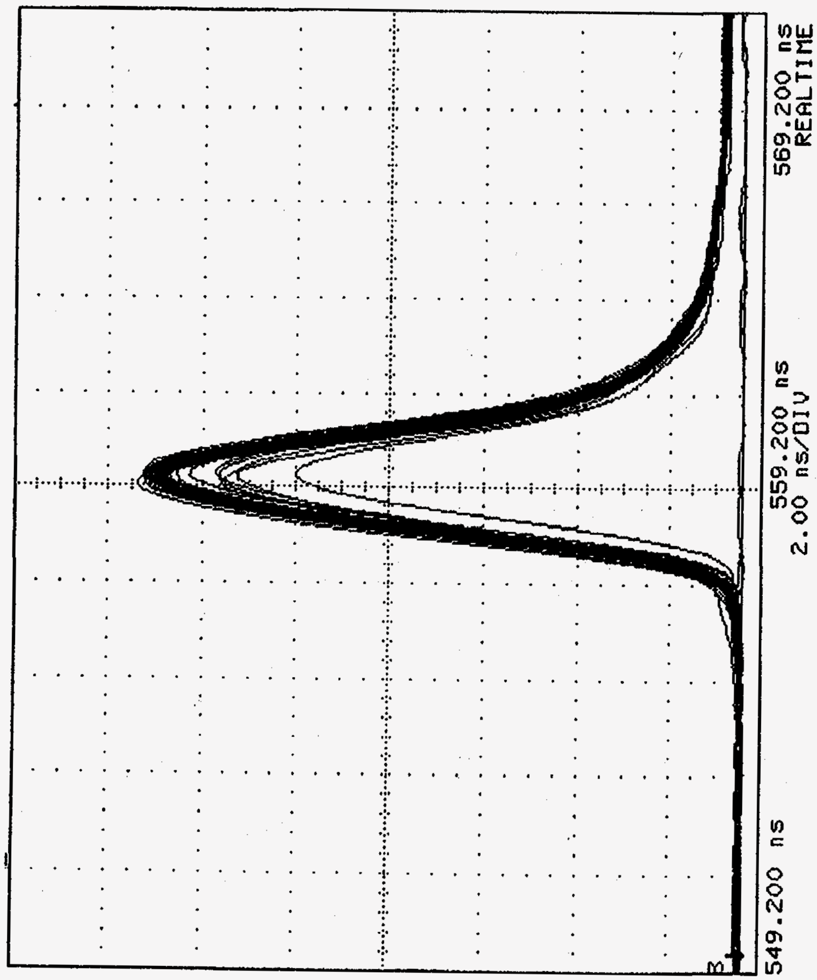

SYNCHRONISATION JITTER ON COMPRESSED BUNCH
capture up to 60 kV & Step to 300kV . - 4/4/97)

(21)

05/06/97
R. Garoby

4. WORK PLAN

4.1 Short term aims (till end 97)

- Build and test the hardware required for the 97-98 shut-down (4 C02 RF systems for the PSB, 2 C80 RF systems for the PS, low level RF and beam controls for all new modes of operation, specification of control's software for 98)
- As far as reasonably achievable {☺ : bnl internal joke}, test prototypes and check all modes of operation during 97
- Beam studies (analysis of longitudinal instabilities, understanding of controlled blow-up mechanism with dual harmonics RF system in the PSB, minimization of longitudinal emittance in the PS, etc.)
- Provide test beams to SPS
- Feasibility study for a 2 GeV Supraconducting Linac
- Define & begin work for the Anti-proton Decelerator ("AD")

4.2 Medium term aims (till end 98)

- Resume operation for physics for the start-up in March 98
- Provide nominal LHC proton beam to SPS for the summer 98
- Build / modify hardware and begin beam studies for the AD

4.3 Long term aims (after 98)

- Start & run the AD
- Implement modifications (if any) for proper handling of the nominal LHC beam in the SPS
- Design and implement a technique to create a void of a few bunches in the PS 40 MHz bunch train
- Prepare Ions injectors' complex for LHC
- Define (implement ?) a scheme to attain the ultimate luminosity in LHC ...

(22)

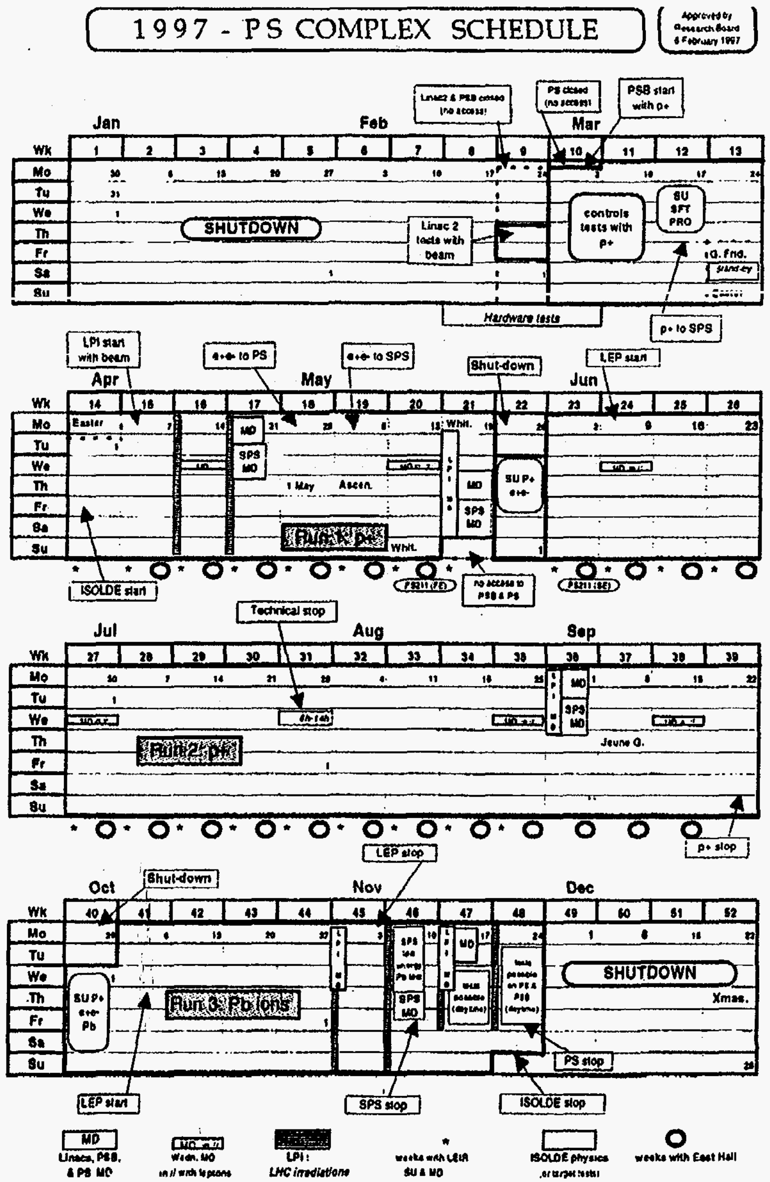

(23)

17/04/97
R. Garoby

PREPARATION OF THE PS COMPLEX FOR THE LHC-ERA IN 1997:

RF AND LONGITUDINAL PHASE PLANE STUDIES

1. PSB (ring 3)

LHC H+	• Acceleration on h=1&2 in ppm • Synchronisation 1 GeV • Longitudinal blow-up (h=10)	Weeks 16-26 (Apr.- Jun.) " Weeks 36-40 (Sept.) Week 35: beam (1 bunch) to the PS
SFTPRO	• High beam intensity acceleration on h=1 & 2 • Analysis & damping (!) of instabilities • Splitting @ 1 GeV • Synchro. after splitting	Weeks 17-40 (Apr.- Sept.) Week 40: beam (2 bunches) to the PS
SFTION.	• Acceleration on h=4 using C02 & C04 (0.72 to 3.86 MHz)	Weeks 36-46 (Sept.-Oct.) Week 47: beam (4 bunches) to the PS

(24)

2. PS

[illegible]	[illegible]	[illegible]
SPS test beams	• 1 to 20 bunches on h=20 @ 26 GeV with frev synchro. on SPS • Recaptured beam on h=84 @ 26 GeV (10^{13} ppp, 0.4 eVs, 9.5 ns) • 1 bunch on h=84 (from 1 bunch on h=20) (5 to 15×10^{10}ppb, 0.14 eVs, 3.8 ns)	Week 16: beam to SPS Weeks 17 Week 18: beam to SPS Weeks 15-22 Week 23: beam to SPS
LHC H+	• Capture on h=8 • Splitting on h=16 • Blow-up and acceleration on h=16	Weeks 35-40 (Sept.)
SFTPRO	• High beam intensity capture / splitting and acceleration on h=16 • Analysis & damping (!) of instabilities	Weeks 40-46 (Oct.)
SFTION	• Capture & acceleration of Pb^{53+} on h=16	Weeks 47-48 (End Nov.)

3. OTHER TASKS ON THE MACHINES

- Test of new 200 MHz blow-up hardware (200 MHz phase-shifter with digital control by GFAS)
- Check phase stabilisation loop for 40 MHz system
- Build and test 40 MHz phase loop
- Set-up and exercise tuning loop for the 40 MHz cavity
- Monitor effects induced by the 40 MHz cavity on the beam. track evolution of multipactor levels.

Domain	Action	Benefits	Comments
PS longitudinal parameters	- increase V_{RF} - reduce $\lvert\eta_{PS}\rvert$	better bunch compression	- expensive and of limited effect - to be investigated but no clear solution yet
Gap in the beam	- "killer" kicker - "barrier-bucket" - bunch splitting	no badly deflected bunches	- beam losses - to be investigated - needs high energy Linac or rebuilt PSB ejection kickers
SPS longitudinal parameters	- reduce $\lvert Z/n\rvert$ - increase $\lvert\eta_{SPS}\rvert$	improved stability in SPS => relaxed requirements on the PS	- under investigation (source of dominant impedance localised) - deserves investigation
New PS ("PS-XXI")	- increase transfer energy - imaginary variable γ_{T_PS}	improved stability in SPS + better bunch compression + improved reliabilility + simplified operation	- major investment - needs upgrade of the transfer channel to SPS - needs further studies
High energy Linac ("SPL")	- increased injection energy in the PS (2 GeV) - no waiting time at PS injection energy - chopped injected beam	minimal long. blow-up + better bunch compression + no badly deflected bunches + reduced transverse emittances + improved reliabilility + simplified operation	- major investment - most effective solution to increase LHC beam brightness - needs further studies

LONG TERM THEMES OF INVESTIGATION

Intensity Related RF Issues at Fermilab

David Wildman

Fermilab

Acknowledgments

Joe Dey
Kathy Harkay
Gerry Jackson
Ioanis Kourbanis
Dave McGinnis
Jim Steimel

Future Plans Requiring Higher Intensities

Collider Run II (1999)

- Increase number of colliding bunches from 6x6 to 36x36
  - Multi-Batch Coalescing
- Increase Pbar production and stacking rate
  - Higher Main Injector Intensity of 6e10 ppb
  - Recycler Ring Barrier Bucket RF system

Tev 33 (before LHC)

- Increase Collider luminosity to 1e33
  - Slip stacking ?
  - Additional Main Injector RF ?
  - A higher frequency RF system for the Tevatron ?

NUMI = NeUtrinos at the Main Injector(2000+)

High intensity fixed target experiments to detect neutrino oscillations

Muon Collider (?)

A fast cycling high intensity proton driver

Three Topics for Discussion

Longitudinal Coupled Bunch Instabilities

Multi-Batch Coalescing (transient beam loading)

Wideband Recycler Ring RF (barrier buckets)

Booster Resistive Wall Monitor

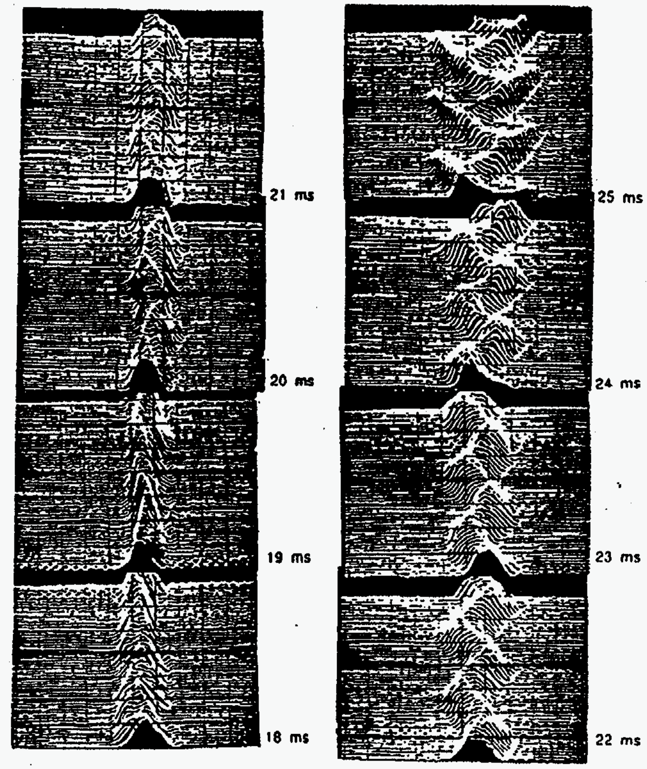

Figure 1.1 Time Evolution of the Bunch Phase (Mountain Range Plots) Through a Portion of the Booster Cycle. Growing dipole oscillations indicative of the coupled-bunch instability are clearly seen. The beam intensity is 1.5×10^{10} protons per bunch, the transition jump system is off, and the RF cavity dampers are out. The horizontal scale is 2 nsec per division. [Ref. 43]

Booster RF Cavity

Upstream Monitor STA 12 Red: No beam
Black: with beam

6/19/90

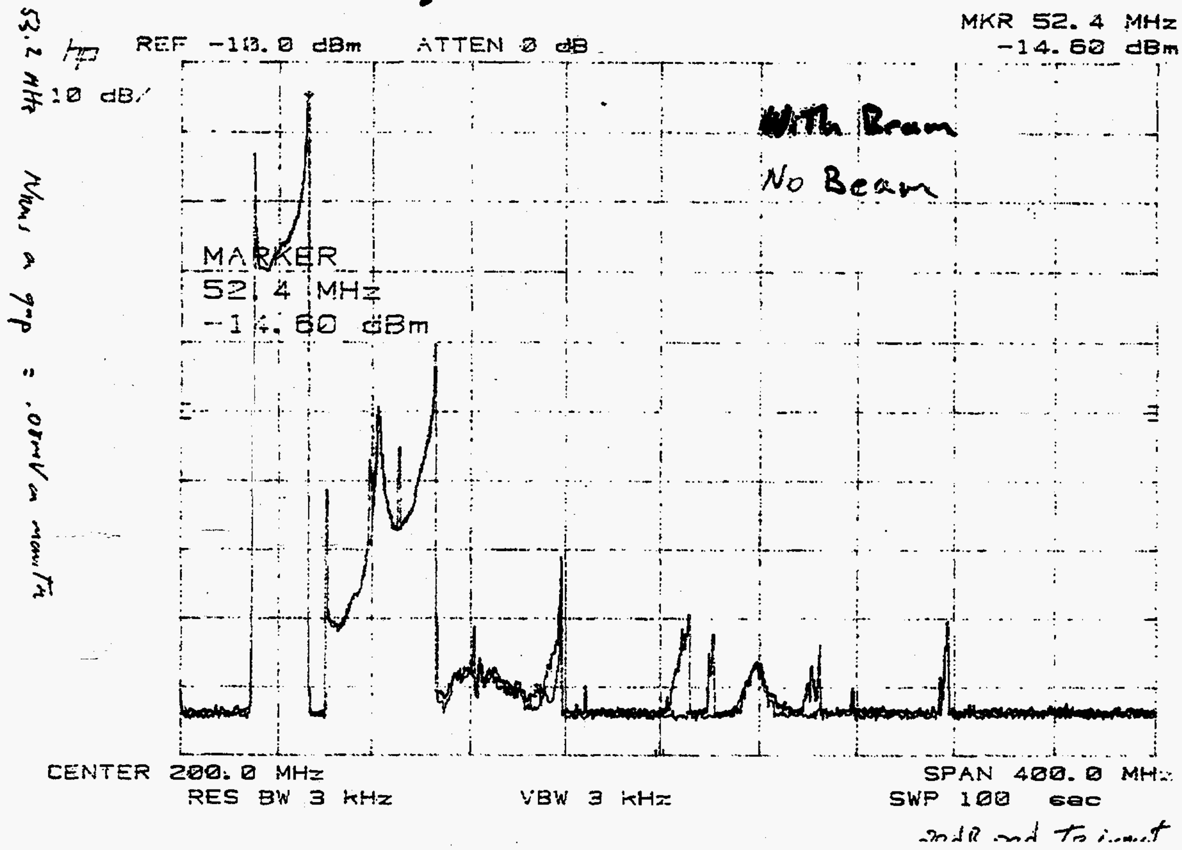

Booster RF Cavity

6/19/90

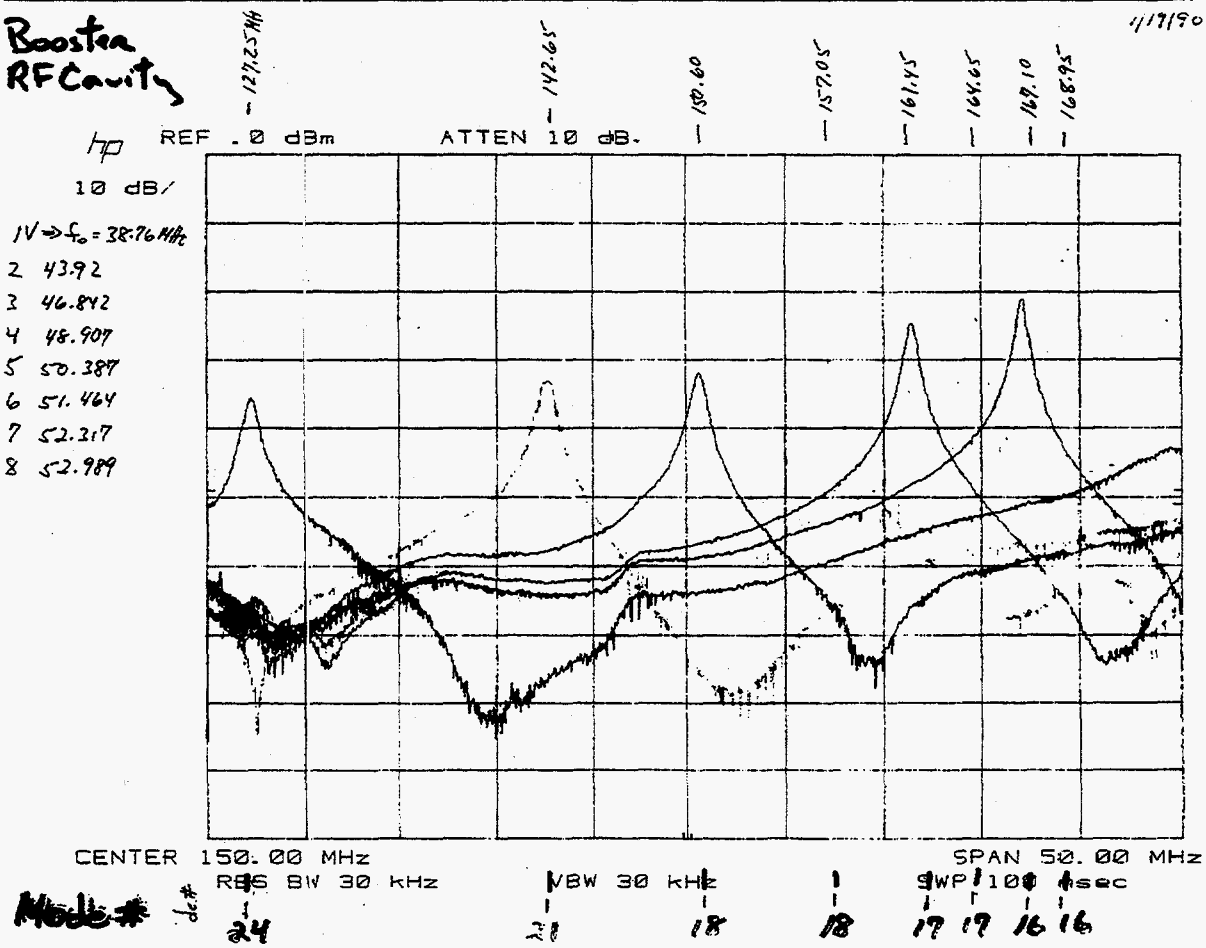

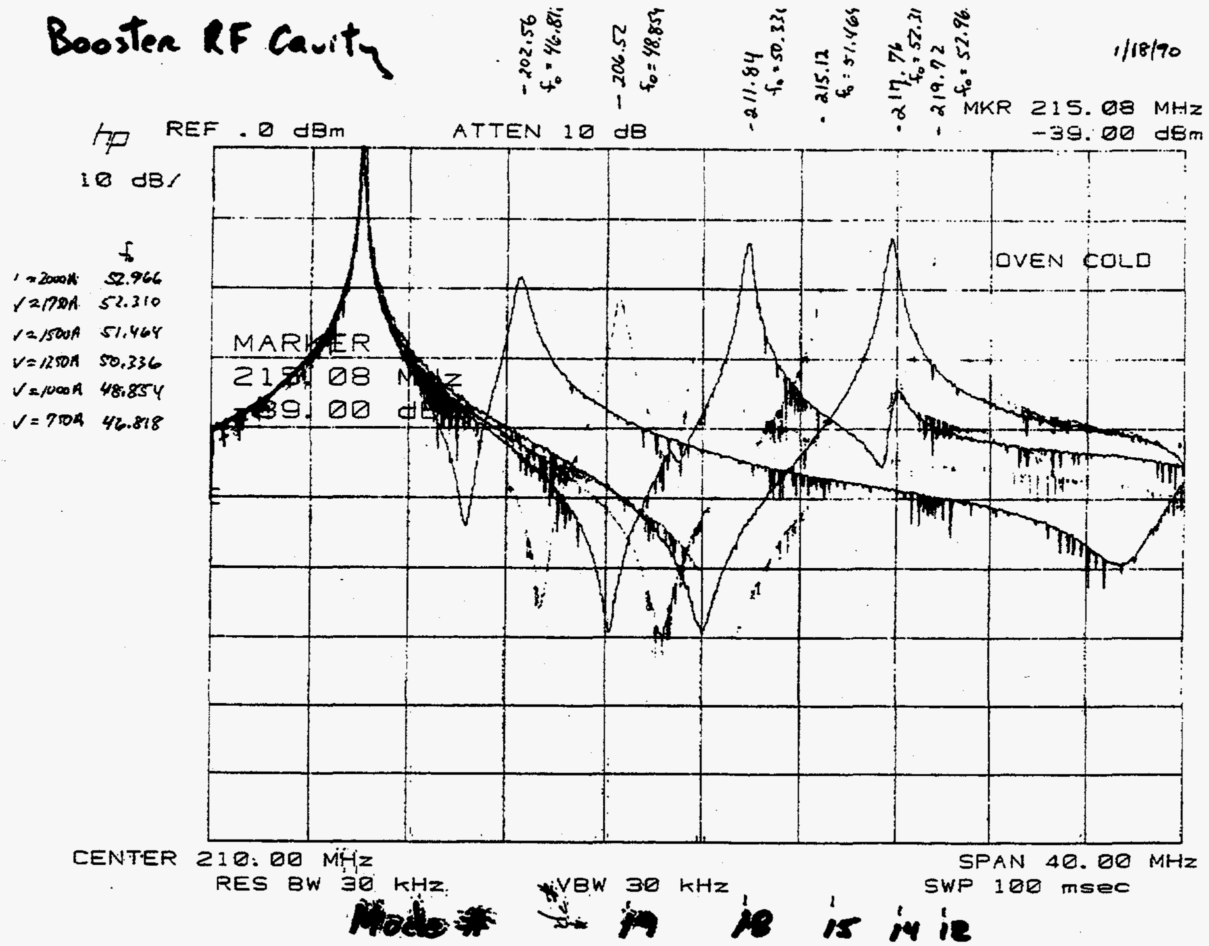

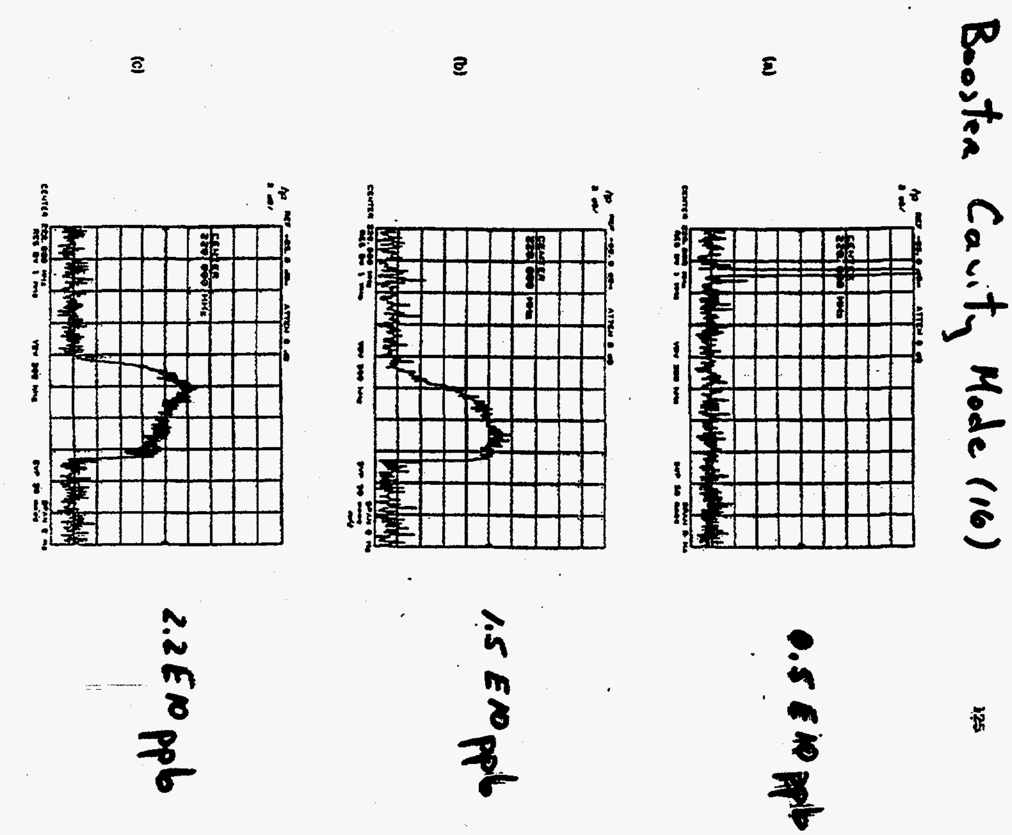

Figure 5.11 Excitation of RF Cavity Mode 16 (220.8 MHz). Shown are three beam intensities: (a) 0.52e10, (b) 1.5e10, and (c) 2.2e10 protons per bunch.

125

Booster Cavity Mode (36)

(a)
(b)
(c)

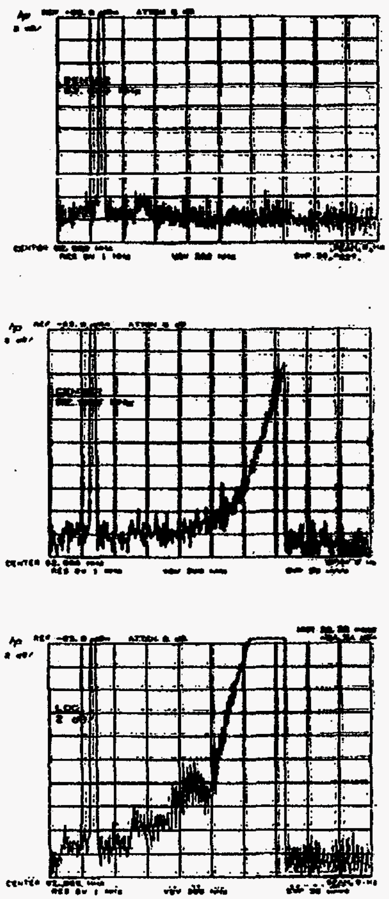

Figure 5.9 Excitation of RF Cavity Mode f2 (82.0 MHz). Shown are three beam intensities: (a) 0.52e10, (b) 1.5e10, and (c) 2.2e10 protons per bunch.

Booster

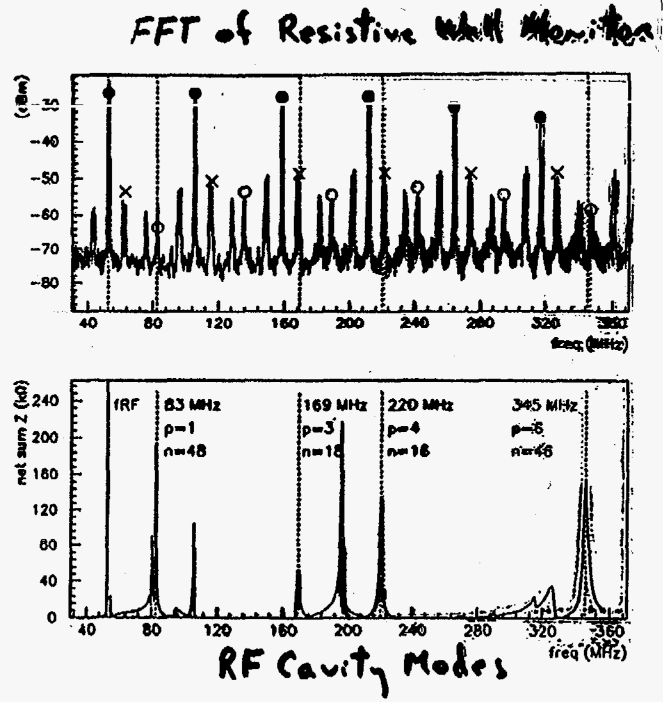

Figure 5.8 Correspondence of RF Cavity HOM Impedance and Coupled-Bunch Mode Spectrum Before HOM Dampers. The RF harmonics are marked with a filled "O", mode 16 with an "X", and mode 48 with an open "O". (R12)

Booster RF Cavity

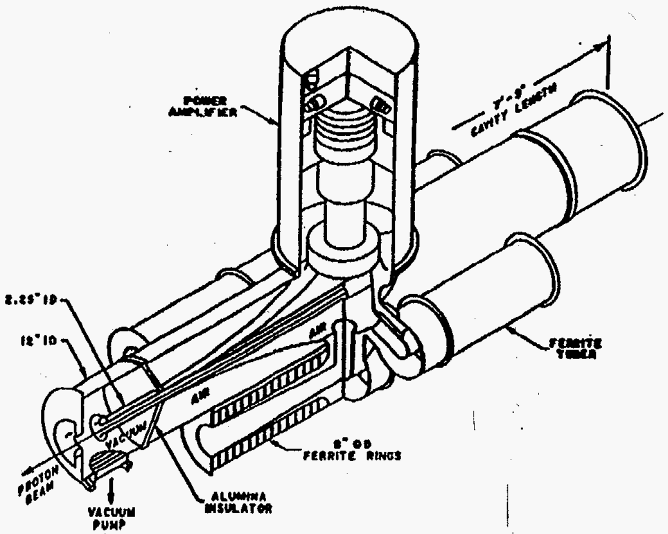

Figure 2.6 Cut-Away Drawing of RF Cavity. (Ref. 5)

Booster Cavity

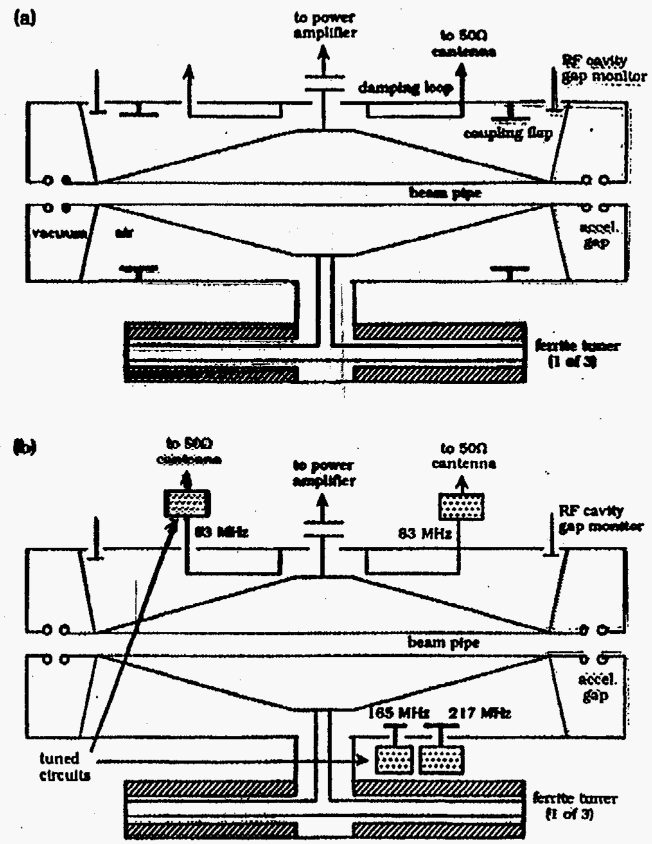

Figure 5.12 RF Cavity Showing Installation of HOM Dampers. Depicted are the (a) nominal and (b) modified cavities.

Booster

(a)

(b)

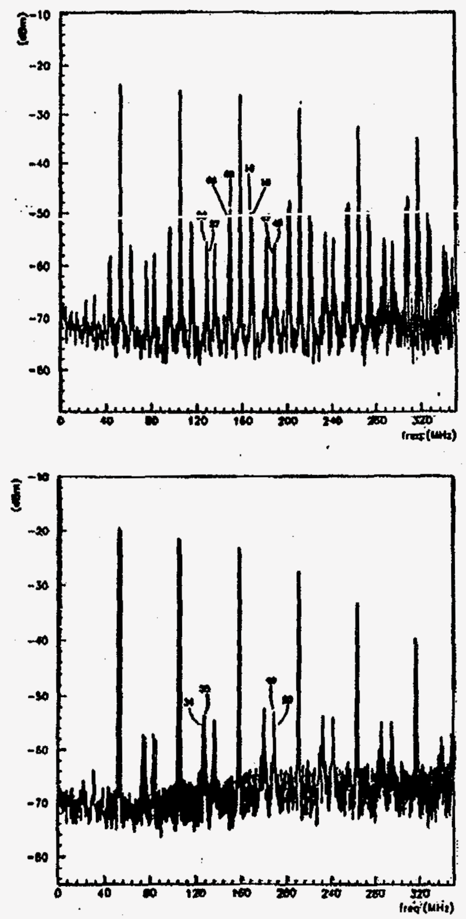

Figure 5.7 Frequency Spectra Showing the Coupled-Bunch Mode Signal Before and After RF Cavity HOM Damping. In (a), the beam intensity is 1.3e12 protons per pulse (HOM dampers out) and in (b), it is 1.9e12 ppp (HOM dampers in). In each case, 16 RF stations are on and the data correspond to 35 msec in the cycle. Mode 16 has been completely suppressed and mode 48 attenuated (recall, the intensity is greater in (b)).

Booster - with passive dampers

FFT of Resistive Wall Monitor

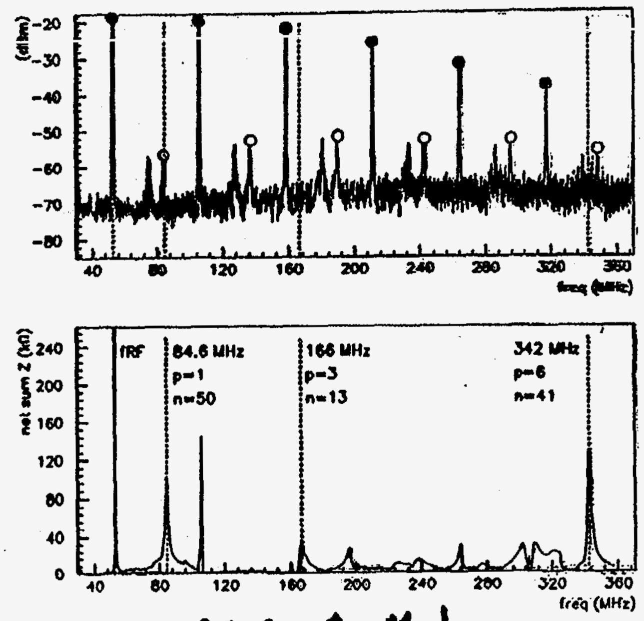

RF Cavity Modes

Figure 5.17 Correspondence of RF Cavity HOM Impedance and Coupled-Bunch Mode Spectrum After HOM Dampers. The RF harmonics are marked with a filled "O" and mode 50 with an open "O". (R36)

Booster

K. Harkay

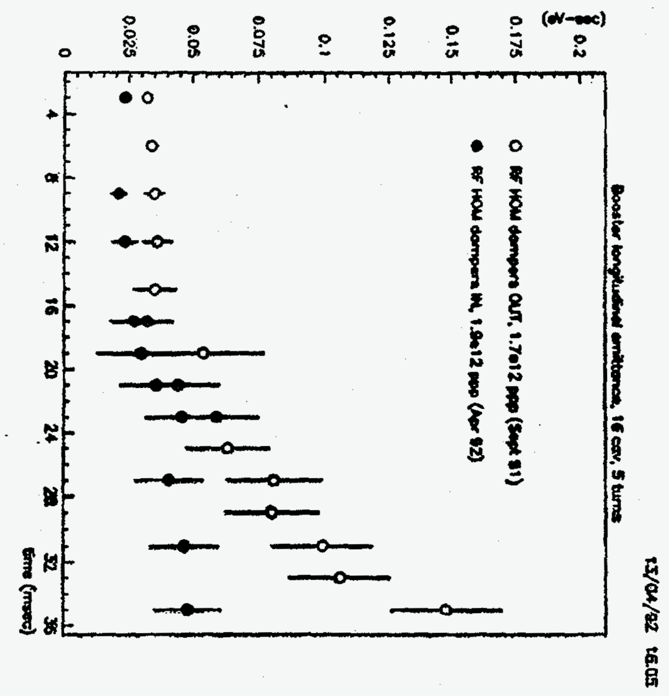

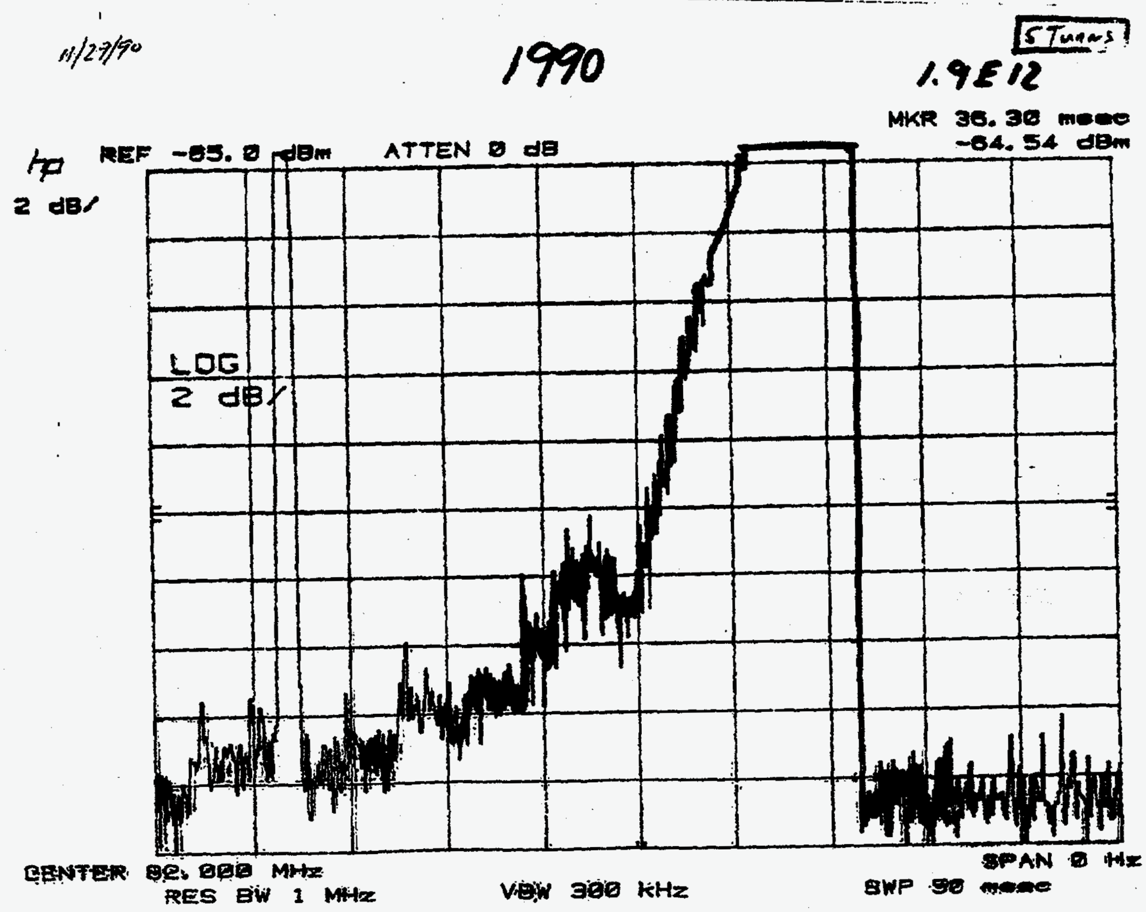

Damping of Booster Mode 36 with an Active Damper

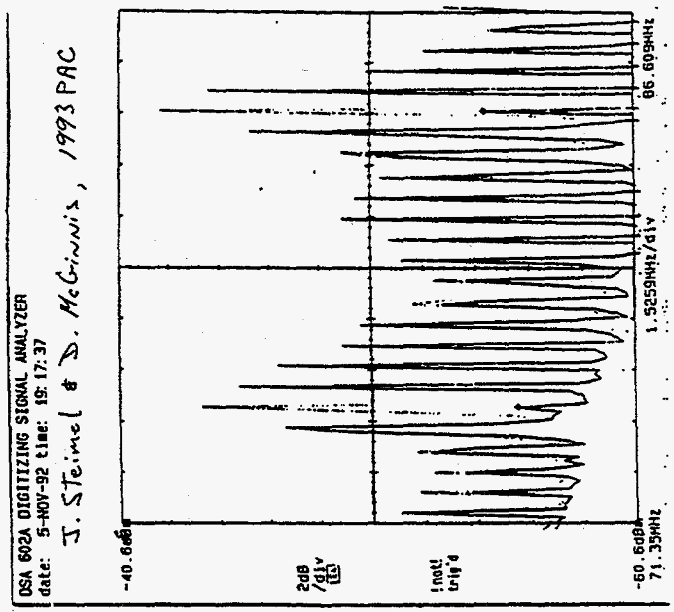

For More Information on Active Dampers:

http://adwww.fnal.gov/proton/other/index.html

2.3 E12 1993 2.3E12

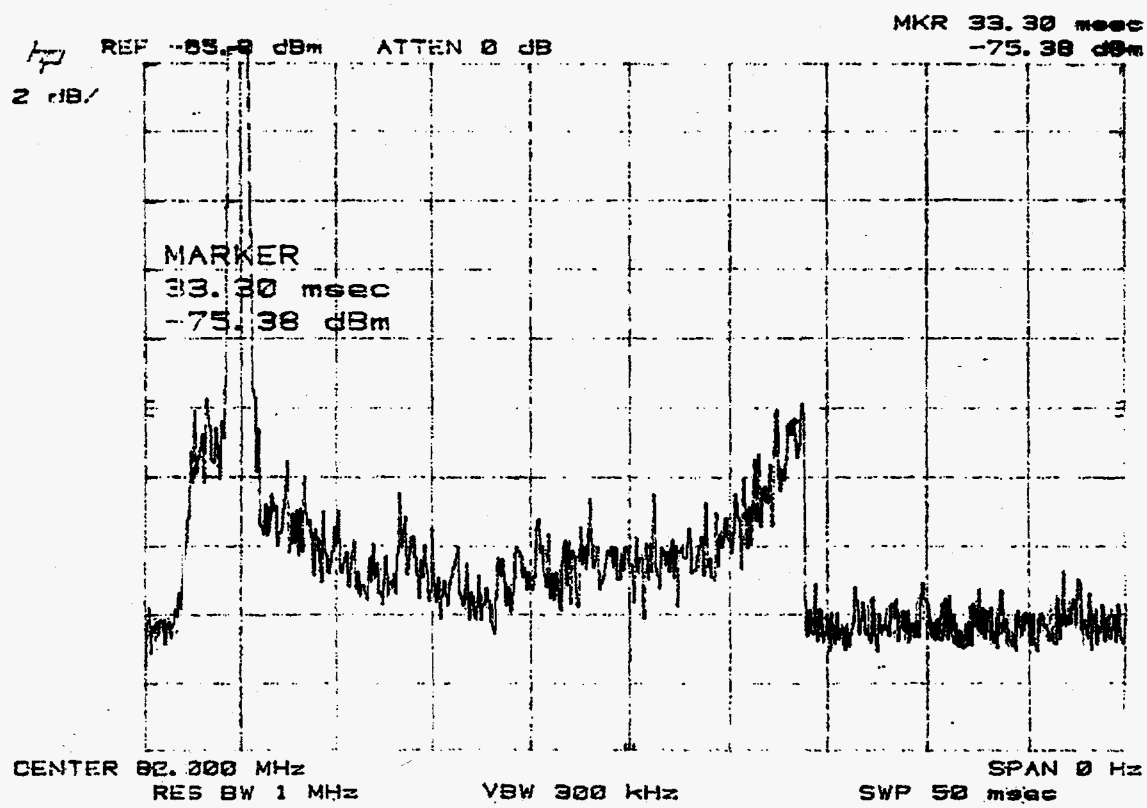

Main Ring Cavity

11/24/92

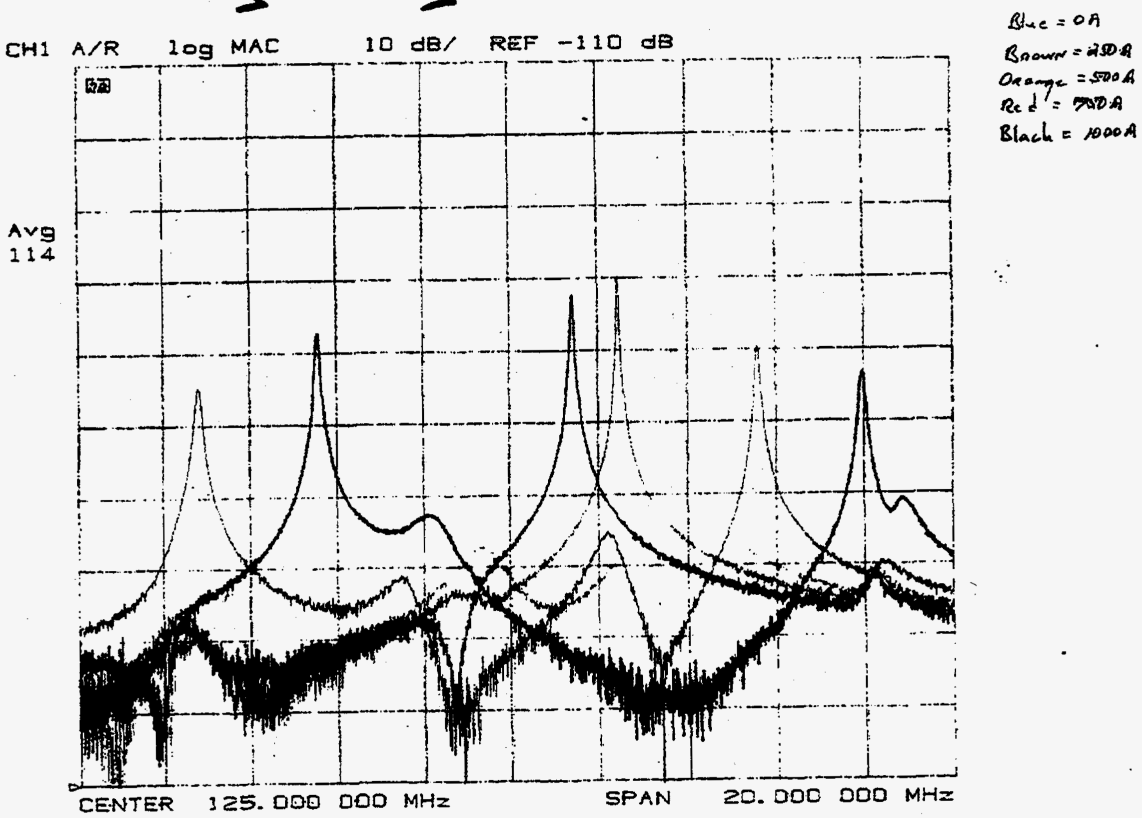

Main Ring Cavity

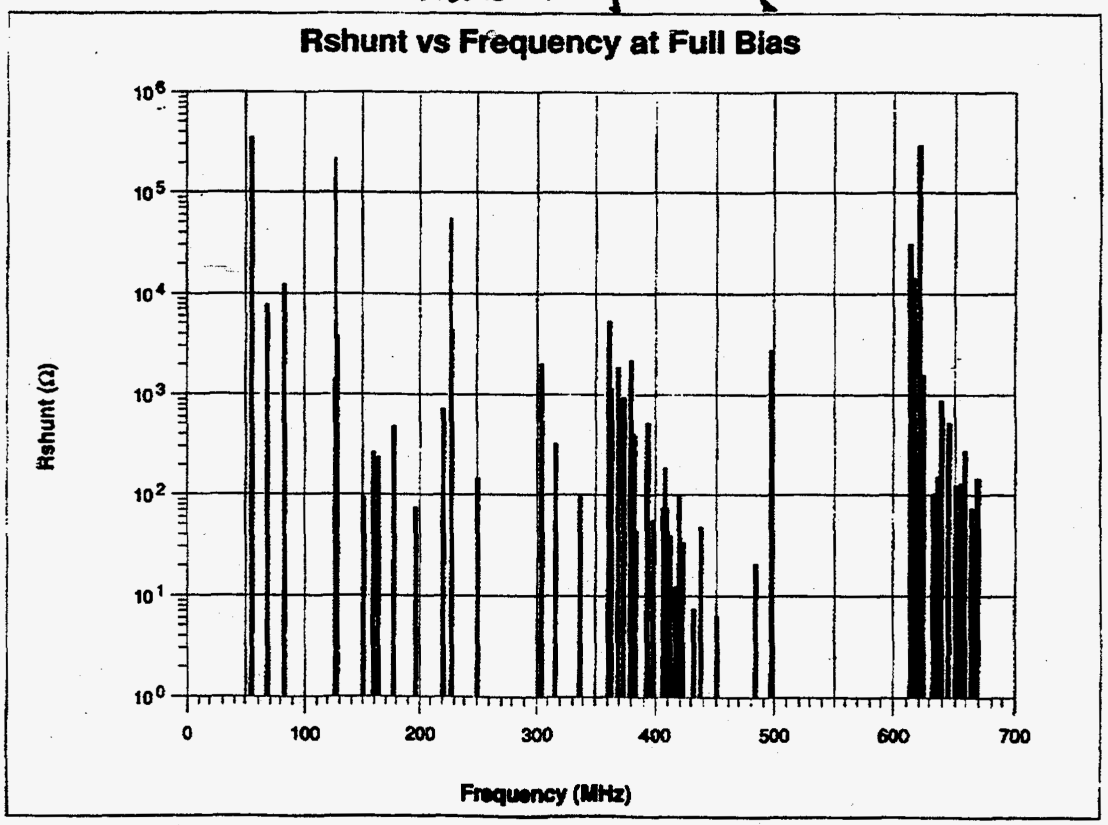

Acquired: 11 JUL 1996 20:51:31.70 Printed: 11 JUL 1996 20:52:29

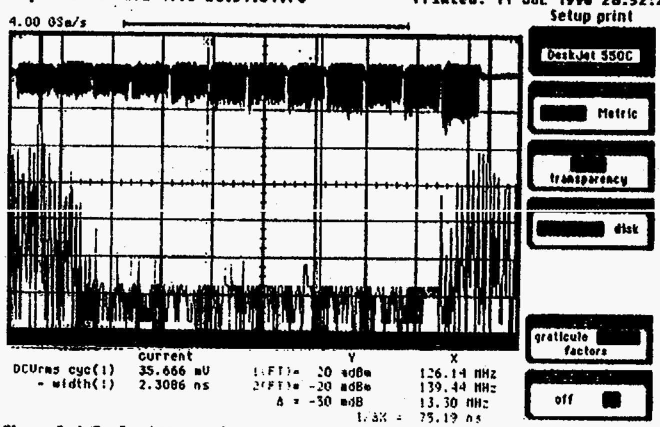

Channel 1 Scale 100 mV/div Offset -300.0 mV Input dc 50 Ohms
Time base Scale 2.10 us/div Position 31.200000 us Reference center
Trigger Mode edge Source trigger 4 Hysteresis normal Holdoff 60 ns
Level 998 mV Slope Pos
Measurement

	current
DCVrms cyc(1)	35.666 mV
- width(1)	2.3086 ns

Marker

	Y	X
1(FT)=	20 mdBm	126.14 MHz
2(FT)=	-20 mdBm	139.44 MHz
Delta =	-50 mdB	13.30 MHz
	1/DX =	75.19 ns

FFT fft magnitude channel 1
Scale 3.00 dBm/div Offset -52.8600 dBm
Scale 6.00 MHz/div Position 132.76000 MHz

.75E13 @ 2.84 sec on 21

Acquired: 11 JUL 1996 15:02:41.30 Printed: 11 JUL 1996 15:03:55

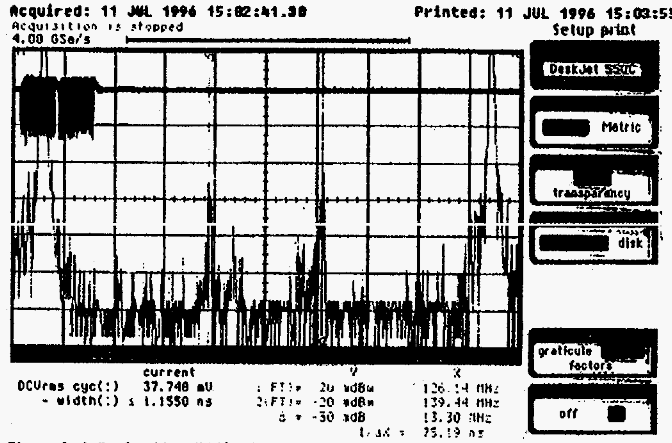

Channel 1 Scale 100 mV/div Offset -300.0 mV Input dc 50 Ohms
Time base Scale 2.10 us/div Position 31.200000 us Reference center
Trigger Mode edge Source trigger 4 Hysteresis normal Holdoff 60 ns
Level 998 mV Slope Pos
Measurement

	current
DCVrms cyc(1)	37.748 mV
- width(1)	<= 1.1550 ns

Marker

	Y	X
1(FT)=	20 mdBm	126.14 MHz
2(FT)=	-20 mdBm	139.44 MHz
Delta =	-50 mdB	13.30 MHz
	1/DX =	75.19 ns

FFT fft magnitude channel 1
Scale 3.00 dBm/div Offset -52.8600 dBm
Scale 6.00 MHz/div Position 132.76000 MHz

2.84 sec on 21
Start of flattop

Longitudinal Coupled Bunch Instabilities

Booster h=84

mode #16 (3rd & 5th harmonic of RF cavities)
passive dampers
mode #36 (fixed frequency drift tube mode)
passive and active dampers

Main Ring h=1113

mode #457 (3rd harmonic of RF cavity)
passive dampers
mode #327 (5th harmonic of RF cavity)
passive damper

Tevatron h=1113

mode #40 (3rd harmonic of RF cavity/
transmission line)
passive damper

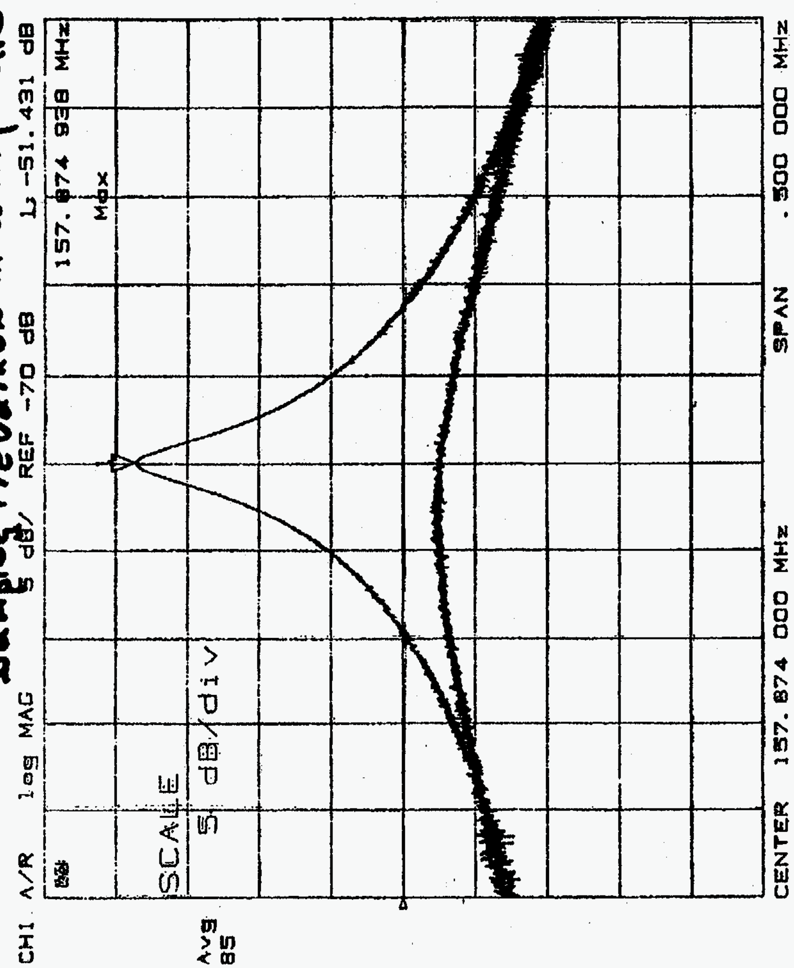

Damping Tevatron RF Cavity Mode

Coalescing Protons in the Main Ring (single batch)

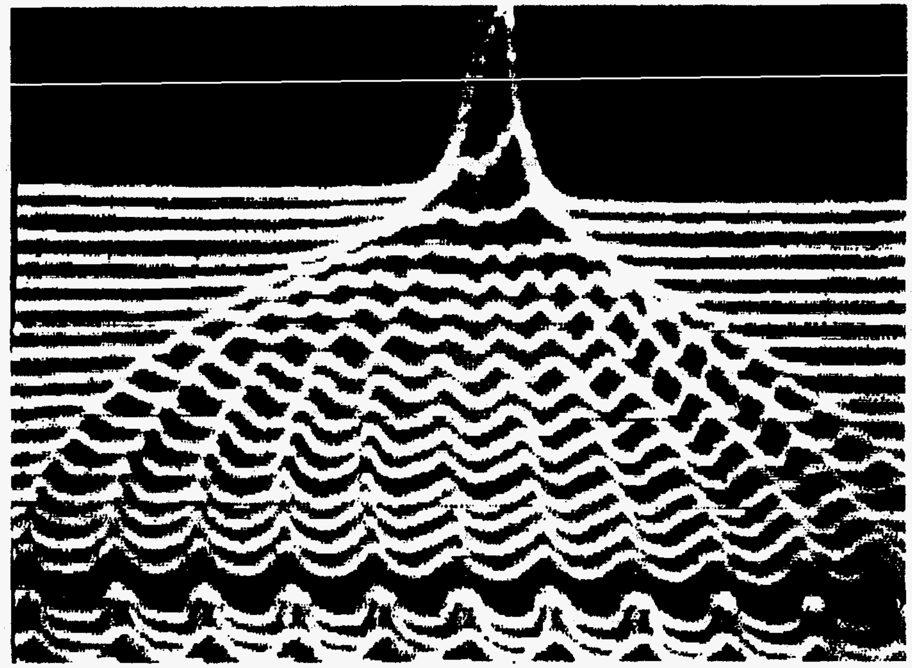

20 ns/div

4 ms/trace

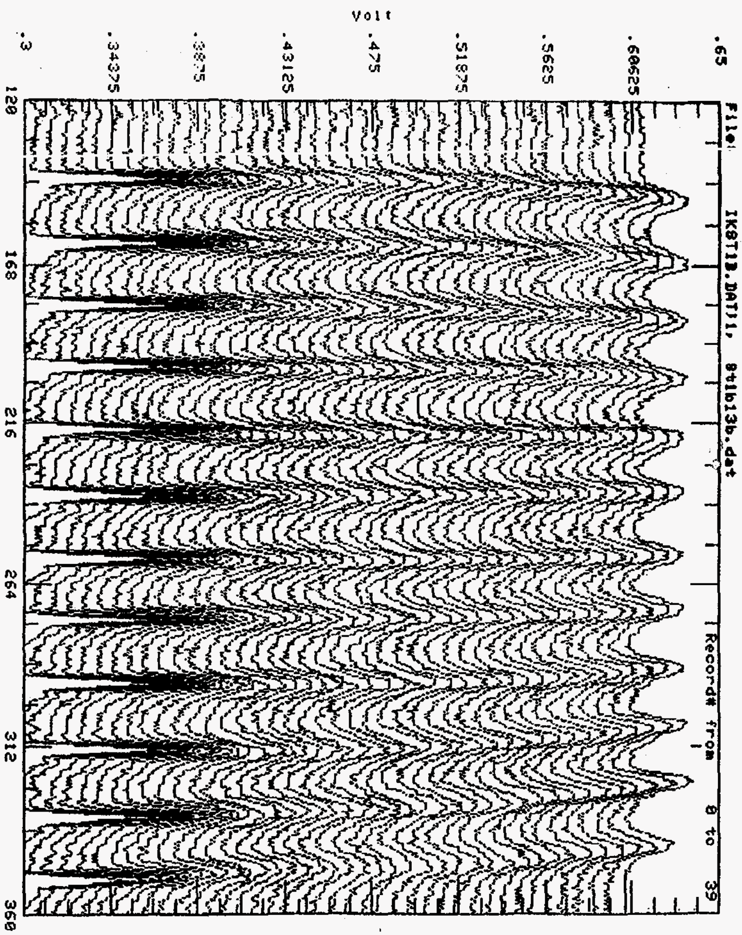

Console Location 10, Mountain Range 9-FEB-1996 13:06 5.21

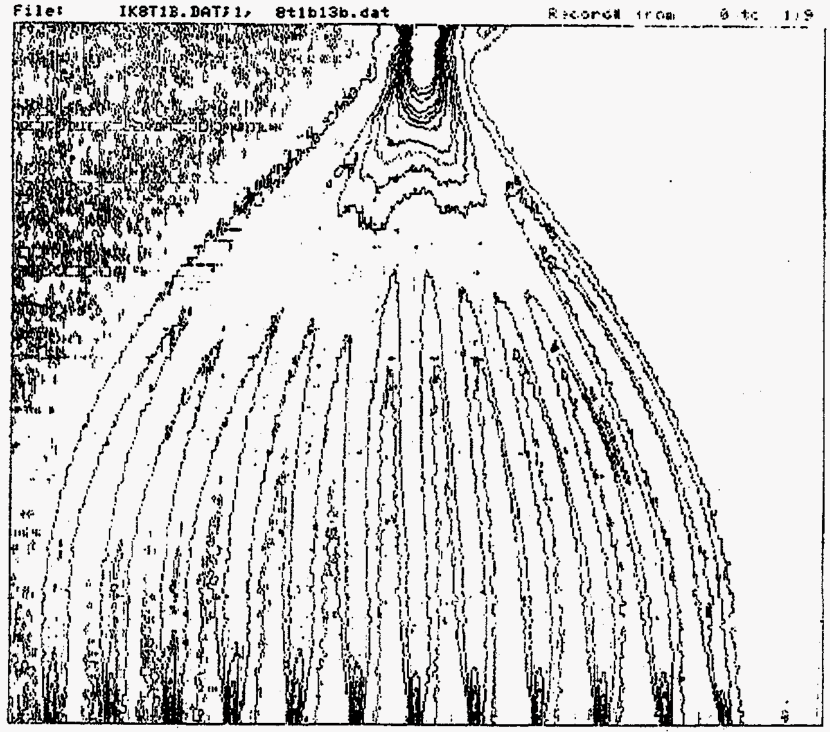

Console Location 8, Contour plot 14-MAR-1996 11:55 41.91

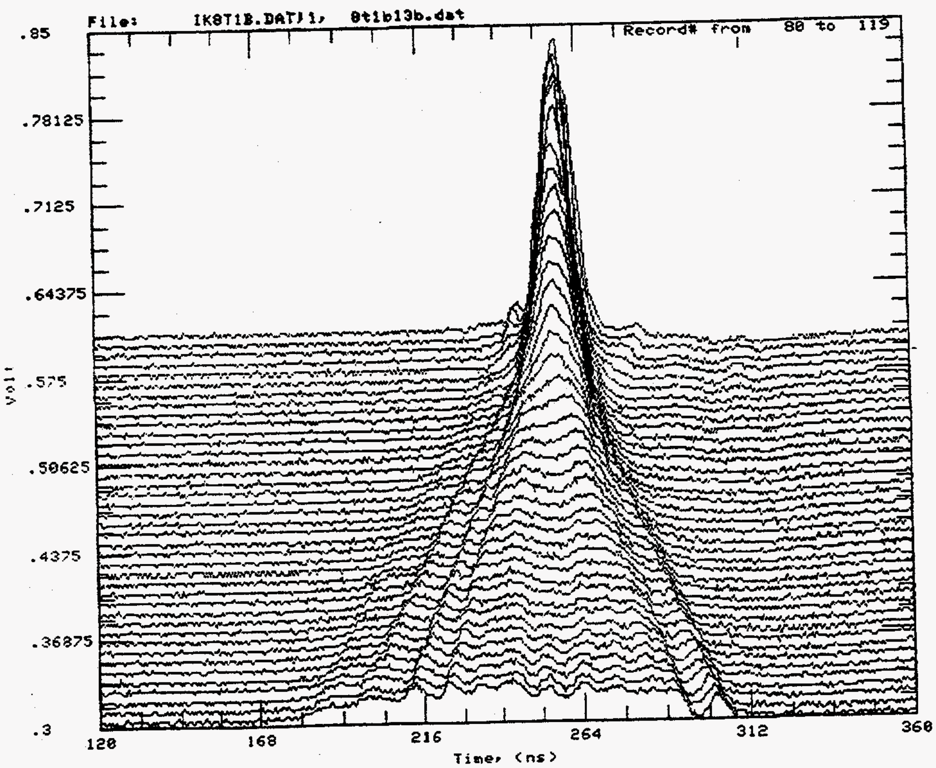

Console Location 10, Mountain Range 9-FEB-1996 13:10 5.45

Coalescing in Main Ring

13 BUNCHES 2.0 E10 ppb

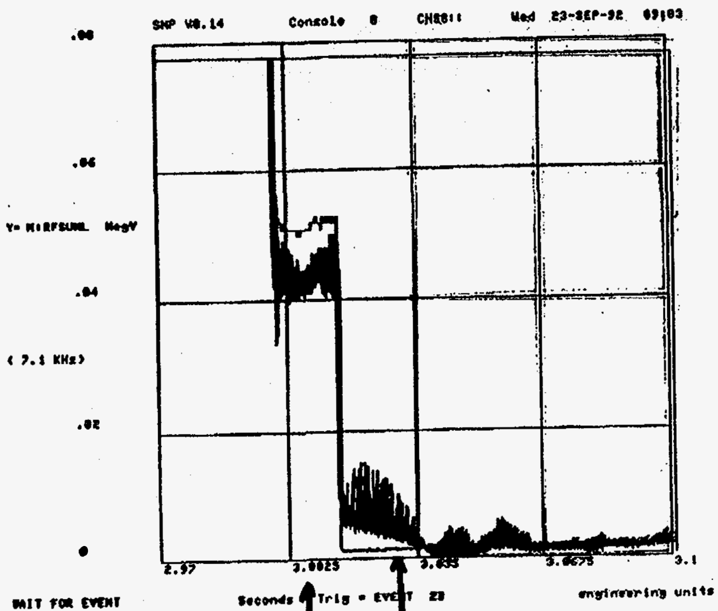

Rotation 53 + 106 MHz

Rotation 2.5 + 5 MHz

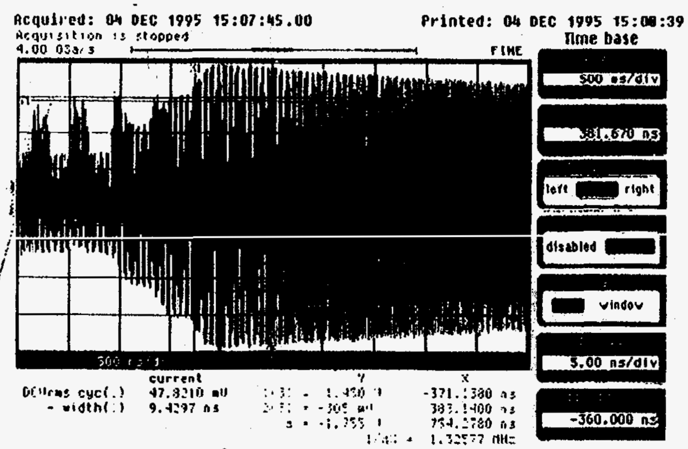

Channel 1 Scale 20 mV/div Offset 0.0 V Input ac 50 Ohms
Channel 3 Scale 500 mV/div Offset 0.0 V Input dc 50 Ohms
Time base Scale 500 ns/div Position 381.670 ns Reference center
Window scale 5.00 ns/div Window position -360.000 ns
Trigger Mode edge Source trigger 2 Hysteresis normal Holdoff 60 ns
Level 170 mV Slope Pos
Measurement

	current
DCVrms cyc(1)	47.8210 mV
- width(1)	9.4297 ns

Marker

	Y	X
1(3) =	1.450 V	-371.1380 ns
2(3) =	-305 mV	383.1400 ns
Delta =	-1.755 V	754.2780 ns
1/DX =		1.32577 MHz

~~53 MHz off~~

106 MHz off

53 + 106 MHz fanback

Main Ring

52

MultiBatch Coalescing (Adiabatic)

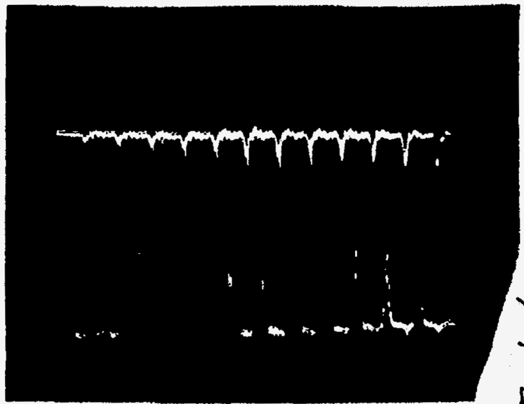

8X10" 12batches 1.2MV at 150 GeV

With shorts

Cavity Shorts IN

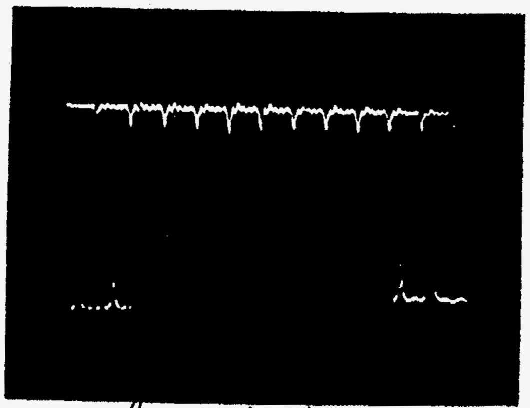

5X10" No shorts

Cavity Shorts Out

Multi-batch Coalescing

3.299sec on 2B 11/5/95

Feedback ON

RF Cavity phase

Feedback off

CPA mons to F3

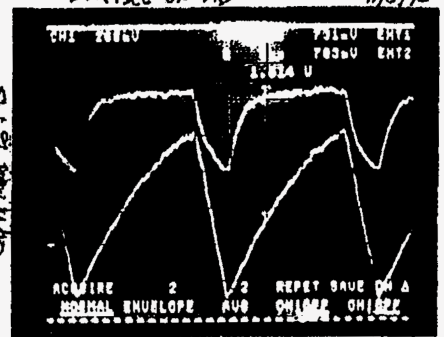

STA 4 with & without (-20dB) Feedback

5μs/div

Multi-Batch Coalescing

Feedforward Off

RF Cavity phase 9°/div

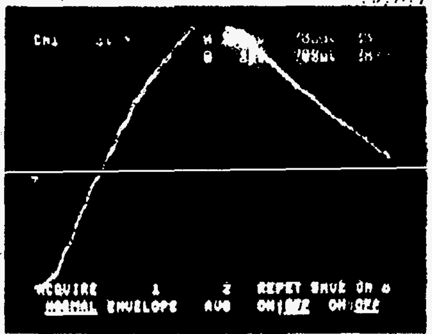

Comp off 12 batches 1E12

1µs/div

Feedforward On

RF Cavity phase 9°/div

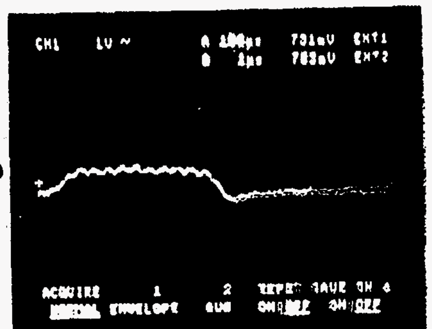

Comp on 12 batches 1E12

1µs/div

Multi-Batch

3 BT NO BLC ~ 6.2E12

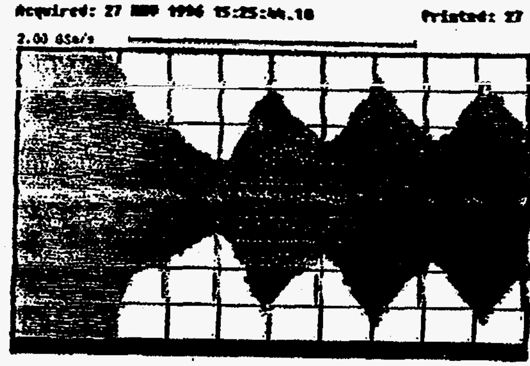

3 B Turn BLC ON (+3db) (-0.5 nsec)

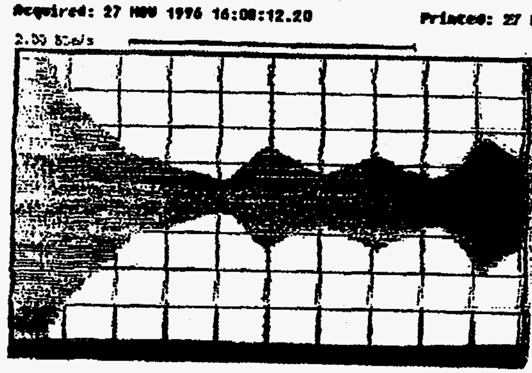

With Feedforward Compensation

COALESCING 4 BATCHES 0.85E12p NO BLC

MOUNTAIN RANGE PLOT OF THE FOURTH BATCH

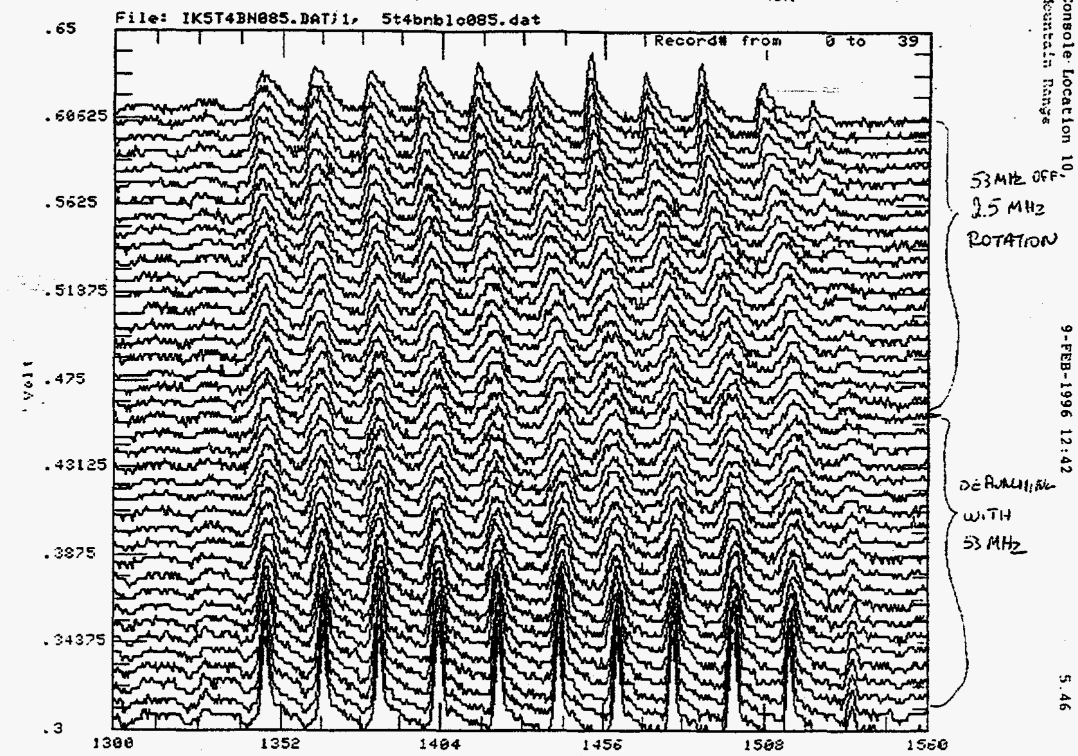

TRACES EVERY 32 TURNS (0.67 msec)

COALESCING 4 BATCHES 0.85E12 BLC ON

MOUNTAIN RANGE PICTURE OF THE FOURTH BATCH

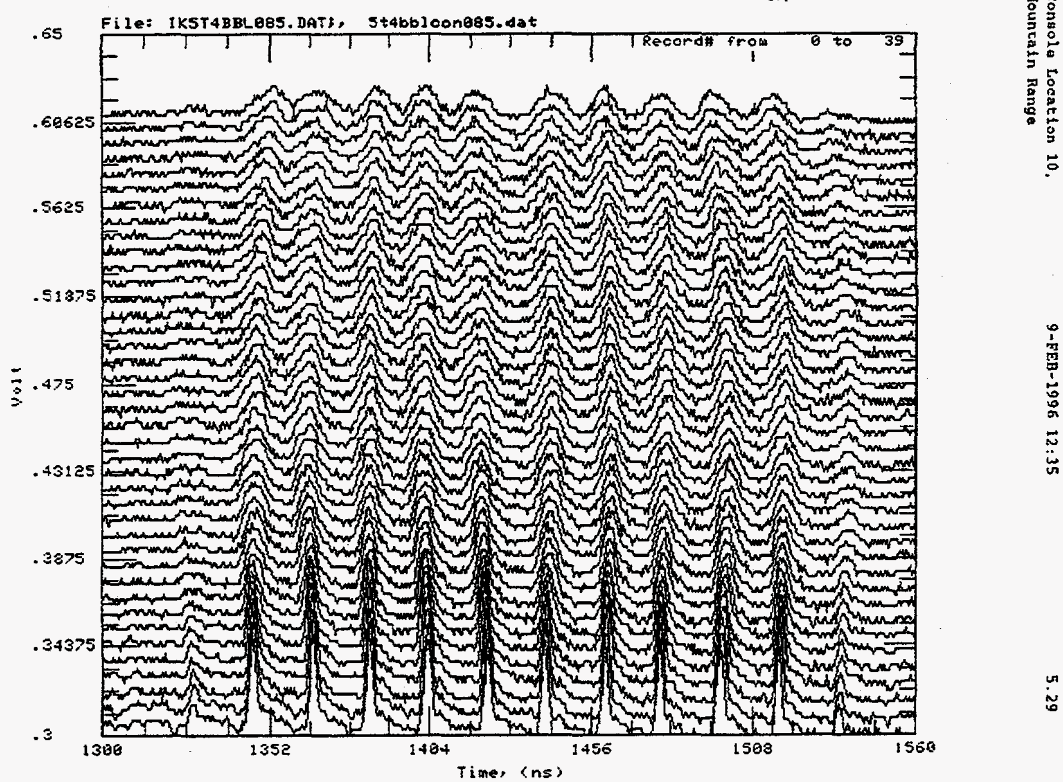

TRACES EVERY 32 TURNS (0.67 msec)

COALESCING 4 BATCHES 0.85E12p NO BLC

MOUNTAIN RANGE PLOT OF THE FOURTH BATCH RECAPTURE TIME

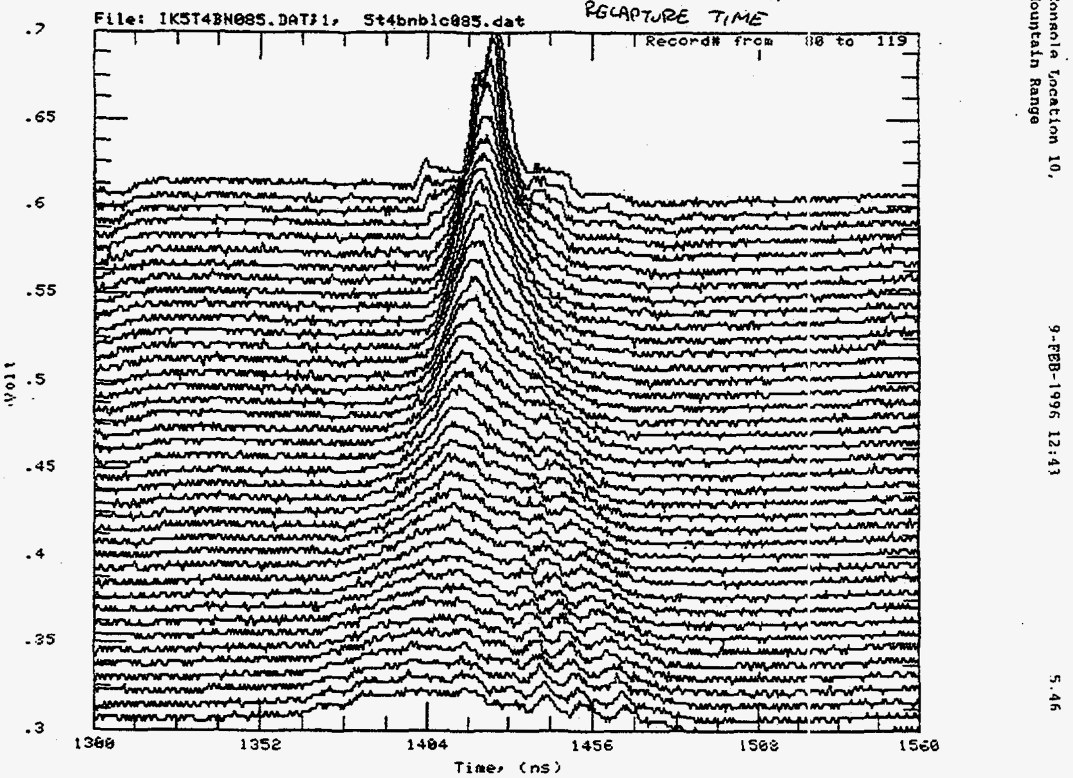

TRACES EVERY 32 TURNS (0.67 msec)

COALESCING 4 BATCHES 0.85E12p BLC ON

MOUNTAIN RANGE PLOT OF THE FOURTH BATCH RECAPTURE TIME

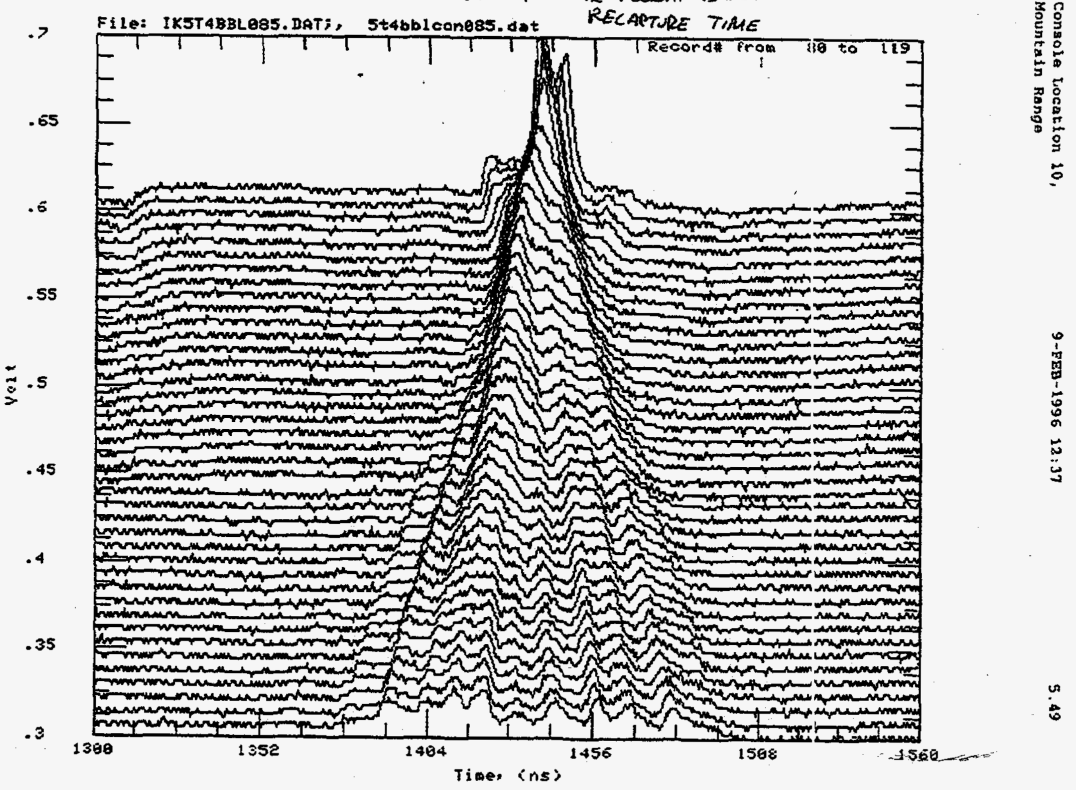

Recycler Ring

An 8 GeV permanent magnet Pbar storage ring

Located above the Main Injector Ring

Dual Purpose: Store and Cool Pbars directly from the Accumulator
Store and Cool Pbars recycled from the Tevatron Collider

Uses Wideband RF system to generate Barrier Buckets for injecting and extracting Pbars

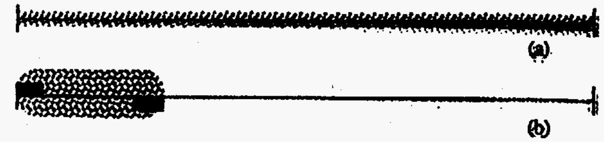

Figure 2.1.23: Full ring phase space sketches of the initial steps of antiproton recycling in the Recycler. In the top drawing (a) the cooled beam starts off basically unbunched (unless an azimuthal gap is necessary for beam clearing reasons). In the bottom drawing (b) a rectangular barrier voltage system adiabatically squeezes the beam into a small fraction of the circumference.

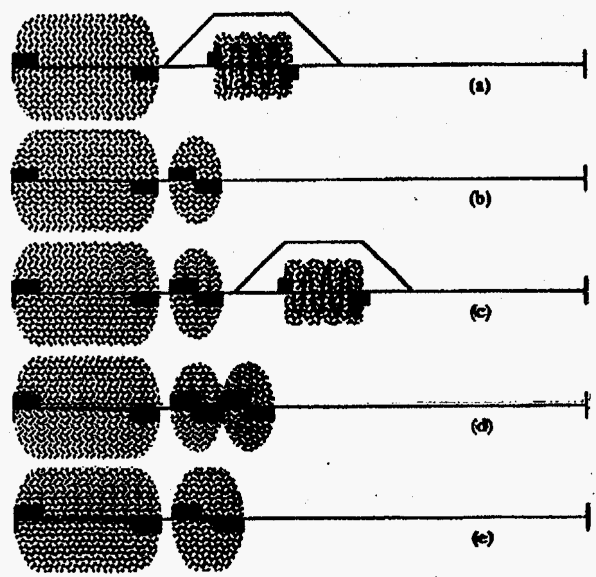

Figure 2.1.25: Recycling of antiproton batches from the Main Injector. The leftmost charge distribution is always the cooled antiprotons. The shown Recycler injection kicker waveform has a rise-time and fall-time of 1 μsec. The recycling process never requires more than 3 pairs of barrier voltage pulses.

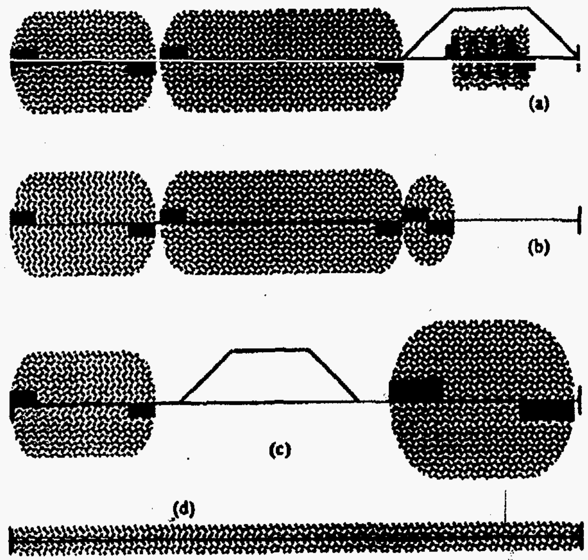

Figure 2.1.30: End of the process of antiproton recycling from the Main Injector. The leftmost charge distribution is always the cooled antiprotons. In (d) the cooled antiprotons have been injected into the Tevatron Collider and the recycled antiprotons have been debunched.

Scope

4 ferrite loaded, 50 ohm RF cavities with a peak accelerating voltage of 2 kV

4 wideband amplifiers, 2500 watts CW, 10 kHz to 100 MHz

Low level RF system to generate barrier bucket pulses

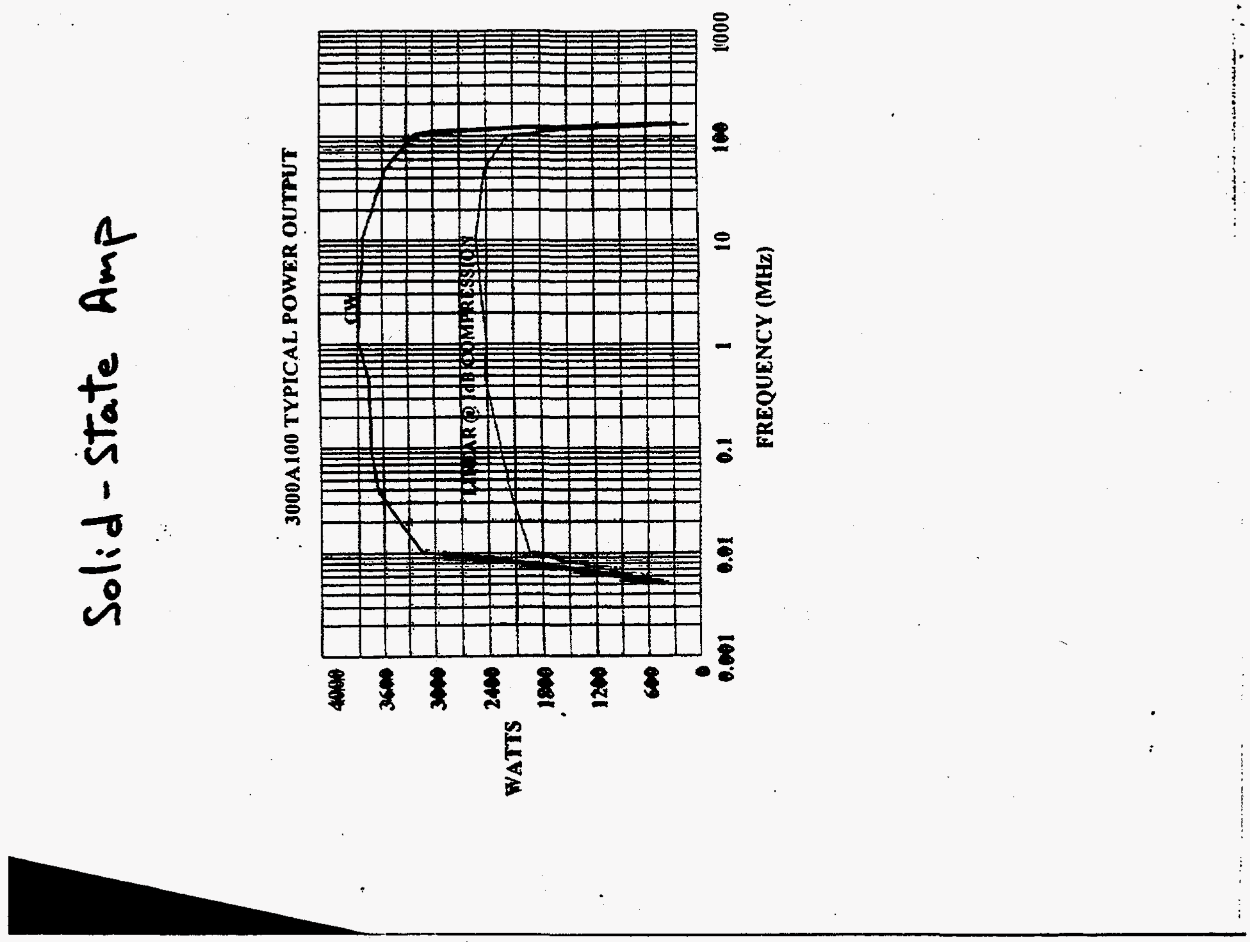
Solid-State Amp
3000A100 TYPICAL POWER OUTPUT
CW
LINEAR @ 1dB COMPRESSION
WATTS
FREQUENCY (MHz)
0.001
0.01
0.1
1
10
100
1000
4000
3600
3000
2400
1800
1200
600
0

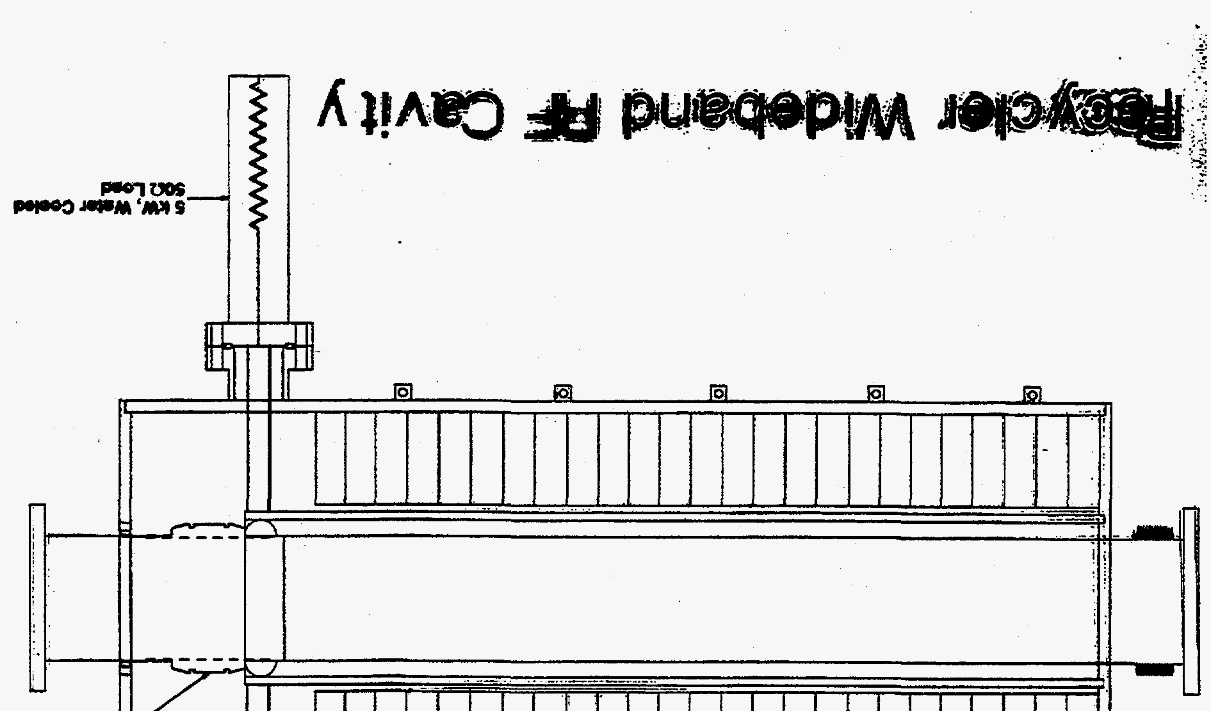
Recycler Wideband RF Cavity
5 kW, Water Cooled
50Ω Load
Ceramic
MnZn Ferrite 12" OD x 6" ID X 1"

Recycler Test

1/15/97

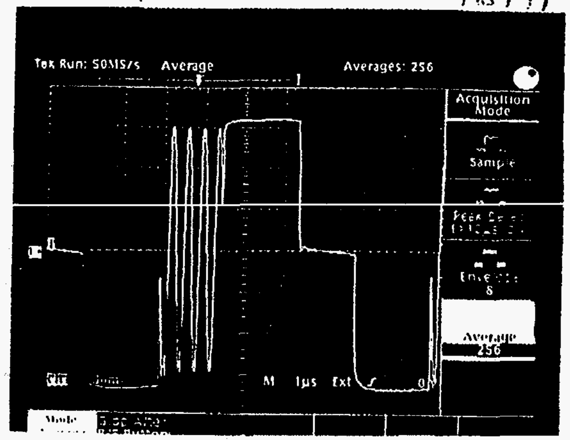

50V/div

1µs/div

1/15/97

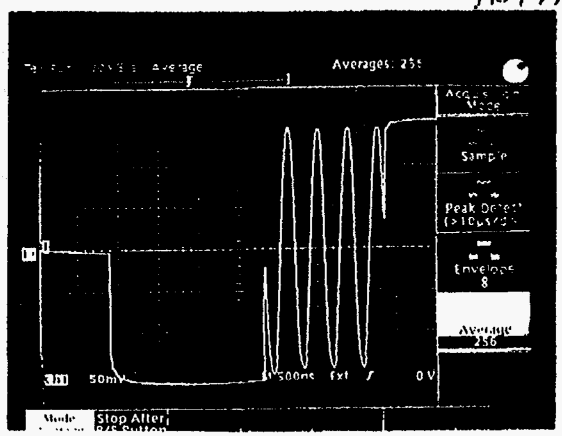

50V/div

Accelerator Complex of Japan Hadron Facility

Chihiro Ohmori
KEK-Tanashi

Accelerator Complex

- **200-MeV linac   high brightness**

accelerated particle	H^- ion
peak beam current	>30(50) mA (25Hz, 400μs)
structures	RFQ + DTL + ACS

- **3-GeV booster   rapid cycling**

intensity	5×10^{13} ppp
repetition rate	25Hz
beam power	0.6 MW
RF frequency	1.99-3.43MHz
RF voltage	~~300~~kV 425
circumference	339.4m (KEK-PS tunnel)

- **50-GeV main ring transition free(negative α)**

intensity	2×10^{14} ppp
acceleration cycle	0.3Hz
RF frequency	3.43-3.51MHz
RF voltage	270kV
momentum compaction	$\sim -10^{-3}$
circumference	1442m (north site of KEK)

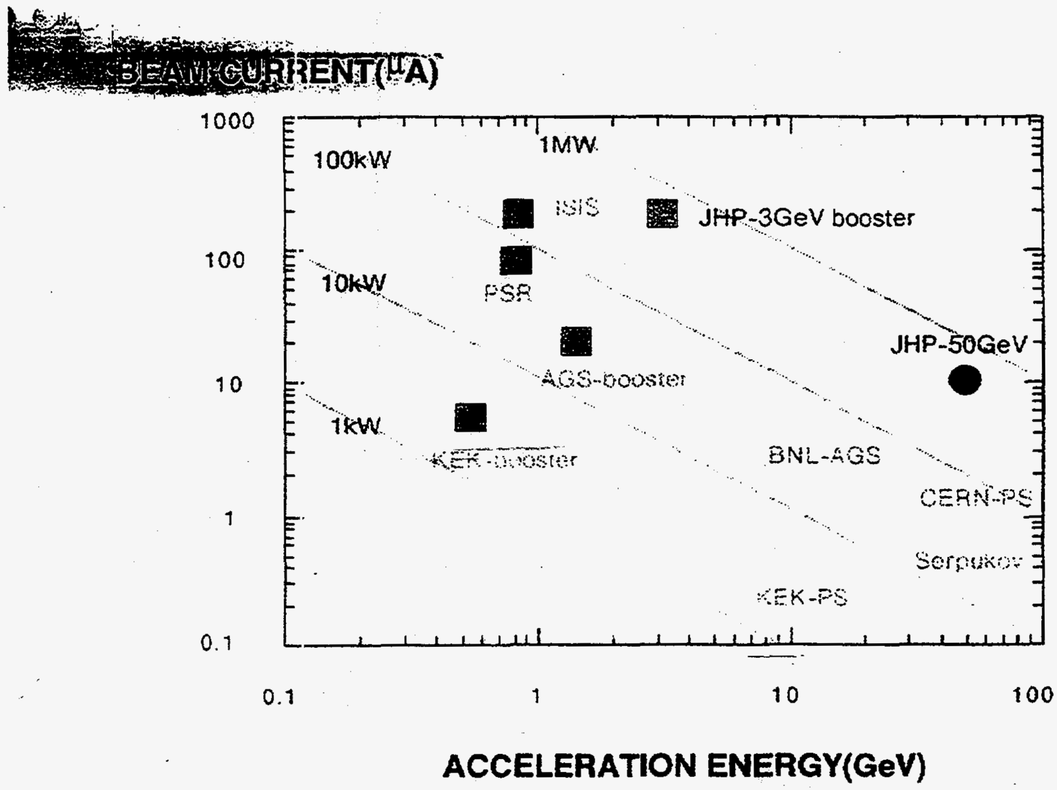

Beam intensities of high-intensity proton synchrotrons.

- 1 -

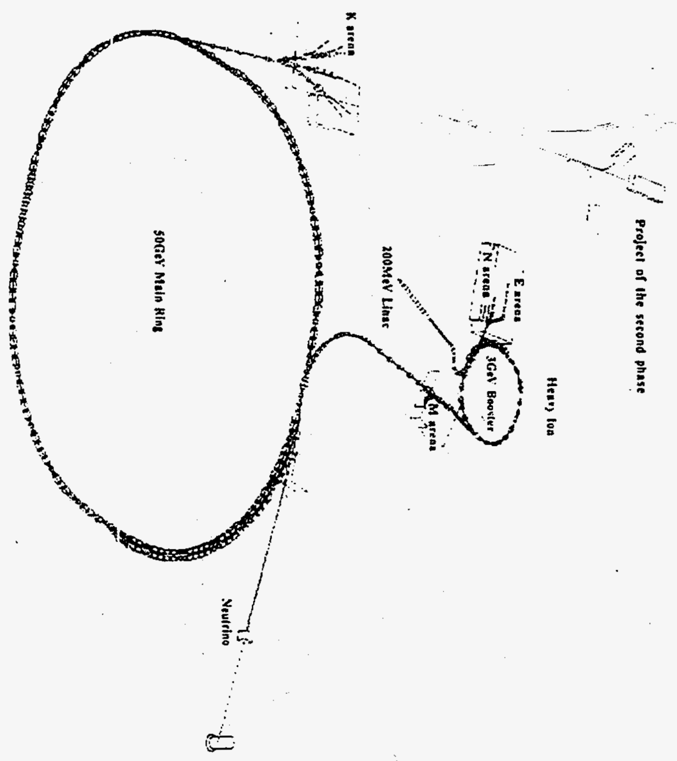

PROPOSED LAYOUT OF THE ACCELERATORS AND EXPERIMENTAL AREAS OF JHP

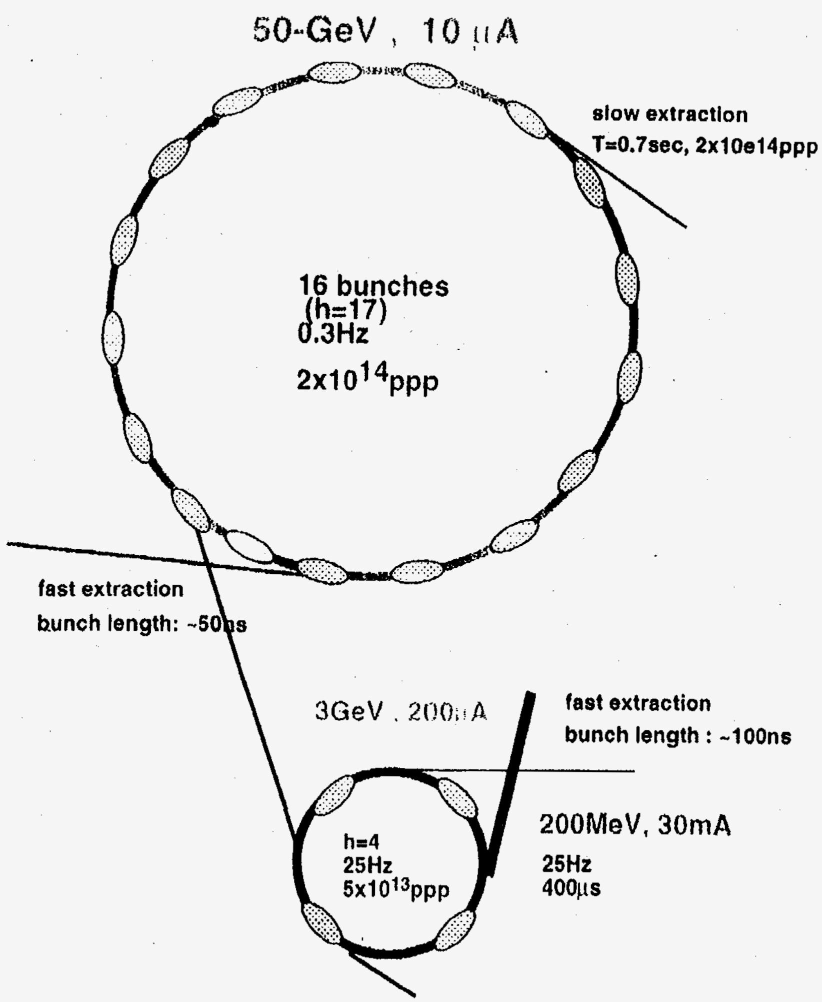

MAIN RING CYCLE

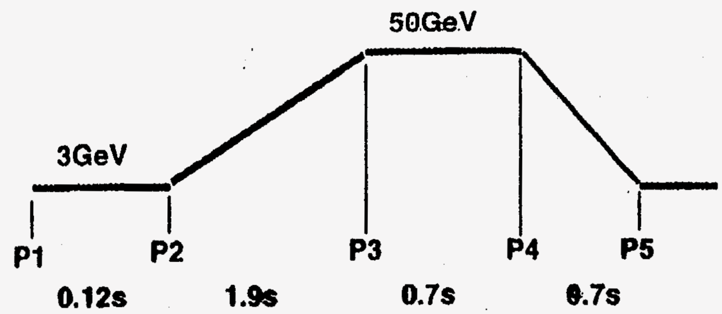

MAIN RING CYCLE:3.42 sec

P1-P2:0.12

P2-P3:1.9

P3-P4:0.7

P4-P5:0.7

h=17, # of bunches:16

BEAM INTENSITY:2x10^{14} ppp

flat top duty dfactor:0.21

Design Issues

50-GeV Main Ring

*Transition-free ring
  Imaginary γ_t lattice: α ~-10^{-3}
*Free from instabilities
  Low impedance ring
*Large dynamic aperture

3-GeV booster

*Tunability ($\nu_{x,y}$)
*Small emittance growth
  Space charge,Coupling(x:y:z)
*Beam scraping

Imaginary γ_t lattice

"4-6-3 lattice"

(1) Stability of linear optics

*Selection of phase advance
*Beam size
*α vs dispersion and tunes
*α vs space charge (Umstatter effects)

(2) Dynamic apertures(DA)

*Chromaticity
*Synchrotron oscillation amplitudes
*Space charge

(3) COD correction
*Dry run

4 - 6 - 3

Super periodicity — module — Cell

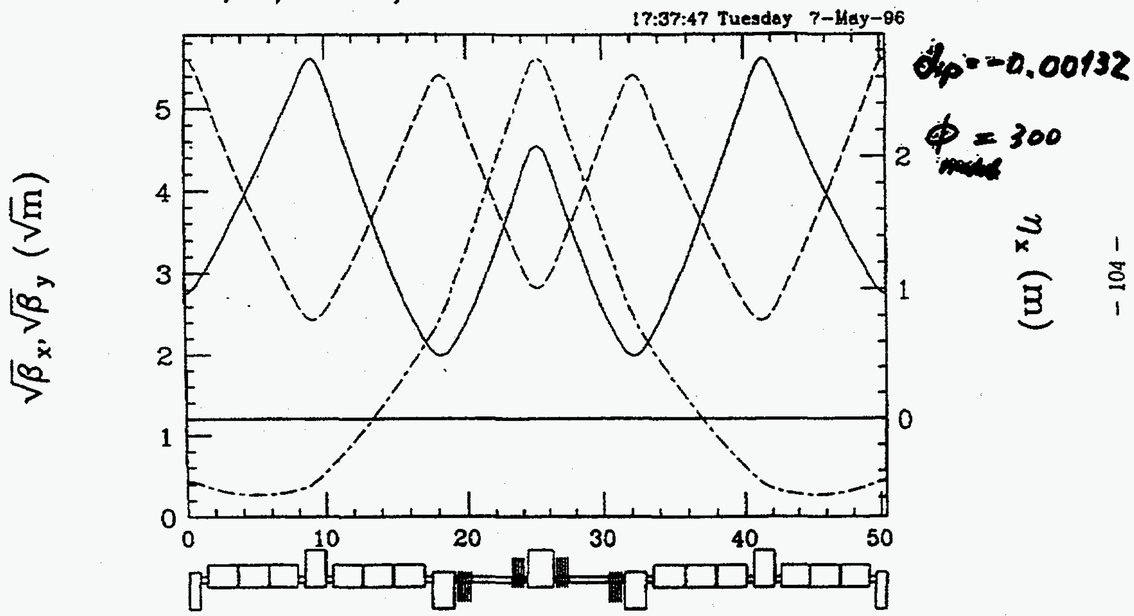

– 104 –

4 · 6 · 3 (I)

β_x : small

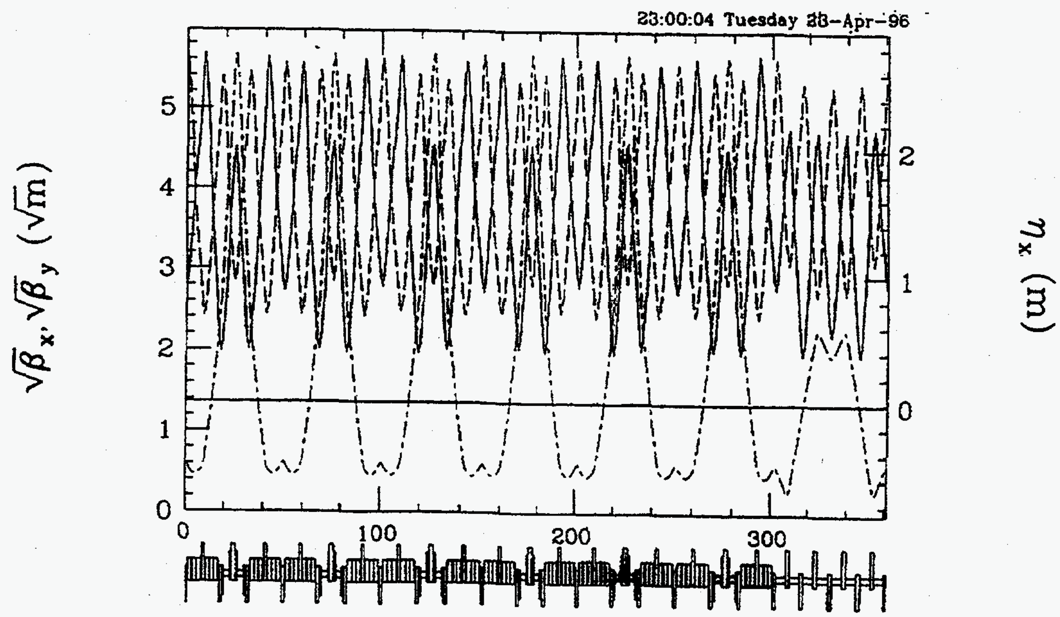

Maximum Apertures of the 50 GeV Main Ring

apertures

$$A_x = \sqrt{\beta_x \varepsilon_x} + \eta_x \left(\frac{\Delta p}{p} \right) + COD + (sagitta)$$

$$A_y = \sqrt{\beta_y \varepsilon_y} + COD$$

$\varepsilon_{x,y} = 53.9\pi mm.mrad$

$\frac{\Delta p}{p} = 0.5\%$

$COD = 5mm$

	horizontal	vertical
B magnet	47 mm (w/o sagitta)	44 mm
Q magnet (max)	53 mm	47 mm

summary of Lattice "4-6-3"

* $\alpha \sim -10^{-3}$

(1) Linear optics stability

*stable operating point O.K.

*beam size ~50mm O.K.

*tunability

$Q_{x,y}, \eta$ vs. α O.K.

*space charge O.K.

(2) Non-linear optics (Dynamic apertures)

*ξ O.K.

*$\Delta p/p$ O.K.

*space charge O.K.

*error fields need optimization

(3) Corrections COD etc. (O.K.)

*"Dry run"

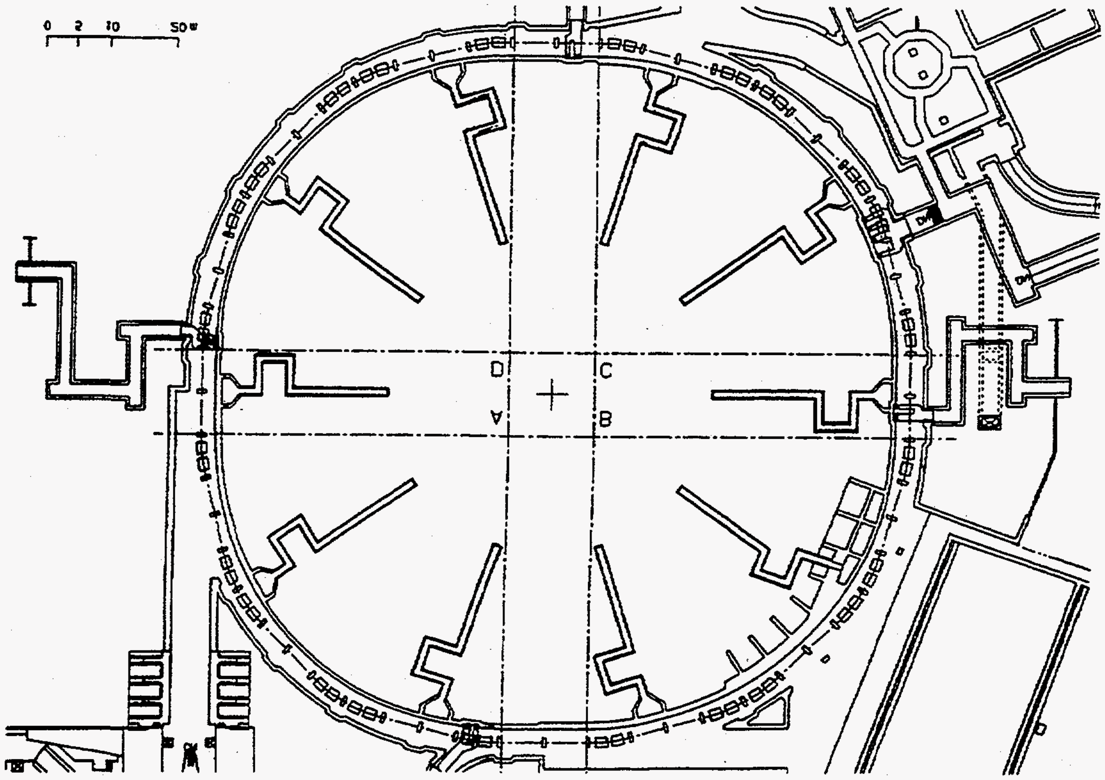

3 GeV booster lattice geometry

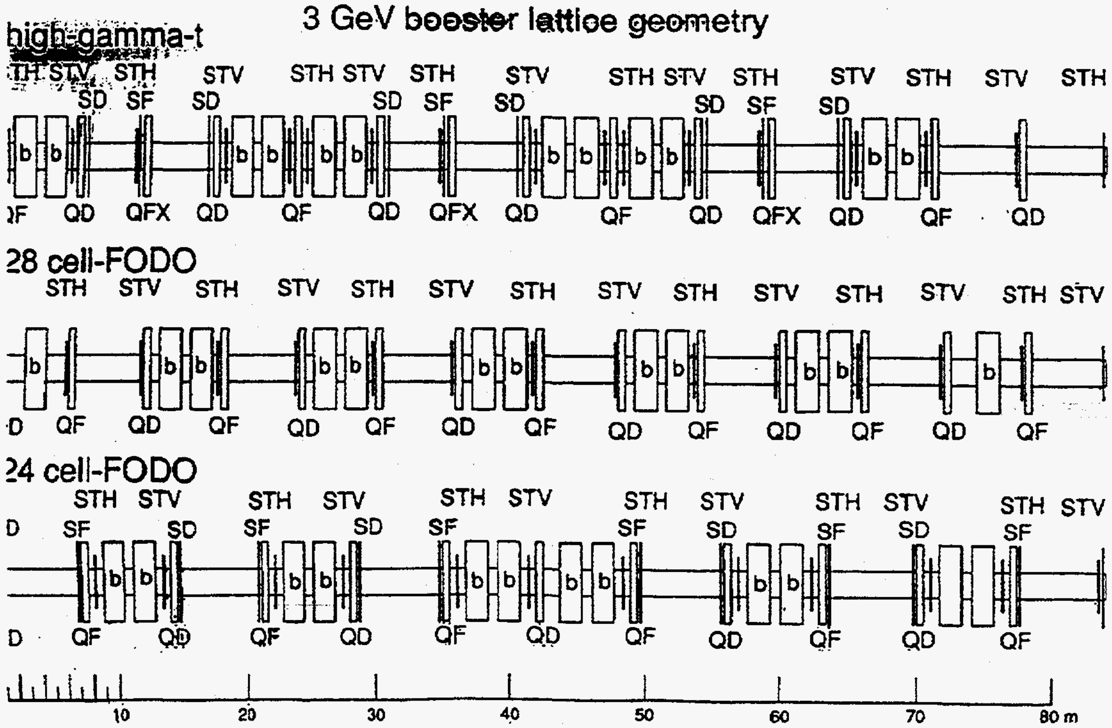

Maximum apertures of the 3 GeV booster

apertures

$$A_x = \sqrt{\beta_x \varepsilon_x} + \eta_x \left(\frac{\Delta p}{p} \right) + COD + (sagitta)$$

$$A_y = \sqrt{\beta_y \varepsilon_y} + COD$$

$$\varepsilon_{x,y} = 340\pi mm.mrad$$

$$\frac{\Delta p}{p} = 0.5\%$$

$$COD = 5mm$$

	horizontal	vertical
B magnet	93 mm	95 mm
Q magnet(max)	106 mm	107 mm

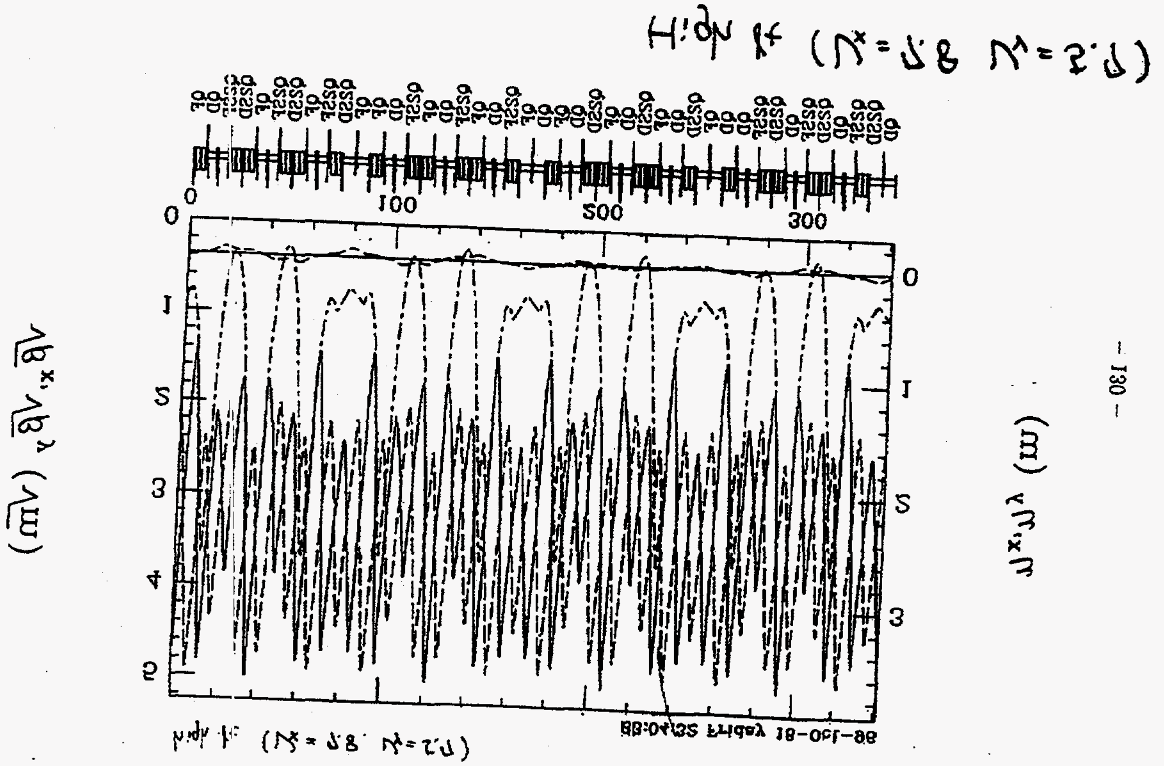

Space Charge Limit

$$N_{inc} = -\frac{\pi \beta^2 \gamma^3 \left(1 + \sqrt{\varepsilon_H / \varepsilon_V}\right) \varepsilon_V \Delta \nu B_f}{r_p F}$$

$$N_{coh} = -\frac{\pi Q_0 h^3 \beta^2 \gamma^3 B_f \Delta \nu}{R r_p F}$$

$\Delta \nu = -0.25$

– 145 –

	Incoherent	Coherent
3 GeV Booster	5.6×10^{13} ppp	1.2×10^{14} ppp
50 GeV Main Ring	4.7×10^{14} ppp	4.2×10^{14} ppp

Summary 3-GeV lattice

	High-γ_t	FODO (28cells)	FODO ([illegible]cells)
$\sqrt{\beta_{max}}$	5	4.6	5.2
η_{max}	$3.6_m (Q_{fx})$	$3.8_m (Q_f)$	$2.6m (Q_f)$
γ_t	~15	~6	~6
A (Q)	large	large	small
A (B)	large	large	small
Injection (Scraper, ...)	○	▲	△
Extraction (1 cell long s.s)	○	△(?)	○
Long. matching with MR	○	△	△

– 141 –

Collective Effect

960505

b)Narrow Band

Longitudinal Coupled-Bunch

RF cavity parasitic mode: $f_p / f_{rf} \approx \dfrac{1}{3B_f}$ **(R.Baartman)**

booster(injection): $R_s < 900\Omega (Q \geq 5, f_p >\sim MHz)$

main ring(injection): $R_s < 700\Omega (Q \geq 5, f_p \sim 15MHz)$

"active damper" , "Q<1 cavity?"

c)Resistive Wall

Transverse Coupled-Bunch

booster: < 0.14MΩ/m

main ring: < 1.4MΩ/m

– 127 –

Collective Effect

960505

a)Broad Band **Space Charge, Inductive Wall**

[1]Microwave Instability

main ring

3GeV(injection) $\left|\dfrac{Z}{n}\right| \leq 20\Omega \ @\varepsilon_L = 1eV \cdot \sec$

space charge impedance $\cong 55\Omega \ \therefore \varepsilon_L \cong 3eV \cdot \sec$

booster:no problem

[2]Negative Mass Instability

Inductive wall : $-\mathrm{Im}\dfrac{Z}{n} \leq 3\Omega \ @\varepsilon_L = 3eV \cdot \sec$

space charge : no problem--capacitive, $\eta<0$ **(~~high~~ imaginary γt lattice)**

– 126 –

Proposed Time Profile of JHP

1997 New Organization

1998 Construction Start

1999 Neutrino Oscillation Experiment at 12-GeV PS

2000

2001 3-GeV Ring Installation into the 12-GeV PS Tunnel

2002 50-GeV Ring completion, First Beam

R&D Works

1 RF Cavity
   New Material
      (Fine-Crystal High-μ Metal)
   Q ~ 1

2 Ceramic Beam Duct
   *booster
      200mm x 240mmx 1m
   *Main Ring
      100mmϕ(i.d) x 2m

3 Main Ring B magnet
   106mm(gap) x 1.5m

4 Booster Magnet Power Supply
   Resonant Network System

72

RF Cavity

Heavy Beam Loading

(1) Beam Power > Cavity Power

(2) Robinson Stability Criterion

Rs ~ small(1kΩ/m)

(3) Coupled Bunch Instability

Q ~ small (Q<5)

Ferrite

(problems)

*nonlinear behavior at large RF field

*low Curie temperature

New Material

"Fine-crystal High-μ Metal"

*high permeability

*Rs ~constant for larger RF field

*Q~1

BEAM DUCT

Requirements

(1) Eddy current	25Hz(3GeV)
	0.3Hz(50GeV)
(2) Impedance	RT<1.4MΩ/m@50GeV
	RT<0.14MΩ/m@3GeV
(3)Thermal shock	Beam hitting
(4)No magnetization	
(5)Ease of fabrication	
(6)Small maintainance	residual activities
(7)Cost	

3-GeV Booster >> Ceramic duct

50-GeV MR >> INCONEL duct

>> Ceramic duct

Control of Resonant Network Systems

２ネットワーク研究のための
テスト電源-ブロックダイアグラム

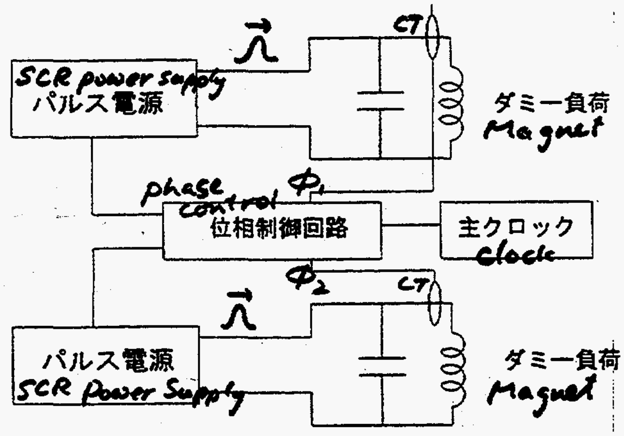

$\Delta\Phi = \phi_1 - \phi_2 \therefore < 8.28\,\mu s$ for $\Delta Q = 0.01$ @ 25 Hz

Overview from Los Alamos:
Current Thinking on RF Upgrade Issues

- PSR Upgrades in Progress
- Space Charge Compensating Inductor
- Barrier Bucket RF
- PSR Instability

  - by Arch Thiessen
  - 8 May, 1997

PSR Upgrades in Progress

PSR parameter list

◆ Beam energy	797 MeV (γ = 1.85, β = 0.84)
◆ Circumference	90.2 m
◆ Bunch length	250 ns
◆ Number of bunches	1
◆ Revolution period	357 ns
◆ Betatron tunes	$\nu_x = 3.18$, $\nu_y = 2.14$
◆ Transition gamma	3.1
◆ Maximum rf voltage	12.5 – 14 kV
◆ Chromaticity, horizontal	-1.28 ± 0.06
◆ Chromaticity, vertical	-0.8 ± 0.2
◆ Momentum spread from linac	0.05%
◆ Momentum spread in PSR	0.5%

PSR parameter list (cont.)

◆ Typical injection time	600 μs
● Typical storage time	10 μs
◆ Max bunched-beam charge stored	6.4 μC (4 x 10^{13} ppp)
◆ Max coasting-beam charge stored	2 μC (1.3 x 10^{13} ppp)
◆ Synchrotron period	720 μs for 10 kV buncher
● Coherent tune shift	0.008

PSR Upgrade Programs In Progress

- LANSCE Reliability Improvement Program (**LRIP**) Phase I (complete!)
  - Improved Beam Availability from ~65% to ~85%
- **LRIP Phase II**
  - Goal is 100 µA @ 20 Hz
  - Direct H- Injection
    - » Construction Starts 1 Aug, '97, Complete 1 March '98
- Short Pulse Spallation Source Enhancement (**SPSS**)
  - Goal Is 200 µA @ 30 Hz, 4×10^{13} protons per pulse
    - » New H- Ion Source
      - 1.5-2x Existing Current at Smaller Emittance
        - Collaboration with K-C Leung, BNL
    - » New RF System
      - Phase I (1997-1998) - New Driver for Existing 2.8 MHz Cavity
        - Needed both for Beam Dynamics and Reliability Improvement
      - Phase II (1999-2000) - New Cavity and RFDriver - Sum 12 KV @ 2.8 MHz, -6 kV @ 5.6 MHz
    - » Building, Cooling Water, and Utilities

Voltage Waveforms Considered

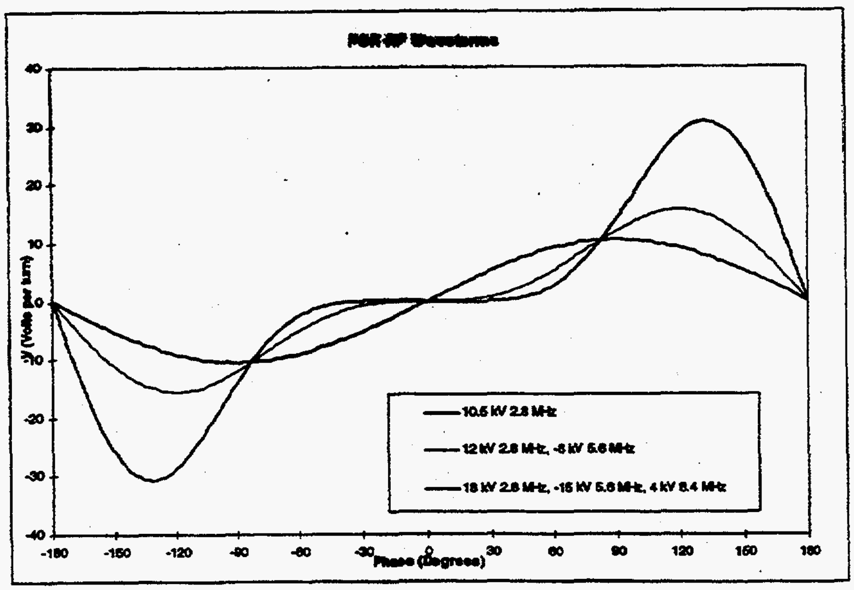

PSR before Upgrade

- Foil Hits 307
- Losses
- 0.15%
- 0.10%
- 0.03%

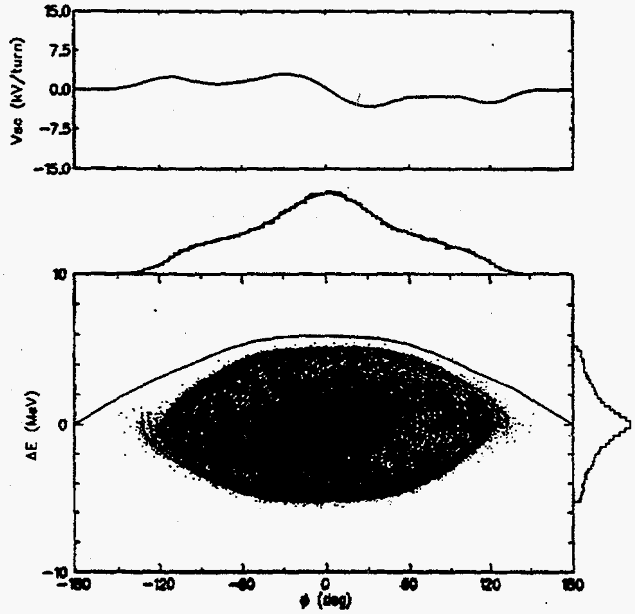

LANSCE

5/08/97 8

PSR with 2 Harmonics

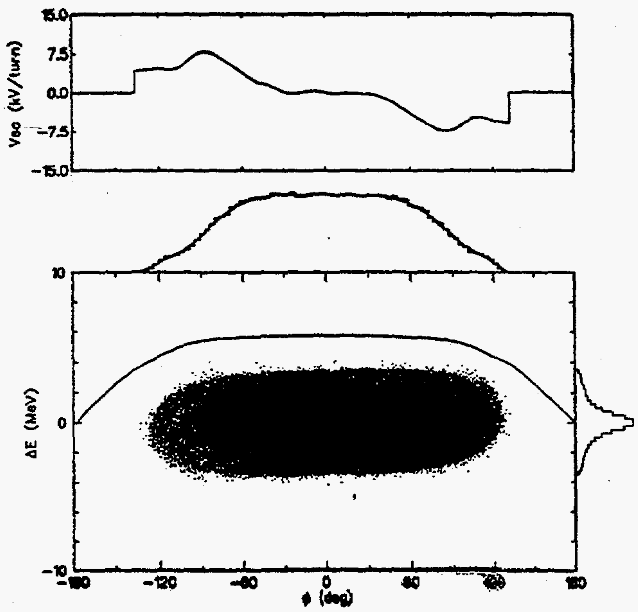

LANSCE

5/08/97 9

Space Charge Compensation with Inductor

Longitudinal Space Charge Control

- Maximum Value is ~1/2 of Applied Voltage after upgrades
  - Up to Now, Propose Control by "Brute Force"
    - » Make Sure $V_{rf} >> V_{sc}$
      - And Test by Tracking with ACCSIM or other code
- In Any Beam
  - V_{sc} α g di/dt - opposite sign from an inductance
    - » Can be compensated with an Inductor if g is a constant
- For PSR
  - For g=3 - inductance required in PSR is about 11 microHenries
  - Actual value of g not well known
    - » at present g~3.9
    - » After LRIP g~3.6
    - » After SPSS g~3.3
  - In Process of Tracking Code (ACCSIM) Modification
    - » for any longitudinal impedance
    - » variation of g with Courant/Snyder invariant

A Test of Space Charge Compensator

- For Space Charge Compensator Test, ~5 microHenries Max
  - Less than 1/2 Amount Needed for Full Compensation
    - » Idea is to see effect
      - bias off vs on
        - beam in gap?
        - Stability threshold ?
    - » Look for other problems caused by inductor
      - change in instability threshold
    - » good ideas for effects to look at?
- Two Days with Access for Installation July 31, 1 Aug
- One 24 hr Day for Tests with Beam
  - Tentatively Scheduled for 2/3 August, 1997

Barrier Bucket at PSR

Barrier Bucket at PSR

- Study Just Getting Underway
  - Tracking Code Not Yet Adapted for Barrier Bucket
- Tradeoff between Injection Time and Voltage
  - Both Are Problems at PsR
    - » Present injection time 250 ns is too long for clean gap
    - » Voltage Available on ~~One Cavity~~, ~10kV is Low
      - h=1.5 - 10 kV ok, but bunching factor low
      - h=2.5 requires 30 kV for full height bucket
  - How Does PSR Work Now?
    - » Not many particles at high dp/p at end of bunch
  - Reasonable options are h=1.5, h=2, h=2.5, h=3 barriers
    - » h=integer ok if Cathode Follower Driver
- Want to Compare with a Traditional 2-Harmonic System

LANSCE

5/08/97 13

SOME QUESTIONS

A) WHAT GAP WIDTH IS NEEDED FOR e-p?

B) WHAT GAP WIDTH IS NEEDED (FOR 2% LOSSES) AFTER LEIP?

C) HOW MUCH ΔE IS NEEDED IN BUNCH?

D) WHAT IS THE MAXIMUM GAP IMPEDANCE ALLOWED?

E) WHAT MIN. AND MAX. BUNCHING FACTORS ARE DESIRED?

F) HOW WELL WILL PASSIVE COMPENSATION WORK? (i.e. WHAT IS "g" AFTER LEIP, HOW MUCH "EXTRA" VOLTAGE WILL BUNCHER NEED TO PROVIDE)

PRESENT OPERATION

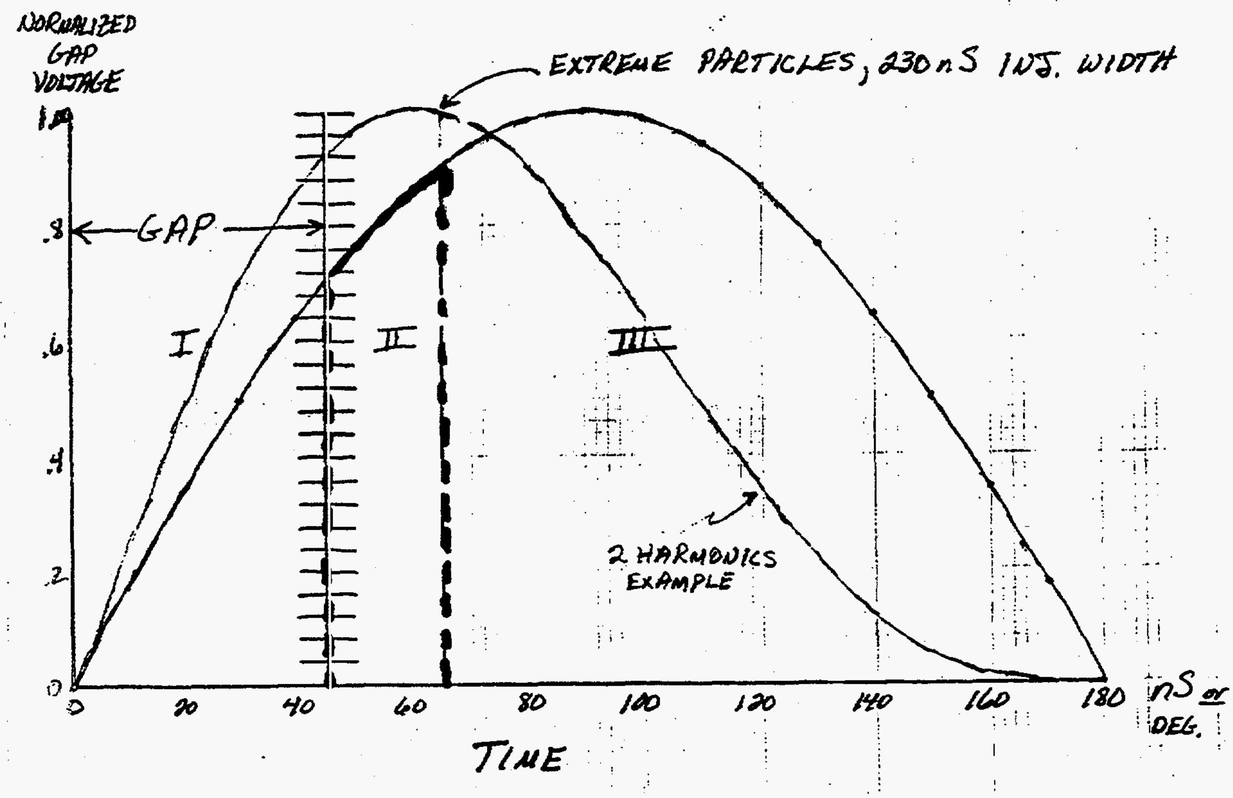

SOME HALF SINUSOIDS

(NOTE: These are appropriate for "high impedance" drives — with cathode followers "any" harmonic is O.K.)

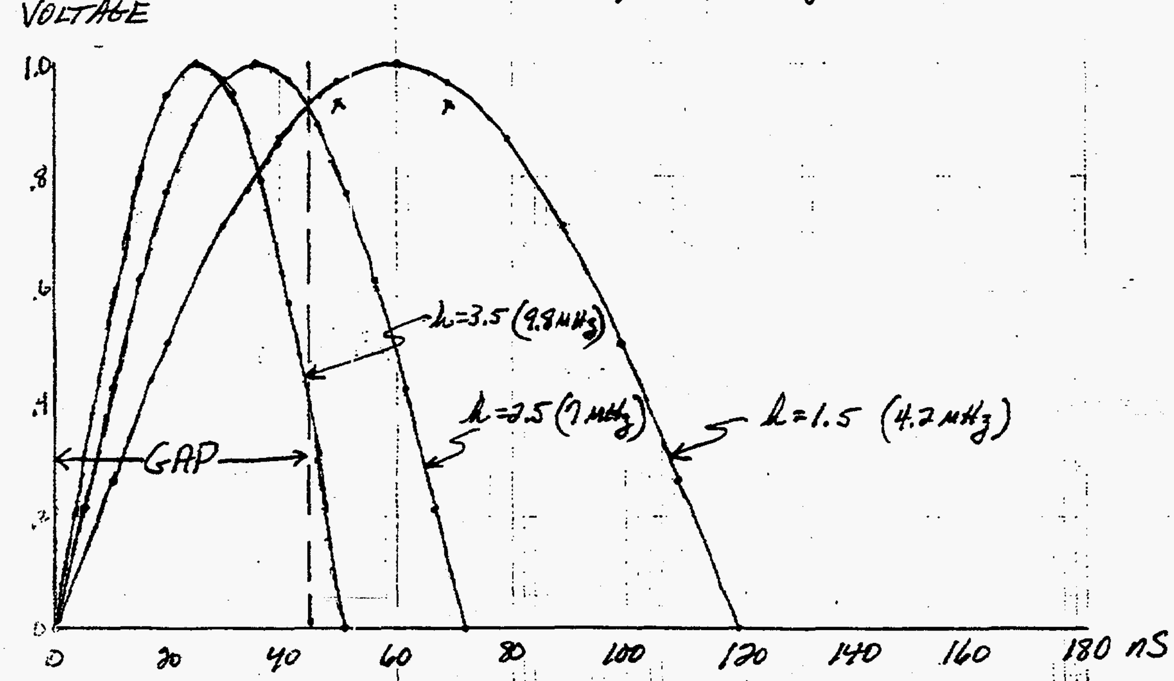

SINUSOID GENERATION IDEAS

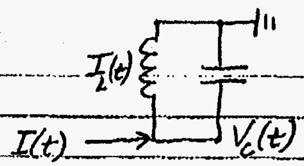

I) ISOLATED SINUSOID

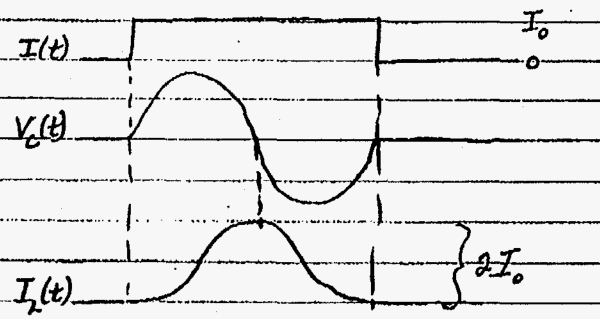

II) ISOLATED HALF-SINUSOIDS

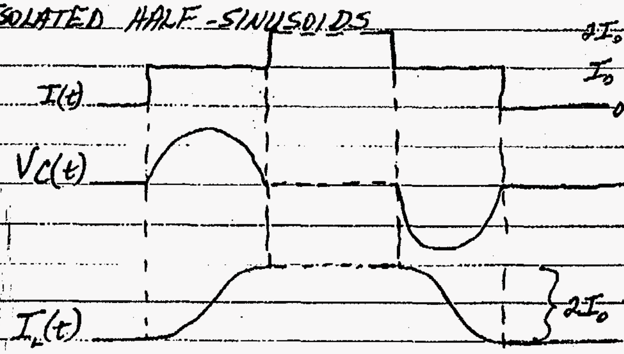

Note: 5% D.F. MAX., EXISTING CATHODE FOLLOWER

(ALSO: 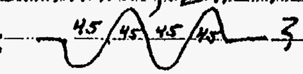 ?)

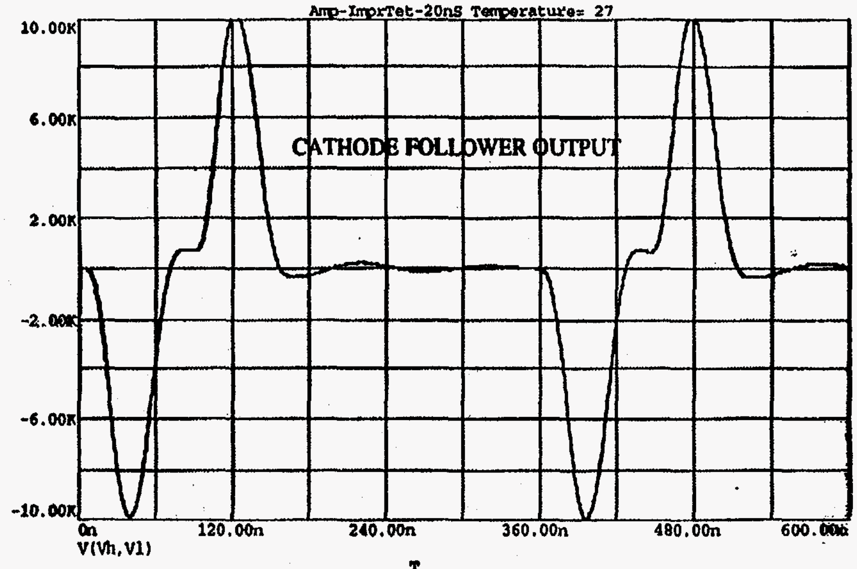

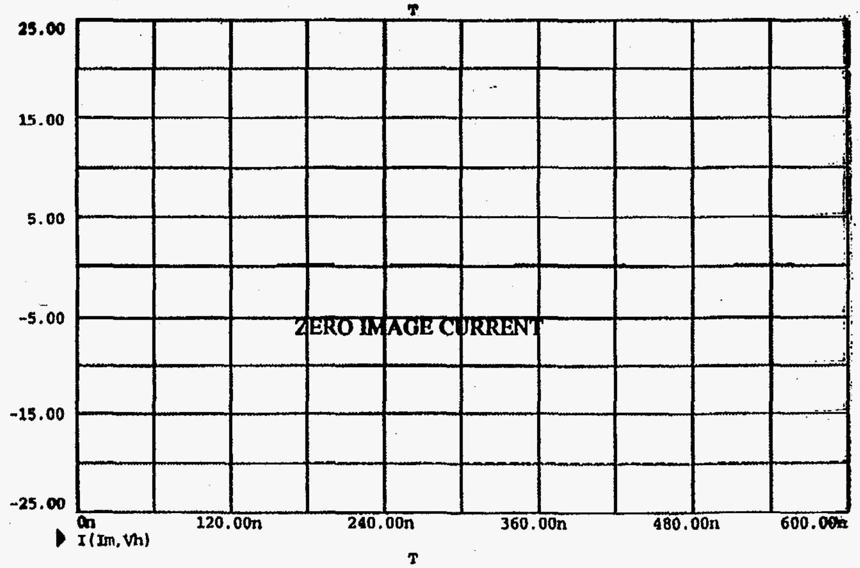

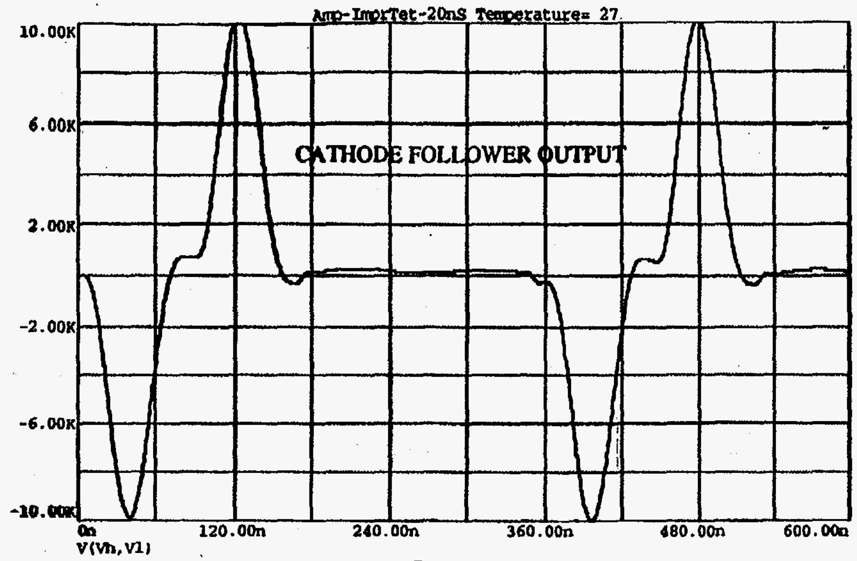

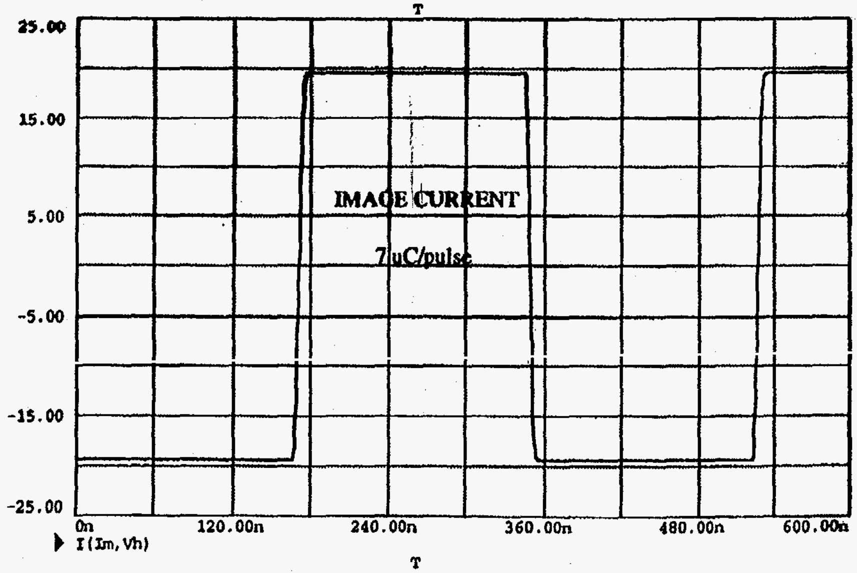

PSR Instability

- A Slide Show

LANSCE

Coasting beam instability signals

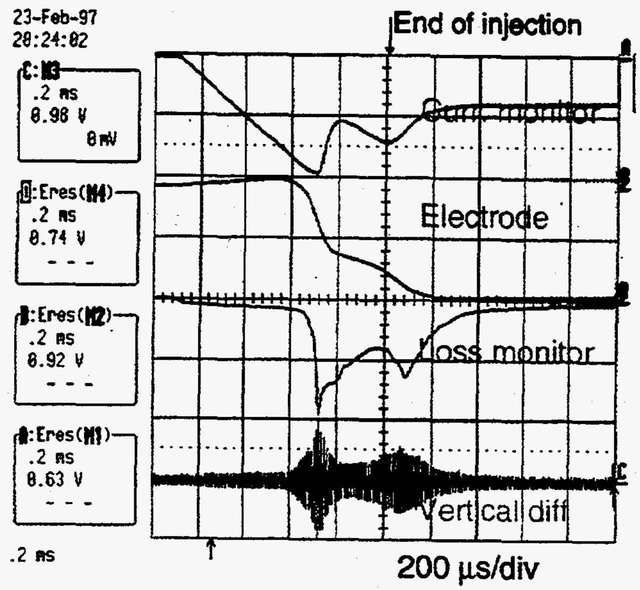

3.0 µC injected
(2.0 µC before instab.)
925 µs injection
250 ns PW
rf off
-1900 V opp. elec.

LANSCE

5/08/97 15

Bunched beam instability signals

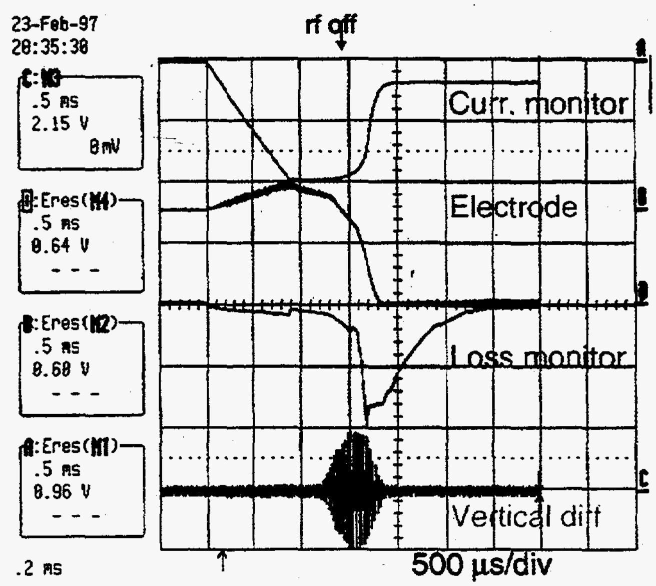

3.0 µC
925 µs injection
250 ns PW
6 kV rf
-1900 V opp. elec.

LANSCE

5/08/97 16

Stable Peak Intensity vs. Buncher Voltage

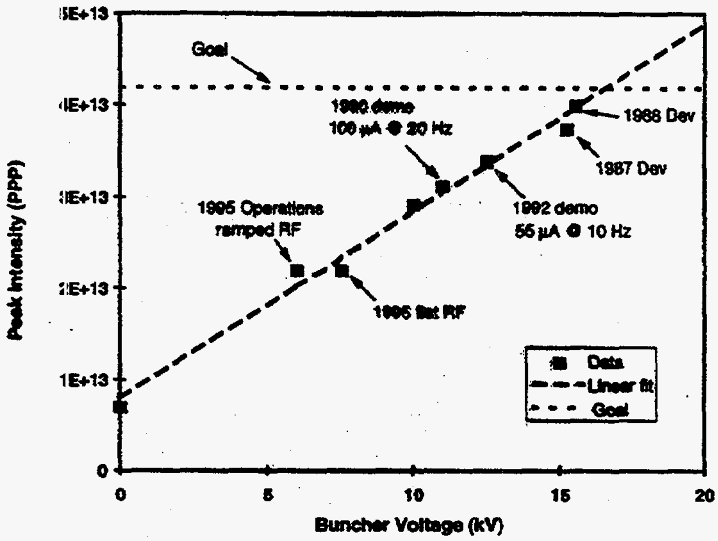

LANSCE

5/08/97 18

Peak Stored Charge vs. Bunch Length

(1989 Data)

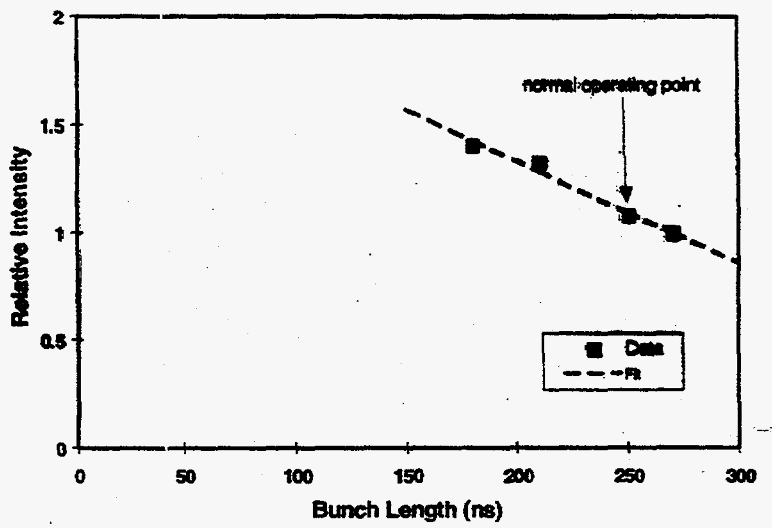

LANSCE

5/08/97 19

Instability from PSR RF System Problems?

- Measured Phase and Amplitude Jump at Extraction
  - Phase Change <5°
  - Amplitude Change <5%
    - » These Result in Tiny Changes in Beam Dynamics
- See Also Arch's Experiment
  - With Open Circuit Drive of Cavity

Logbook - Arch's Test: With Open Circuit Buncher Drive

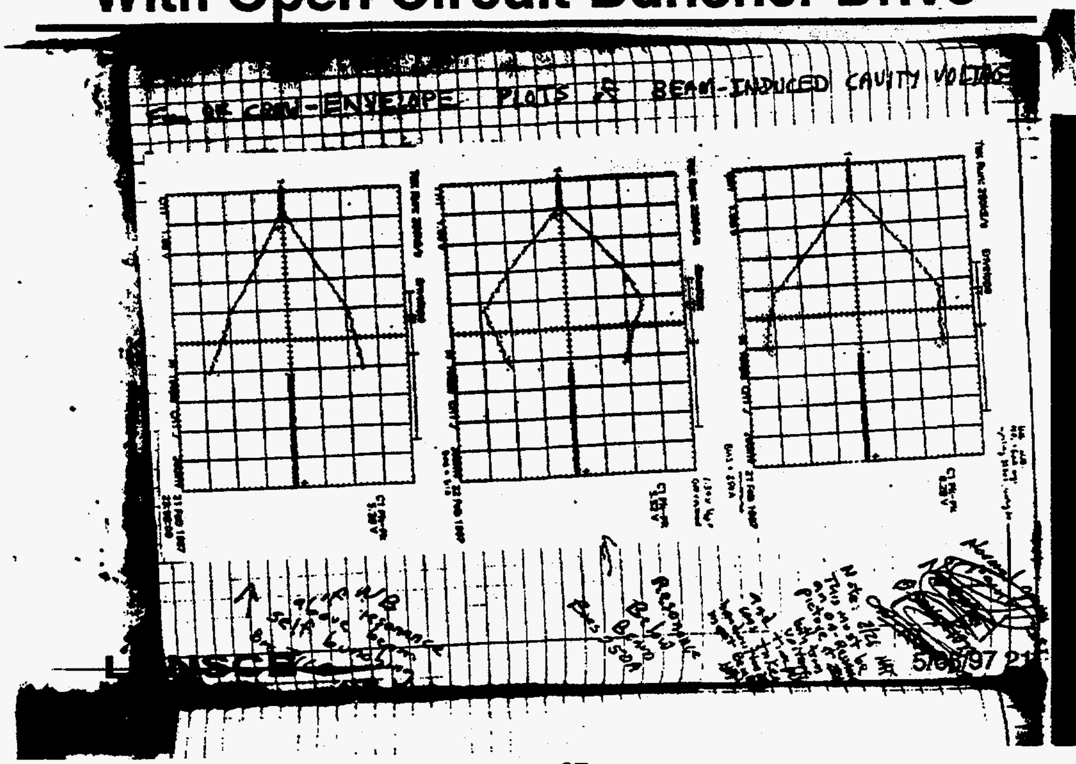

Instability from Beam in Gap?

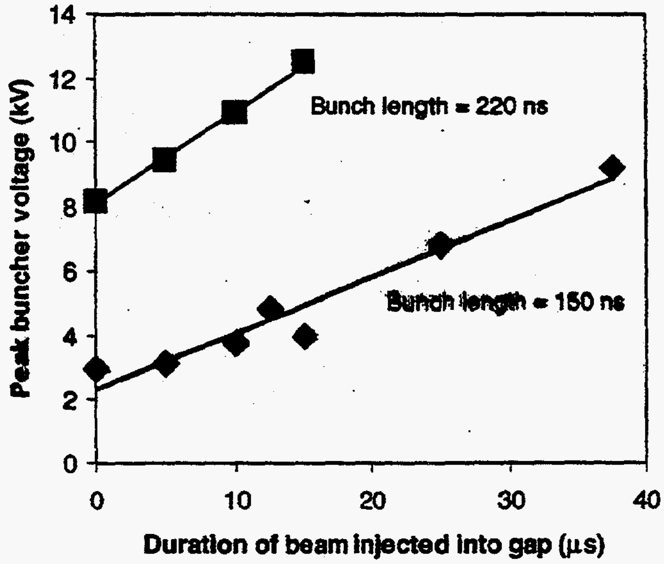

LANSCE 5/08/97 22

Logbook - Beam in Gap

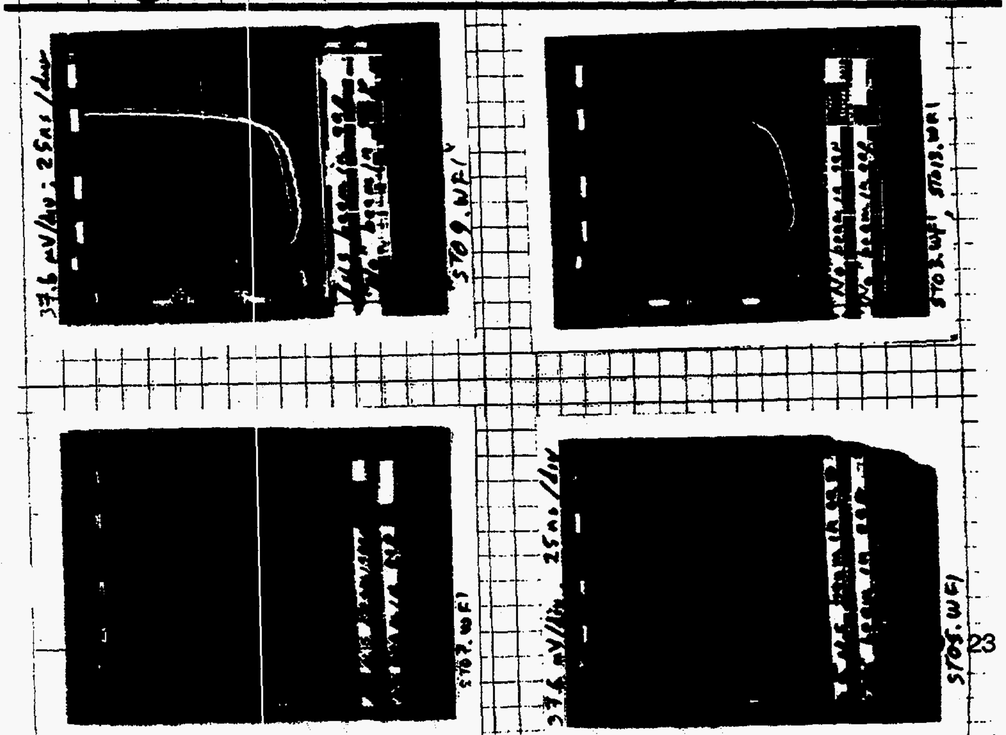

23

Signal power vs. time

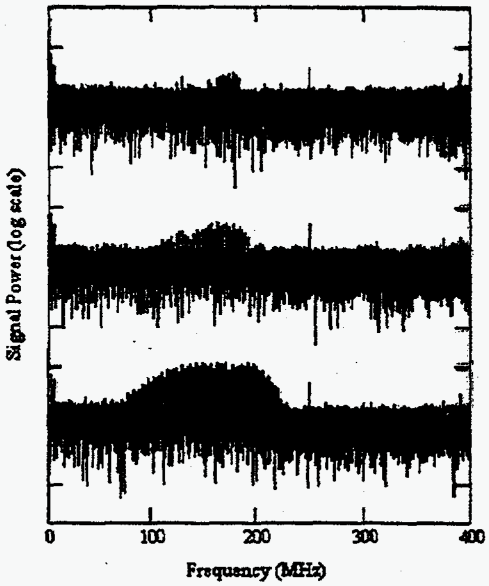

- Signal power at t, t + 60 μs, and t + 160 μs from wide band stripline beam position monitor.
- Power begins at about 175 MHz, then spreads in width and amplitude.

$$f = \frac{1}{2\pi}\sqrt{\frac{2Nr_e c^2(1-\eta_e)}{\pi b(a+b)R}}$$

Data from SRWM41 ΔV, 4/7/97. WM41VD.ON2

LANSCE

5/08/97 24

Peak frequency vs. intensity

- The peak in the signal spectrum depends on the beam intensity.
- Top spectrum is twice the intensity of the bottom spectrum
- Beam conditions for the top and bottom spectra are the same except for the beam intensity and the buncher voltage.

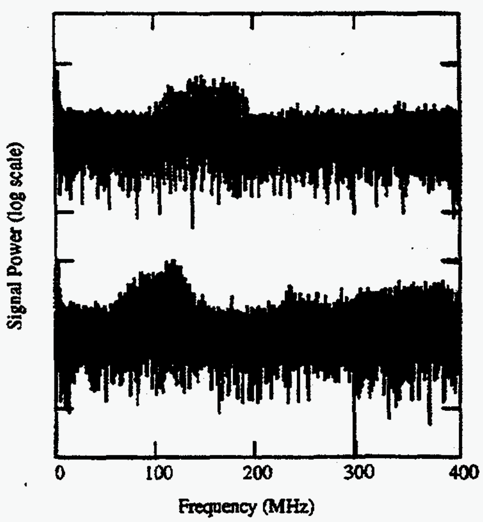

$$f = \frac{1}{2\pi}\sqrt{\frac{2Nr_e c^2(1-\eta_e)}{\pi b(a+b)R}}$$

SRWM41 ΔV from 13/Apr/97 data. WM41VD.4C, SRWM41VD.4F

LANSCE

5/08/97 25

Where Vertical Instability Grows: 2nd Half of Bunch

- CERN BPM Vertical Difference
  - three traces at different times

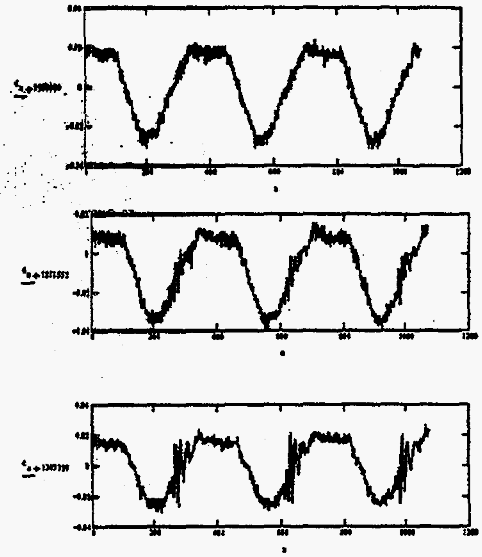

Vertical oscillations and beam density

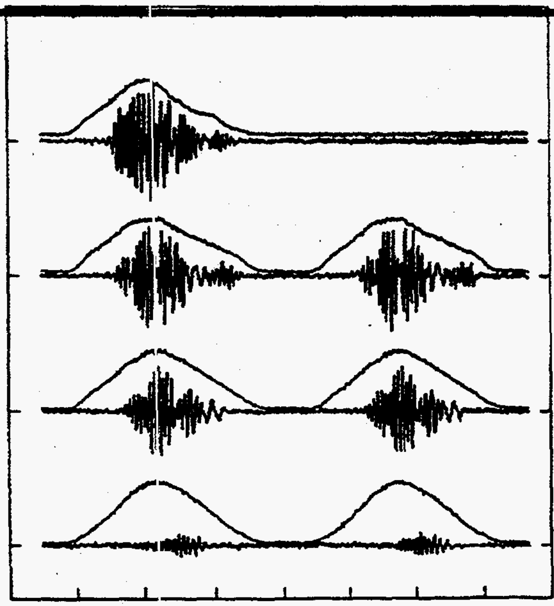

- WM41VD.4B
- WC41.4B
- Data taken Apr. 14, 1997
- Data at t, t+115 μs, t+230 μs, t+345 μs

Transverse oscillation λ correlated with ρ

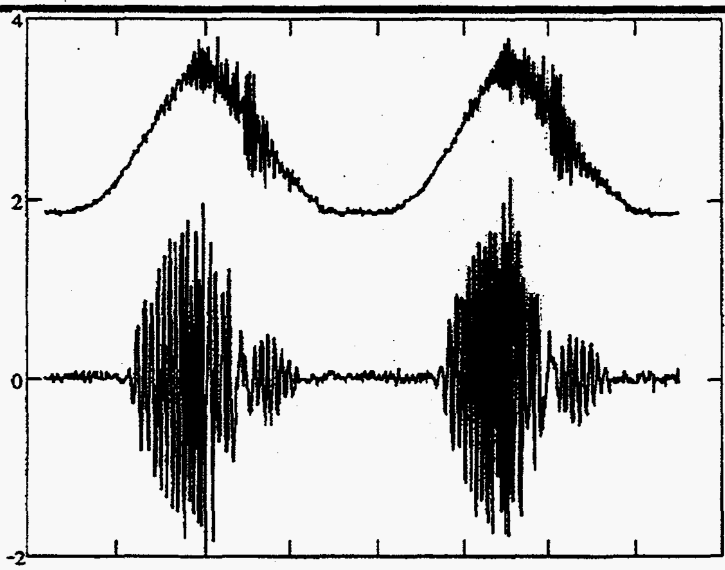

SRCM41 (top)
SRWM41 ΔV (Bot)
Data from 22/Feb/97

Sources of electrons

For each injected proton, we have:

- "Convoy" electrons — 1
- SEM from stripper foil from convoy electrons — 0.1 - 1
- Knock-on electrons from stripper foil — 1.3
- SEM from foil from circulating protons — 6
- Thermionic emission from foil — <0.02

- SEM from beam loss — 0.01 - 1
  (2 to 200 electrons created per proton lost)
- Residual gas ionization — 0.0001
- Electron multiplication from electron osc. — ?

Conclusions

- Study of Inductor for Space Charge Compensation Underway
  - An Experiment Planned for August
    - » If logistics work out
- Studying Barrier Bucket for PSR Underway
  - No Results Yet
- PSR Instability is e-p
  - Frequency Dependence
  - Starts in 2nd Half of Bunch
    - » But Source of Electrons
    - » And Mechanism for Growth
      - Not Yet Understood

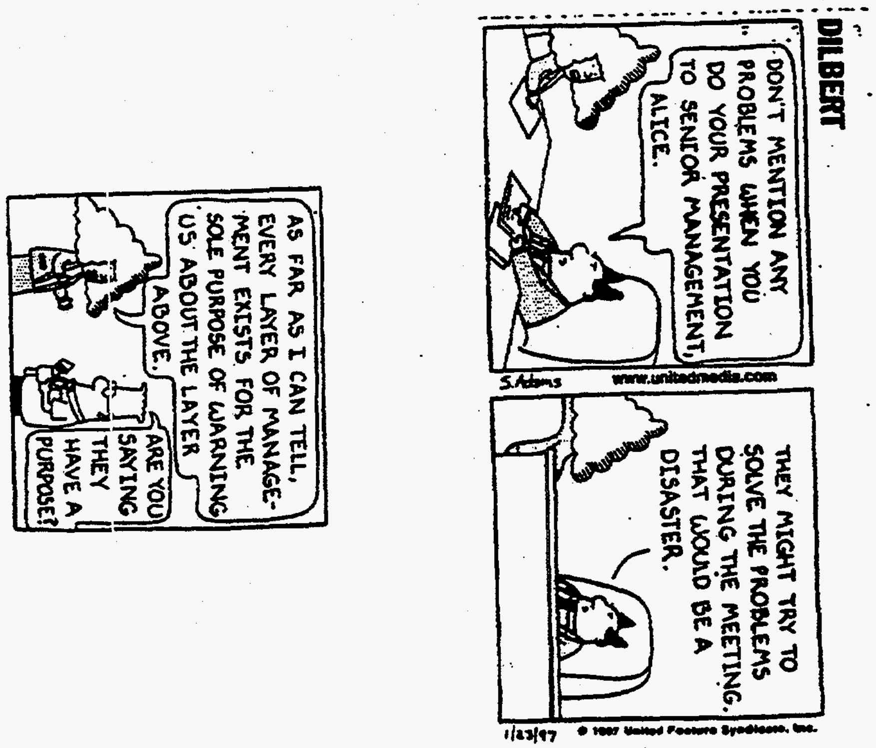

Session on Barrier Cavity Issues

M. Blaskiewicz

The working group on barrier cavity issues included two presentations. Masahito Yoshii presented plans for the AGS barrier cavity upgrade and Chihiro Ohmori presented plans for the JHF.

Plans for the AGS barrier cavity upgrade included cavity design and materials as well as drive considerations. The system will produce two single period sine wave pulses of amplitude 80 kV and period 250 ns (1/ 4 MHz) at a rep rate of 350 kHz. There will be one rf station for each pulse. Since the cavity is run in a non-resonant mode the cavity voltage V and generator current I are related via $V \approx IR/Q$ where R/Q is the ratio of shunt impedance to cavity Q for the resonant mode at 4 MHz.

Yoshii stressed the need for a high inductance and a low capacitance so that the necessary waveform could be obtained with minimum generator current. The AGS philosophy is to use a fairly low loss ferrite (Philips 4B2 or 4L2) to obtain the high inductance and to control the shape of the voltage waveform by careful adjustment of the generator. This technique minimizes the peak generator current required for a given gap voltage and cavity R/Q. The generator supplies current in one direction only, which reduces cost.

The total voltage of 80 kV is obtained using 8 gaps with 10 kV per gap. Such a design does not require high voltage feedthroughs and a prototype of a single cell using Philips 4L2 has achieved the necessary voltage.

The JHF design included an upgrade of the KEK Booster as well as a the new high energy JHF. Accelerating voltages of 10 kV/meter are required. The KEK design differs from the AGS design mainly in the choice high permeability material. Ohmori agreed that large inductance with small capacitance was needed, but is more inclined toward the very high permeability and lossy FINEMET. For a truly isolated voltage pulse the system requires a push-pull current drive, but the voltage waveform from a half sine wave current pulse was not far from ideal. The low Q leads to large power dissipation in the cavity, but FINEMET has a 600 C Curie temperature. Additionally, the low quality factor reduces the shunt impedance of parasitic modes which should reduce instability problems. A prototype cavity has been built and has achieved 11 kV/ meter. Studies of feedback and beam loading are underway.

AGS Barrier Cavity

* M. Yoshii (KEK)
M. Meth (BNL)
R. Spitz (BNL)

May 7 1997
Barkner Hall Room B
BNL, Upton NY, USA

CONTENTS

- ✓ AGS Barrier Requirements
- ✓ Design Principles
  - ✓ permeability : μ
  - ✓ μQ-product : μQ
  - ✓ capacitance : C
- ✓ Ferrites
  - ✓ μ(r) measurement
  - ✓ sample measurement
- ✓ Cavity Capacitance
- ✓ New AGS Barrier Cavity
  - ✓ design
  - ✓ 1/8 model
  - ✓ drive circuit
- ✓ Summary

MAY 7-97
M.YOSHII
Mini-Workshop

AGS Barrier Requirements

- ✓ 80 kV per each station
- ✓ Two Barrier Stations
  the length of station should be
  less than 102 inches (2.6m)
- ✓ 4 MHz
  cf. the revolution frequency at AGS
  injection is 357 kHz

Design Principles

✓ <u>to minimize the drive-tube current</u>

✓ high cavity inductance

✓ square current waveform

✓ simple structure

The total current required for the barrier gap voltages is,

$$I(t) = \omega C V_o \left(1 + \frac{\sin(\omega t)}{Q}\right) + V_o \cos(\omega t)\left(\omega C - \frac{1}{\omega L}\right).$$

And, the peak current on resonance is,

$$I_p = \omega C V_o \left(1 + \frac{1}{Q}\right).$$

Therefore, following three basic parameters for the cavity ; μ, μQ-product and total C are chosen in order to <u>minimize total tube current</u>.

✓ Capacitance per gap < 200 pF

- to keep the average rf-current as low as possible

✓ μQ-product > 2000

- to keep the peak rf-current as low as possible

✓ **μ > 500 :**

- to get a high gap voltage, $V \propto L \frac{dI}{dt}$
- also, to make a cavity short

MAY 7-97
M.Yoshii
Mini-workshop

Radial Dependence of Ferrite μ and Magnetic Flux

G. Rakowsky (BNL) " RF Accelerating Cavity For AGS Conversion"
: μ(r) , B(r) distributions under biasing conditions

Idc 0

- μ has radial-dependence

  For a given Idc,
  μ increases with radius
  H_{rf} decrease as radius

  ->Magnetic Flux becomes uniform

Idc = 0 or weekly biased

- μ is uniform in a ferrite
  -> Magnetic Flux has radial dependence.

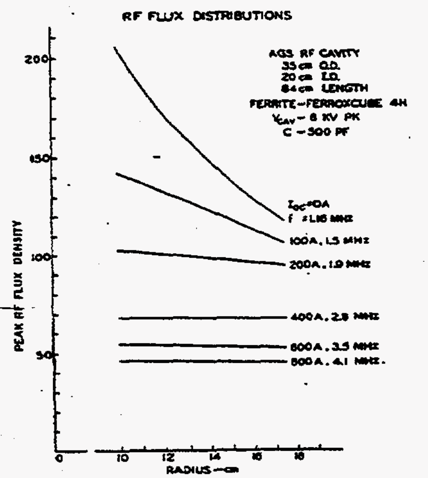

5

MAY 7-97
M.Yoshii
Mini-workshop

Measurements of Permeability and Flux Distribution

- 100 turns of primary winding for biasing
- 30 turns of pick-up coil (5 positions along the radial direction)
- 4L2 ø500 x ø200 x 25.4mm

Measurement

- single cycle of magnetization with sinusoidal biasing
  ± 15 A -> ± 1500 AT

- How to calculate B and H.

$$\overline{H} = \frac{\text{total current crossing inside a core}}{\text{average magnetic length}} = \frac{NI}{\pi \overline{d}} \quad (1)$$

where $\overline{d} = \dfrac{ID + OD}{2}$.

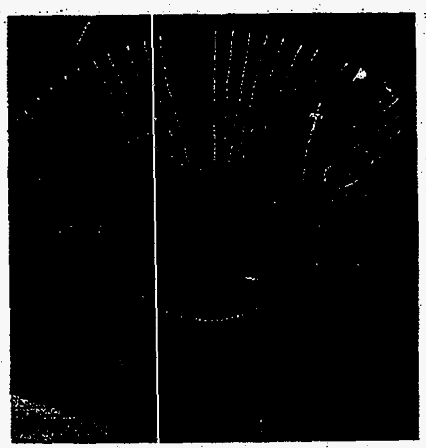

6

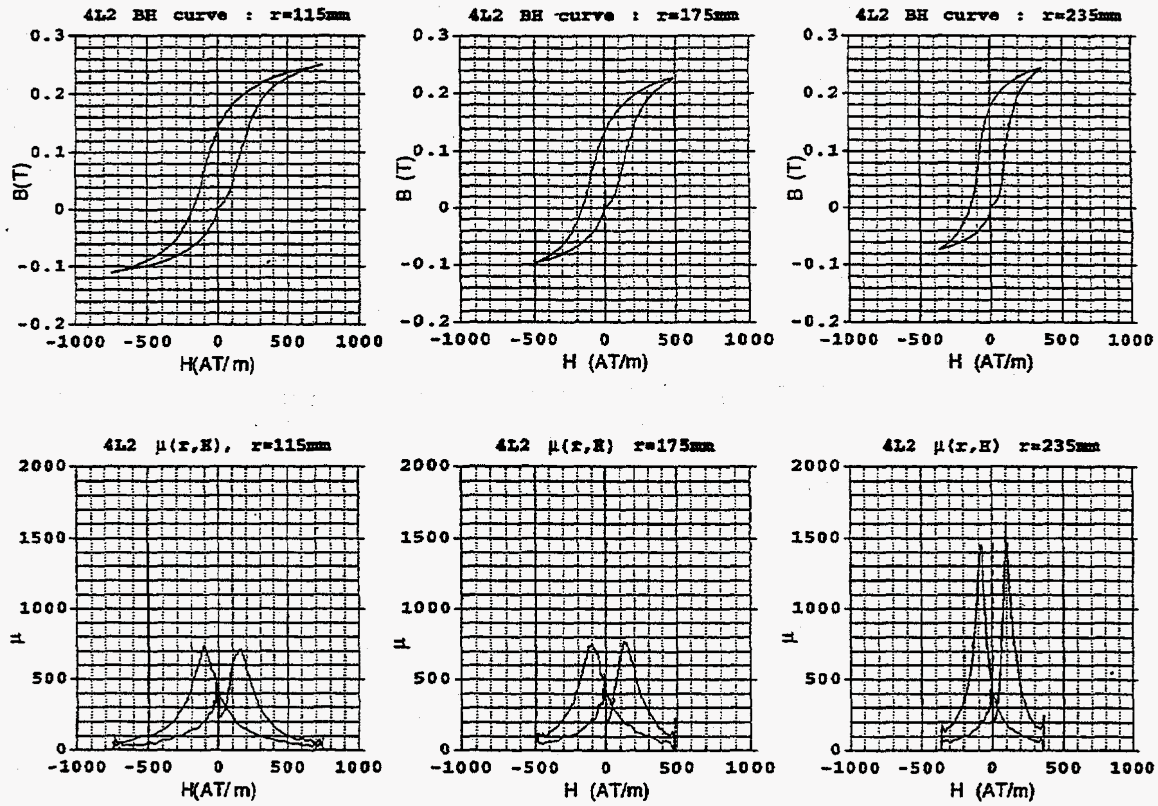

Differential $\mu = \frac{\Delta B}{\Delta H}$

MAY 7-97
M.Yoshii
Mini-workshop

- An induced voltage at each pick-up is

$$\varepsilon^{(n)} = -\frac{d\left(N^{(n)}\phi^{(n)}\right)}{dt} \quad (volts), \qquad (2)$$

where N is the turn-number of pick-up coil , ø is a magnetic flux through the coil and a suffix (n) denotes the pick-up position.

As a flux $\phi^{(n)} = \int_S \vec{B}^{(n)} \cdot d\vec{S}^{(n)}$, $\quad B^{(n)} = \frac{d\phi^{(n)}}{dS^{(n)}} \approx \frac{flux\ nth.\ pick-up}{crossectional\ area}$ (3).

The time-integration of eq.(2) gives $\phi^{(n)}(t) = \frac{1}{N^{(n)}} \int_0^t \varepsilon^{(n)}(t)\,dt$ (4).

From (3) and (4), then, the average flux density B_n at n-th pick-up is given by

$$\overline{B}^{(n)}(t) = \frac{1}{N^{(n)} S^{(n)}} \int_0^t \varepsilon^{(n)}(t)\,dt \qquad (5).$$

In the measurements all data are discretely sampled. So, Integration in eq.(5) must be re-written by,

$$\overline{B}_k^{(n)} = \frac{\Delta t}{N^{(n)} S^{(n)}} \sum_{j=0}^{k} \varepsilon_k^{(n)} \qquad (6)$$

---

for example, in our case,

N = 30 turns , S = 763 x10^{-6} m^2 , $\Delta t = 200\,\mu sec$

$$\overline{B}_k^{(n)} = 8.75 \times 10^{-3} \sum_{j=0}^{k} \varepsilon_j^{(n)} \left(\frac{volts \cdot sec}{meter^2}\right)$$

Sample measurements

The Ferrite materials are required at 4MHz

$\mu > 500$

$\mu Q > 2000$

Philips: 4A11, 4B3, 4L2

TDK: L6H

Ceramic Magnetics : CMD10, CMD5005

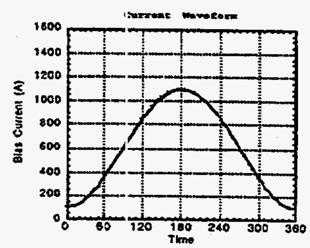

Bias Current : 100 ~ 1100 A

Differential $\mu_\Delta = \frac{\Delta B}{\Delta H}$

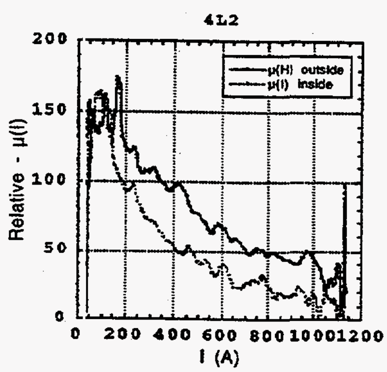

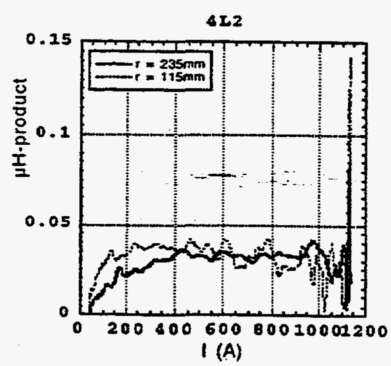

MAY 7-97
M.YOSHII
Mini-Workshop

Samples

Table - 1. List of dimensional parameters of tested samples

Name	Maker	I.D (mm)	O.D (mm)	t (mm)	AL/μ_r (pH)
4A11	Philips	20.	30.	8.	649.
4B3	Philips	20.	30.	8.	649.
4L2	Philips	20.	30.	8.	649.
L6H	TDK	19.	31.	8.	772.
CMD10	CM	33.	27.	15.	602.
CMD5005	CM	38.	25.	13.	986.

Measurements

- conditions : 4 turns winding for measuring 4A11, 4B3, 4L2, CMD10 and CMD5005
  5 turns for L6H
- instruments : HP8751A Network Analyzer
  with HP87512A Transmission/Reflection Test Set
  for 4A11, 4B3, 4L2 and L6H measurements

  HP3753A Network Analyzer
  with HP85044A Transmission/Reflection Test Set
  for CMD10 and CMD5005 measurements
- frequency range : 100kc to 10 Mc or 300 kc to 10 Mc

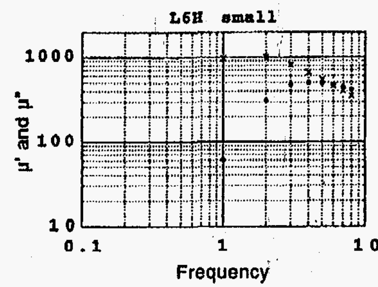

μ' = 660, Q = 1.3 (μQ = 860) at 4MHz

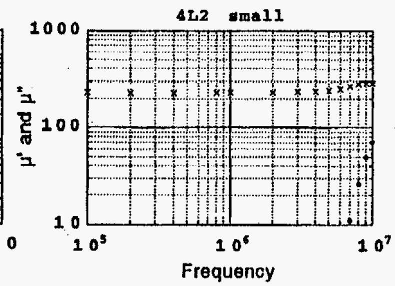

μ' = 240, Q = 29 (μQ = 6900) at 4MHz

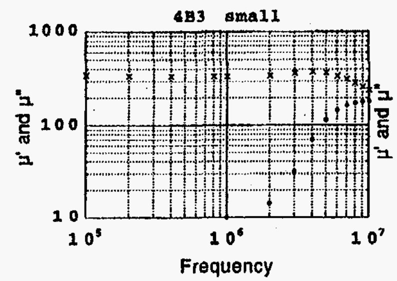

μ' = 370, Q = 5.7 (μQ = 2100) at 4MHz

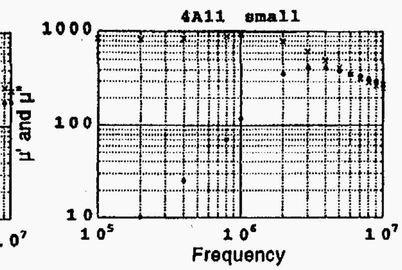

μ' = 490, Q = 1.2 (μQ = 590) at 4MHz

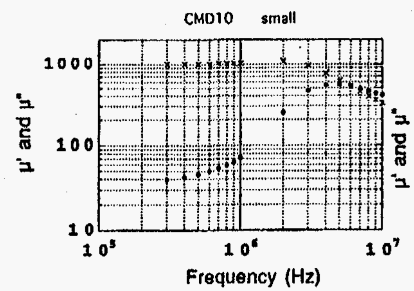

μ' = 780, Q = 1.4 (μQ = 1100) at 4MHz

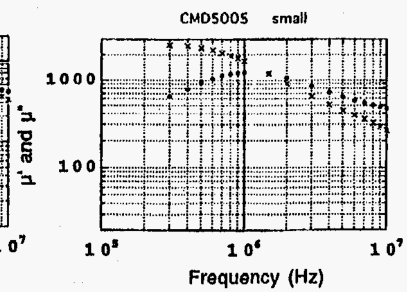

μ' = 505, Q = 0.7 (μQ = 346) at 4MHz

14

Capacitance Measurement :

$$f^{-2} = LC_{gap} \quad : C_{gap} \textit{ unknown}$$
$$f^{-2} = L(C_{gap} + C_{ext}) \quad : C_{ext} \textit{ known}$$

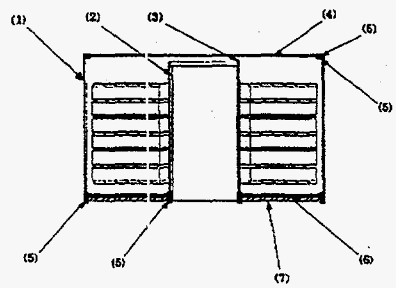

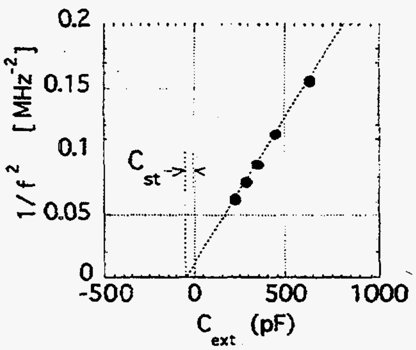

FIGURE - 2 : Typical plot

13

MAY 7-97
M.YOSHII
Mini-Workshop

Cavity Capacitance

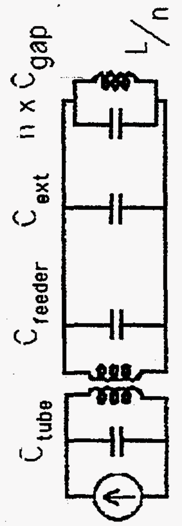

Total Capacitance : $C_T = C_{tube} + C_{feeder} + C_{ext} + nC_{gap}$

C_{tube} : tube capacitance : 100 pF

C_{ext} : trim capacitance for tuning : as low as possible

C_{feeder} : stray capacitance etc., , , unknown (?!)

C_{gap} : gap capacitance unknown (?!)

n : the number of gaps

Considering a resonant condition ,

$$(2\pi f)^{-2} = \left(\frac{C_{tube} + C_{feeder} + C_{ext}}{n} + C_{gap}\right)L.$$

Contribution of C_{tube}, C_{feeder} and C_{ext} to C_T becomes less with n.

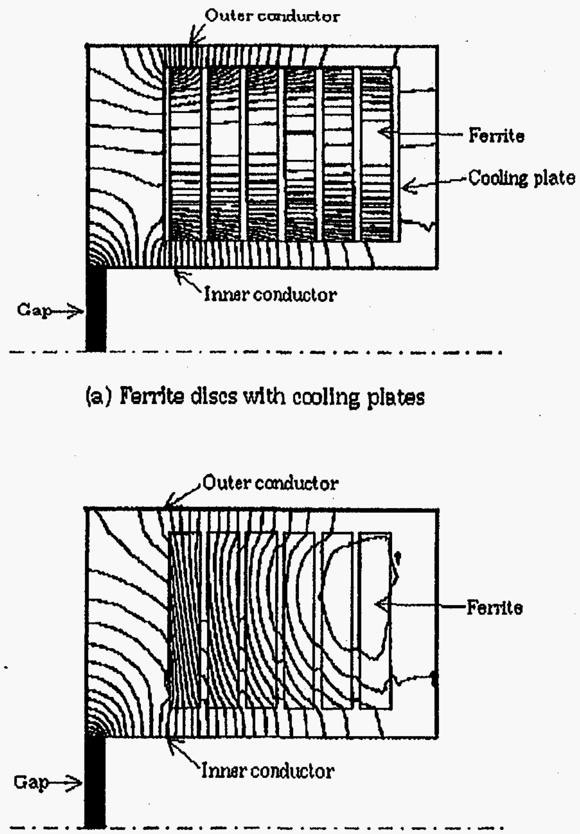

(a) Ferrite discs with cooling plates

(b) Ferrite discs with no cooling plate

FIGURE - 5 Superfish Field Plots :
Electric field lines in the ferrite loaded cavities with the cooling plates (a), and without the plates (b) are displayed. Each cross-sectional view shows a half of the cavity

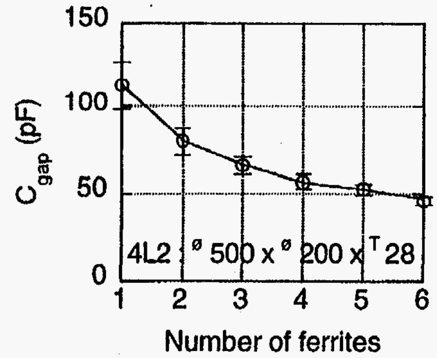

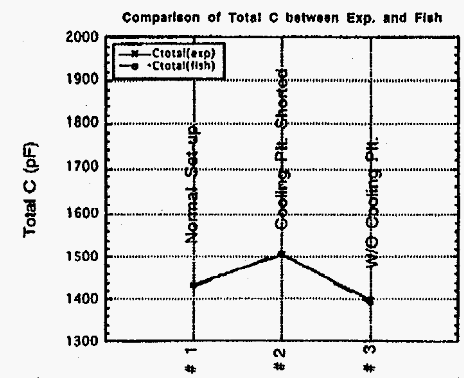

	Name	<μ'>	<Q>	Lp(μH)/gap	CT (pF)	Cext (pF)	Total Irf	Rsh	Pw/ring (kW)	Pw density (W/cc)	P (kW)
0	8-Gap Cavity									r = r1	
1											
2											
3	OD = 500 mm										
4	ID = 200 mm										
5	t = 28.1 mm										
6	Co = 50 pF										
7											
8	N = 6										
9	8 gaps										
10											
11											
12	4A11	490	1.2	25.7	61.7	-86.3	227	97	11	6.6578	517.00
13	4B3	370	5.7	11.8	134.3	-494.8	318	211	5	3.0514	236.95
14	4L2	240	30.0	7.4	213.3	-1126.1	443	700	1	0.92029	71.464
15	L6H	850	1.3	32.0	49.5	-183.8	176	131	8	4.9319	382.98
16	CMD10	780	1.4	36.4	43.5	-232.0	150	180	7	4.0224	312.35
17	CMD5005	505	0.7	47.4	33.4	-313.1	163	104	10	6.1710	479.20
18											
19											
20	< Brf >	157									
21	B max @ r = r1	258									
22											
23	Vgap total (kV)	10.0									
24	Frequency (MHz)	4.00									

$$N \frac{\mu}{2\pi} \ell_F \ln\frac{r_2}{r_1}\left(1+\frac{1}{Q^2}\right)$$

New Cavity Design

1. 8 gaps
2. 10 kV / gap
3. Ferrite
   500 x 200 x 28
   4B2 (?) 4L2 (?)
4. Cooling plates
   electrically floated
5. $N_f = 6$

20

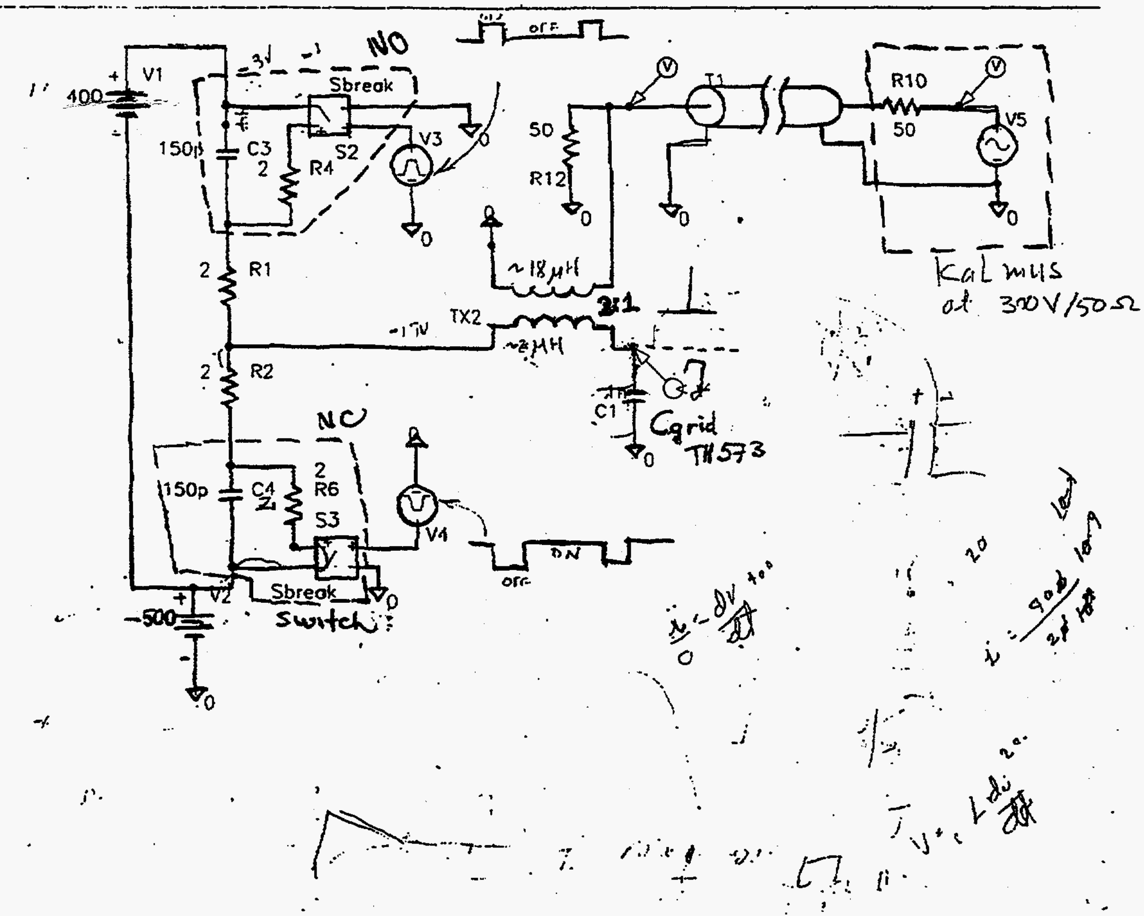

19

AGS BARRIER CAVITY (cross-sectional view)

- The AGS barrier cavity consists of 8 cells of a re-entrant ferrite loaded cavity. Total gap voltage is required to be 80kV at 4MHz. And, the cavity is going to be driven by one TH 558 power tetrod (500kW).

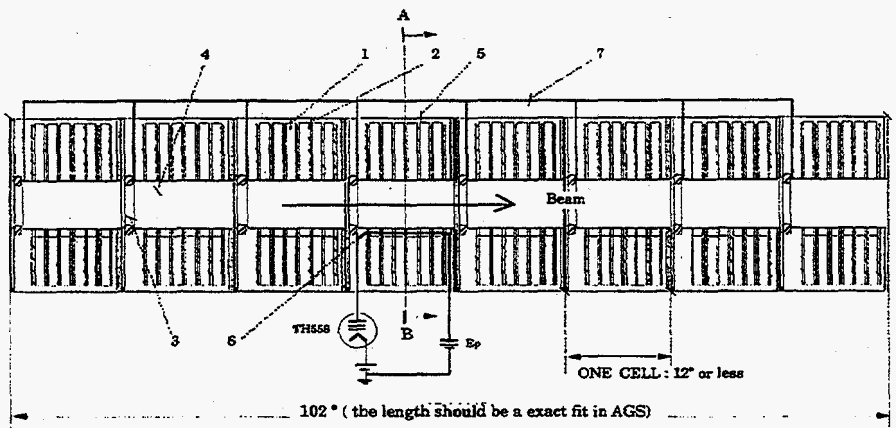

1. Ferrite disc : ø500 x ø200 x t28 (mm) , 6 per cell
2. Cooling Plate : 1/4" thick , 7 plates per cell
3. Accelerating Ceramic Gap : max. 10kV gap voltage at 4MHz
4. Beam Pipe : bore should be as same as a present pipe
5. Outer Conductor of the Cavity
6. RF Power Feed Line
7. Bus Bars Cell Connection

View A - B

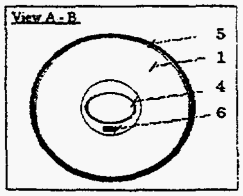

March 26 1997
M.YOSHII

22

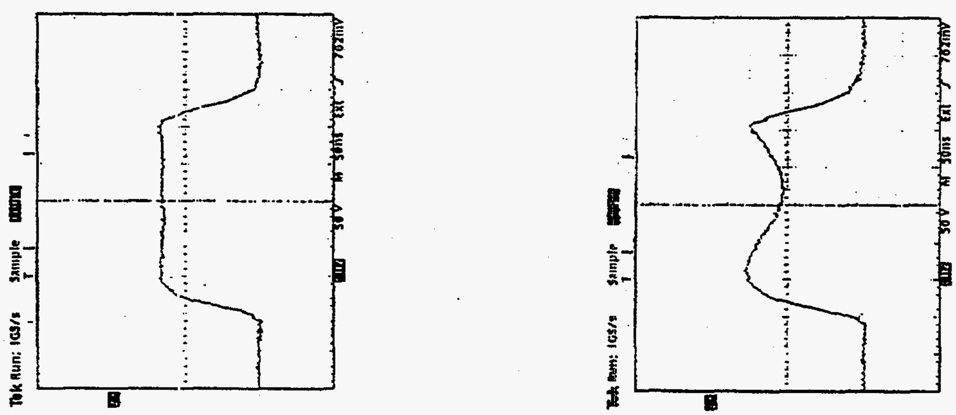

21

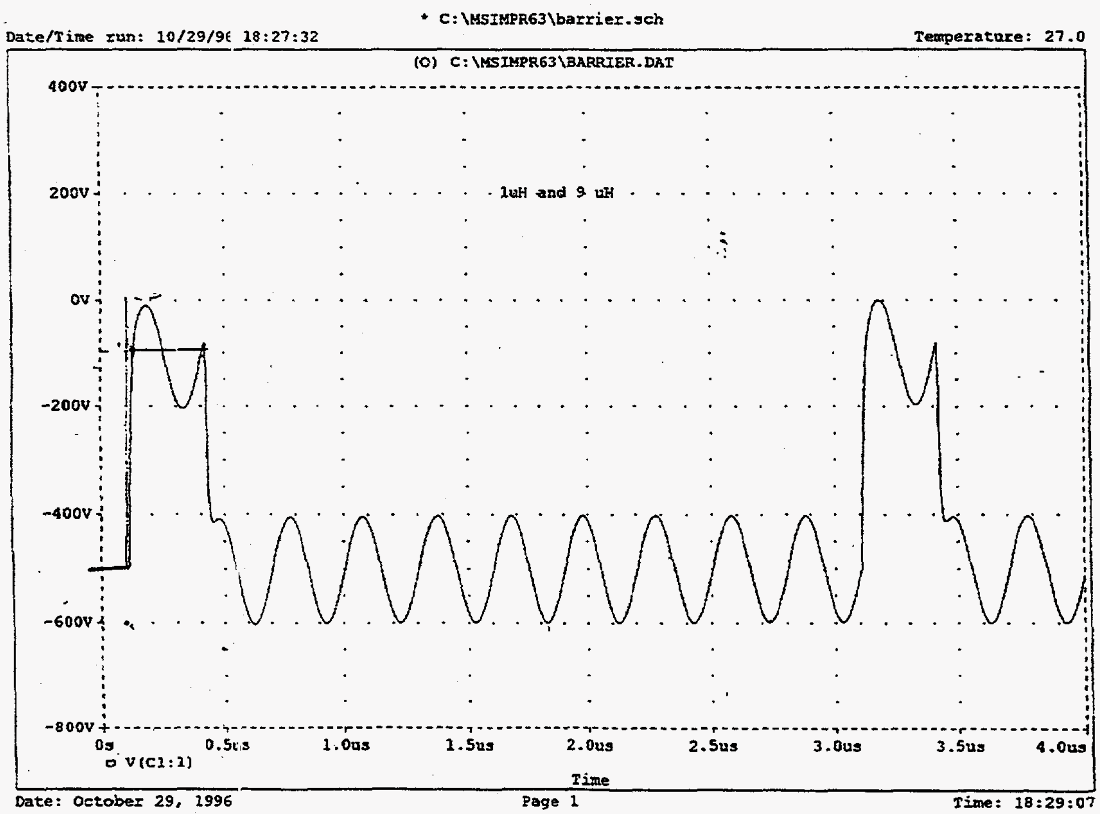
* C:\MSIMPR63\barrier.sch
Date/Time run: 10/29/96 18:27:32
Temperature: 27.0
(O) C:\MSIMPR63\BARRIER.DAT
400V
200V
0V
-200V
-400V
-600V
-800V
1uH and 9 uH
0s
0.5us
1.0us
1.5us
2.0us
2.5us
3.0us
3.5us
4.0us
V(C1:1)
Time
Date: October 29, 1996
Page 1
Time: 18:29:07

Kenny's cavity (1/8 model)

Results of High Power Test

6 x 4L2 Ferrites

Vgap
(10kV/div)

Vgrid
(100V/div)

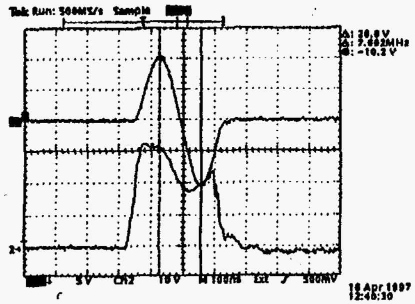

Irf
(40A/div)

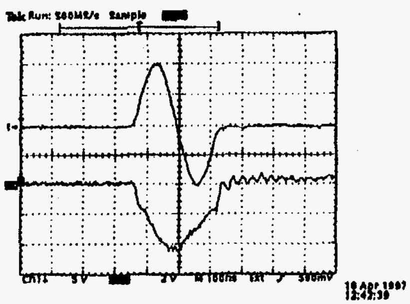

Vg = -375 V, f = 3.8 Mhz

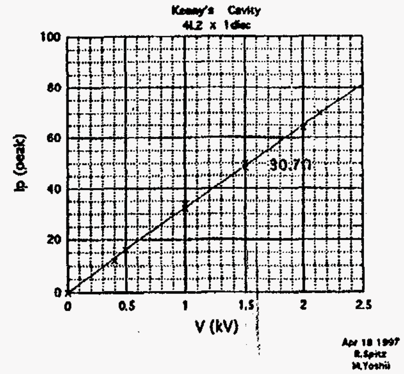

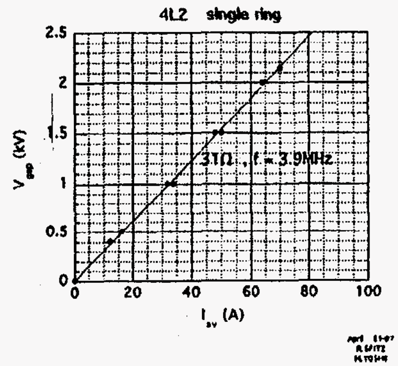

4B3 x 2 discs

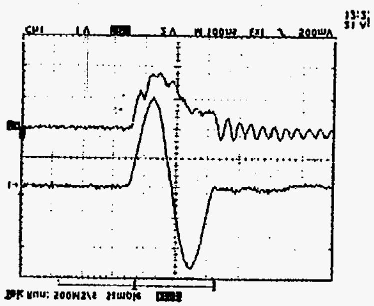

f = 3.7 MHz
Q = 2
V_{peak} = 2.8kV
I_{ave} = 44 A
ωL = 59

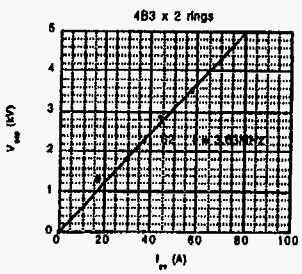

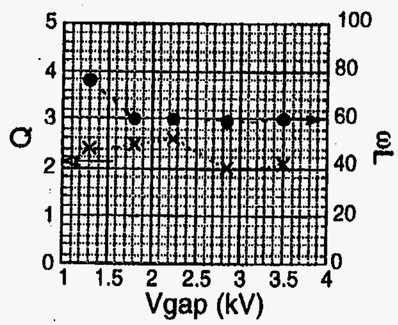

MAY 7-97
M.YOSHII
Mini-Workshop

SUMMARY

In order to minimize the driving current ;<400A

N dependence of gap capacitance and the effect of cooling plates have been studied

>> $C_{gap} \approx const. + C_1/N$

>> cooling plates must be electrically isolated

Experimental results explained G.Rakousky's representations about μ and flux distribution in a ferrite

(as far as major magnetizing process)

Sample measurements

there were only two interesting ferrite found.

New design

8 gap, 80 kV per station, six rings per gap

basic design has been done

1/8 model cavity

10 kV gap voltage with 6 x 4L2 was achieved

(2.2 kV !! per ring with one 4L2)

new grid drive circuit has been test well

As a minor problem,

no satisfied ferrite material yet

fast grid circuit needs some improvements

to need dumping the ringing on the plate current

R&D Works for RF System of JHF

Chihiro Ohmori
KEK-Tanashi

REQUIREMENTS FOR RF SYSTEMS

	Booster	Main Ring
RF VOLTAGE	~450 kV	270 kV
RF FREQUENCY	1.99-3.43 MHz	3.43-3.51 MHz
REPETITION RATE	25Hz(50Hz)	0.3 Hz
CIRCULATING CURRENT	4 - 7 A	6.4 - 6.6 A
I_B	8 - 14 A	12.8 - 13.2 A

REQUIREMENTS FOR RF SYSTEMS

NEED HIGH VOLTAGE

SPACE IN BOOSTER IS LIMITED
(24*6m STRAIGHT SECTION).

50 Hz OPERATION NEEDS 800~900 kV

~40 kV/CAVITY/3~4M
>10 kV /m (>13 kV/m)

10 Hz OPERATION FOR MAIN RING (in future)

>10 kV /m

REQUIREMENTS FOR RF SYSTEMS

STABILITY FOR BEAM LOADING

CIRCULATING CURRENT	4 - 7 A
I_B	~14 A
Y (= I_B/I_0)	< 1.4
I_0	10 A

To handle Beam without direct feedback.

REQUIREMENTS FOR MAGNETIC CORE

ASSUME ~20 CORES PER METER
2.5 cm thickness

V > 500 V

R > 100 Ω

SUMMARY OF MAGNETIC CORE MEASUREMENTS

	CORE FOR BOOSTER	CORE FOR MAIN RING
HITACHI N5C	NOT GOOD	NEED BIG CORE
PHILIPS 4M2	OK	NOT GOOD (HIGH LOSS EFFECT)
TDK SY2	NOT GOOD	NEED BIG CORE
FINEMET FT3	PROBABLY OK	OK

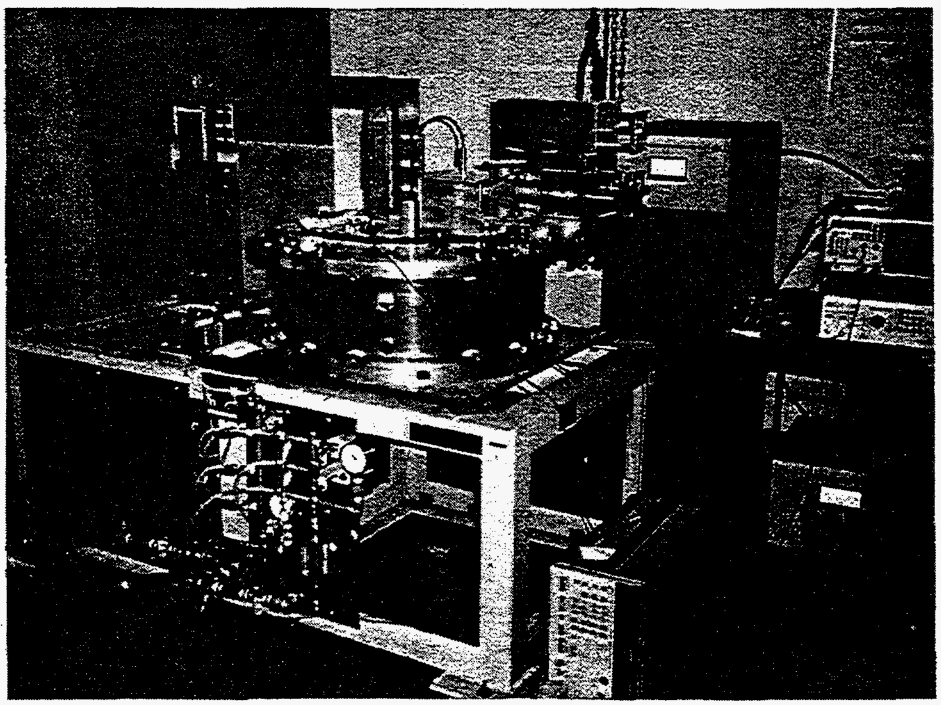

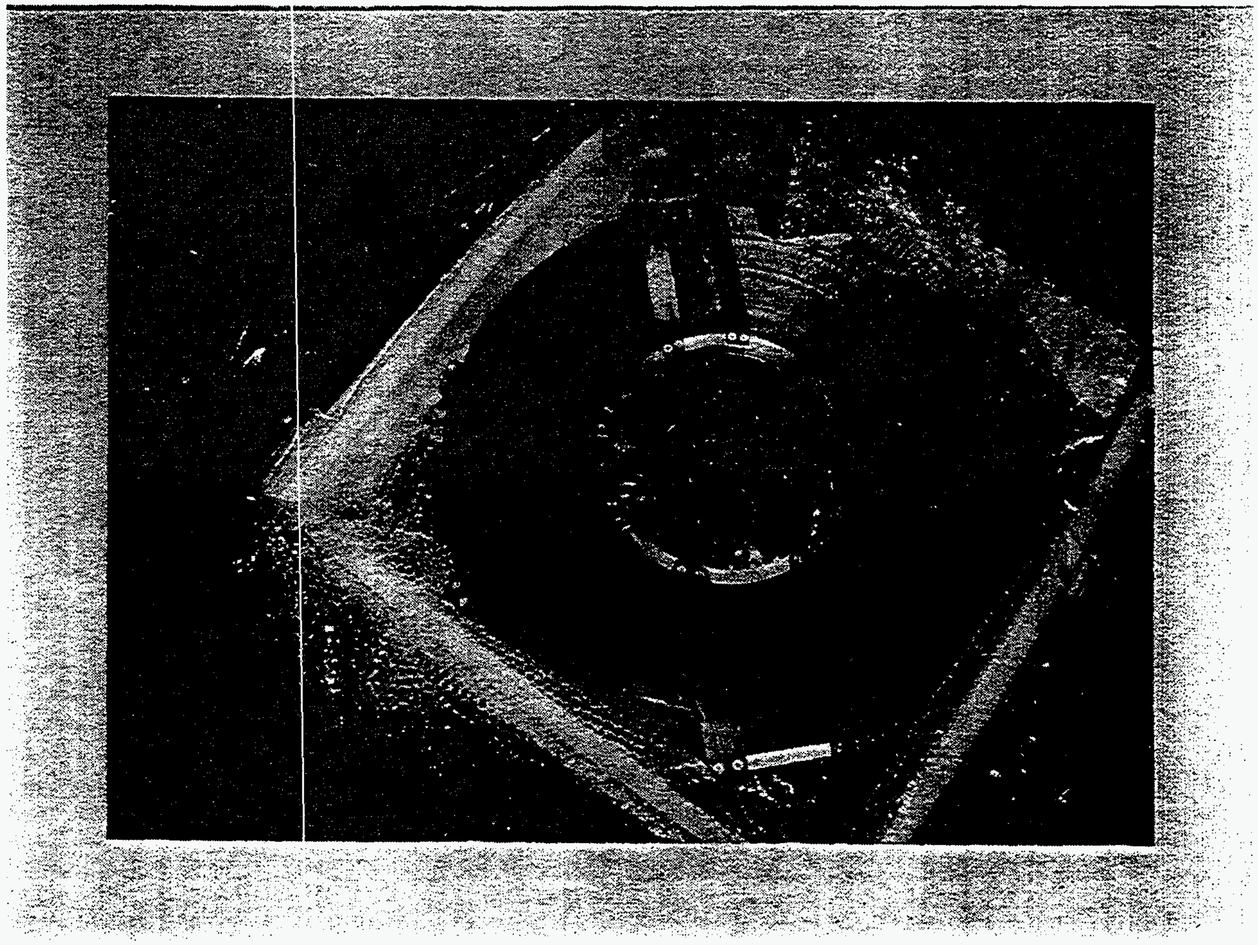

What is FINEMET?

Soft Magnetic Material with very fine crystallized structure.

High Permeability 1931@3.3MHz
Low Quality factor 0.63@3.3MHz
R 76 Ω@3.3MHz
R~100 Ω for new core as O.D. is large (67cm).

Very High Curie Temperature ~600 deg.C

Very Stable for Temperature and RF Power

Very thin tape, Easy to make a big core

Not Saturated @ 10 A

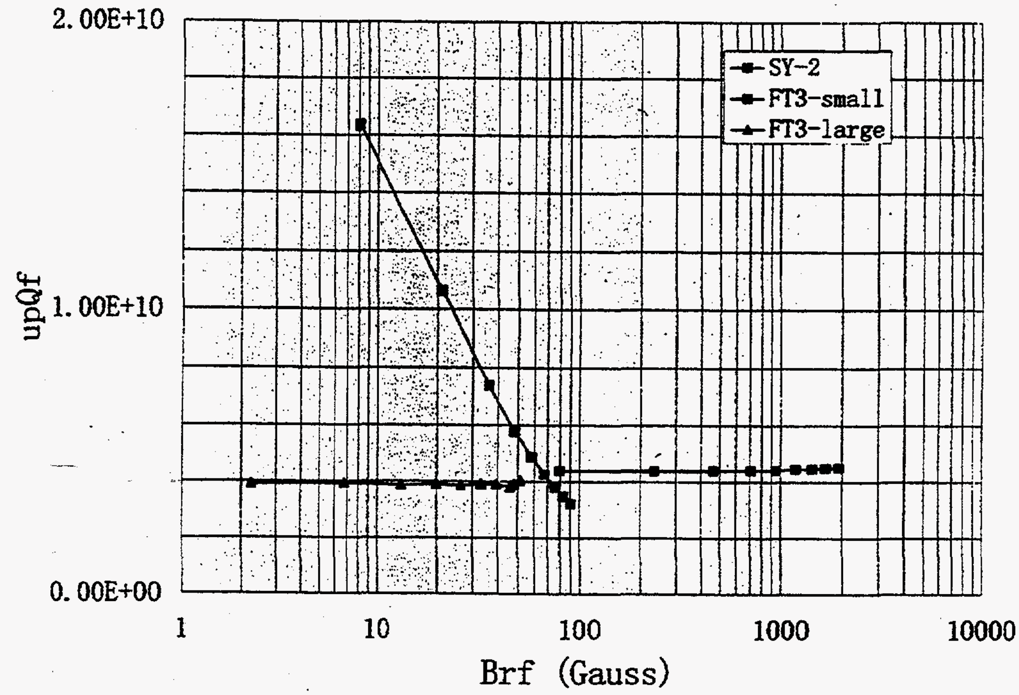

FINEMET CAVITY

Suitable for Barrier Bucket RF

Easy to make an isolated pulse

Many possibility for RF gymnastics

To store more particles
To change RF frequency
To make empty bucket

Decrease Peak intensity

To flatten Bunch shape

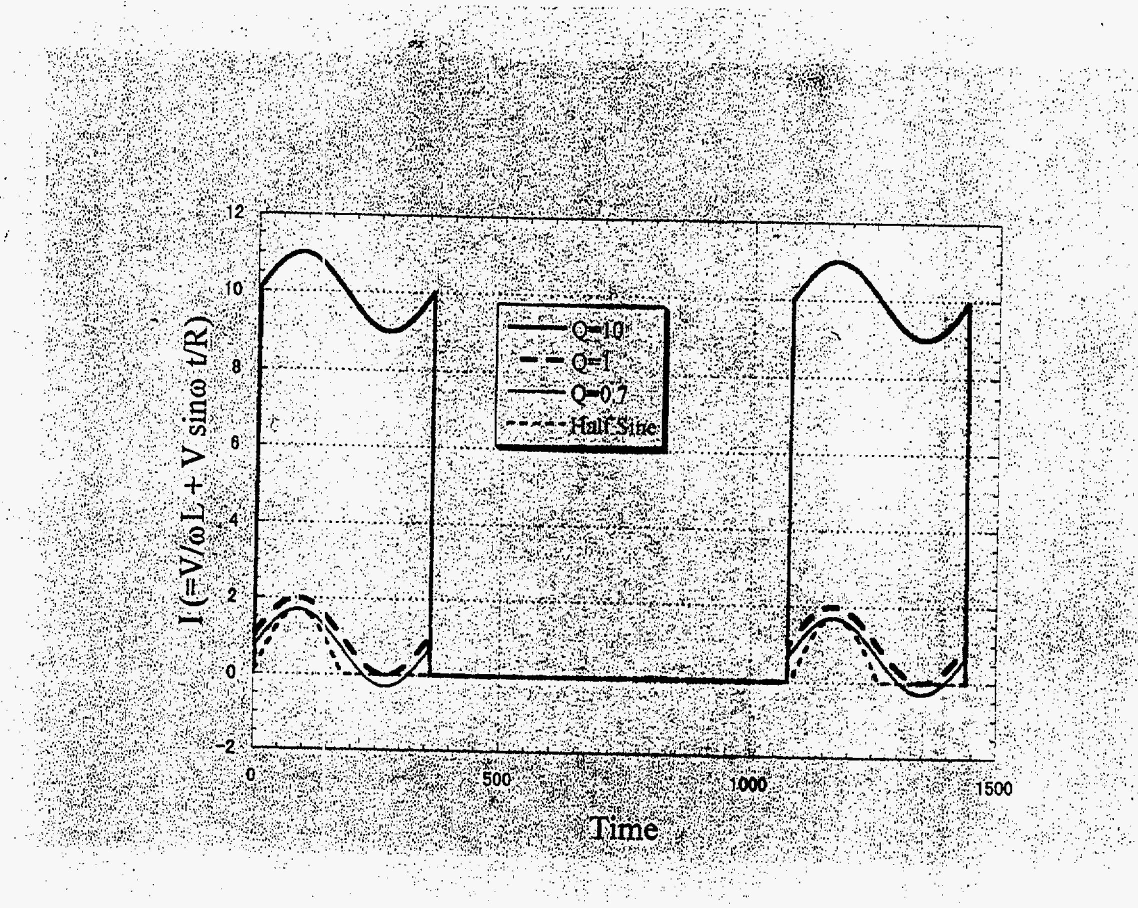

Barrier Bucket

JHP synchrotrons : very high intensity machines.

To reduce beam loss is important issue.

Stable operation @ high intensity

Reduction of S.C. tune shift.

To change Beam distribution

To store more particles in rings

Barrier Bucket is very attractive !!!

FINEMET CAVITY

Dump wake field quickly

Good for instabilities,
Coupled bunch as H=4 for Booster
as H=17 for Main Ring

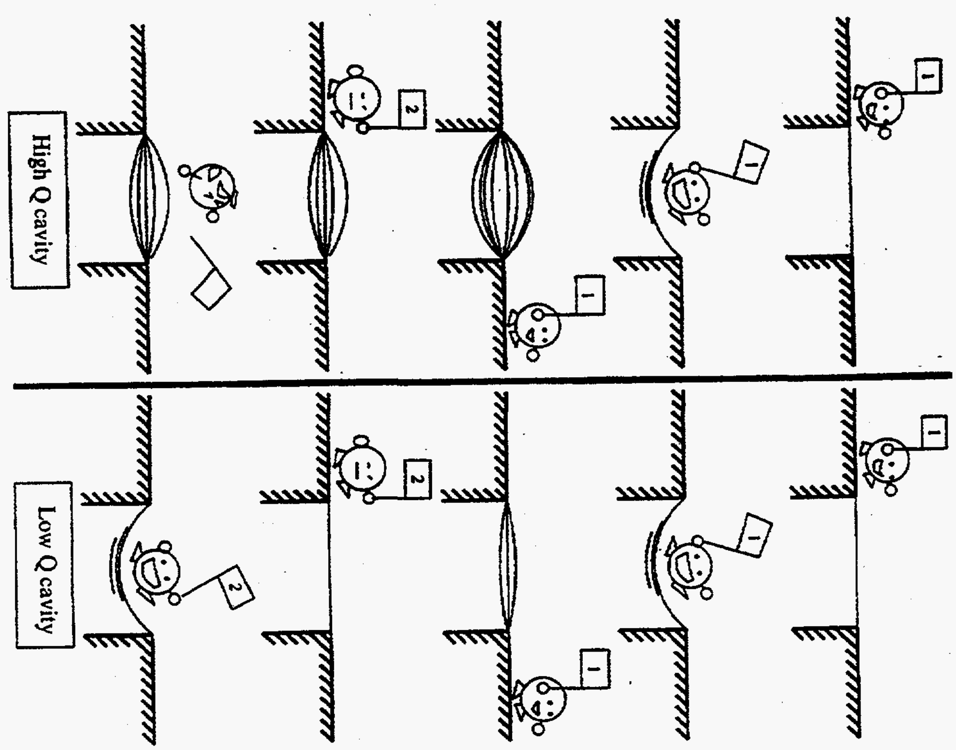

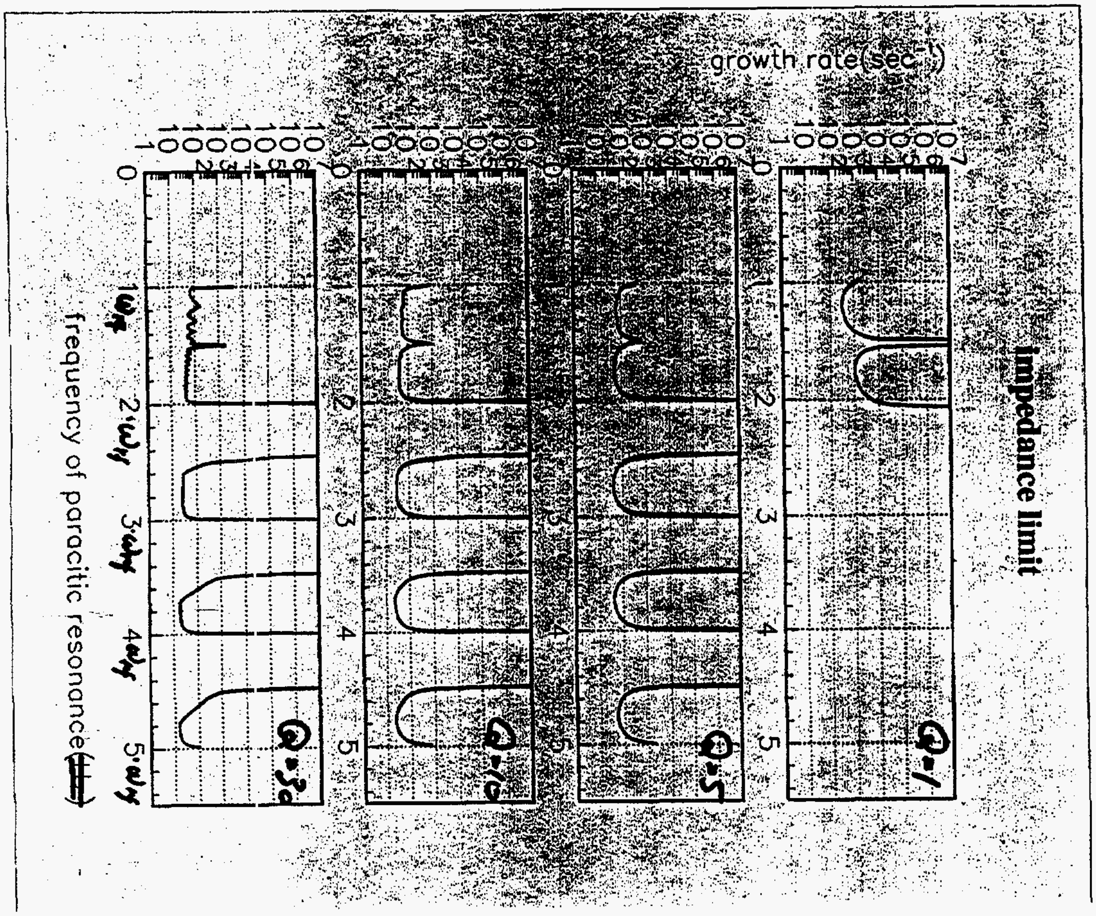

ft3 series グラフ 3

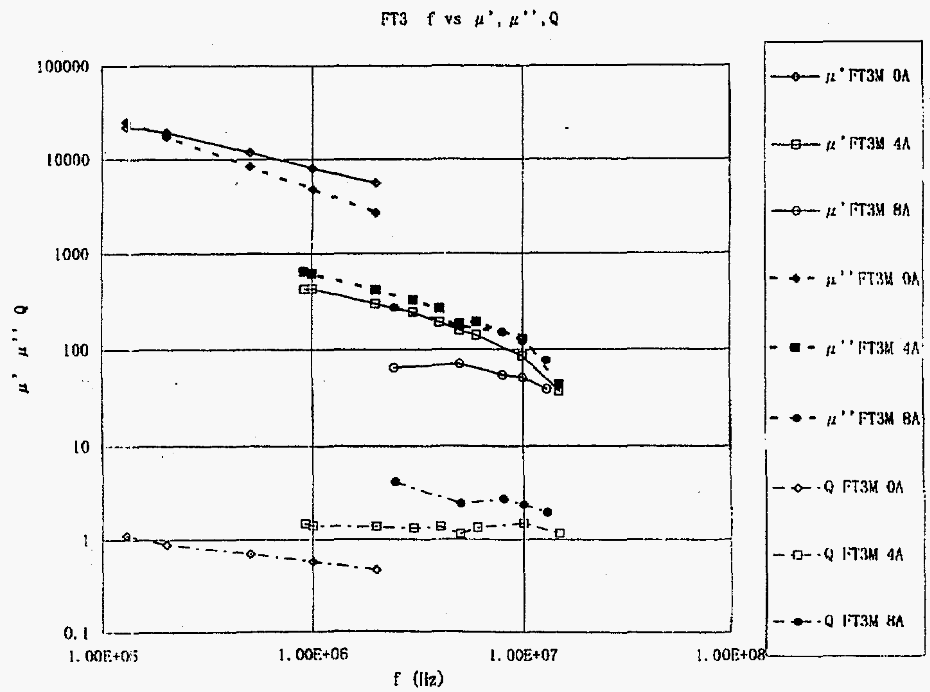

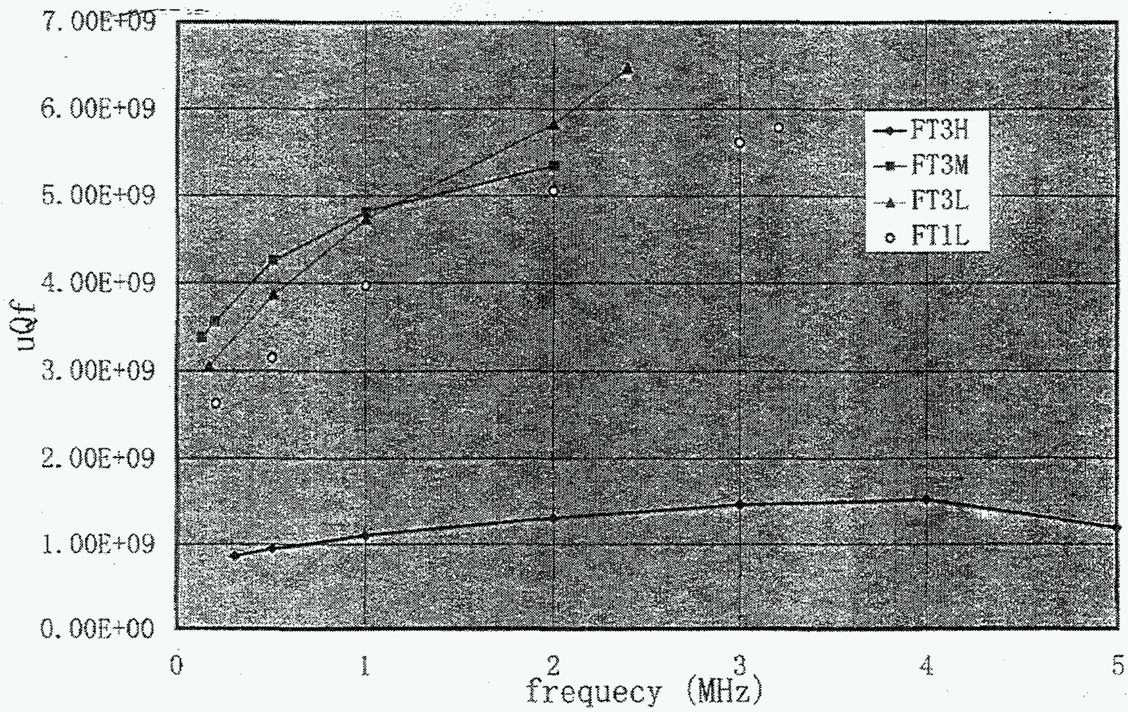

$$Q = \frac{R}{\omega L} = \frac{\mu'' \ln\frac{b}{a}}{\mu' \cdot \ln\frac{b}{a}}$$

FT3 f vs μ', μ'', Q

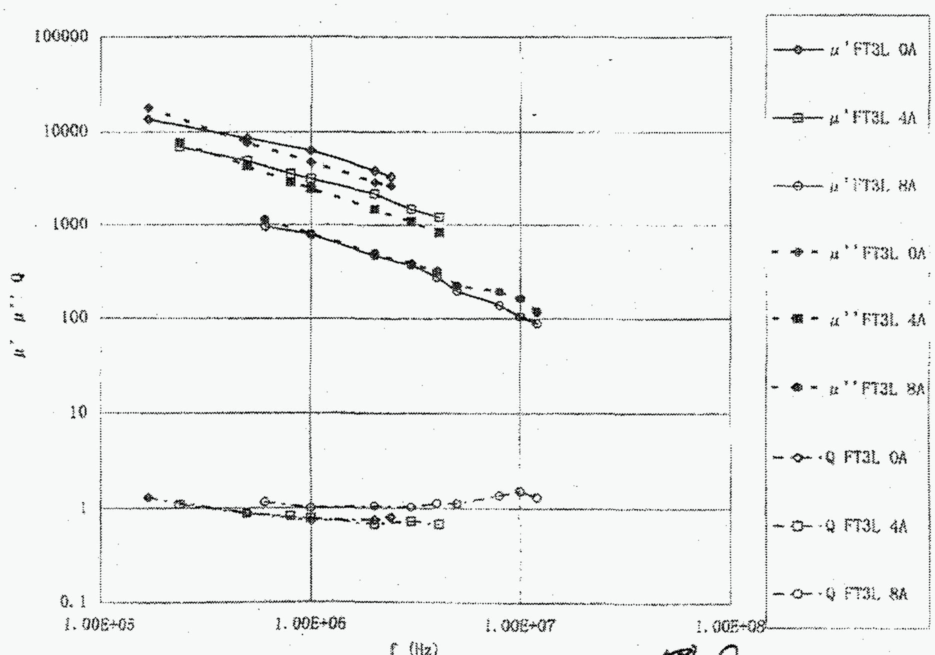

$$Q = \frac{R}{\omega L}$$

The aim of the 30 kW test cavity is to prove the following:

- The required accelerating voltage of 10 kV/m can be obtained.
- The isolated pulse for the barrier bucket can be generated.
- The frequency of the parasitic resonance is very high and/or the quality factor is low enough to avoid the dangerous growths of the instabilities.
- The beam loading and transient beam loading effects are controllable.

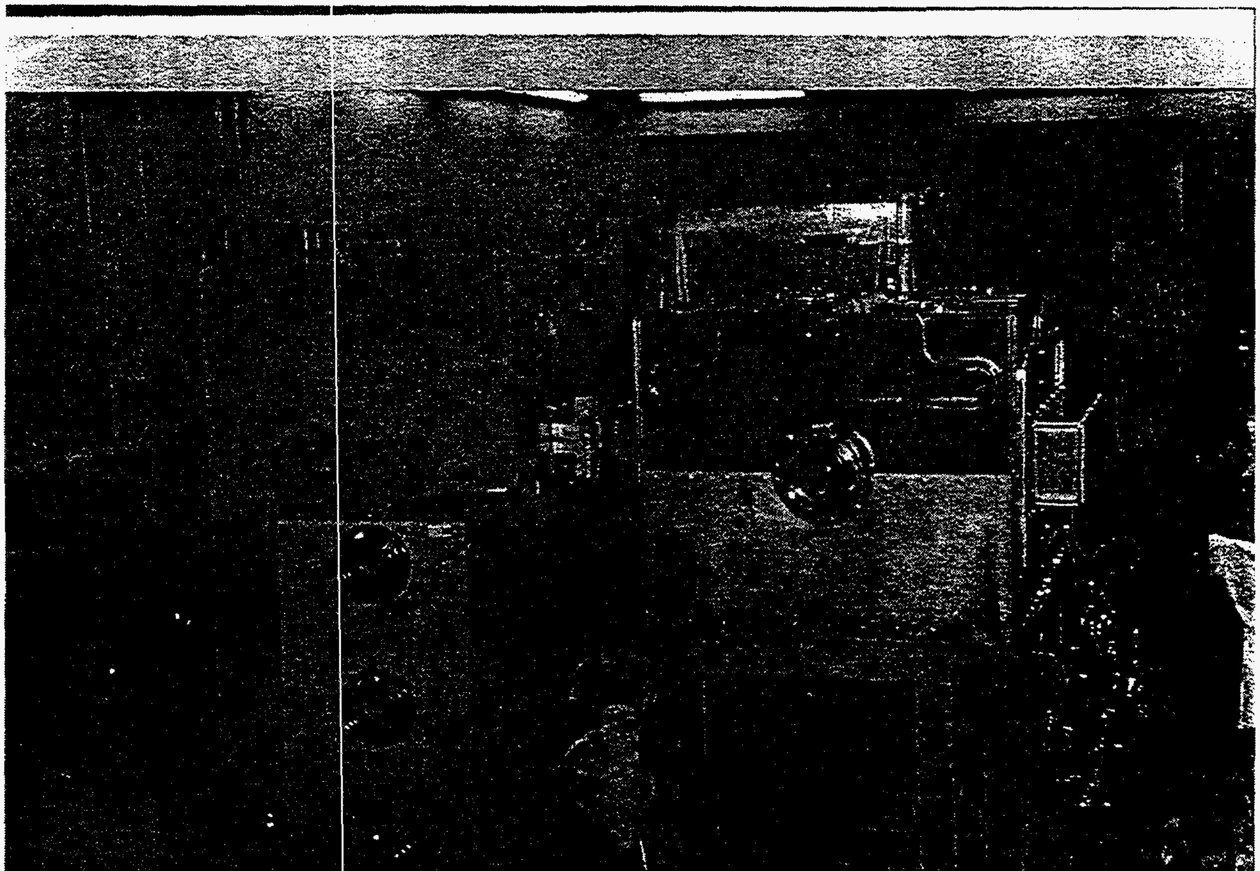

The test cavity and amplifier. Behind the cavity, there are a high voltage station and a power

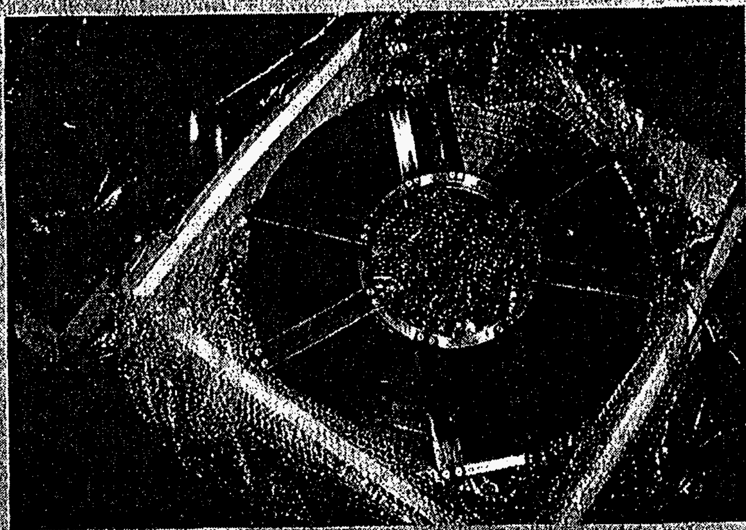

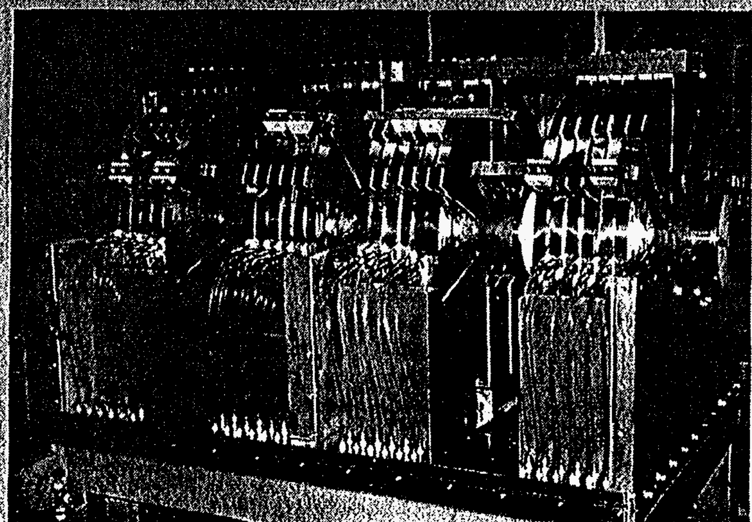

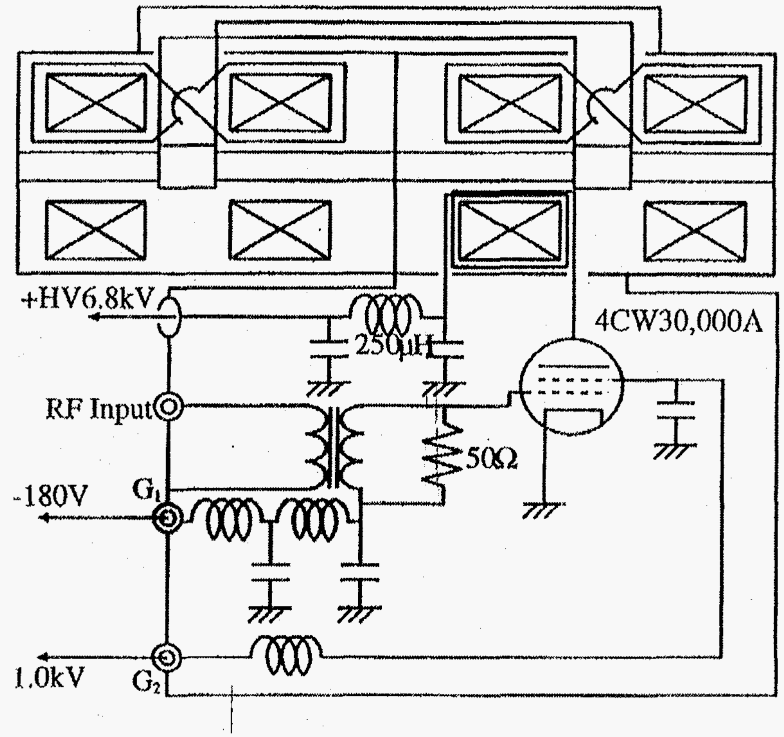

+HV6.8kV
250μH
4CW30,000A
RF Input
50Ω
-180V
G1
1.0kV
G2

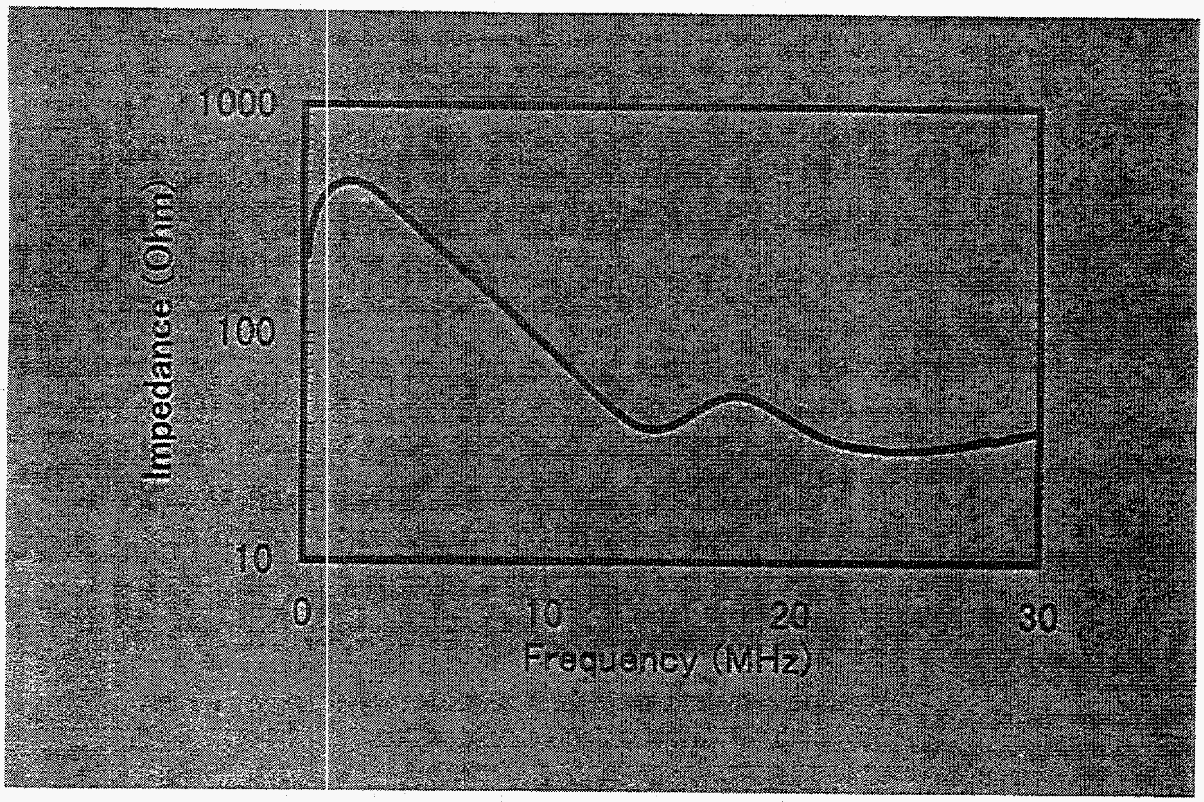
Impedance (Ohm)
1000
100
10
0
10
20
30
Frequency (MHz)

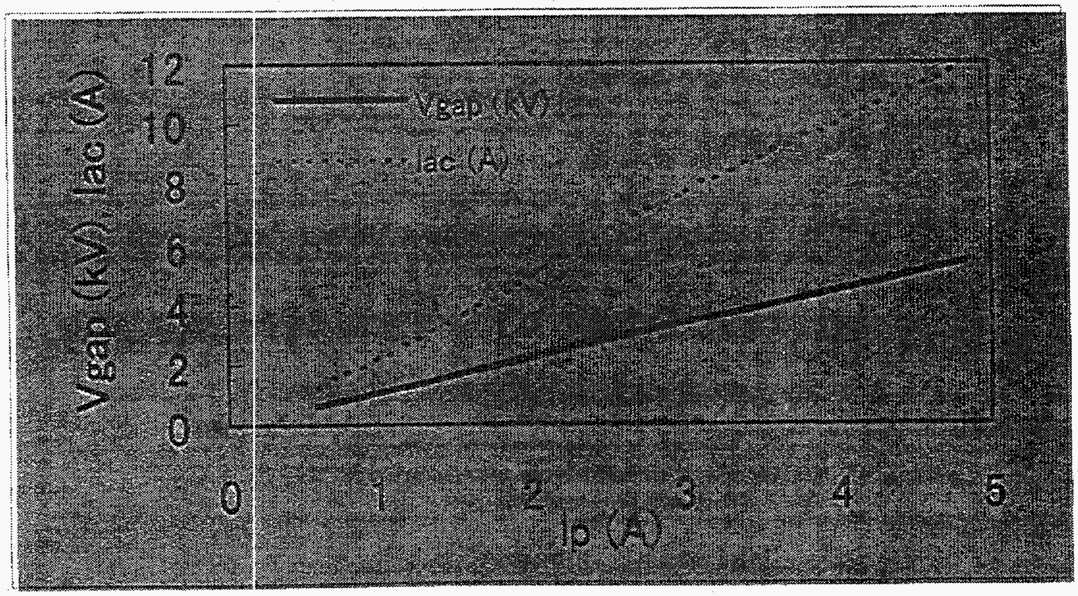
Vgap (kV), Iac (A)
12
10
8
6
4
2
0
Vgap (kV)
Iac (A)
0
1
2
3
4
5
Ip (A)

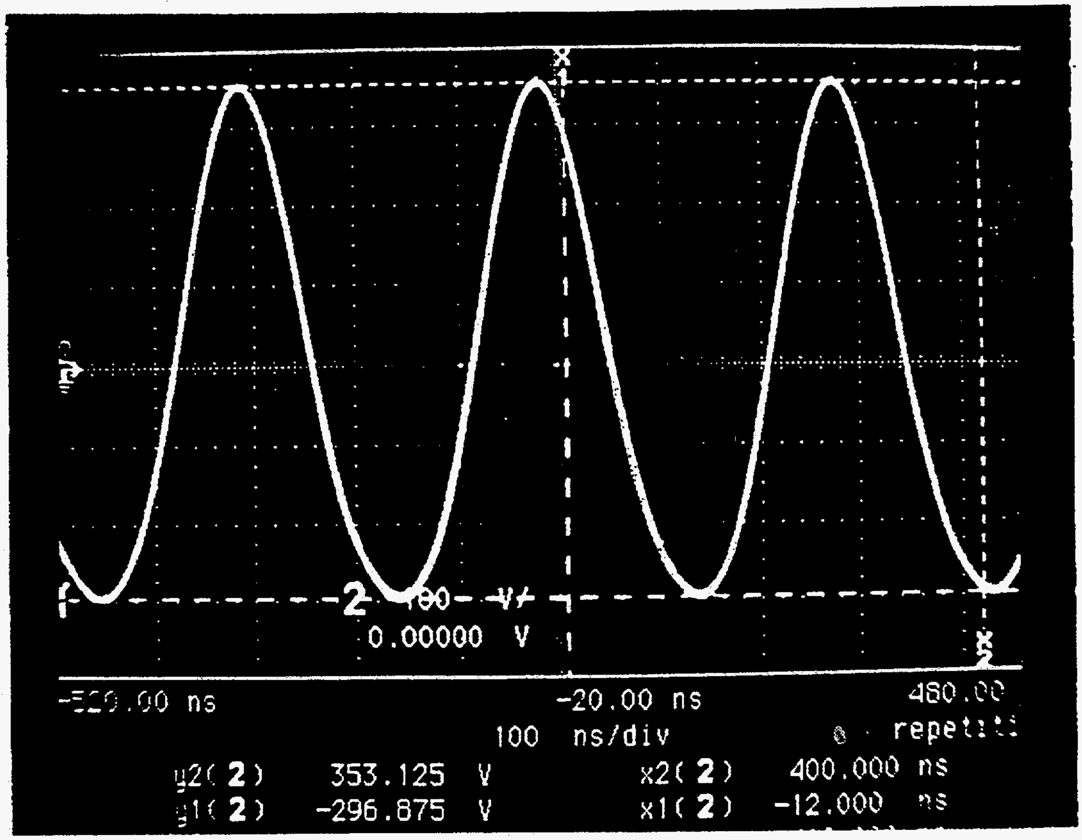

The typical RF voltage signal in the class AB operation.

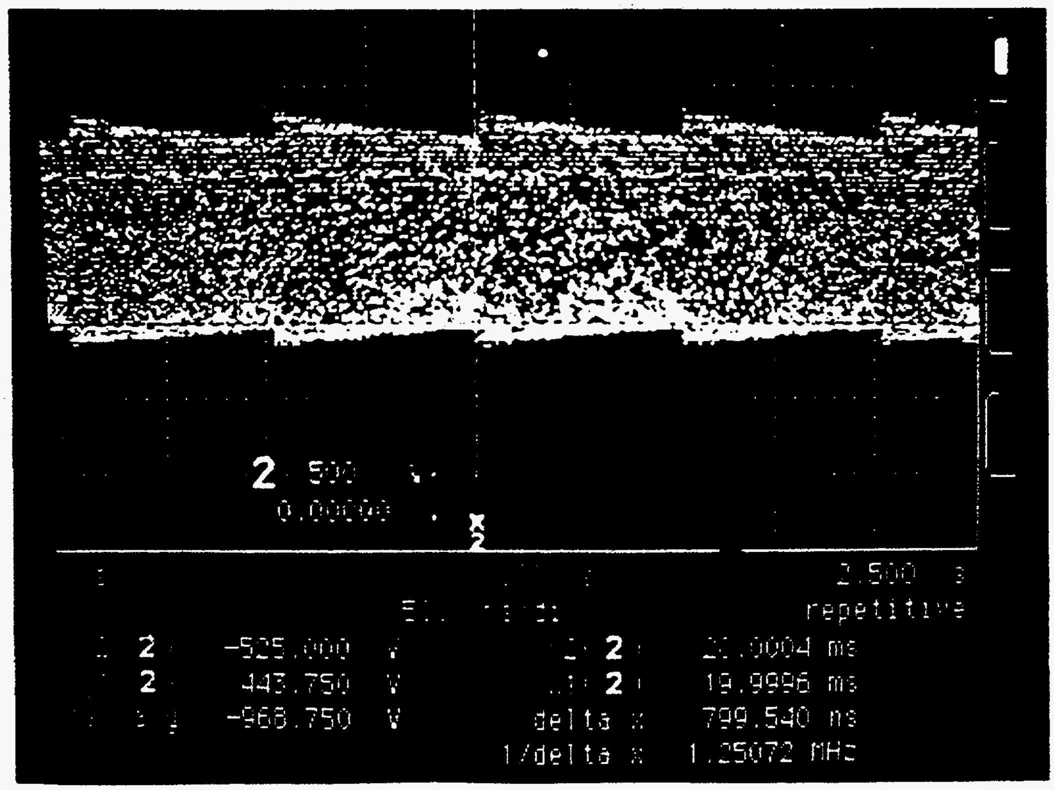

The RF voltage signal for the frequency sweep of the range of 2 to 3.4 MHz. The repetition is 1 Hz.

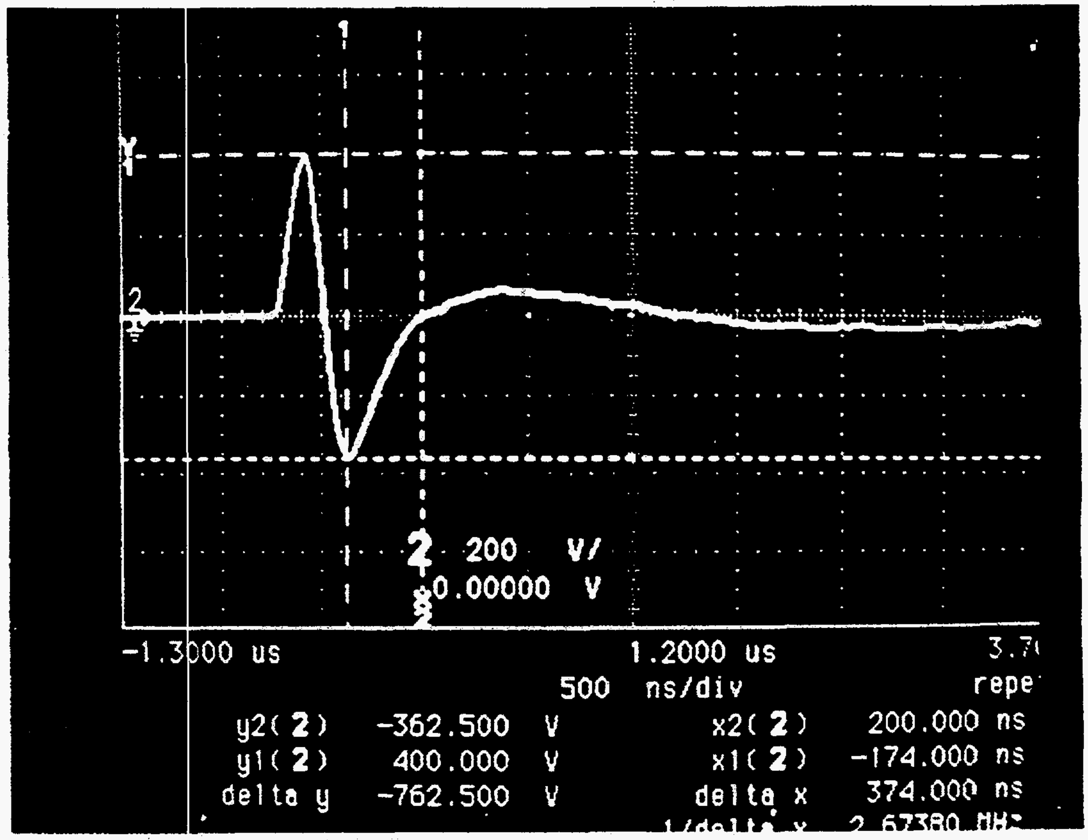

The typical voltage signal in the class AB operation for the barrier bucket.

Beam Loading

RF system does not include the tuning loop.→Simpler

for Fundamental Frequency

Y=1.4 was chosen for stable operation

If no tuning system, compensation technique is required.

Ex.: feed-forward

Beam Loading

- Electron Gun will be ready in summer.
  About 200 keV, 7 A, 1μs

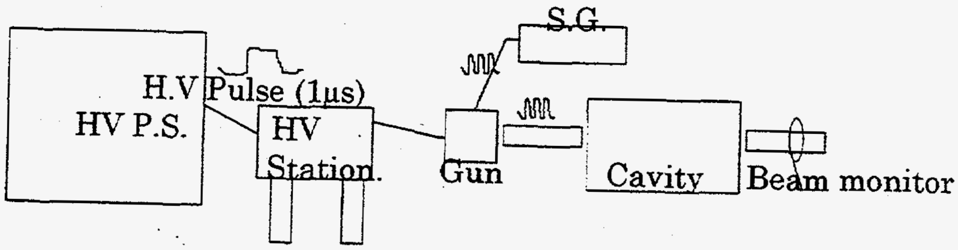

Aims:

Beam Loading Effects

Fundamental, Higher Order(Distortion of RF Bucket)

Transient Beam Loading

Compensation Techniques.

---

for 2nd(3rd) harmonics

Component in the beam current is about 30% (for half-sine) of the fundamental component.

Impedance is also about 30% of that at the RF frequency.

Effects are about 10 % of those by RF frequency components.

It may be possible to compensate by feed back and/or feed-forward techniques.

Transient Beam Loading

As Q-value is low, effects excited by other bunches have been damped, automatically.

Because of fast response, compensation is applicable.

CONCLUSIONS

The test cavity using a new material has been developed.

The voltage more than the designed value has been obtained. In order to achieve the higher voltage, a new material is being developed.

The impedance measurement shows that the cavity has no dangerous parasitic resonance.

An isolated pulse for the barrier bucket was generated and the maximum voltage of 11.3 kV was obtained.

However, the distortion of RF voltage was not small because of the class B operation of the single tube. It is expected that the distortion will be improved by the planned modification of the amplifier to a push-pull amplifier.

Session on Longitudinal Emittance Control

R. Garoby

On the issue of emittance control, representatives of Brookhaven and CERN have presented their aims and worries for achieving the level of performance ultimately needed by their respective future high energy machines. One step further in the future, the issue of longitudinal space-charge effects and possible cure in the 3 GeV proton driver for the proposed muon collider was described.

1. For RHIC at Brookhaven the gymnastics taking place in the AGS are the dominant source of longitudinal emittance blow-up (J.M. Brennan). Recent results have been shown, where the final bunch emittance approaches 0.7 eVs/u, for an initial design goal of 0.2 eVs/u. Two directions are pursued for solving the problem:
a) improvement of the gymnastics in the AGS. Many of the reported imperfections are attributed to the lay-out and adjustment of the low level RF hardware, and solutions are being designed (J.M. Brennan).
b) increase to 0.5 eVs/u of the nominal emittance accepted by RHIC. A larger emittance is beneficial at injection energy because it reduces intra-beam scattering. The first bottleneck used to be at transition because RHIC ramping rate is limited by the superconducting magnets, and transition is crossed slowly. But thanks to the newly agreed transition jump scheme, bunches of 0.5 eVs/u can now be accelerated with less than 10 for the second bottleneck due to the rebucketing (bunch transfer from a 28 MHz into a 196 MHz bucket), but improvement is possible doing it slightly above transition energy, where acceptance is largest (J. Kewisch).

2. For LHC at CERN most longitudinal beam characteristics are established in the PS. Specifications result from SPS characteristics (RF frequency and single bunch beam stability at injection) and LHC requirements (25 ns bunch spacing and number of protons per bunch), and the overall emittance budget is tight (E. Jensen). The undergoing LHC injectors project is implementing the most economical means to approach the nominal performance. Results will be obtained already in 1998. The hope is that the combination of these improvements with the planned SPS upgrade programme will help achieve the full beam performance needed at injection in LHC. Controlled longitudinal blow-up is a necessary ingredient and future plans include the use of a new method to generate flat-topped bunches corresponding to hollow distribution (S. Hancock). A promising technique for tomography in the longitudinal phase plane is under investigation for monitoring beam characteristics, even in the presence of non-linearities and/or time-varying potential.

3. Space-charge in the proton driver rings of the muon collider dangerously reduces the longitudinal focusing given by RF (K.Y. Ng). Compensation by an inductive impedance is a tempting challenge, which is under investigation. The design presented is based on a 2.4 m ferrite cylinder surrounding the beam with perpendicular bias by a solenoidal field to follow the variation of potential well distortion between 1 and 3 GeV. Tests are planned in the PSR ring at Los Alamos which suffers from similar effects.

Third ICFA Mini-Workshop on High Intensity, High Brightness Hadron Accelerators Brookhaven National Laboratory May 7-9, 1997

Controlled Longitudinal Blow-ups

S. Hancock CERN

As the name suggests, the purpose of a blow-up is to increase the longitudinal emittance of the beam in a reproducible fashion. This reduces the peak beam current and hence the so-called Laslett tune shift, which is important at low energy. It also increases beam stability by increasing the spread of synchrotron frequencies of particles in a bunch.

In the special case of a stationary bucket, the synchrotron frequency, fs, may be expressed in terms of the complete elliptic integral of the first kind.

```
fsratio[r_] := (Pi/2) / EllipticK[ Sin[ phihat[r]/2 ]^2 ]
phihat[r_] := ArcCos[1 - 2 r^2]

Plot[
  fsratio[r],
  {r, 0,1}, PlotRange->{0,1.5},
  AxesLabel->Map[FontForm[#,{"Courier-Bold",10}]&, {"r","fs/fs0"}]];
```

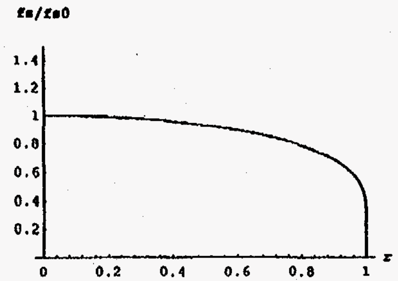

Here, r is the synchrotron amplitude and varies from 0 at the centre of the bunch to 1 at the bucket separatrix.

The addition of a phase-modulated, high-frequency RF modifies fs depending upon the voltage and frequency ratios and upon the amplitude of the phase modulation. Normalized to the unperturbed small-amplitude synchrotron frequency, the modified value is

```
perturbedfsratio[r_] := fsratio[r] *
  (1 + VRFratio BesselJ[0, Amod] BesselJ[1, 2 r hratio] / (2 r))
```

for VRFratio < 0.3 and integer hratio. The SFTPRO cycle, for example, typically has VRFratio ~ 6kV/45kV, hratio = 479/20, Amod = Pi for BU1 and VRFratio ~ 10kV/40kV, hratio = 433/20, Amod = Pi for BU2. However, whatever the frequency ratio of the two RF systems, the underlying principle of blow-ups is the same:

Phase space dilution occurs when particles at a certain amplitude have a synchrotron frequency which is resonant with the frequency of the phase modulation. This results in non-zero dr/dt for those particles.

Experiments, with both integer and non-integer hratio, support the theory. See CERN/PS 92-40 (RF).

```
Plot[
  Evaluate[
    perturbedfsratio[r] /. {VRFratio->0.1, hratio->22, Amod->{1.6,3.8}}
  ],
  {r, 0,1}, PlotRange->{0,1.5},
  AxesLabel->Map[FontForm[#,{"Courier-Bold",10}]&, {"r","fs/fs0"}]];
```

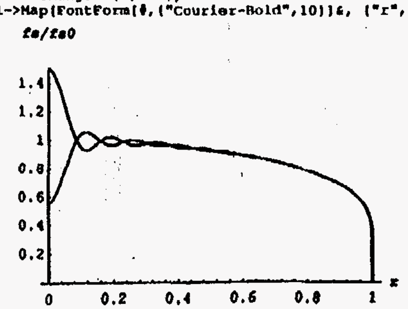

MOTIVATION

$$\text{(Laslett) Tune shift, } \Delta Q \propto -\frac{1}{B_f}$$

$$\text{Bunching factor, } B_f = \frac{\text{DC beam current}}{\text{Peak beam current}}$$

Can increase B_f

- by employing second-harmonic cavities to modify the bucket, but this
  - "wastes" RF voltage
  - introduces phasing complications
- by modifying the distribution of particles in phase space.

Projected (1-D) Density, $p(t)$

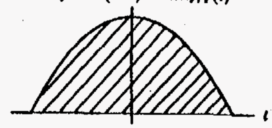

$p(t)$ = Line charge density function

Phase Space (2-D) Density, $\mathcal{P}(r)$

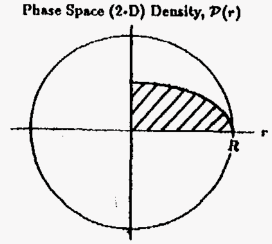

$$\mathcal{P}(r) = -\frac{1}{\pi}\int_r^R \frac{p'(t)}{\sqrt{t^2 - r^2}}dt$$

[Krempl, MPS/Int. BR/74-1]

$p(t)$ = Rectangular $\Rightarrow$ $\mathcal{P}(r) \propto \frac{1}{\sqrt{R^2 - r^2}}$ i.e., a "hollow bunch".

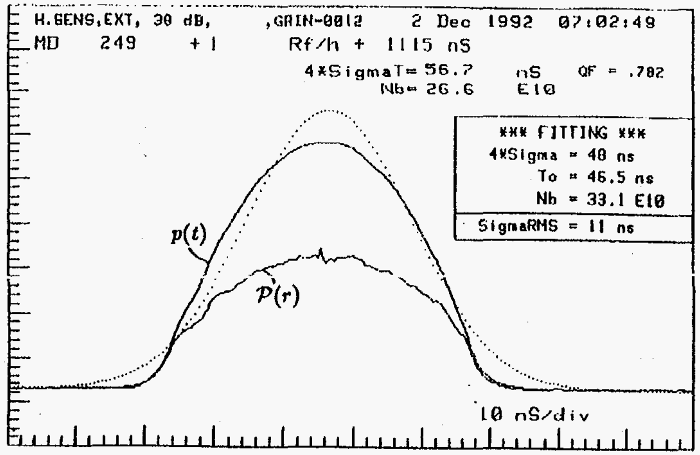

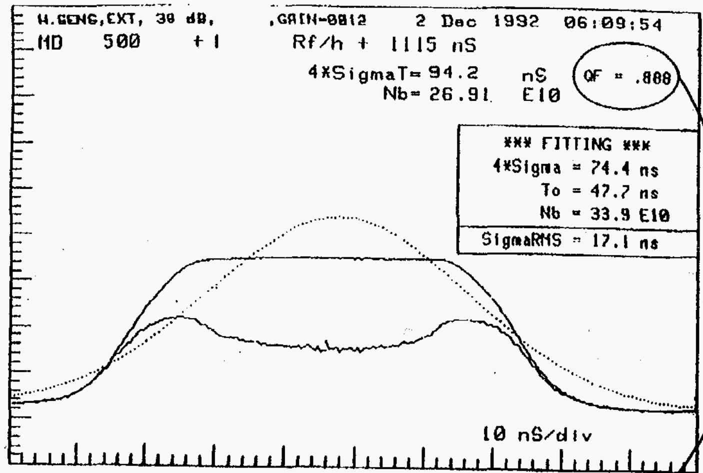

$$Q_f = \frac{\text{Mean (over } \pm\sqrt{3}\sigma_{t,rms}\text{) line charge density}}{\text{Peak line charge density}}$$

$p(t) = \text{Rectangular} \Rightarrow Q_f = 100\%$

$p(t) = \text{Parabolic} \Rightarrow Q_f = 80\%$

$p(t) = \text{Gaussian} \Rightarrow Q_f = 66\%$

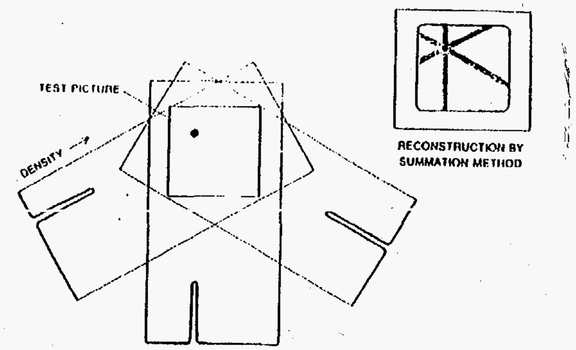

SUMMATION METHOD is a rough technique for reconstructing images from a series of projections. Here three projections are made of a simple two-dimensional test picture containing a single point. Each projection is a one-dimensional distribution of the density, or darkness, across the test picture as it is seen from a specific angle. In the case of this test picture the projection looks the same from all directions. The picture can be reconstructed from the projections: the density of each point on the reconstructed picture is estimated by adding up the densities of all the rays going through that point. The reconstruction of the single point is a "star," or spokelike image. The star is the "point-spread function" of the reconstruction technique. It approximately demonstrates the nature of summation method.

COMPLEX PICTURE CAN BE RECONSTRUCTED with a photographic analogue of the summation method devised by B. K. Vainshtein of the Institute of Crystallography in Moscow. The projection of the picture is made by moving a sheet of film across it as the film is exposed to light. The result is a "streak picture," a set of parallel lines whose darkness depends on the total density of the original picture along each line. A series of such projections can be made at various angles. The reconstruction is obtained by superposing the streak pictures photographically. Reconstruction at right was made with 18 projections spaced at intervals of 10 degrees.

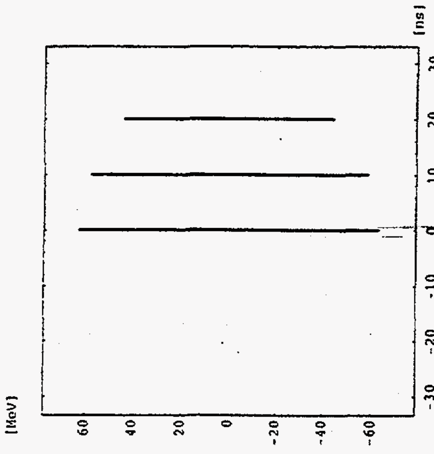
[MeV]
60
40
20
0
-20
-40
-60
-30
-20
-10
0
10
20
30
[ns]

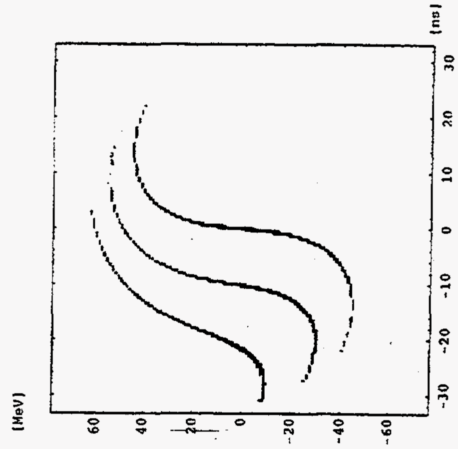
[MeV]
60
40
20
0
-20
-40
-60
-30
-20
-10
0
10
20
30
[ns]

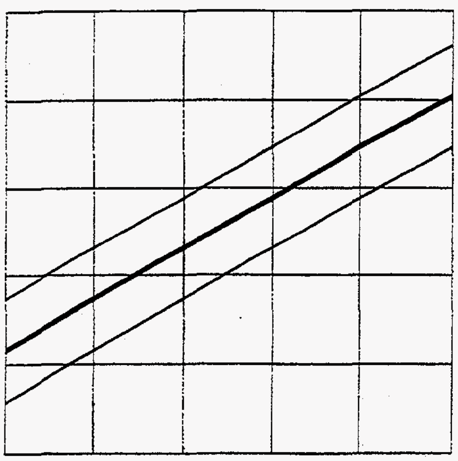

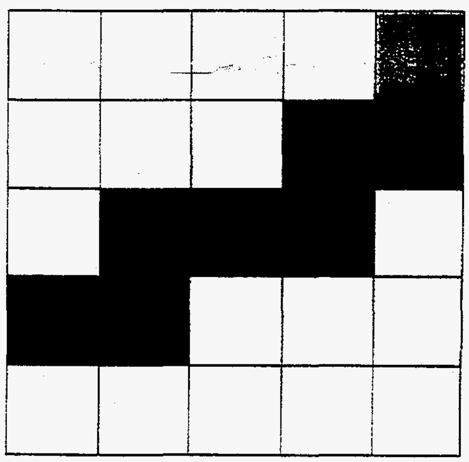

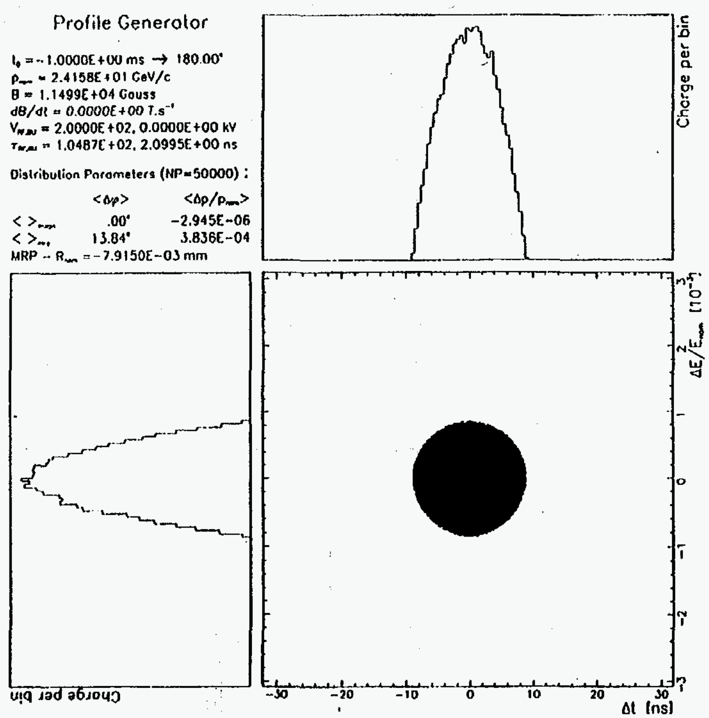
Profile Generator
t_ϕ = -1.0000E+00 ms → 180.00°
p_{nom} = 2.4158E+01 GeV/c
B = 1.1499E+04 Gauss
dB/dt = 0.0000E+00 T.s^{-1}
V_{RF} = 2.0000E+02, 0.0000E+00 kV
τ_{RF} = 1.0487E+02, 2.0995E+00 ns
Distribution Parameters (NP=50000) :
<Δφ> <Δp/p_{nom}>
< >$_{mean}$ .00° -2.945E-06
< >$_{rms}$ 13.84° 3.836E-04
MRP - R_{nom} = -7.9150E-03 mm
Charge per bin
ΔE/E_{nom} [10^{-3}]
Δt (ns)

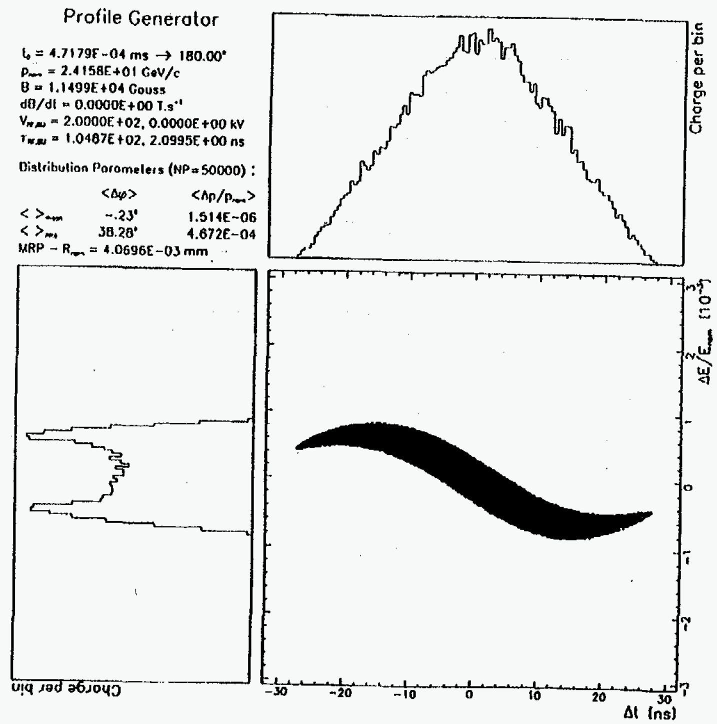
Profile Generator
t_ϕ = 4.7179E-04 ms → 180.00°
p_{nom} = 2.4158E+01 GeV/c
B = 1.1499E+04 Gauss
dB/dt = 0.0000E+00 T.s^{-1}
V_{RF} = 2.0000E+02, 0.0000E+00 kV
τ_{RF} = 1.0487E+02, 2.0995E+00 ns
Distribution Parameters (NP=50000) :
<Δφ> <Δp/p_{nom}>
< >$_{mean}$ -.23° 1.514E-06
< >$_{rms}$ 38.28° 4.672E-04
MRP - R_{nom} = 4.0696E-03 mm
Charge per bin
ΔE/E_{nom} [10^{-3}]
Δt (ns)

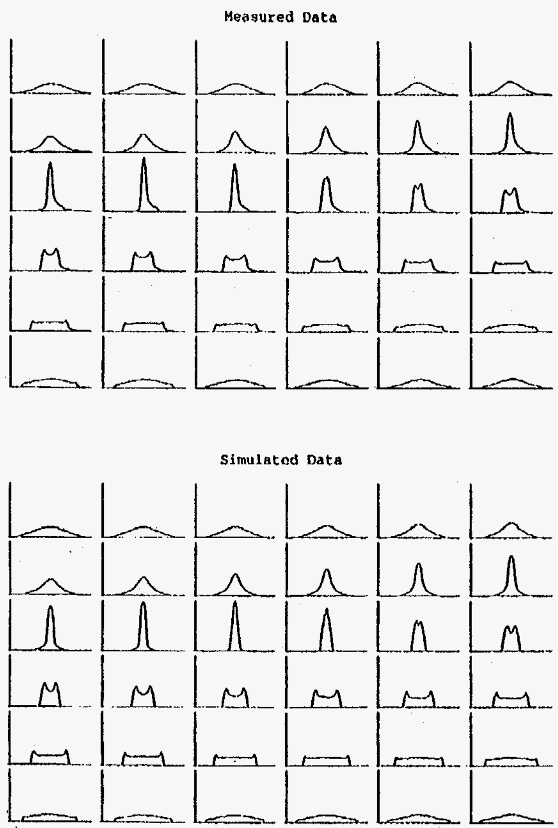

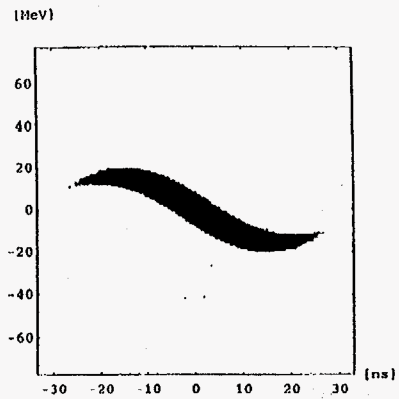

Original Distribution

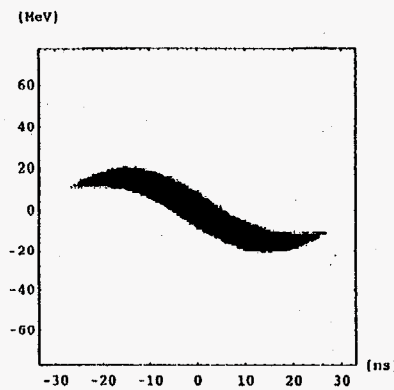

Reconstruction by Maps

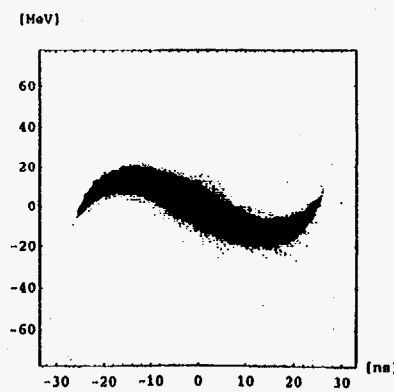

cf. "ART"

Advantages of the New Algorithm

- Large-amplitude motion is correctly treated.
- The constraint on trigger rate (re-arm deadtime) is relaxed.
- Computational investment in the maps benefits repeated use with different data - as in optimization.
- Replacement of the Runge-Kutta integration by full-blown tracking would permit the reconstruction of:
  - ◊ arbitrarily complex (even no) RF;
  - ◊ non-adiabatic processes;
  - ◊ self fields
  - ◊ particles outside the bucket (but NB normalization).

Question Marks

- How fast can it be made to run?
- Minimum number of profiles required.
- "Free" parameters: n, gain.
- Influence of the phase loop.

Ref: CERN PS/RF/Note 97-06

CERN injector complex

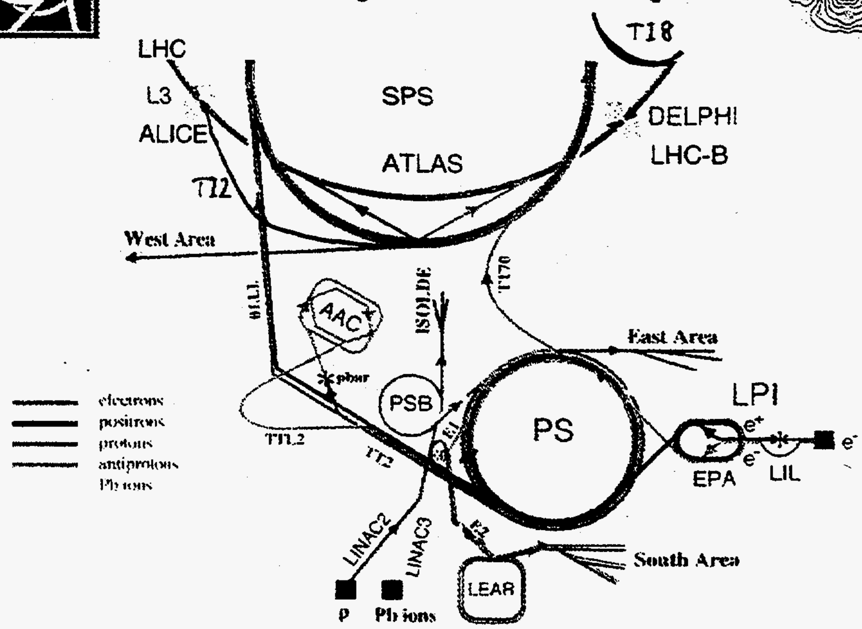

May 7-9, 1997 3rd MINI-WORKSHOP ON HIGH INTENSITY, HIGH BRIGHTNESS HADRON COLLIDERS *Erk JENSEN*

LHC filling scheme

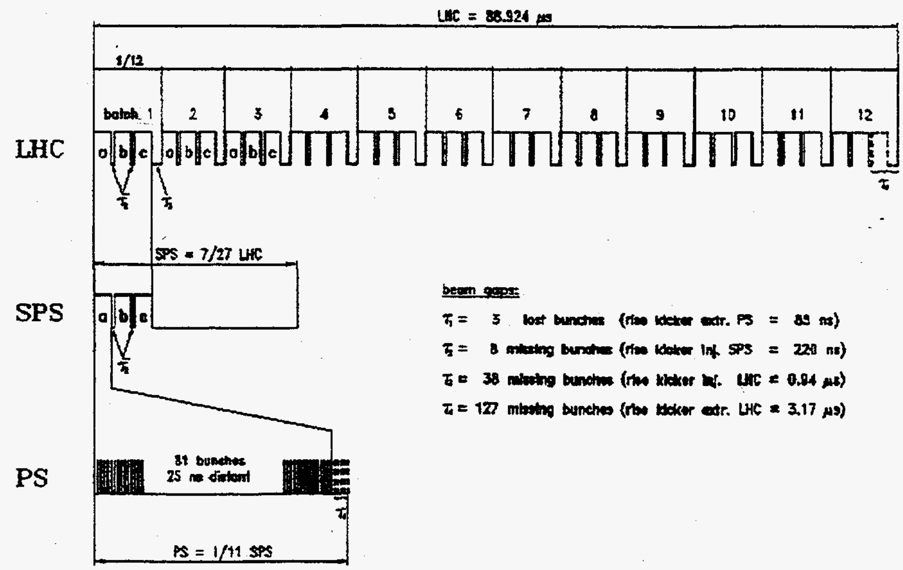

May 7-9, 1997 3rd MINI-WORKSHOP ON HIGH INTENSITY, HIGH BRIGHTNESS HADRON COLLIDERS

LHC beam ε_{long} "budget"

Machine & process		E_{kin}	p	$\varepsilon_{longitudinal}$ [bunch]	h	$\varepsilon_{longitudinal}$ *) [LHC bunch]	bunch length	$\Delta p/p$ **) [2 σ]	RF
		GeV	GeV/c	eVs		eVs	ns	10^{-3}	MHz
Linac		0.05	0.31	(0.65)		**0.06**	(1667)	2	(0.60)
PSB	capture	0.05	0.31	1.20	1	**0.11**	1600	4.9	0.6
	acc. (+ contr. bu?)	1.40	2.14	1.45	1	**0.14**	190	2.5	1.75
CPS	injection	1.40	2.14	1.45	8	**0.14**	190	2.5	3.5
	acceleration	2.74	3.56	1.50	8	**0.14**	66	4.1	3.69
	b split + contr. bu (200 MHz)	2.74	3.56	1.00	16	**0.19**	46	4	7.38
	acceleration	25.5	26.4	1.00	16	**0.19**	24	1	7.6
	adiabatic debunching	25.5	26.4	(0.25)	84	**0.25**	(25)	0.2	40
	adiabatic rebunching	25.5	26.4	0.36	84	**0.36**	12	0.7	40
	bunch rotation	25.5	26.4	0.36	84	**0.36**	4	2.2	40
SPS	filamentation on inj. plateau	25.5	26.4	0.52	4620	**0.52**	4.3	3	200
	acc. + contr. bu (800 MHz)	450	451	1	4620	**1**	2.5	0.6	200
	bunch compression	450	451	1	9240	**1**	1.7	0.8	400
LHC	injection	450	451	1	35640	**1**	1.7	0.9	400
	acceleration (+ contr. bu ?)	7000	7001	2.5	35640	**2.5**	1	0.2	400

*): Phase space area attributed to one LHC bunch, or (total CPS longitudinal emittance)/84 or (PSB bunch emittance)/10.5.

**): Bunch half height. For upright elliptical bunch, $\varepsilon_{longitudinal}=\Delta W*(\text{bunch length})*\pi/2$ $\Delta p / p=\gamma / (\gamma^2-1)\ \Delta W / (m_0 c^2)$

bunch parameter limitations

10^{11} protons/bunch

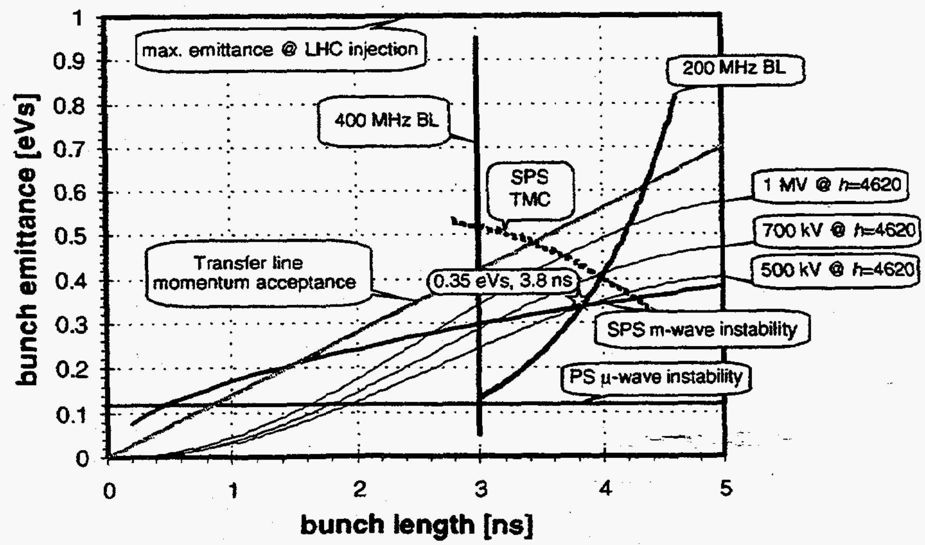

the most stringent bunch parameter limitations

- **SPS microwave instability** $\varepsilon_{l,\max} \propto \sqrt{\left|\frac{Z}{n}\right| \cdot N \cdot \frac{l_{bunch}}{|\eta|}}$
  "Keil-Schnell-Boussard", $|Z/n| \approx 10\ \Omega$ assumed.
  γ_t: 23 ↘ 19 (decreases also capture voltage)?
- **TMC (transverse mode coupling)**
  $Z_t = 23$ MΩ/m, Q=1 @ 1.3 GHz assumed
- **200 MHz periodic transient beam loading (BL)**
  Zcav ≈ 360 kΩ assumed
- **400 MHz BL**
  300 kW installed power assumed
- **Transfer line momentum acceptance**
  $6 \cdot 10^{-3}$ total assumed

Quasi-adiabatic compression on h=84 to 600 kV (!)

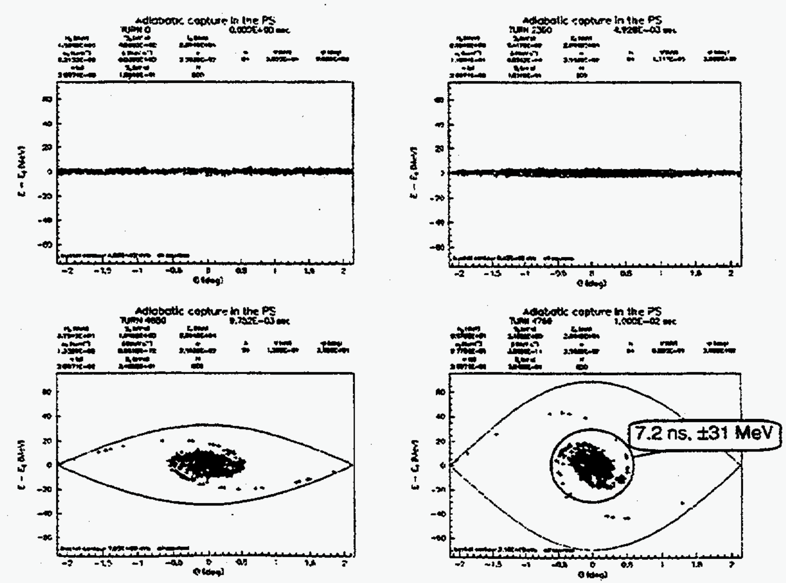

Animation: http://nicewww.cern.ch/~jensene/www/htm_40/Bunching.html

40 MHz cavity

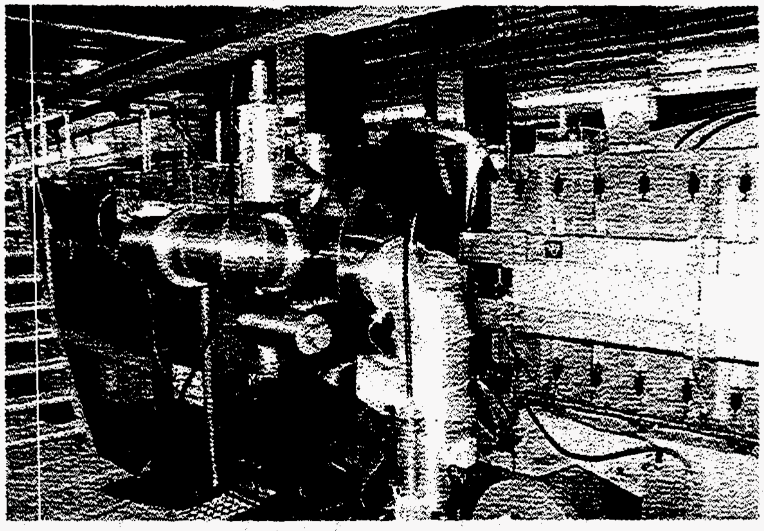

May 7-9, 1997 3rd MINI-WORKSHOP ON HIGH INTENSITY, HIGH BRIGHTNESS HADRON COLLIDERS

First 40 MHz bunches

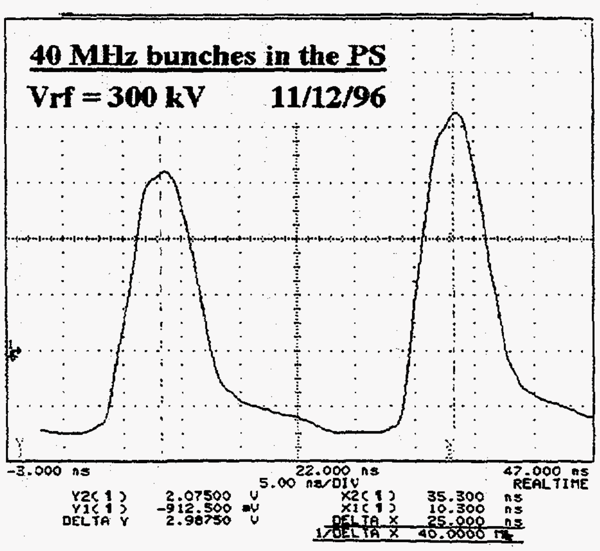

May 7-9, 1997 3rd MINI-WORKSHOP ON HIGH INTENSITY, HIGH BRIGHTNESS HADRON COLLIDERS

Bunch rotation test

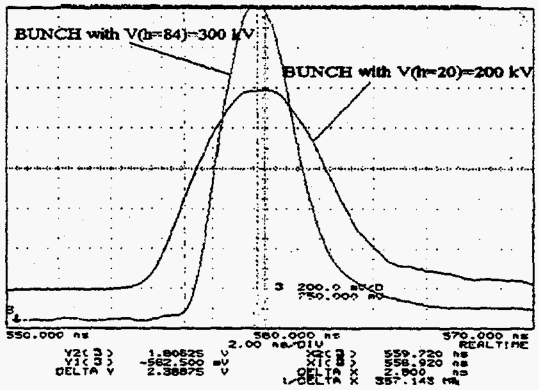

Synchronisation jitter

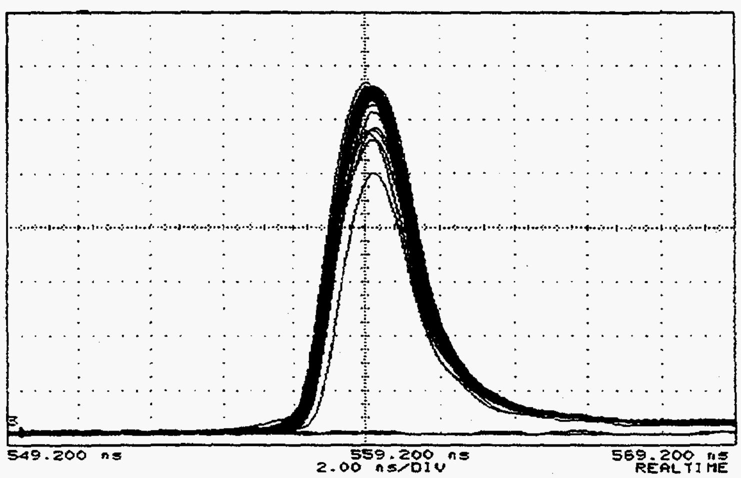

SYNCHRONISATION JITTER ON COMPRESSED BUNCH
(Ad. capture up to 60 kV & Step to 300kV . - 4/4/97)

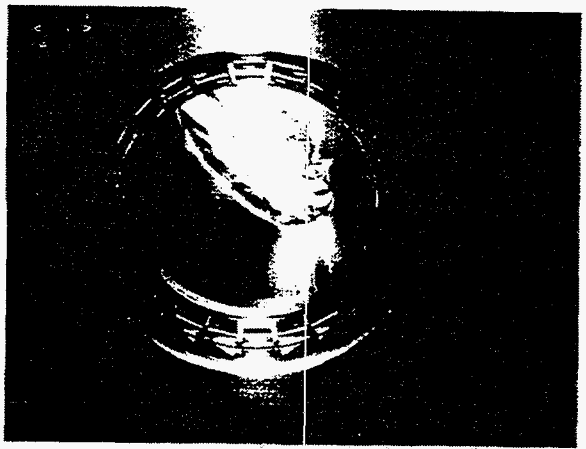
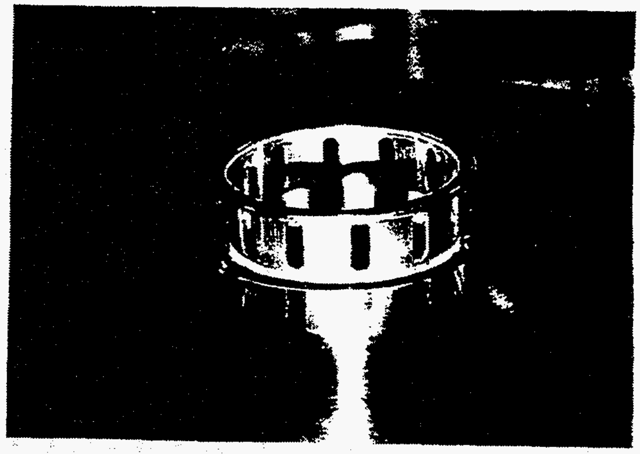
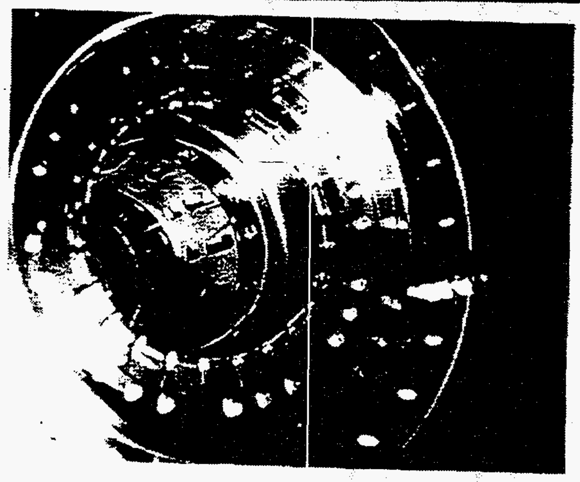
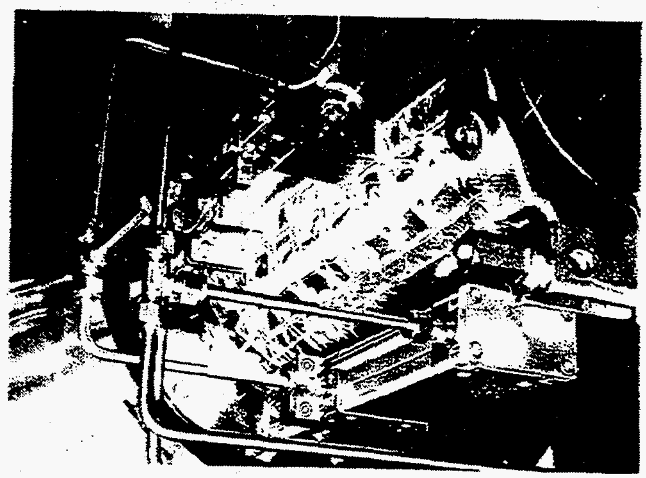

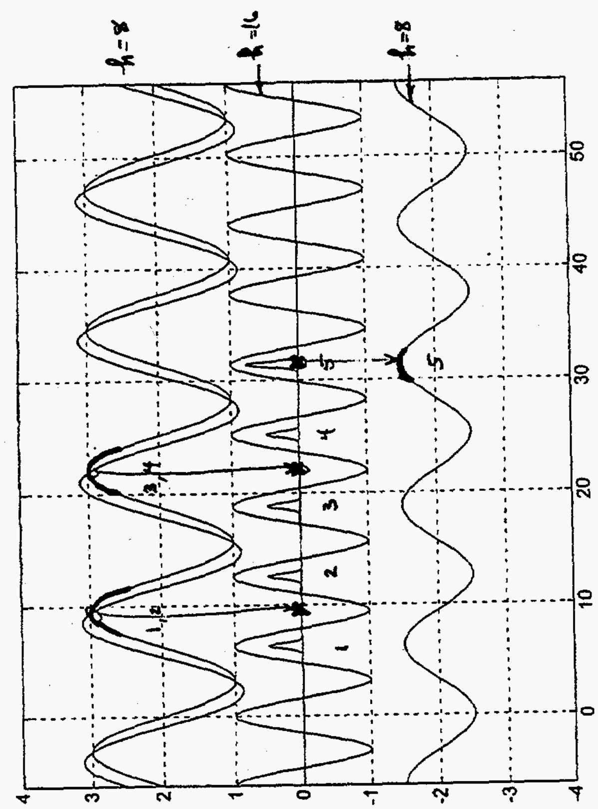

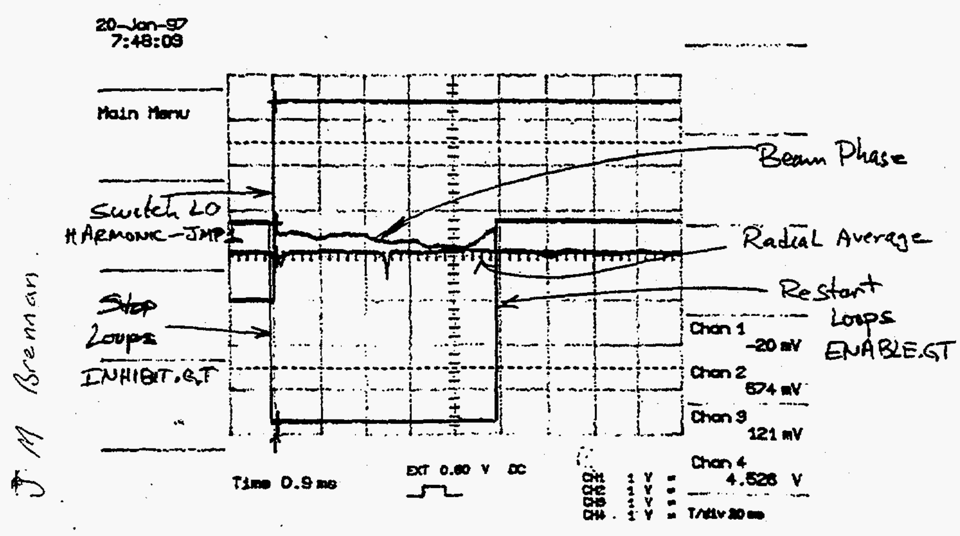
20-Jan-97
7:48:09
Main Menu
Switch LO
HARMONIC-JMP2
Stop
Loops
INHIBIT.GT
Beam Phase
Radial Average
Restart
Loops
ENABLE.GT
Chan 1
-20 mV
Chan 2
574 mV
Chan 3
121 mV
Chan 4
4.526 V
Time 0.9 ms
EXT 0.80 V DC
J M Brennan

Page 1

MRange_ch3
Last modified on 1/9/97 at 8:09 PM

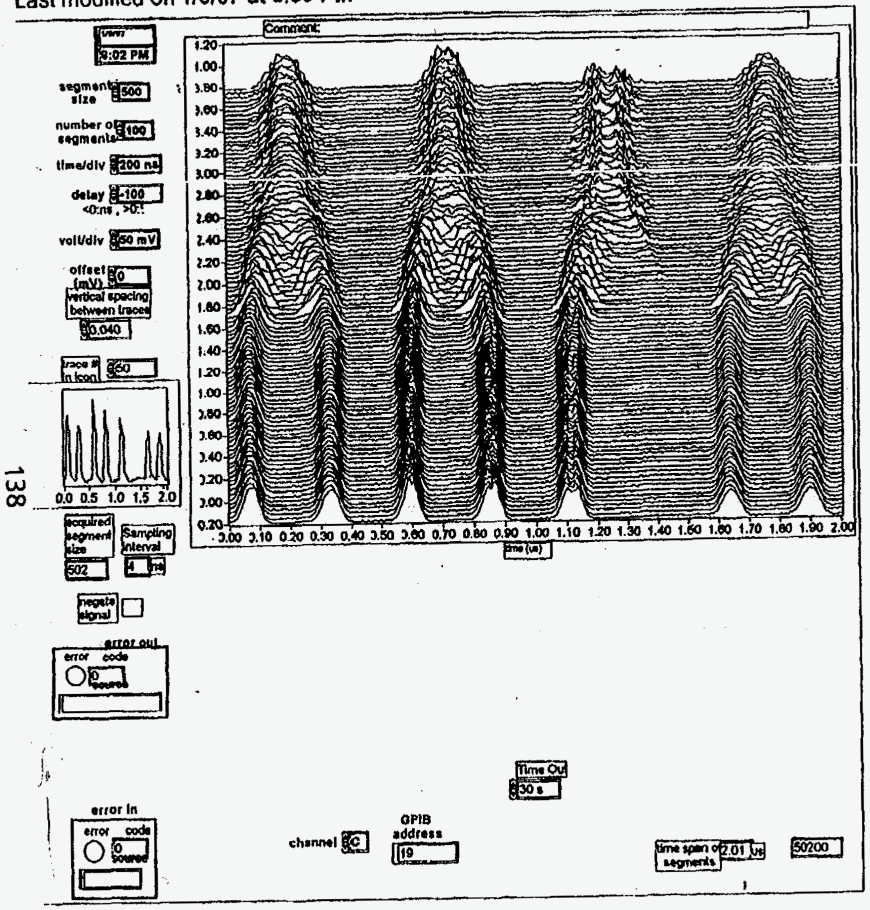

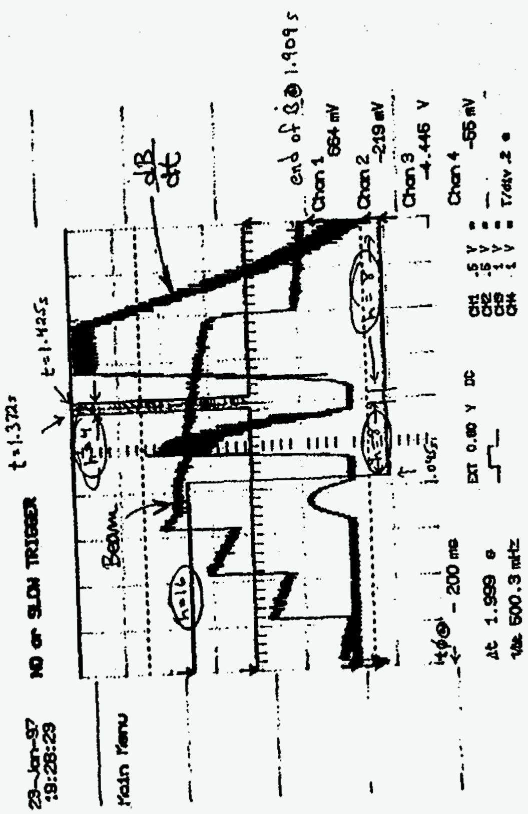

SEB mode

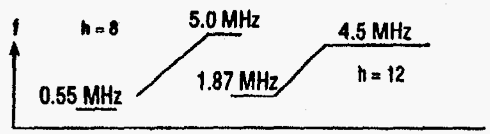

RHIC mode

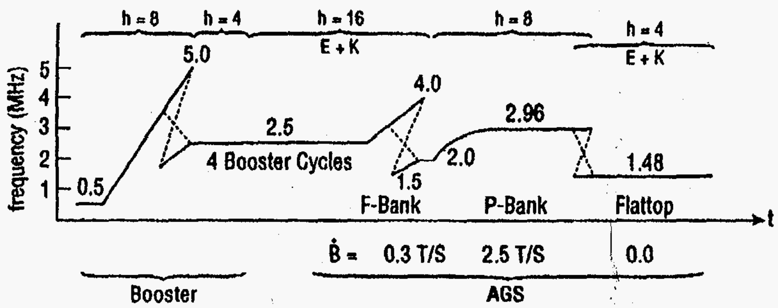

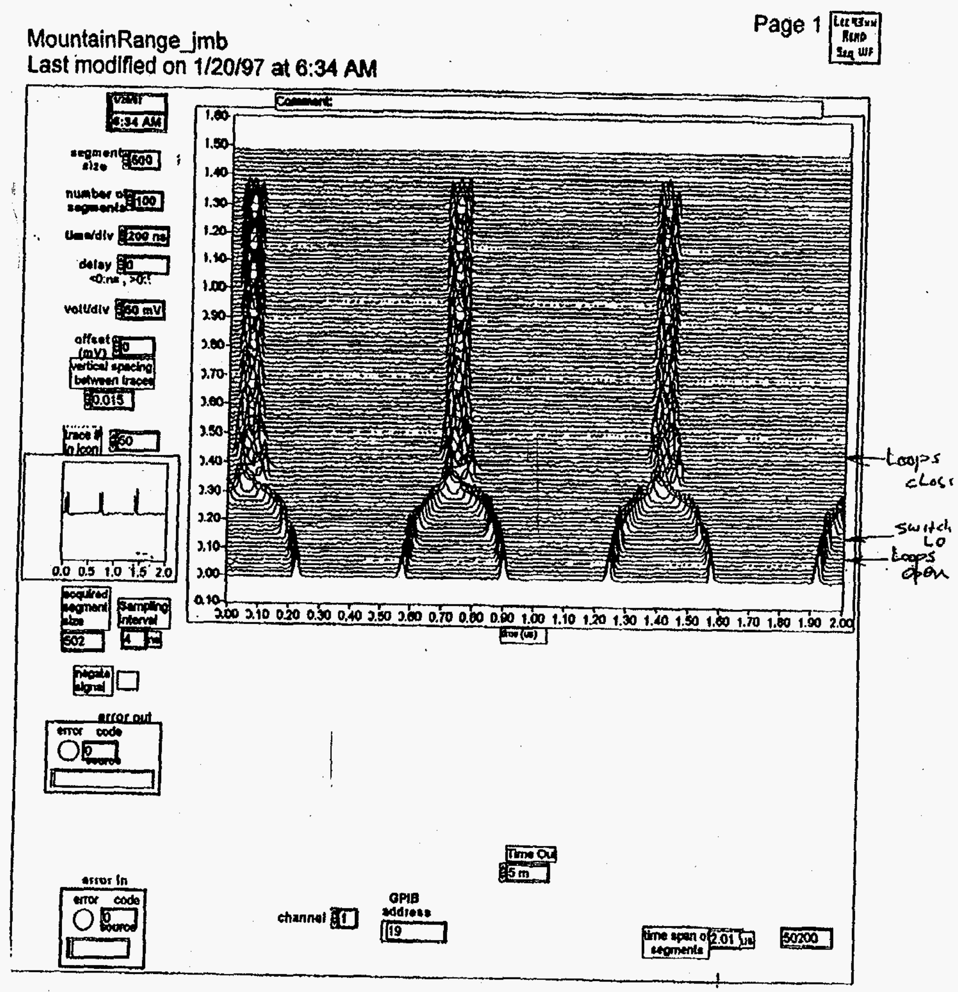

2048 turns per trace   Trev = 2.7μs

MRange_ch3
Last modified on 1/9/97 at 6:43 PM

Page 1

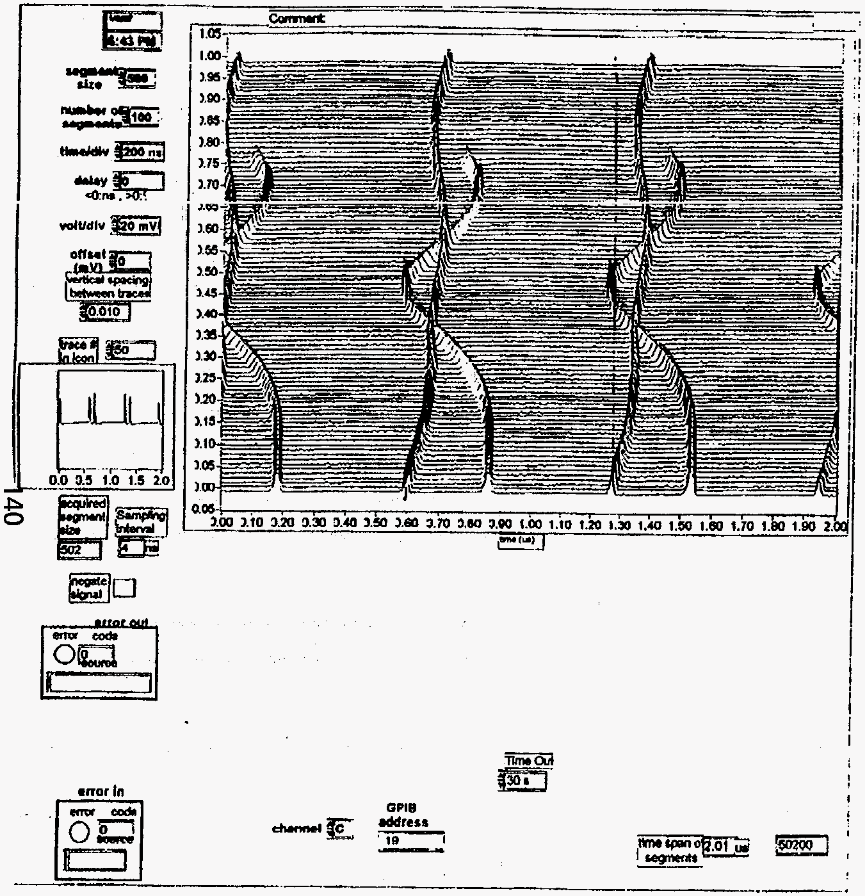

140

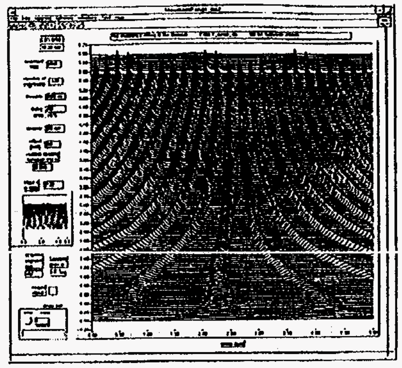

Booster Cycle

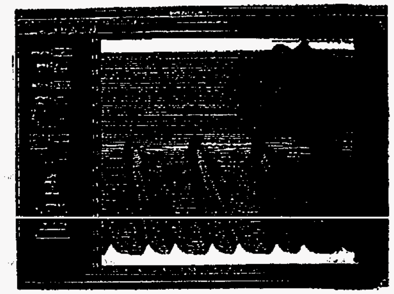

$h = 8 \rightarrow 4$ $\Delta T \cong 100\,\mu S$

⇕

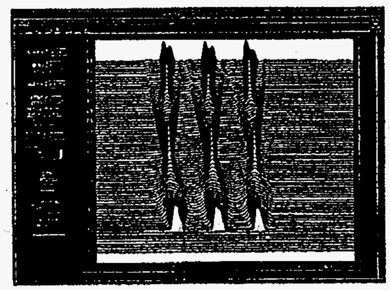

In AGS, after
+32 → +77 Stripping
↓

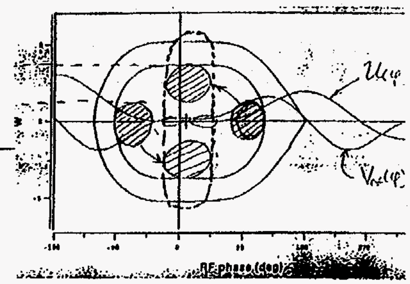

Merge in Double rf

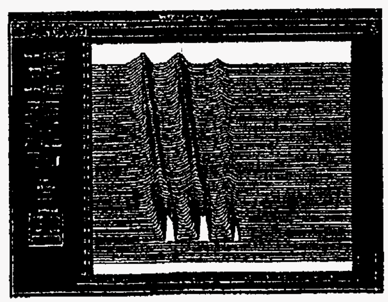

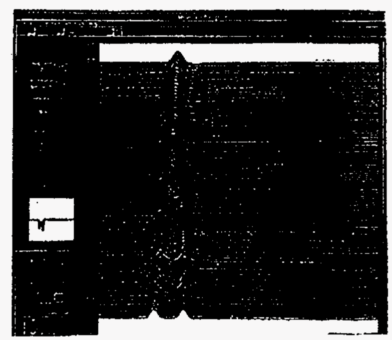

Mismatch at AGS Injection

- Momentum Error
- Bucket shape mismatch, need more Vrf for ΔE
- New batch perturbs old batch via phase loop
- Batch-by-batch phase Loop, bunch shape damper

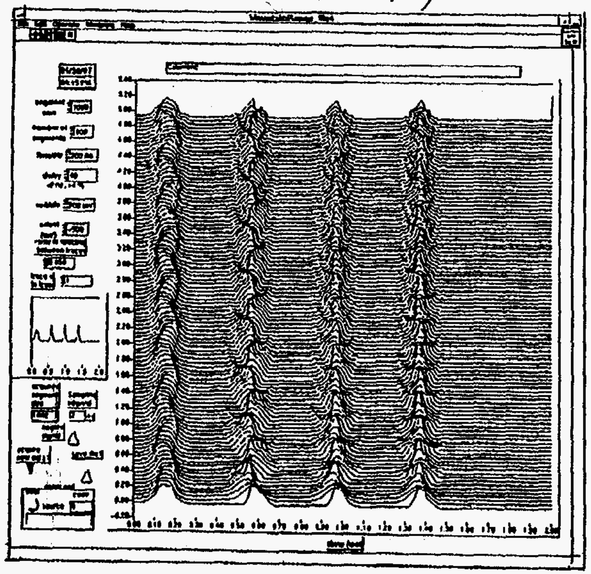

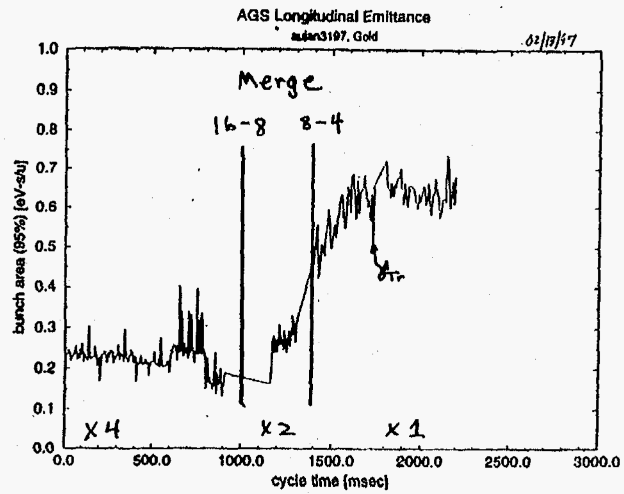

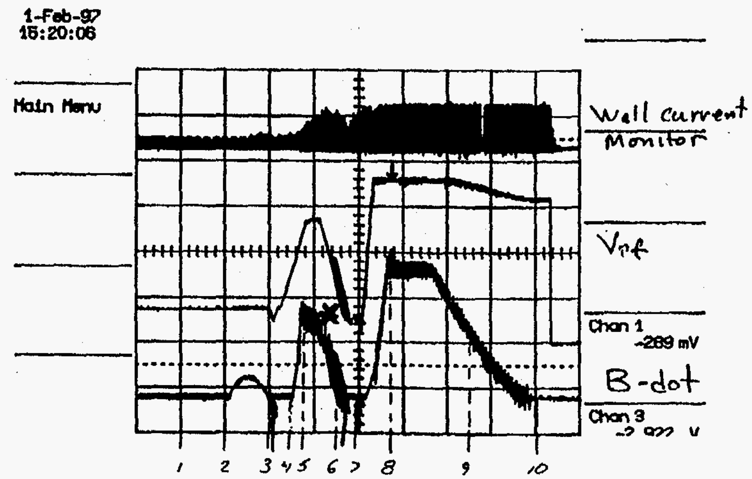

$\ast\ \delta\left(\frac{\dot{B}}{V_{rf}}\right)$ is Large + fast!

Space-Charge Effects and Ferrite Compensation

K.Y. Ng and Z. Qian

(May 7, 1997)

I INTRODUCTION

- C. Ankenbrandt suggested 2 rings for the proton driver.
- We concentrate on the first ring where space-charge is more important.

Kinetic Energy	1 GeV injection, $\gamma = 2.06579$, $\beta = 0.87503$
	3 GeV extraction
Cycle rate	15 Hz
Circumference, C	237.10 m f_0 = 1.106 MHz
Rf harmonic, h	2 or 4 for 2 or 4 bunches
Transition, γ_t	7
Bunching factor, B	0.25
No. per bunch, N_B	2.53×10^{13} I_{AV} = 4.48 amp/bunch
95% bunch area, A	1 eV-s
95% emittance, ϵ_{N95}	$200 \times 10^{-6}\,\pi$ m

II TRANSVERSE TUNE SPREADS

- Laslett tune shift at injection

$$\Delta\nu = -\frac{3N_{\text{total}}r_p}{2\gamma^2\beta\epsilon_{N95}B} = \begin{cases} -0.199 & \text{2 bunches, good} \\ -0.397 & \text{4 bunches, manageable} \end{cases}$$

This is an incoherent effect and cannot be compensated by ferrite.

III MICROWAVE INSTABILITIES

- For parabolic bunch,

$\hat{\delta}$ ↓

$$B = 0.25 \Longrightarrow \begin{cases} \hat{\tau} = 84.73 \text{ ns or } \hat{\ell} = 22.23 \text{ m} & \text{for } h = 2 \\ \hat{\tau} = 42.37 \text{ ns or } \hat{\ell} = 11.12 \text{ m} & \text{for } h = 4 \end{cases}$$

5.49 × 10⁻

1.098 × 10

- Using Krinsky-Wang criterion and a bunch area of 1 eV-s,

$$\left|\frac{Z_\parallel}{n}\right| < \frac{2\pi E|\eta|}{e\beta^2 I_p}\left(\frac{\sigma_E}{E}\right)^2 = \begin{cases} 71.27\ \Omega & \text{for } h = 2 \\ 142.5\ \Omega & \text{for } h = 4 \end{cases}$$

Note: If the Boussard-modified Keil-Schnell criterion is used, these limits will be 1.67 times larger.

- Space-charge impedance:

  With $\epsilon_{N95} = 2 \times 10^{-4}\pi$ m, bunch area 1 eV-s, and assuming

  a momentum dispersion of ~2 m, $<\beta>= 7.28$ m

  beam radius is $a = 3.35$ cm and 3.85 cm for $h = 2$ and 4.

  Using a 5 cm radius beam pipe,

$$\left.\frac{Z_\parallel}{n}\right|_{\rm spch} = i\frac{Z_0}{2\gamma^2\beta}\left(1 + 2\ln\frac{b}{a}\right) = \begin{cases} i91.1\ \Omega & \text{for } h = 2 \\ i76.8\ \Omega & \text{for } h = 4 \end{cases}$$

  Note: Same size as the stability limit. However, we are below transition, hopefully, microwave instability will not develop.

- Assume pipe radius of 5 cm. Cutoff freq is 2.30 GHz, or harmonic $n_{\rm cutoff} = 2074$. Tunes: $\nu_x = \nu_y = 5.18$.

$$|Z_\perp| < F\frac{4\nu\beta}{eRI_{\rm peak}}(\Delta E)_{\rm FWHM}|(n-\nu)\eta + \nu\xi| = 31.56\ {\rm M}\Omega/{\rm m}$$

- With $b = 5$ cm, $a = 3.35$, 3.85 cm for $h = 2$, 4,

$$Z_\perp|_{\rm spch} = i\frac{RZ_0}{\beta^2\gamma^2}\left(\frac{1}{a^2} - \frac{1}{b^2}\right) = \begin{cases} i2.21\ {\rm M}\Omega/{\rm m} & h = 2 \\ i1.23\ {\rm M}\Omega/{\rm m} & h = 4\,. \end{cases}$$

  Therefore transverse microwave instability will not happen.

IV POTENTIAL-WELL DISTORTION

- A particle at distance s from bunch center sees a longitudinal space-charge $E_{z\,\mathrm{sp\ ch}}$ field and a potential drop per turn:

$$E_{z\,\mathrm{sp\ ch}} = -\frac{eg_0}{4\pi\epsilon_0\gamma^2}\frac{d\lambda}{ds}, \qquad g_0 = 1 + 2\ln\frac{b}{a}$$

$$V_{\mathrm{sp\ ch}} = E_{z\,\mathrm{sp\ ch}}C = -\left(\frac{3\pi I_{\mathrm{av}}Z_0 g_0}{4\gamma^2\beta}\right)\left(\frac{R}{\hat{\ell}}\right)^2\frac{s}{\hat{\ell}} = \begin{cases} 11.1\,\frac{s}{\hat{\ell}}\ \mathrm{kV} & \text{for } h=2 \\ 37.4\,\frac{s}{\hat{\ell}}\ \mathrm{kV} & \text{for } h=4 \end{cases}$$

- On the other hand, neglecting space charge, the synchrotron tune and required rf are

$$\nu_s = \frac{|\eta|\hat{\delta}}{\omega_0\hat{\tau}} = \begin{cases} 0.000919 \\ 0.003677 \end{cases} \qquad V_{\mathrm{rf}}\cos\phi_0 = \frac{2\pi\beta^2 E}{|\eta|h}\nu_s^2 = \begin{cases} 18.41\ \mathrm{kV} & \text{for } h=2 \\ 147.3\ \mathrm{kV} & \text{for } h=4 \end{cases}$$

- For $\phi_0 = 0$, rf voltage seen by end particle of bunch is

$$V = V_{\mathrm{rf}}\sin\frac{h\omega_0\hat{\ell}}{\beta c} = V_{\mathrm{rf}}\sin\frac{3\pi B}{2} = 0.924V_{\mathrm{rf}}$$

- The potential-well distortion is large compared with rf voltage required if there is no space-charge, especially for $h = 2$.

- We wish to compensate this distortion by ferrite. The frequency is roughly is at ~ 2.2 MHz and ~ 4.4 MHz for $h = 2$ and 4.

to $\frac{7}{2}\times 2.2 = 7.7$ MHz to $\frac{14}{4}\times 4.4$ MHz = 15 MHz

V FERRITE COMPENSATION

- The voltage drop per turn due to space charge can be written as

$$V_{\text{sp ch}} = \left(i\frac{3\pi I_{\text{av}}}{2}\right) \frac{Z_{\|}}{n}\bigg|_{\text{sp ch}} \left(\frac{R}{\hat{\ell}}\right)^2 \frac{s}{\hat{\ell}}$$

Thus, it can be canceled by adding an inductance.

- Consider using a hollow cylinder of ferrite of inner and outer radii b and d and length ℓ. Impedance introduced is

$$\frac{Z_{\|}}{n}\bigg|_{\text{ferrite}} = -i\frac{Z_0\omega_0}{2\pi c}\mu'\ell \ln\frac{d}{b}$$

For example, with $\mu' = 1000$, $d = 5.5$ cm, $b = 5$ cm, to cancel a space-charge Z/n of $\sim 100\ \Omega$, a length of $\ell = 63$ cm will be enough.

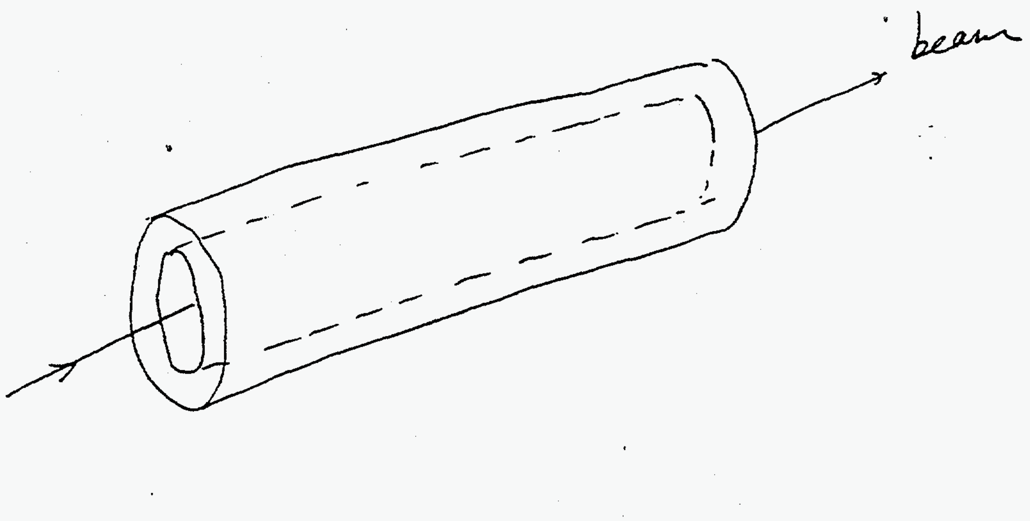

V.1 Loss

- One way to include loss is to write

$$\mu = \mu' + i\mu'' \qquad \text{and} \qquad Q = \frac{\mu'}{\mu''}$$

$$Z_{\parallel} = \left(\frac{1}{Q} - i\right) \left|Z_{\parallel}\right|_{\text{spch}}$$

- We want material with large μ'. However, μ'' will usually be large as well.

- Since the real part is proportional to frequency, we need to sum many harmonics to compute the total loss. For *each* bunch,

$$\text{Current :} \quad I(t) = I_{\text{av}} + \sum_{n=1}^{\infty} I_n \cos n\omega_0 t$$

$$\text{Power :} \quad P = \tfrac{1}{2} \sum_{n=1}^{\infty} n I_n^2 \frac{\left|Z_{\parallel}/n\right|_{\text{spch}}}{Q}$$

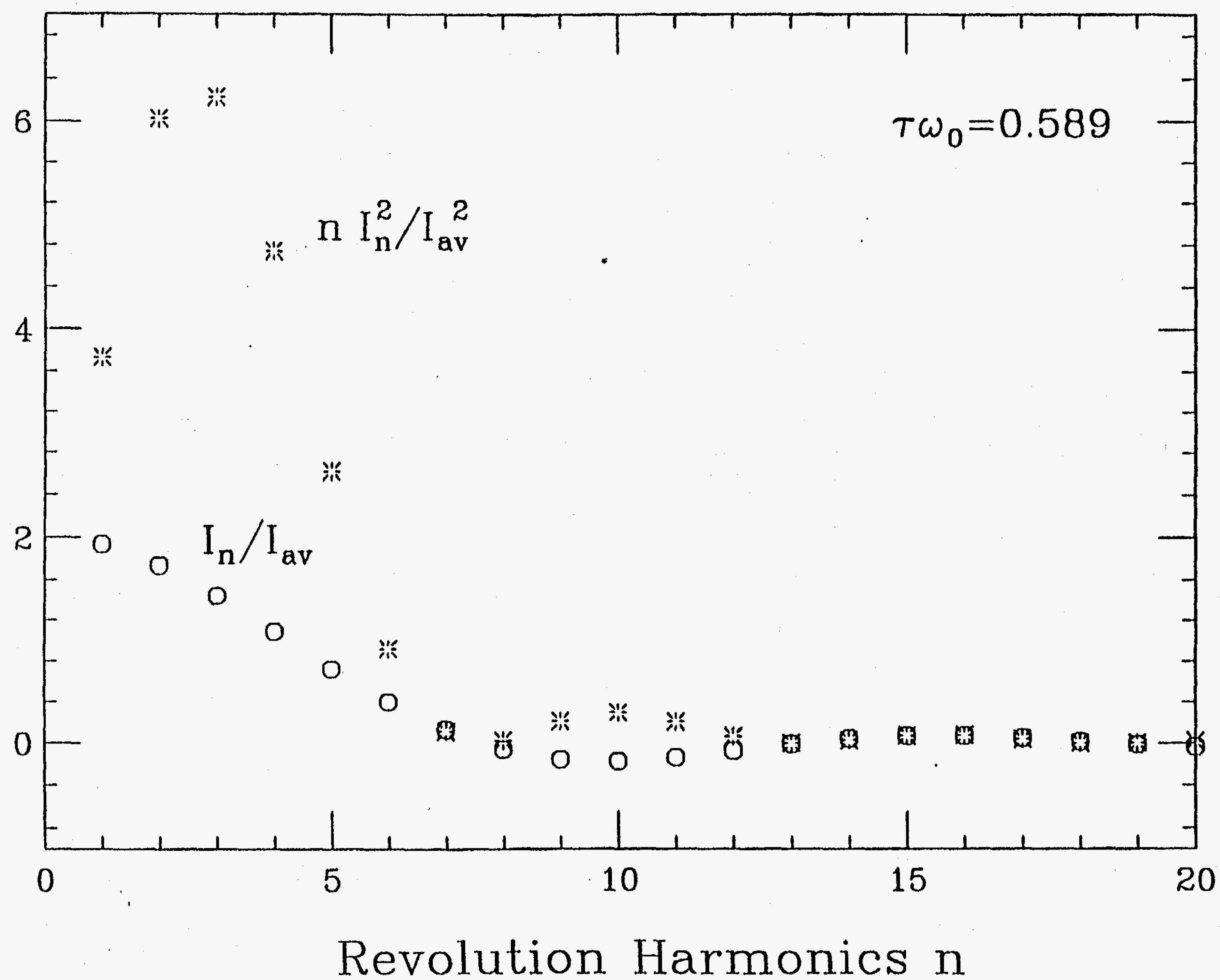
$\tau\omega_0$=0.589
$n\ I_n^2/I_{av}^2$
I_n/I_{av}
0
2
4
6
0
5
10
15
20
Revolution Harmonics n

- If we assume Gaussian distribution, the summation can be approximated by integration to give, $\hat{\tau} = \sqrt{5}\sigma_\tau$,

$$P = \frac{I_{\rm av}^2 |Z_\parallel/n|_{\rm spch}}{Q(\sigma_\tau\omega_0)^2}.$$

For $h = 2$, $|Z_\parallel/n|_{\rm spch} = 100\ \Omega$, and $Q = 1$, the power loss is $P = 25.6$ kw, parabolic, (29.2 kw by above formula).

Need to sum up to at least $n \sim 4/(\sigma_\tau\omega_0) = 7$ for $h = 2$.

For $h = 4$, need to sum to at least $n = 14$, and loss per bunch is 102.2 kw, 4 times larger.

- Average Loss per particle per turn is 6.5 kV.

Worst of all, because of the short wake (small Q), center of bunch loses much more than the ends.

Such position-dependent loss is hard to compensate.

- There are other problems like (1) high frequency response of ferrite, (2) effect of electric permittivity ϵ, (3) transverse effects.

- If loss is small (see below), the problem can be solved analytically.

VI FERRITE-LOADED WAVEGUIDE

- Here, the assumptions are (a) a perfectly conducting medium outside ferrite and (b) the ferrite insertion is infinitely long.

- The boundary-value problem has been solved in Phys. Rev. **D42**, 1819 (1990).

- The transverse and longitudinal wakes of the m-th azimuthal is

$$W_m(z) = \frac{Z_0 c\ell}{2\pi m d^{2m+1}} \sum_{\lambda=1}^{\infty} \tilde{F}_{rm\lambda}(x_{m\lambda}) \sin \frac{x_{m\lambda} z}{d\sqrt{\epsilon\mu - 1}} \cdot$$

$$W'_m(z) = \frac{Z_0 c\ell}{2\pi(1+\delta_{0m}) d^{2m+2}} \sum_{\lambda=1}^{\infty} \tilde{F}_{zm\lambda}(x_{m\lambda}) \cos \frac{x_{m\lambda} z}{d\sqrt{\epsilon\mu - 1}}$$

where $x_{m\lambda}$ is the λ-th zero of some combinations of modified Bessel functions of order m.

- The above are just summations of sharp resonances.

There are analytic expressions if the ferrite layer is thin.

$$Z_{\parallel}(\omega) \sim \int W'_0(z)\, e^{-i\omega z/c}\, d\left(\frac{z}{c}\right)$$

$$Z_{\perp}(\omega) \sim \int W_1(z)\, e^{-i\omega z/c}\, d\left(\frac{z}{c}\right)$$

Monopole ($m = 0$)

- If $\delta = \frac{t}{b} \ll 1$, $x_{01} = \sqrt{\frac{2\epsilon}{\delta}}$, *and* $\tilde{F}_{z01} = 4$. t = thickness of ferrite

Resonance frequency is

$$\omega_{01} = \frac{x_{01}c}{d\sqrt{\epsilon\mu - 1}} = \frac{c}{d}\sqrt{\frac{2\epsilon}{\delta(\epsilon\mu - 1)}} \longrightarrow \frac{c}{d}\sqrt{\frac{2}{\mu\delta}} \qquad \text{when } \epsilon\mu \gg 1$$

$$\frac{Z_\parallel}{n} = -i\frac{\omega_0 Z_0}{2\pi c}\left(\mu - \frac{1}{\epsilon}\right)\ell\delta$$

- Result is ϵ independent when $\epsilon\mu \gg 1$.

- For $\mu = 1000$, $\delta = 0.1$, $d = 5.05$ cm, $\ell = 63$ cm,

$$f_{01} = 840 \text{ MHz}, \qquad \frac{Z_\parallel}{n} = -i100\ \Omega$$

($\mu'' \sim 1000$)

But if loss is included as perturbation, loss is $\sim$ 76.8 kV per turn near bunch center and almost zero at both ends.

- For the low-loss Yttrium-iron garnet, $\mu = 3$, $\epsilon = 8$, $\ell = 63$ cm,

$$f_{01} = 15.3 \text{ GHz} \qquad \frac{Z_\parallel}{n} = -i3\ \Omega$$

VII HIGH TRANSVERSE DC BIAS

- From KE 1 GeV injection to KE 3 GeV, the space charge impedance will be reduced by a factor of 4.58. We would like the inductance of the ferrite to decrease by the same factor.

- This can be accomplished by passing a DC bias field through the ferrite. To reduce loss, we suggest the bias field $\perp$ field due to the bunch particles.

  This can be done by putting a solenoid outside the ferrite.

- Use a dc biased field H_c in z-direction, so high that the magnetization $\vec{M}$ inside the ferrite is saturated and becomes $\hat{z}M_s$.

- The ac field $\vec{H}_1$ from beam particles is in the x-y plane. This ac field causes the magnetization to precess about H_c, or creating an ac magnetization $\vec{M}_1$ in the x-y plane.

- Thus, we have

$$\vec{H} = \hat{z}H_c + \vec{H}_1\,, \qquad \vec{M} = \hat{z}M_s + \vec{M}_1$$

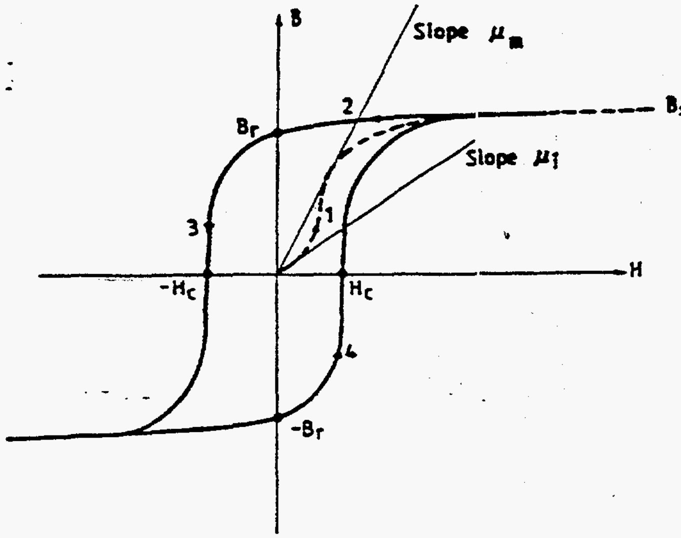
B
Slope μ_m
2
B_r
B_r
Slope μ_i
1
3
-H_c
H_c
H
4
-B_r

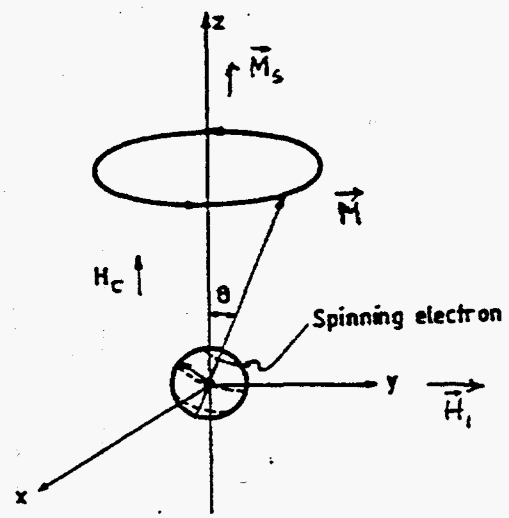
z
$\vec{M}_s$
$\vec{M}$
H_c
θ
Spinning electron
y
$\vec{H}_i$
x

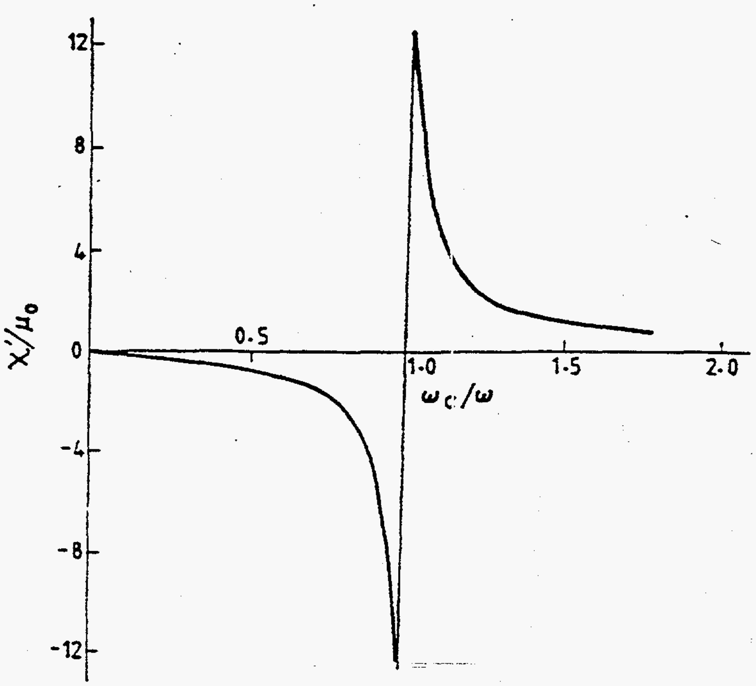
12
8
4
0
-4
-8
-12
0.5
1.0
1.5
2.0
χ'/μ_0
ω_c/ω

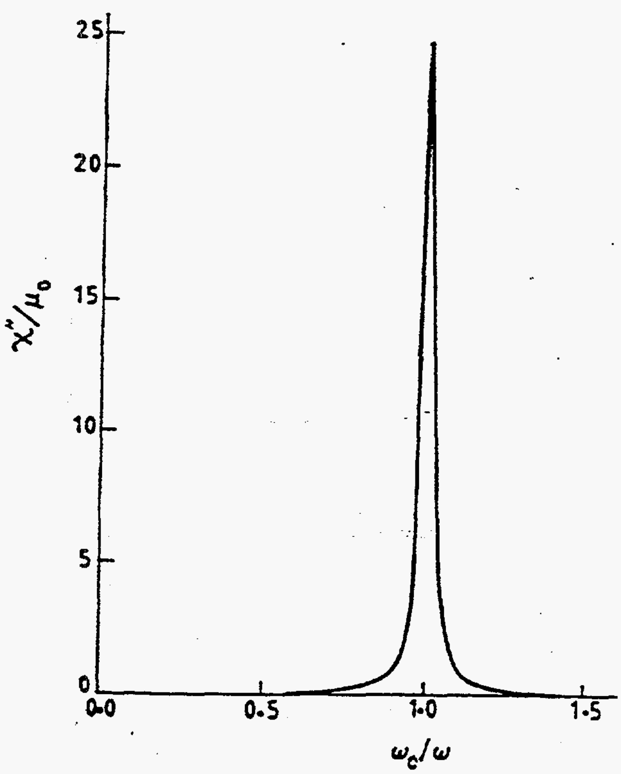
25
20
15
10
5
0
0.0
0.5
1.0
1.5
χ''/μ_0
ω_c/ω

- When $|\vec{H}_1| \ll H_c$, the equation of motion is

$$\frac{d\vec{M}}{dt} = \gamma(\hat{z}M_s \times \vec{H}_1 + \hat{z}\vec{M} \times H_c)$$

where $\gamma = 2.80 \times 2\pi$ MHz/Oersted is the gyromagnetic ratio of the electron. Defining the magnetic susceptibility tensor $\overleftrightarrow{\chi}_r$ as $\vec{M}_1 = \overleftrightarrow{\chi}_r \vec{H}_1$, the solution is

↑ reversible

Stationary soln. or particular soln.

$$\overleftrightarrow{\chi}_r = \begin{pmatrix} \chi & -j\kappa & 0 \\ j\kappa & \chi & 0 \\ 0 & 0 & 1 \end{pmatrix} \qquad \overleftrightarrow{\mu}_r = 1 + \frac{\overleftrightarrow{\chi}_r}{\mu_0}$$

where

$$\frac{\chi}{\mu_0} = \frac{\omega_c \omega_m}{\omega_c^2 - \omega^2}, \qquad \frac{\kappa}{\mu_0} = \frac{\omega \omega_m}{\omega_c^2 - \omega^2} = \frac{\chi}{\mu_0}\frac{\omega}{\omega_c}$$

and

$$\omega_c = \gamma H_c, \qquad \omega_m = \gamma \frac{M_s}{\mu_0}$$

- There is a resonance at the gyromagnetic resonant frequency $\omega_c = \gamma H_c$, which is proportional to the dc H_c. This explains why we want H_c to be large so that the resonance effect can be avoided.

- Loss can be included by letting $\omega_c \longrightarrow \omega_c - i\omega\alpha$, giving

$$\frac{\chi'}{\mu_0} = \frac{\left(\frac{\omega_m}{\omega}\right)\left(\frac{\omega_c}{\omega}\right)\left[\left(\frac{\omega_c}{\omega}\right)^2 - 1 + \alpha^2\right]}{\left[\left(\frac{\omega_c}{\omega}\right)^2 - 1 - \alpha^2\right]^2 + 4\left(\frac{\omega_c}{\omega}\right)^2 \alpha^2}$$

$$\frac{\chi''}{\mu_0} = \frac{\left(\frac{\omega_m}{\omega}\right)\alpha\left[\left(\frac{\omega_c}{\omega}\right)^2 + 1 + \alpha^2\right]}{\left[\left(\frac{\omega_c}{\omega}\right)^2 - 1 - \alpha^2\right]^2 + 4\left(\frac{\omega_c}{\omega}\right)^2 \alpha^2}$$

Note that, actually the above depend on only M_s and α.

- Usually the ac field comes from a cavity. Then, ω will not be changed by very much and can be considered fixed except very near to the resonance. Therefore, χ is plotted as a function of H_c This explains why the formulas have been written as a function of ω_c/ω.

- In our application, the ac field comes from the beam particles. So ω has the range of the bunch spectrum. For $h = 2$, $\omega/(2\pi)$ varies up to $\frac{7}{2}\times$ ~ 2.2 MHz, or 7.7 MHz and for $h = 4$, up to $\frac{14}{4}\times$ ~ 4.4 MHz. ~ 15 MHz

- The merit of this application is the low loss, because the ferrite is saturated, there will not be hysteresis loss. The only loss is due to spin wave which is small. The disadvantage is μ' is usually small.

Application

- Choose Ferramic Q-1, which has saturated flux density of 3300 Gauss at 25 Oersted.
- Thus, $M_s = 3300 - 25 = 3275$ Gauss.
- Choose $H_c = 25$ Oe.

  This gives resonant frequency $\omega_c/(2\pi) = \gamma H_c = 70$ MHz.

  Up to 10 MHz, $\mu' \sim M_s/H_c = 131$.
- With ferrite thickness $t = 1$ cm, to cancel $|Z_\parallel/n|_{\text{sp ch}} = 100\ \Omega$, we need a length of $\ell = 2.4$ m of ferrite is required.
- At extraction, want μ' to be reduced to $131/4.58 = 28.6$.

  The biased field should be raised to $H_c = M_s/\mu' = 114.5$ Oe.
- At low frequencies, the loss is $\mu'' \longrightarrow \dfrac{\alpha\omega\omega_m}{\omega_c^2}$.
- Take a typical value of $\alpha = 0.05$, we find μ'' varies linearly from 0 and reaches 0.5 at 5 MHz when $H_c = 25$ Oe at injection, and is reduced by a factor of $4.58^2 = 21.0$ when $H_c = 114.5$ Oe at extraction.

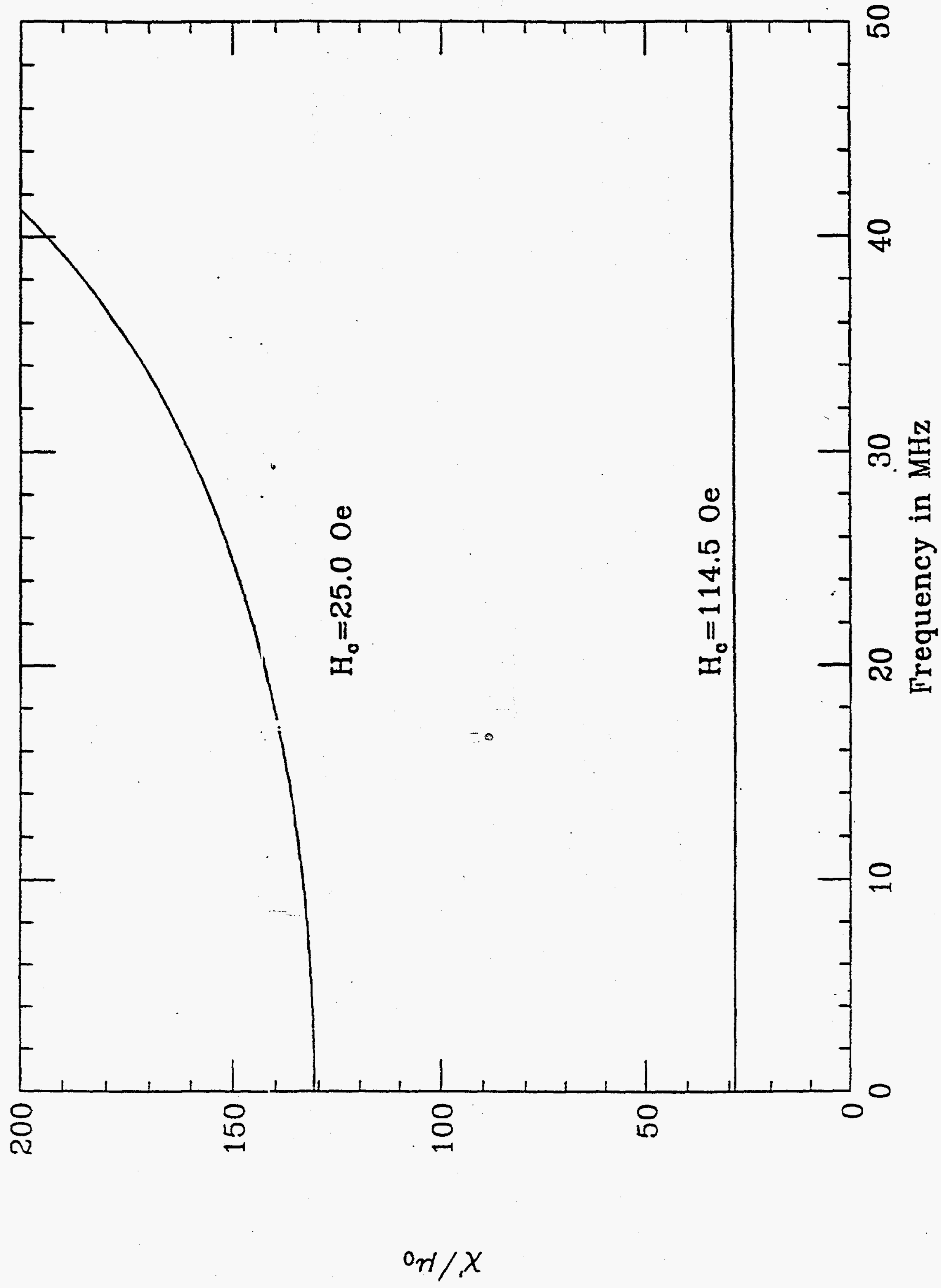

H_c=25.0 Oe
H_c=114.5 Oe
Frequency in MHz
0
10
20
30
40
50
200
150
100
50
0
χ/μ_0

VIII CONCLUSIONS

1. The most serious space-charge effect Laslett tune shift for $h = 4$.

2. Longitudinal microwave instability seems to be safe .

3. Potential-well distortion needs ferrite compensation.

4. Ordinary compensation without DC bias field gives large μ' and also large μ'' of the order of 1000. The loss is about 100 kV per turn and is position dependent along the bunch.

5. Large transverse DC bias beyond saturation eliminate hysteresis loss. Only loss is due to spin wave and is tiny.

6. However, large transverse DC bias gives small μ', but is still good enough. Total ferrite length of 2.4 m is required if thickness is 1 cm.

7. From injection energy of 1 GeV to extraction energy of 3 GeV, the DC bias field need to be increased quadratically with energy from 25 Oe to 114.5 Oe. Hopefully, this can be accomplished by using a solenoid.

ICFA Workshop
May 8, 1997

RHIC Operation with Increased Longitudinal Bunch Area (I)

Jie Wei, Brookhaven National Laboratory

I. Introduction

II. Intrabeam Scattering at Injection

III. Transition Crossing

IV. Storage and Luminosity

V. Conclusions

part (II) by Jörg Kewisch

I. Introduction

Results of 1997 Sextant Test:

- Intensity: typical 2×10^8, up to 4×10^8 /bunch
- Bunch area: typical $S = 0.5 \pm 0.1$ eV s/u

Au^{79+} beam during 1997 sextant test

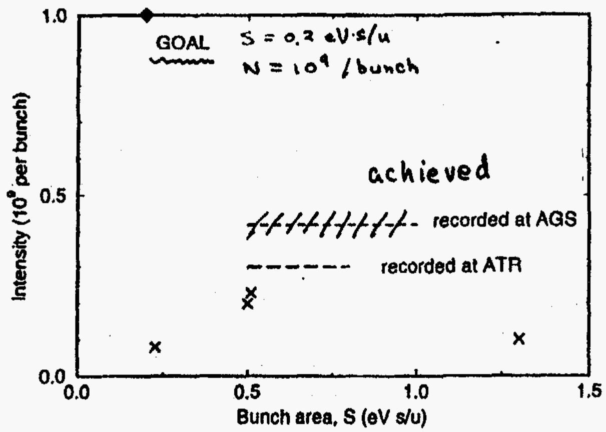

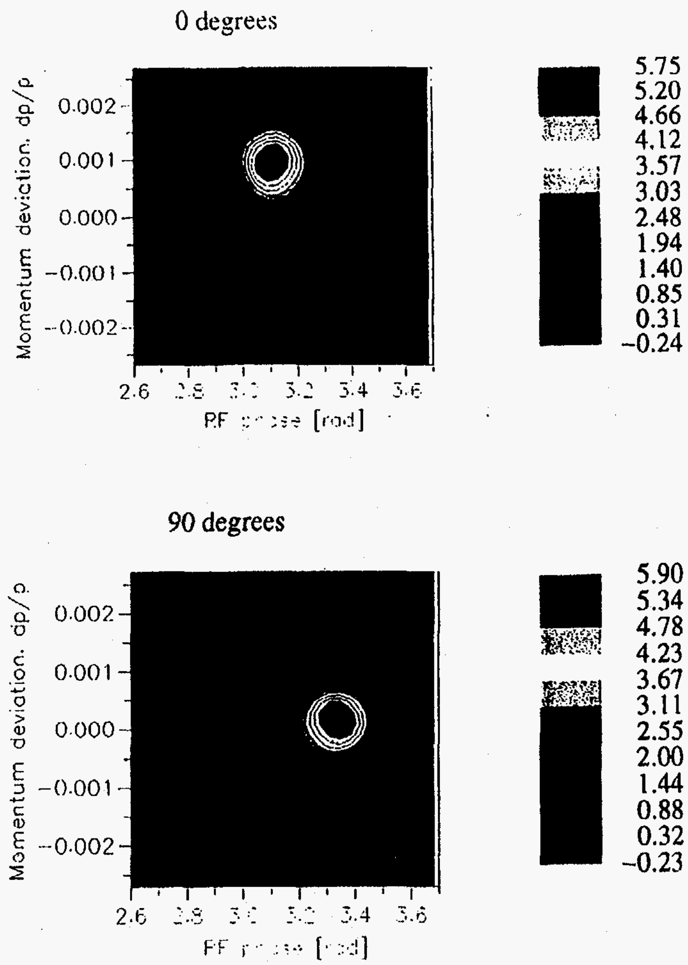

Figure 1: Au^{77+} Beam exhibiting dipole motion in an AGS RF bucket

1

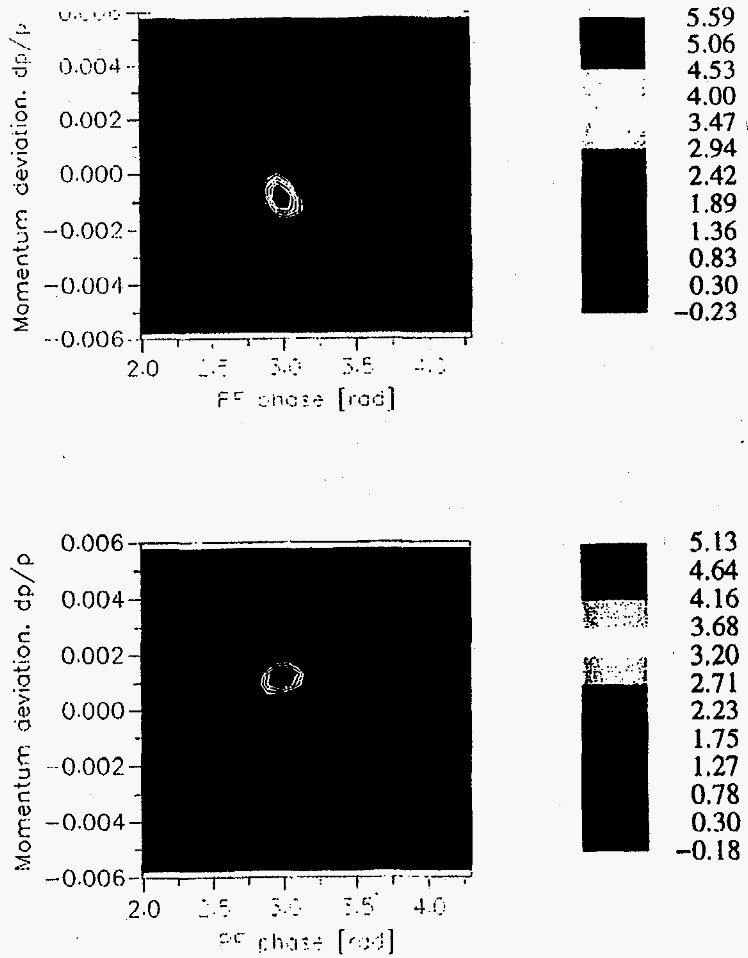

Figure 2: Two distinct globs of charge of Au^{77+} due to imperfect tuning rotating in an AGS rf bucket (110 degree)

2

Longitudinal phase-space reconstruction:

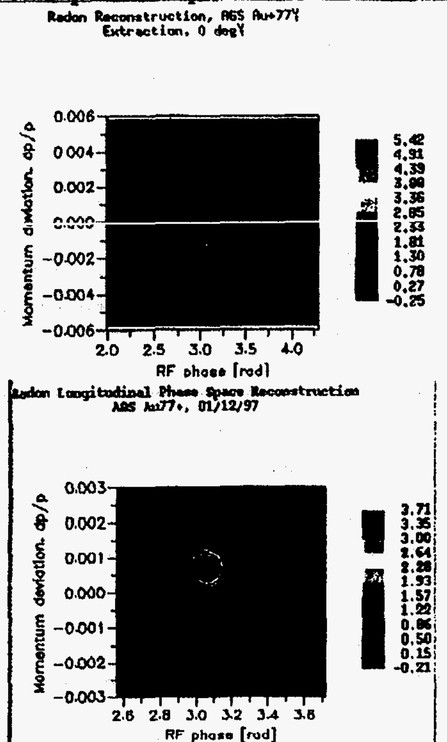

Figure 5: Longitudinal phase space of a Au^{77+} beam in AGS reconstructed with RADON on (a) Dec. 15, 1996 and (b) Jan. 12, 1997, showing improvement of merging at bunch coalescing.

Possible problems with increased bunch area:

*• emittance growth and particle loss at transition;

(Johnson) chromatic nonlinear effect

• re-bucketing (28 MHz ⟶ 196 MHz);

to be discussed by Jörg

• consequences in intrabeam scattering (injection & storage).

IBS @ injection

Luminosity performance & IBS @ storage

V. Mane, et. al.

II. Intrabeam Scattering at Injection

Quasi-equilibrium condition: "equal temperature"

(below transition)

$$\frac{\sigma_x}{\beta_x} \approx \frac{\sigma_y}{\beta_y} \approx \frac{\sigma_p}{\gamma}, \quad \gamma \ll \gamma_T. \qquad (1)$$

√ **For** $\frac{\sigma_{x,y}}{\beta_{x,y}} \gg \frac{\sigma_p}{\gamma}$: (low longitudinal temperature)

$$\begin{bmatrix} \frac{1}{\sigma_p}\frac{d\sigma_p}{dt} \\ \frac{1}{\sigma_x}\frac{d\sigma_x}{dt} \end{bmatrix} \sim 42.4 L_c r_0^2 E_0 \frac{Z^4 N}{A^2 \gamma \epsilon_x \epsilon_y S} \begin{bmatrix} \frac{\gamma \sigma_x}{\beta_x \sigma_p} \\ -\frac{\beta_x \sigma_p}{2\gamma \sigma_x} \end{bmatrix} \qquad (2)$$

For $\frac{\sigma_{x,y}}{\beta_{x,y}} \ll \frac{\sigma_p}{\gamma}$: (high longitudinal temperature)

$$\begin{bmatrix} \frac{1}{\sigma_p}\frac{d\sigma_p}{dt} \\ \frac{1}{\sigma_x}\frac{d\sigma_x}{dt} \end{bmatrix} \sim 27 L_c \ln\chi \, r_0^2 E_0 \frac{Z^4 N}{A^2 \gamma \epsilon_x \epsilon_y S} \begin{bmatrix} -\frac{\gamma^2 \sigma_x^2}{\beta_x^2 \sigma_p^2} \\ \frac{1}{2} \end{bmatrix} \qquad (3)$$

* strong dependence on energy
* proportional to 6-D phase space density
* $\sim \frac{Z^4}{A^2}$, problem for Au^{79+}

IBS growth at RHIC injection:

- mainly occurs in longitudinal direction;
  Lower longitudinal temperature
- with $S = 0.2$ eV·s/u, the growth time is about <u>3 minutes</u>;
- the growth rate can be reduced by increasing σ_p (rf voltage);
- with $S = 0.5$ eV·s/u, the growth time is about <u>20 minutes</u>;.

III. Transition Crossing

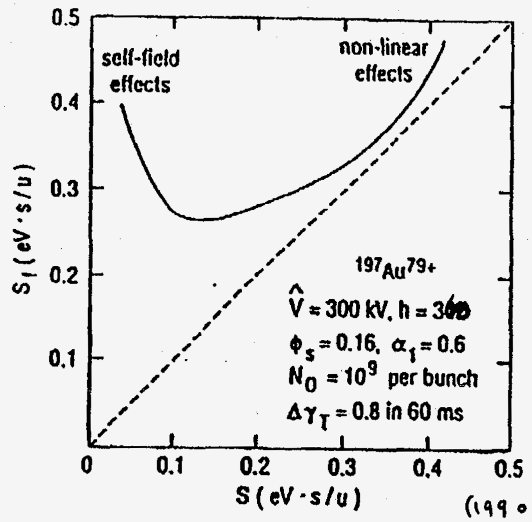

(1990 result)

Figure 2: Effects of chromatic nonlinearities and self fields at transition.

Recent progress in transition design:

- a "first-order, matched" γ_T-jump lattice,

  $\alpha_1 = -0.6$ remains almost constant during the jump;

  $\alpha_1 = +0.6$ (old) → $\alpha_1 = -0.6$ (new)

- two quadrupole corrector families, one for γ_T-jump, the other for optical optimization;

  Peggs, Tepikian, Trbojevic

- chromatic nonlinear effects greatly reduced.

$$\frac{\Delta S}{S} \sim (\alpha_1 + 1.5) \cdot \sigma_p$$

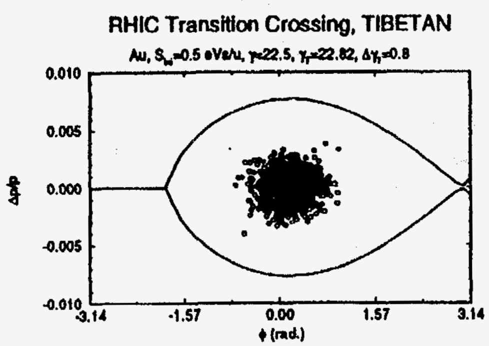

V_{rf} = 300 kV

* low enough to have a smaller σ_p

* high enough to compensate beam induced fields, especially in storage cavities.

γ_T - jump and α_1 variation:

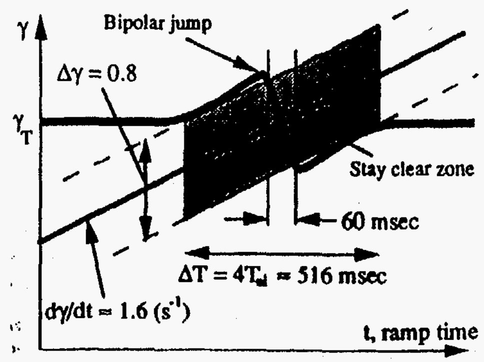

Figure 1 Transition is crossed almost 10 times faster with the nominal RHIC bipolar transition jump than without. Not to scale.

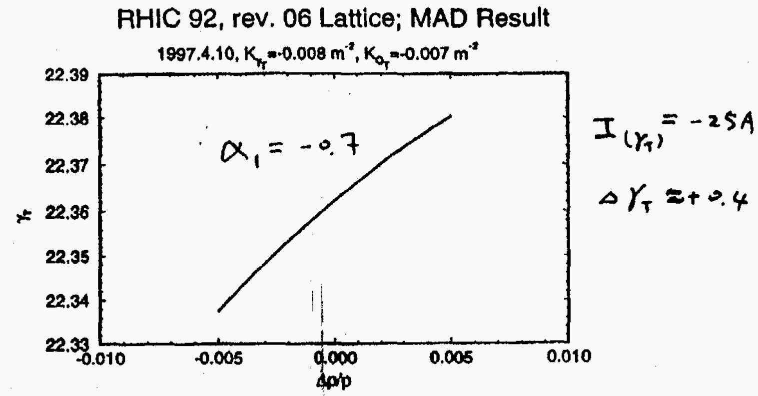

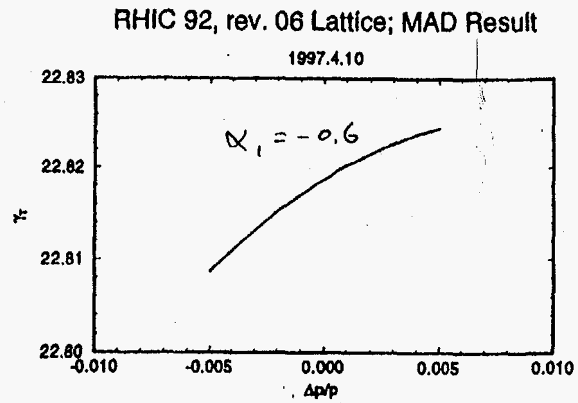

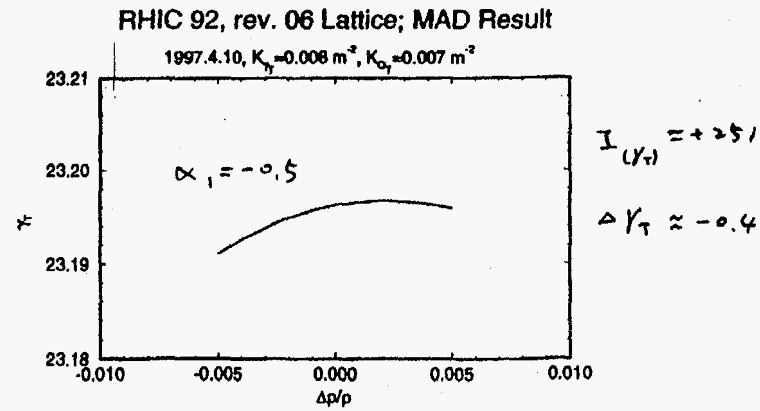

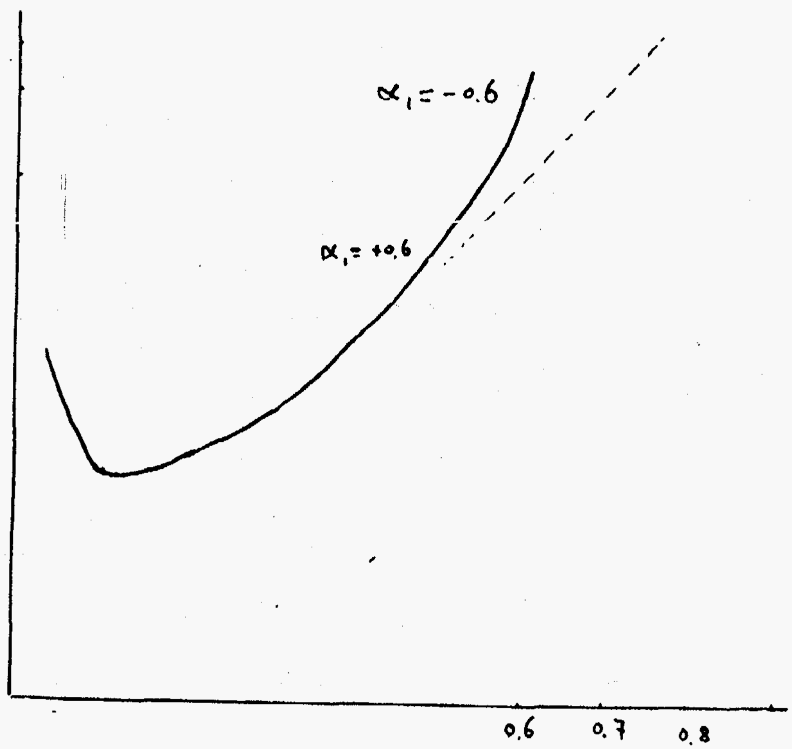

emittance growth after transition:

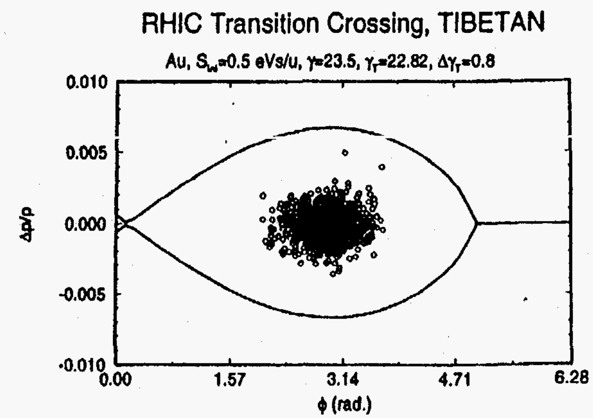

$\alpha_1 = -0.6$
(new)
negligible
growth

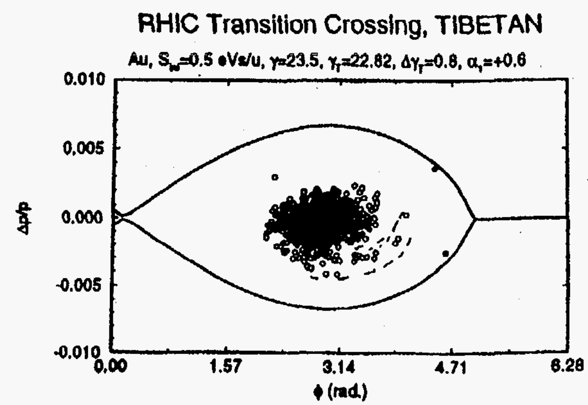

$\alpha_1 = +0.6$
(old)
considerable
growth

IV. Storage and Luminosity

Intrabeam Scattering growth at storage:

- growth occur in both transverse and longitudinal directions with similar rates;
- there exists *no* equilibrium state (negative-mass regime) (above transition)

$$\begin{bmatrix} \frac{1}{\sigma_p}\frac{d\sigma_p}{dt} \\ \frac{1}{\sigma_x}\frac{d\sigma_x}{dt} \end{bmatrix} \sim 34.6 L_c r_0^2 E_0 \frac{Z^4 N}{A^2 \gamma_T \epsilon_x \epsilon_y S}. \qquad (4)$$

* always grows

* weak dependence on energy

* proportional to 6-D phase space density

* $\sim \frac{Z^4}{A^2}$ problem for Au^{79+}

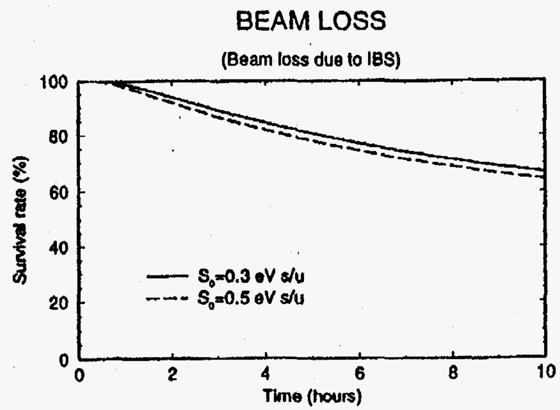

* fills the bucket in 1 ~ 2 hours

* beam escapes from the bucket

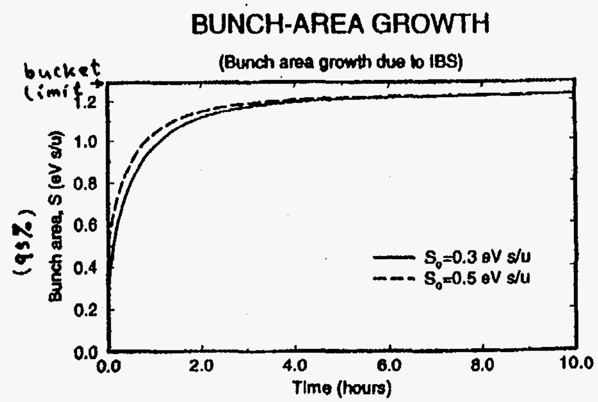

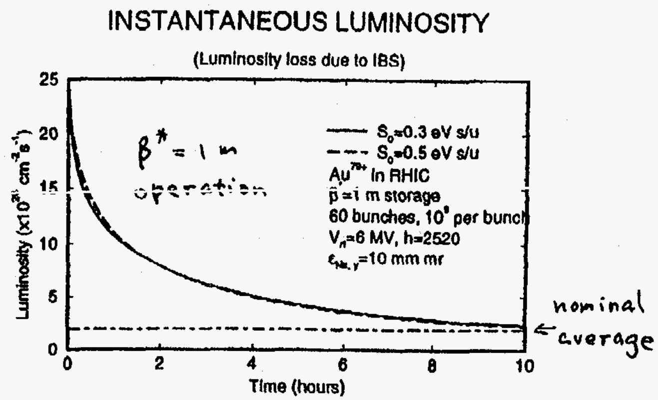

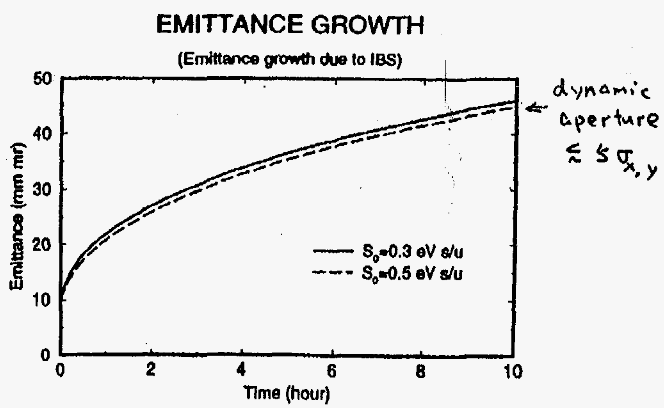

V. Conclusions

<u>With an increased longitudinal emittance:</u>

- intrabeam scattering growth at injection will be reduced;
- Current γ_T-jump scheme is adequate for efficient transition crossing;
- No significant change is expected in luminosity performance during collision.
- Re-bucketing process will be discussed by Jorg.

Rebucketing in RHIC

Jörg Kewisch

Motivation:
Short bunches (rms < 20 cm) are required for optimum detector design. (20 cm rms = 50 cm 95%)

Question:
If the requirement for the longitudinal bucket area is relaxed from 0.2 eV sec/u to 0.45 eV sec/u, how does that effect the particle loss during rebucketing

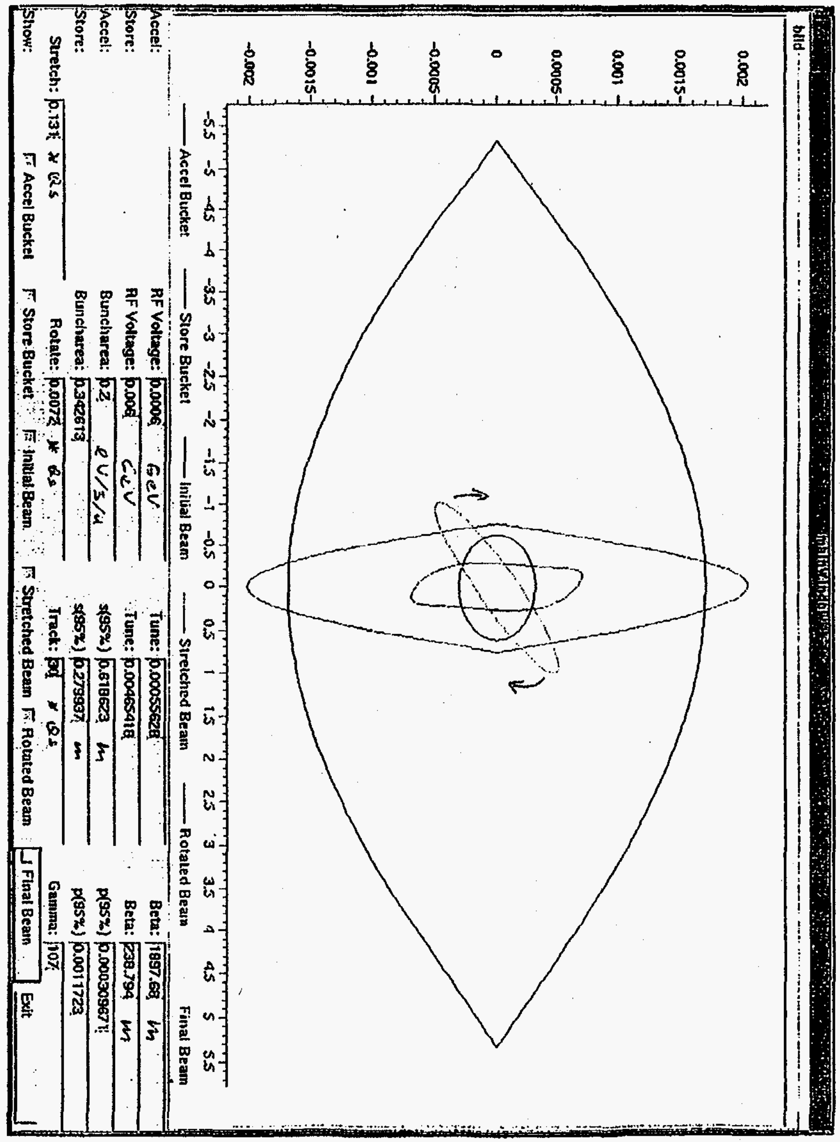

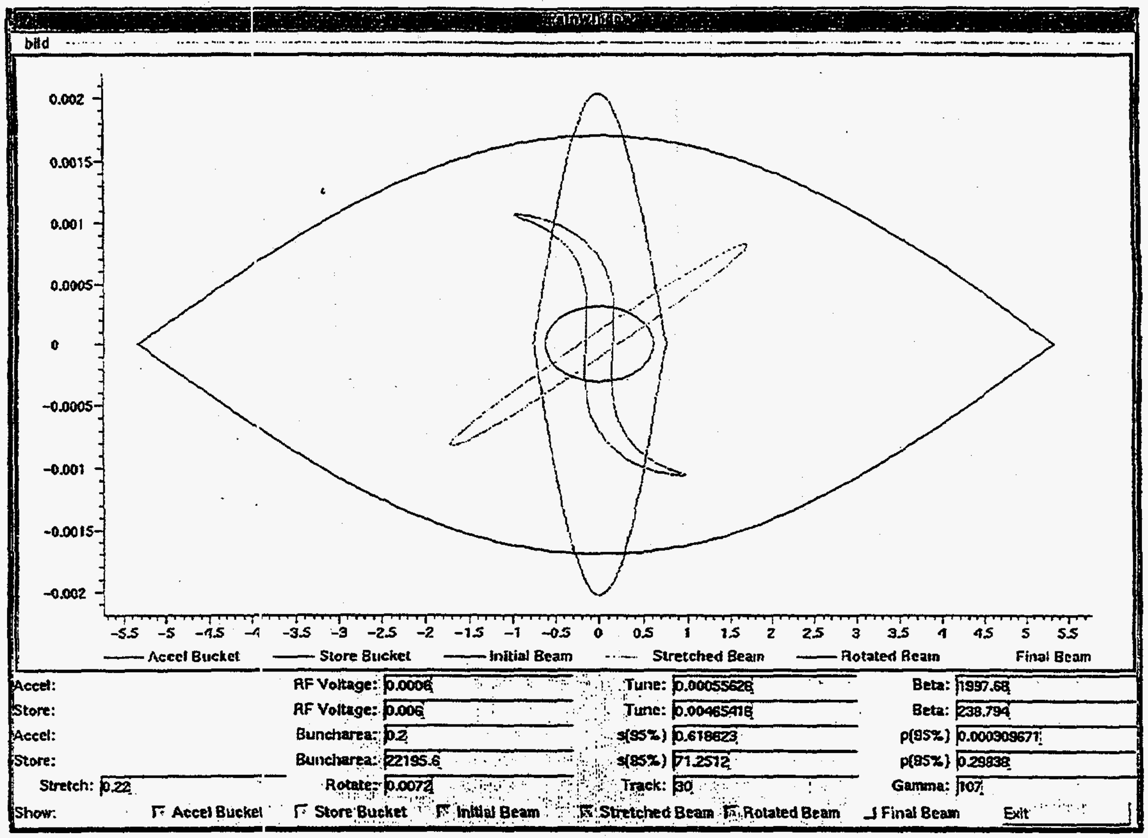
bild
0.002
0.0015
0.001
0.0005
0
-0.0005
-0.001
-0.0015
-0.002
-5.5 -5 -4.5 -4 -3.5 -3 -2.5 -2 -1.5 -1 -0.5 0 0.5 1 1.5 2 2.5 3 3.5 4 4.5 5 5.5
Accel Bucket
Store Bucket
Initial Beam
Stretched Beam
Rotated Beam
Final Beam
Accel: RF Voltage: 0.0006 Tune: 0.00055626 Beta: 1997.68
Store: RF Voltage: 0.006 Tune: 0.00465418 Beta: 238.794
Accel: Buncharea: 0.2 s(95%) 0.618623 p(95%) 0.000309671
Store: Buncharea: 22195.6 s(95%) 71.2512 p(95%) 0.29838
Stretch: 0.22 Rotate: 0.0072 Track: 30 Gamma: 107
Show: Accel Bucket Store Bucket Initial Beam Stretched Beam Rotated Beam Final Beam Exit

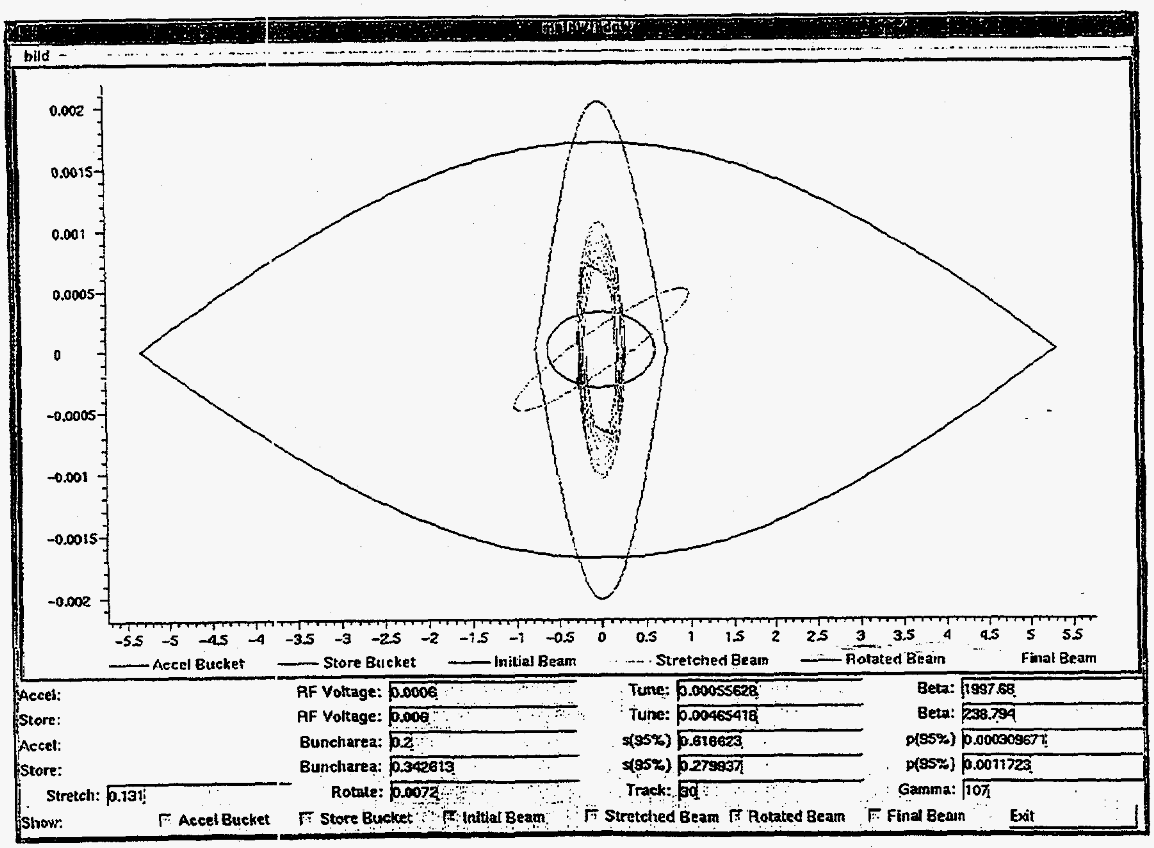
bild
0.002
0.0015
0.001
0.0005
0
-0.0005
-0.001
-0.0015
-0.002
-5.5 -5 -4.5 -4 -3.5 -3 -2.5 -2 -1.5 -1 -0.5 0 0.5 1 1.5 2 2.5 3 3.5 4 4.5 5 5.5
Accel Bucket
Store Bucket
Initial Beam
Stretched Beam
Rotated Beam
Final Beam
Accel: RF Voltage: 0.0006 Tune: 0.00055628 Beta: 1997.68
Store: RF Voltage: 0.006 Tune: 0.00465418 Beta: 238.794
Accel: Buncharea: 0.2 s(95%) 0.618623 p(95%) 0.000309671
Store: Buncharea: 0.342613 s(95%) 0.279937 p(95%) 0.0011723
Stretch: 0.131 Rotate: 0.0072 Track: 30 Gamma: 107
Show: Accel Bucket Store Bucket Initial Beam Stretched Beam Rotated Beam Final Beam Exit

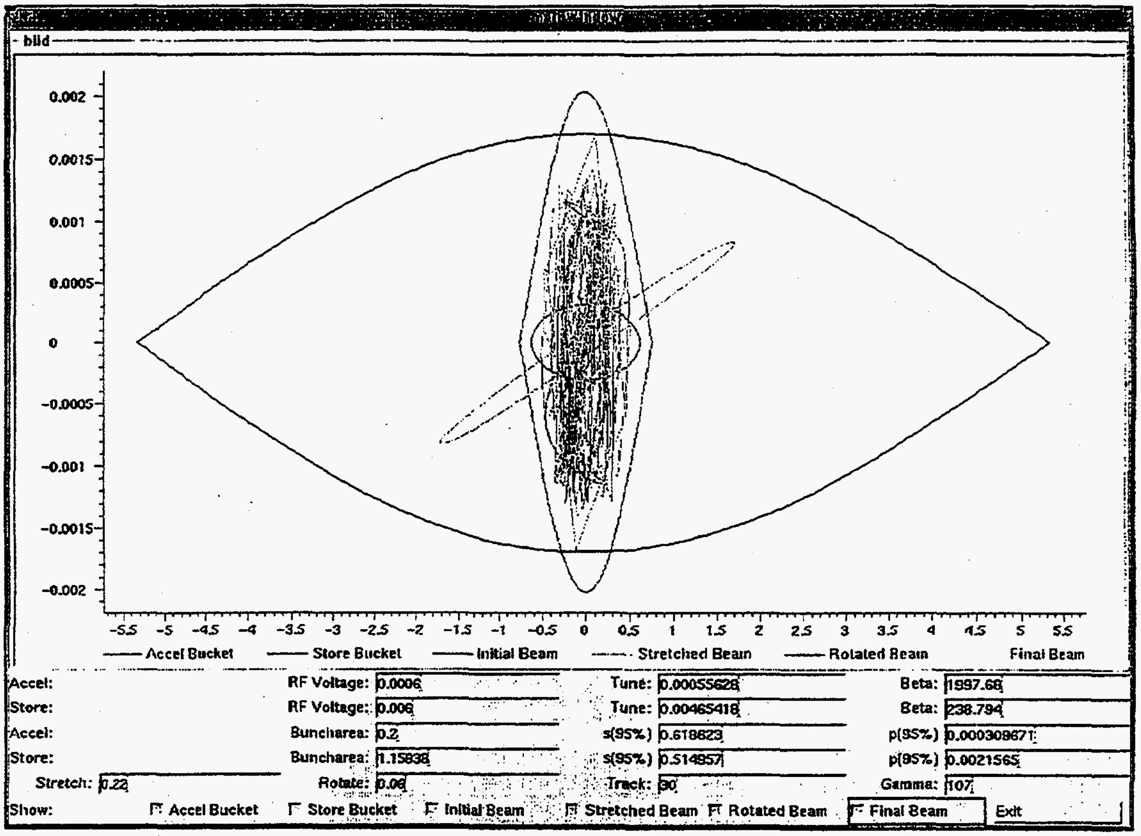
bild
0.002
0.0015
0.001
0.0005
0
-0.0005
-0.001
-0.0015
-0.002
-5.5 -5 -4.5 -4 -3.5 -3 -2.5 -2 -1.5 -1 -0.5 0 0.5 1 1.5 2 2.5 3 3.5 4 4.5 5 5.5
Accel Bucket
Store Bucket
Initial Beam
Stretched Beam
Rotated Beam
Final Beam
Accel:
Store:
Accel:
Store:
Stretch: 0.22
RF Voltage: 0.0006
RF Voltage: 0.006
Buncharea: 0.2
Buncharea: 1.15838
Rotate: 0.06
Tune: 0.00055628
Tune: 0.00465418
s(95%) 0.618623
s(95%) 0.514957
Track: 30
Beta: 1997.68
Beta: 238.794
p(95%) 0.000309671
p(95%) 0.0021565
Gamma: 107
Show:
Accel Bucket
Store Bucket
Initial Beam
Stretched Beam
Rotated Beam
Final Beam
Exit

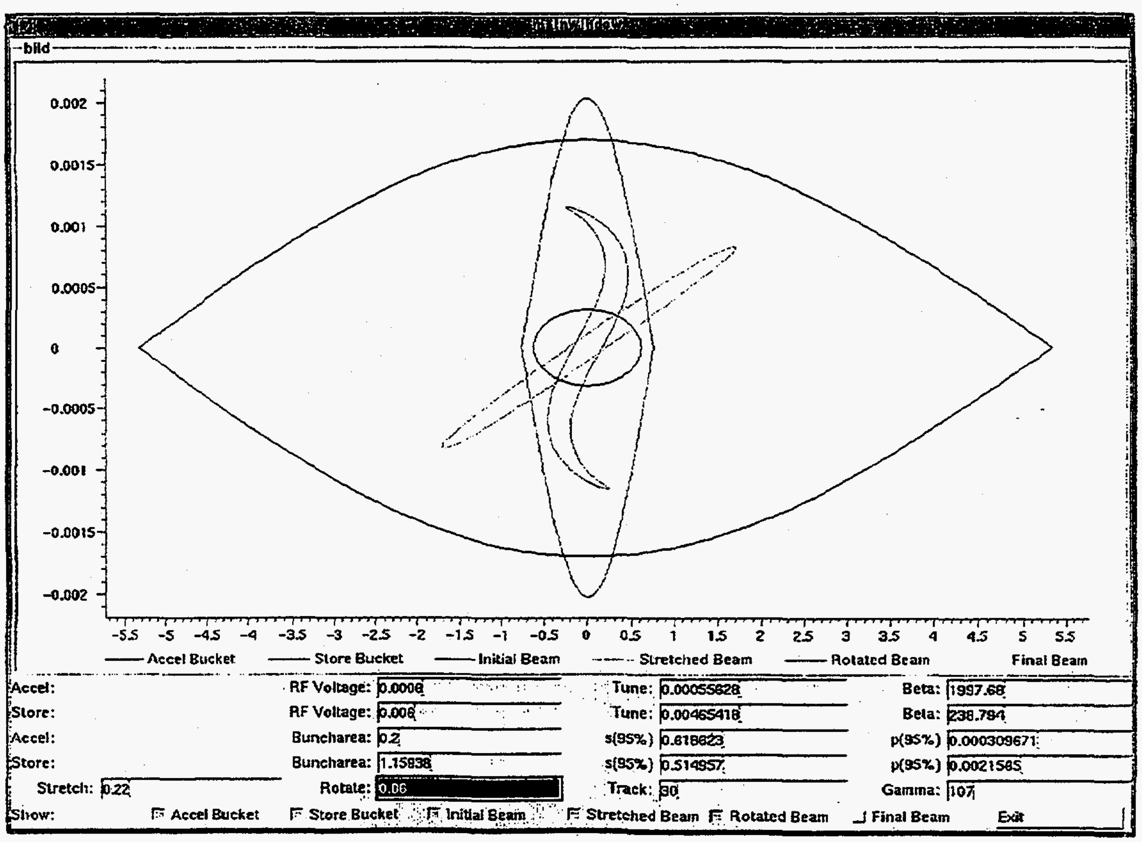
bild
0.002
0.0015
0.001
0.0005
0
-0.0005
-0.001
-0.0015
-0.002
-5.5 -5 -4.5 -4 -3.5 -3 -2.5 -2 -1.5 -1 -0.5 0 0.5 1 1.5 2 2.5 3 3.5 4 4.5 5 5.5
Accel Bucket
Store Bucket
Initial Beam
Stretched Beam
Rotated Beam
Final Beam
Accel:
Store:
Accel:
Store:
Stretch: 0.22
RF Voltage: 0.0006
RF Voltage: 0.006
Buncharea: 0.2
Buncharea: 1.15838
Rotate: 0.06
Tune: 0.00055628
Tune: 0.00465418
s(95%) 0.618623
s(95%) 0.514957
Track: 30
Beta: 1997.68
Beta: 238.794
p(95%) 0.000309671
p(95%) 0.0021565
Gamma: 107
Show:
Accel Bucket
Store Bucket
Initial Beam
Stretched Beam
Rotated Beam
Final Beam
Exit

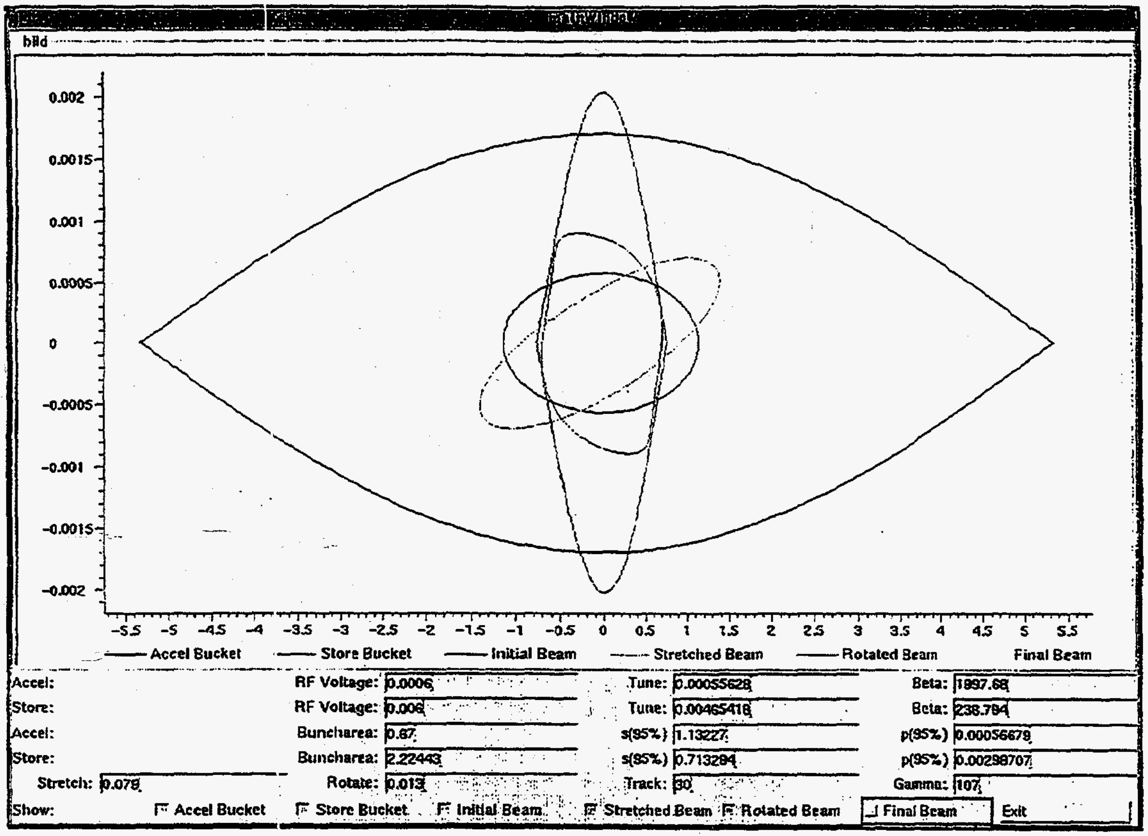

bild
0.002
0.0015
0.001
0.0005
0
-0.0005
-0.001
-0.0015
-0.002
-5.5 -5 -4.5 -4 -3.5 -3 -2.5 -2 -1.5 -1 -0.5 0 0.5 1 1.5 2 2.5 3 3.5 4 4.5 5 5.5
Accel Bucket
Store Bucket
Initial Beam
Stretched Beam
Rotated Beam
Final Beam
Accel: RF Voltage: 0.0006 Tune: 0.00055628 Beta: 1997.68
Store: RF Voltage: 0.006 Tune: 0.00465418 Beta: 238.794
Accel: Buncharea: 0.87 s(95%) 1.13227 p(95%) 0.00056679
Store: Buncharea: 2.22443 s(95%) 0.713284 p(95%) 0.00298707
Stretch: 0.078 Rotate: 0.013 Track: 30 Gamma: 107
Show: Accel Bucket Store Bucket Initial Beam Stretched Beam Rotated Beam Final Beam Exit

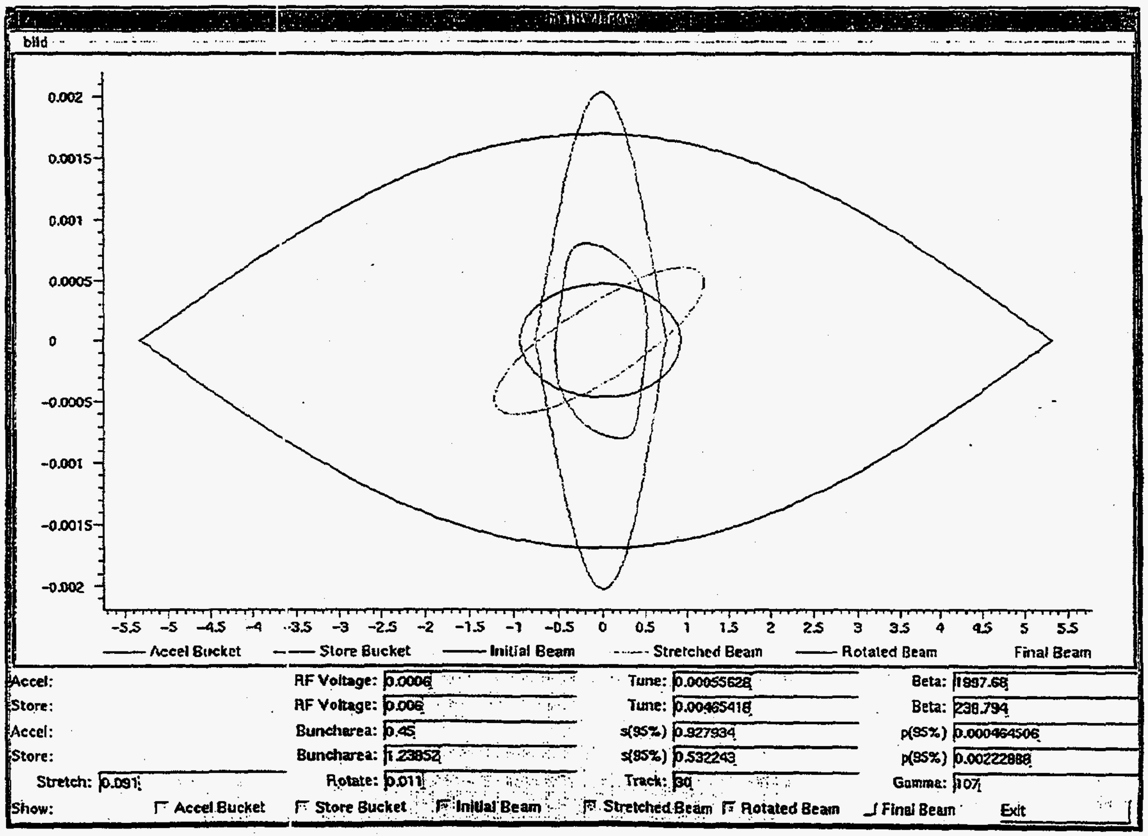

bild
0.002
0.0015
0.001
0.0005
0
-0.0005
-0.001
-0.0015
-0.002
-5.5 -5 -4.5 -4 -3.5 -3 -2.5 -2 -1.5 -1 -0.5 0 0.5 1 1.5 2 2.5 3 3.5 4 4.5 5 5.5
Accel Bucket
Store Bucket
Initial Beam
Stretched Beam
Rotated Beam
Final Beam
Accel: RF Voltage: 0.0006 Tune: 0.00055628 Beta: 1997.68
Store: RF Voltage: 0.006 Tune: 0.00465418 Beta: 238.794
Accel: Buncharea: 0.45 s(95%) 0.927934 p(95%) 0.000464506
Store: Buncharea: 1.23852 s(95%) 0.532243 p(95%) 0.00222888
Stretch: 0.091 Rotate: 0.011 Track: 30 Gamma: 107
Show: Accel Bucket Store Bucket Initial Beam Stretched Beam Rotated Beam Final Beam Exit

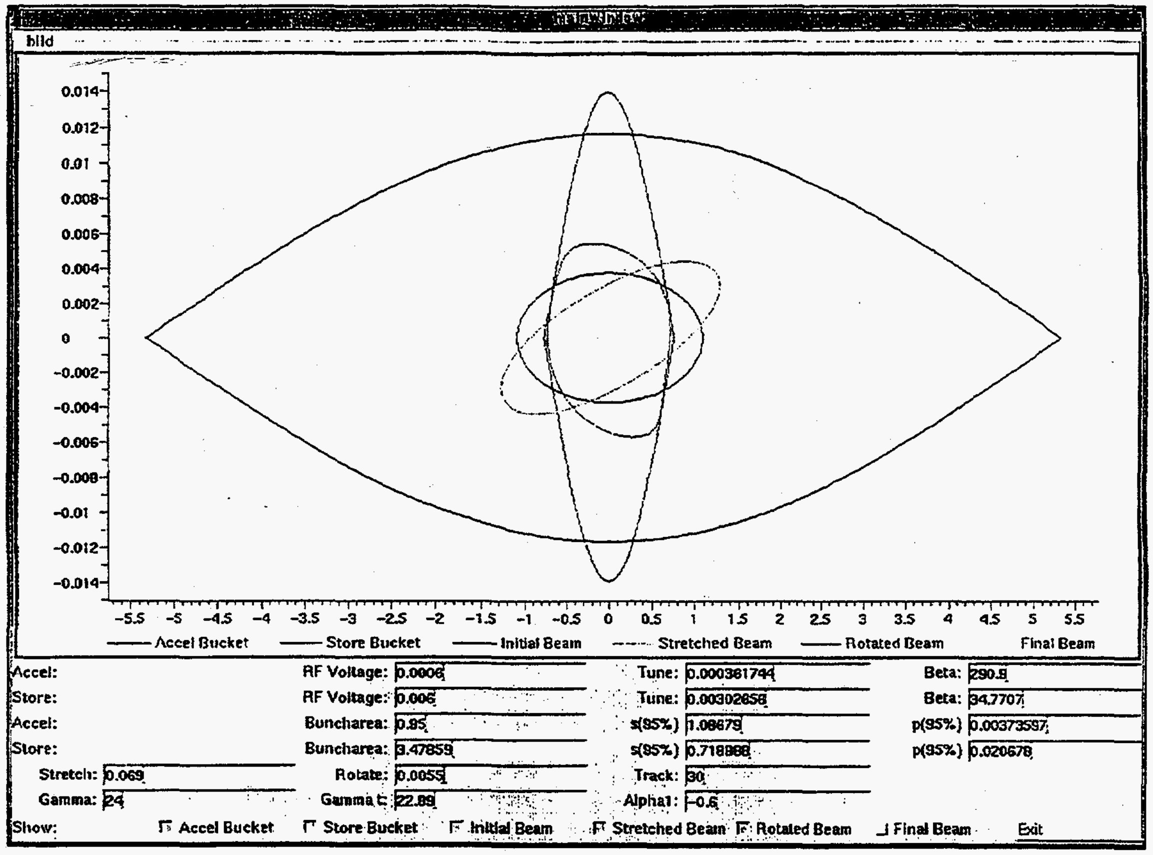
bild
0.014
0.012
0.01
0.008
0.006
0.004
0.002
0
-0.002
-0.004
-0.006
-0.008
-0.01
-0.012
-0.014
-5.5 -5 -4.5 -4 -3.5 -3 -2.5 -2 -1.5 -1 -0.5 0 0.5 1 1.5 2 2.5 3 3.5 4 4.5 5 5.5
Accel Bucket
Store Bucket
Initial Beam
Stretched Beam
Rotated Beam
Final Beam
Accel: RF Voltage: 0.0006 Tune: 0.000381744 Beta: 290.8
Store: RF Voltage: 0.006 Tune: 0.00302658 Beta: 34.7707
Accel: Buncharea: 0.85 s(95%) 1.08679 p(95%) 0.00373597
Store: Buncharea: 3.47859 s(95%) 0.718988 p(95%) 0.020678
Stretch: 0.069 Rotate: 0.0055 Track: 30
Gamma: 24 Gamma t: 22.89 Alpha1: -0.6
Show: Accel Bucket Store Bucket Initial Beam Stretched Beam Rotated Beam Final Beam Exit

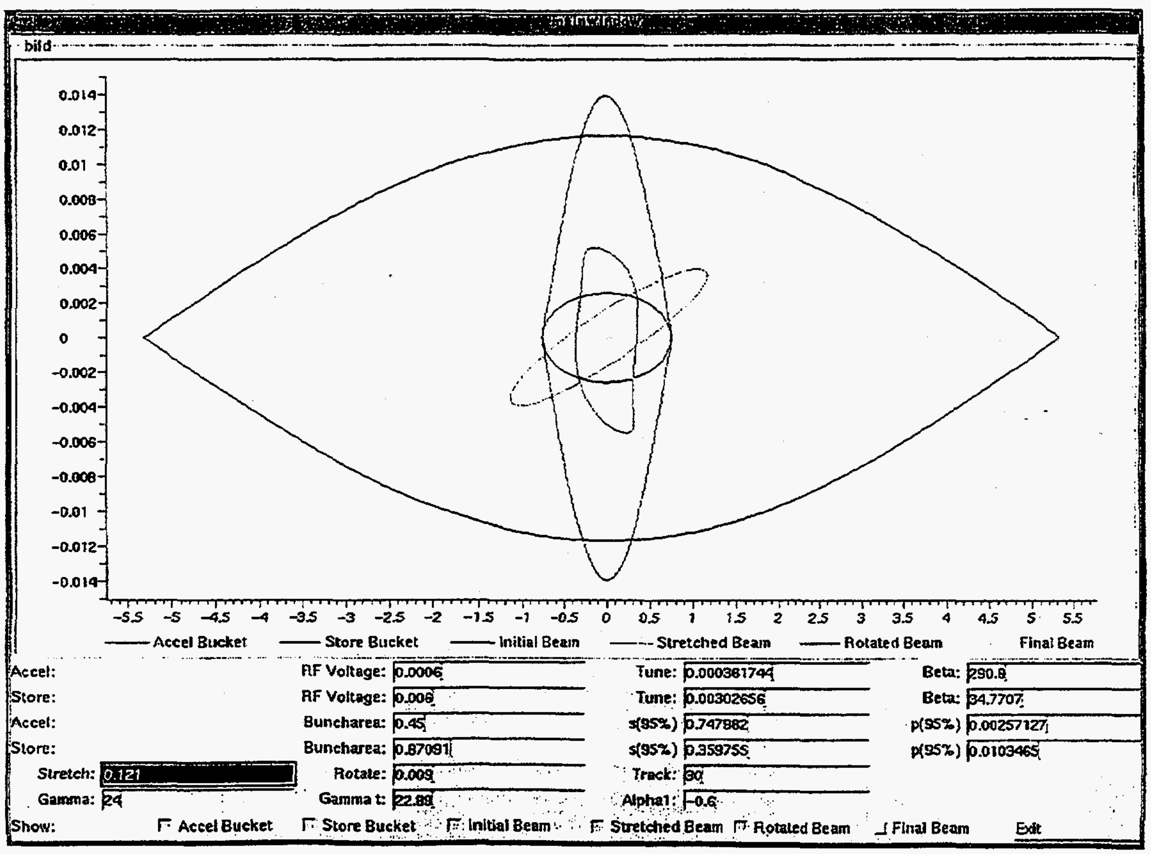
bild
0.014
0.012
0.01
0.008
0.006
0.004
0.002
0
-0.002
-0.004
-0.006
-0.008
-0.01
-0.012
-0.014
-5.5 -5 -4.5 -4 -3.5 -3 -2.5 -2 -1.5 -1 -0.5 0 0.5 1 1.5 2 2.5 3 3.5 4 4.5 5 5.5
Accel Bucket
Store Bucket
Initial Beam
Stretched Beam
Rotated Beam
Final Beam
Accel: RF Voltage: 0.0006 Tune: 0.000381744 Beta: 290.8
Store: RF Voltage: 0.006 Tune: 0.00302656 Beta: 34.7707
Accel: Buncharea: 0.45 s(95%) 0.747882 p(95%) 0.00257127
Store: Buncharea: 0.87091 s(95%) 0.359755 p(95%) 0.0103465
Stretch: 0.121 Rotate: 0.009 Track: 30
Gamma: 24 Gamma t: 22.89 Alpha1: -0.6
Show: Accel Bucket Store Bucket Initial Beam Stretched Beam Rotated Beam Final Beam Exit

Conclusion

Particles are captured up to (sigma):

Condition	Sigma
at storage 0.2 eV sec/u	8.3
at storage 0.45 eV sec/u	3.75
after transition 0.45 eV sec/u	5.4
after transition 0.45 eV sec/u, V=800kV	5.9

174

To do:

- Extend tracking program to simulate rebucketing while ramping
- ???

Session on Longitudinal Instabilities

K.Y. Ng

There were 3 talks in this session. The first talk was by Y.H. Chin and H. Tsutsui on "Microwave Instability in a Barrier Cavity". A bunch inside a barrier bucket behaves like a coasting beam because the bunch particles drift most of the time. However, it is also a bunch because of its finite length, and therefore we can talk about bunch modes. Chin and Tsutsui demonstrated the equivalence between mode-crossing instability and the Boussard-Keil-Schnell microwave instability. Although this equivalence had been demonstrated for a resonant impedance by many authors, they were the first to demonstrate mode-crossing instability for a pure inductive impedance below transition, which is predicted by the Boussard-Keil-Schnell theory. They expanded the bunch modes in terms of orthogonal functions and compute the eigen-modes as a function of bunch current. They also wrote a code to track the bunch particles in the longitudinal phase space, and verified that the onsets of instability agree with theory. The code is a tracking in the time domain and approximates a bunch as a series of triangular bunches.

The second talk by M. Blaskiewicz is on "Fast Particle-Particle Update Scheme" in tracking. When tracking N particles involving binary interaction, the number of steps per turn is usually $\mathcal{O}(N^2)$, which rises sharply when more particles are required. First, the time-order of the particles are sorted, which takes $\mathcal{O}(N \ln N)$ steps. Once the ordering is known, the positions of the particles can be updated using a recurrence relation, which takes $\mathcal{O}(N)$. Thus, for each turn, the number of steps is reduced from $\mathcal{O}(N^2)$ to $\mathcal{O}(N \ln N)$, and the saving in time is very significant.

The third talk by J. Rose is on "Stability in RHIC" against longitudinal coupled-bunch instability. ZAP and analytic formula computations for bunches passing through the the 28 MHz cavity shows instabilities driven by only the first few higher-harmonic modes (HOM). This is because the form factor falls off as the inverse of both the HOM frequency and the square of the bunch length. Since the bunches in RHIC will be long, the form factor is less than 0.6. Note that this is rather conservative; for a Gaussian bunch distribution, the form factor will fall off very much faster. Some passive de-Qing had been performed on these offensive modes, so that the growth rates for the unstable modes will be within the range of the injection damper rate of 10 sec^{-1}. From the MAFIA computation of the HOM dampers, it appears that there should not be any problem concerning longitudinal coupled-mode instability.

176

Longitudinal Bunched-Beam Instabilities in a Barrier RF System

KEK

Yong Ho Chin
and
Hiroshi Tsutsui

1997 Particle Accelerator Conference
Vancouver, Canada
May 13, 1997

Introduction

- Barrier RF System

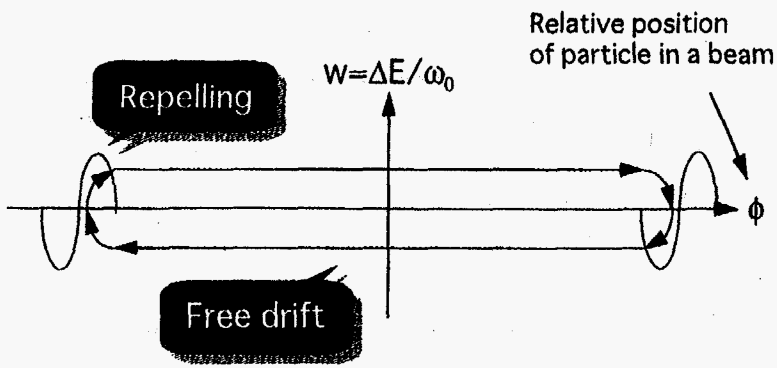

- Characteristics of a barrier RF system
  - A very flat bunch --> A smaller peak current
  - A variable bunch length
  - A small synchrotron frequency (ν_{rms}=17Hz at JHF)
  - Synchrotron frequency proportional to the energy deviation --> A spread is comparable to the frequency itself
  - A strong Landau damping effect

- Collective stability of a bunched-beam in a barrier bucket
  - Keil-Schnell-Boussard criterion would give a reasonable estimate, IF
    - the wave length of beam density modulation is much shorter than the bunch length
    - the instability growth is much faster than the synchrotron motion.

How do we know without calculation ?

If not, or no way to know if the coasting approximation is good or not, what should replace Keil-Schnell-Boussard criterion?

A need to develop a theory proper to a bunched-beam

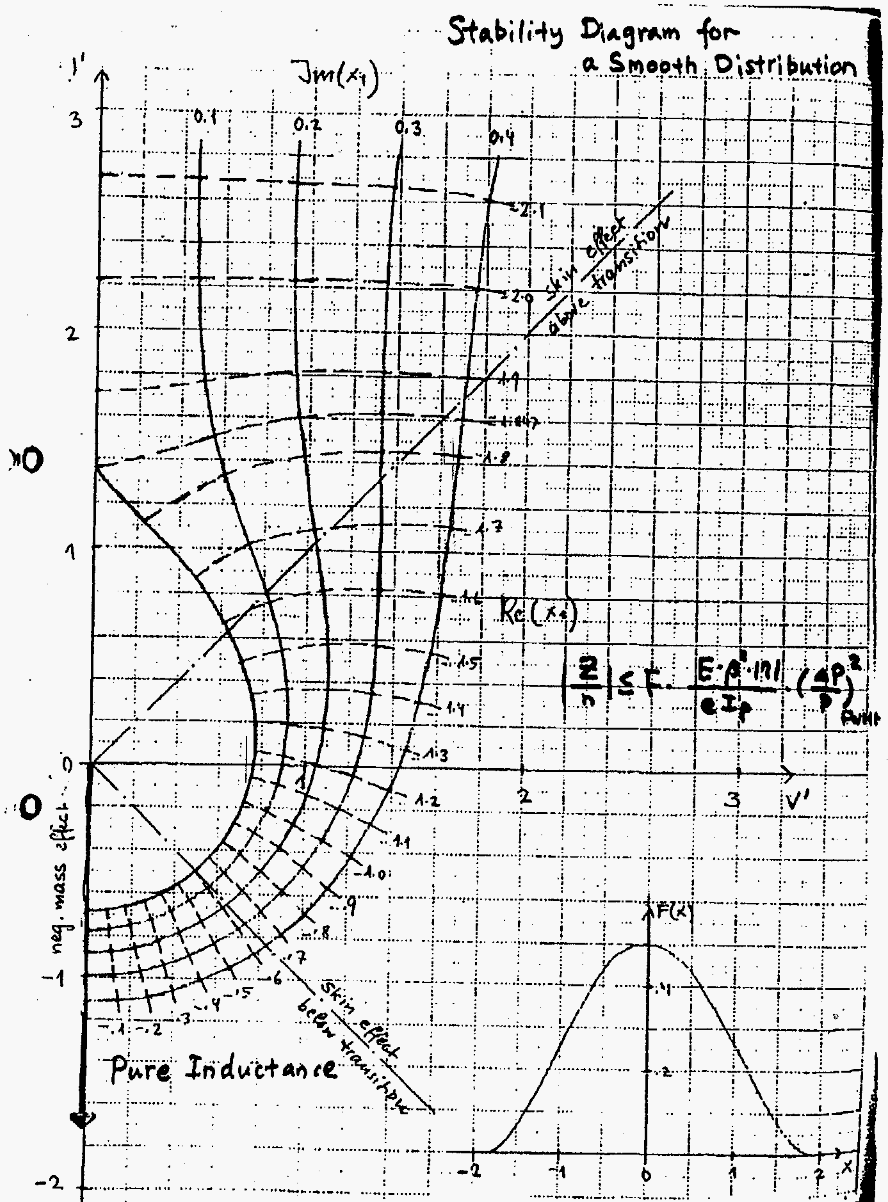

Fig. 6 - Quartic distribution

Coasting Beam Mode Number "n"

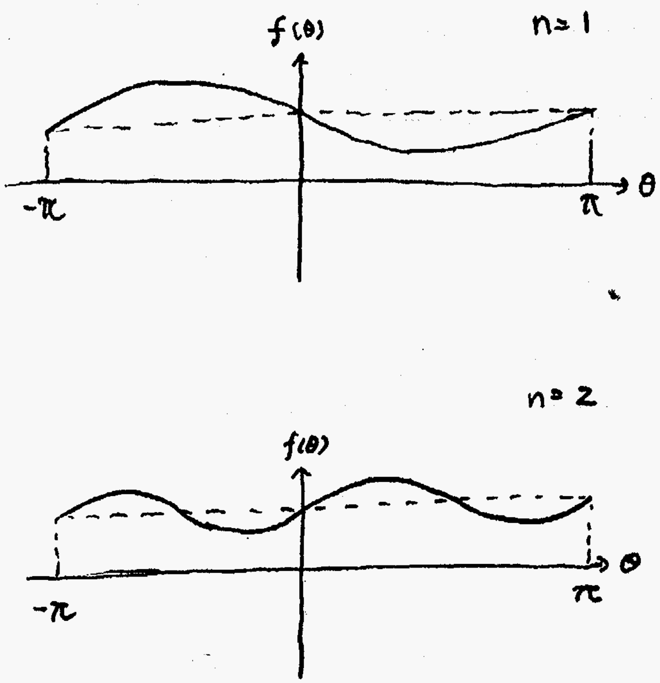

- Main framework of the newly developed theory
  - No coasting beam approximation
  - Vlasov equation for evolution of phase space distribution
  - Synchrotron and energy mode expansion
  - Action-angle variables to describe the squarish particle trajectory in phase space
  - A Gaussian energy distribution
  - A full inclusion of Landau damping effect
- A simulation code ECLIPS (Evaluation Code for Longitudinal Instabilities in a Proton Synchrotron) was also developed.
- Their application to JHF 50 GeV proton synchrotron at injection show good agreements.
- We will demonstrate (as Sacherer predicted)

Microwave and negative mass instabilities in a coasting beam → transform → Mode-coupling instabilities in a bunched-beam

BUNCH LENGTHENING AND MICROWAVE INSTABILITY

F.J. Sacherer
CERN, Geneva, Switzerland

Introduction and Summary

A single-bunch instability that leads to blow-up of bunch area and microwave signals (100 MHz to 3 GHz) has been observed in the PS[1] and the ISR[2]. A similar instability may cause bunch lengthening in electron storage rings. Attempts to explain this as a high-frequency coasting-beam instability require e-folding rates faster than a synchrotron period, and wavelengths shorter than a bunch length. In this case, the usual Keil-Schnell coasting-beam criterion[3] is used, but with local values of bunch current and momentum spread, as suggested by Boussard[1]. This yields $|Z/n| \approx 13\ \Omega$ for the ISR, and values about five to ten times larger for the PS. The restrictions mentioned above, however, are not fulfilled near threshold, or for frequencies as low as 100 MHz.

A direct approach, without coasting-beam approximations, is presented in this paper. The basic idea is that the usual bunched-beam modes[4], dipole, quadrupole, sextupole, etc., become unstable at intensities sufficiently high for their coherent frequencies to cross, as indicated in Fig. 1. If $Z(\omega)$ is known, the frequency shifts can be computed, and surprisingly, one finds thresholds near the coasting beam values, but with fewer assumptions.

The lowest thresholds occur for wakefields that decay in about a bunch length. In general, lowering Q-values does not help, since the threshold depends on the area under the resonance curve. For very rapidly decaying wakes, the bunch is stable, in agreement with a conjecture of Hereward[5]. Only one wavelength along the bunch is sufficient for instability.

The main results are presented here (Part 1), while the derivations are given elsewhere[6] (Part 2). For other approaches, see references 7 to 10.

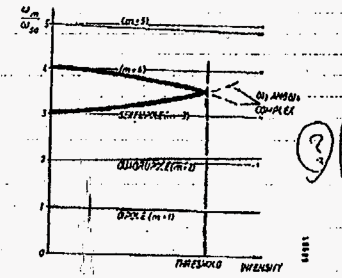

Fig. 1 Coherent frequencies ω_m versus intensity

Modes of Oscillation

For low intensities, a bunch can oscillate in the usual dipole, quadrupole and higher modes (Fig. 2) with frequencies near harmonics of the synchrotron frequency, $\omega_m \approx m\omega_{s0}$. The oscillating part of the line density $\lambda_m(t)$ is approximately sinusoidal, and a little thought

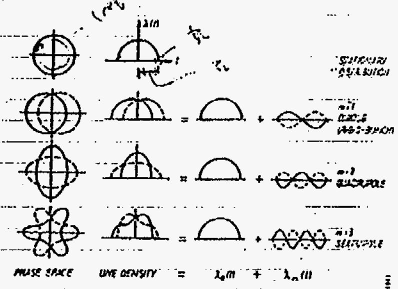

Fig. 2 Low-intensity modes of oscillation

shows it to be a standing wave with fixed nodes, so there is no instability if the wakefield decays before the next bunch arrives[4]. However, at sufficiently high intensities for two coherent frequencies to merge as indicated in Fig. 1, the two standing waves add to give travelling waves, one moving forward and one backward along the bunch, one of which is stable and the other unstable. This is the connection with the coasting-beam travelling-wave modes.

Fig. 3 Envelope of frequency spectra for the stationary distribution and for modes m and m+1

The spectra for the low intensity modes are shown in Fig. 3. Mode m is peaked near the frequency $(m+1)/(2\tau_L)$ of the sine wave $\lambda_m(t)$, and extends $\pm 1/\tau_L$ Hz corresponding to the bunch length τ_L sec. For example, mode m = 5 for a 1 nsec bunch is centred at 3 GHz, and lies mostly above the pipe cut-off.

The actual spectrum is a line spectrum within the envelopes of Fig. 3. For one bunch, the frequencies

$$f_p = pf_0 + mf_s\ , \qquad -\infty < p < \infty \qquad (1)$$

occur, where f_s is the synchrotron frequency and f_0 is the revolution frequency in Hz. For M equally spaced bunches, only every M^{th} line occurs,

$$f_p = (n + pM)f_0 + mf_s\ , \qquad -\infty < p < \infty \qquad (2)$$

*) A longitudinal chromaticity due to the dependence of the synchrotron frequency on momentum deviation would lead to a head-tail instability analogous to the transverse case, but this effect has been estimated to be very small[11].

Vlasov analysis

Square model

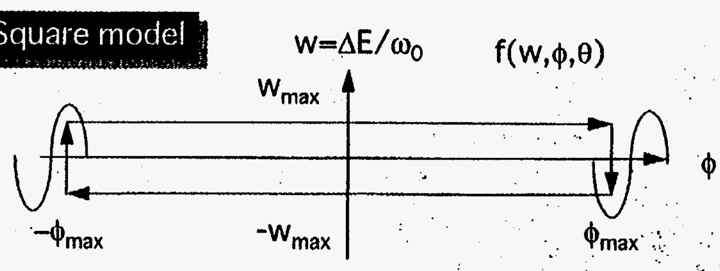

Since the particle trajectory is a complicated function of w and ϕ, let us introduce the action-angle variables.

$I = \frac{1}{2\pi}\int dw\, d\phi = \frac{2}{\pi}\phi_{max} w_{max}$ — Action=area in □

[illegible] — Angle=phase of motion

[illegible] — Synchrotron frequency proportional to I (or ΔE_{max})

Vlasov eq. for the phase space distribution $f(I,\psi,\theta)$

$$\frac{\partial f}{\partial \theta} + \psi' \frac{\partial f}{\partial \psi} + I' \frac{\partial f}{\partial I} = 0$$

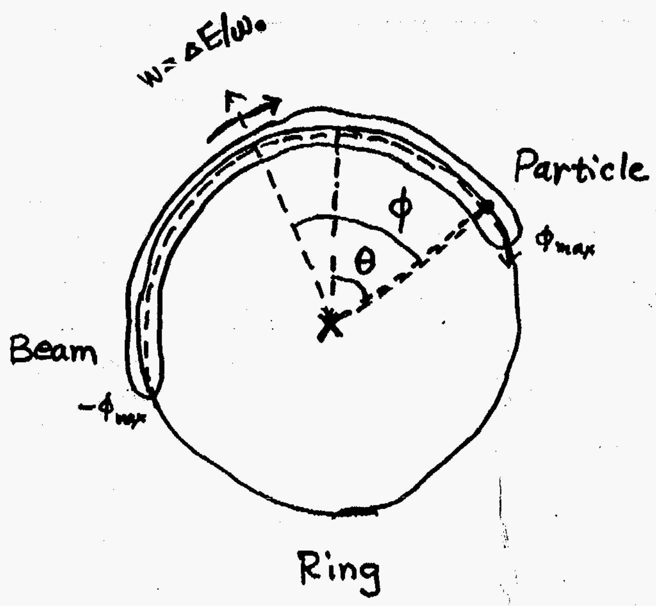

- Perturbation method + separate factorization with respect to I and ψ + Fourier expansion

$$f(I,\psi,\theta) = f_0(I) + \sum_{m=-\infty}^{\infty} f_m(I)\exp(im\psi)\exp(-i\Omega\theta)$$

Line charge density $\rho(\phi)$

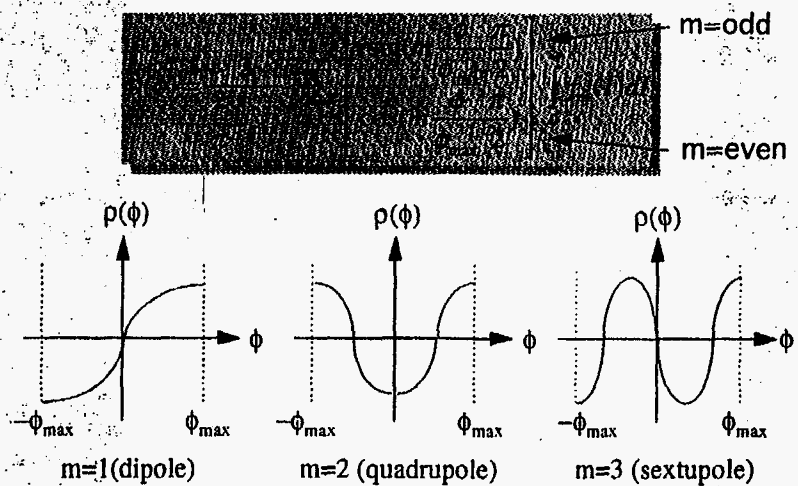

corresponds to "n=1" coasting beam mode when $\phi_{max}=\pi$

- Using impedance $Z(\omega/\omega_0)$ and Fourier transform of $\rho(\phi)$, $\tilde{\rho}(v)$

$$I' = -e^2 N \frac{\phi_{\max}}{\pi^2} \mathrm{sgn}(w) \sum_{p=-\infty}^{\infty} Z(p+\Omega)\tilde{\rho}(p+\Omega)$$
$$\times \exp(-i(p+\Omega)\phi - i\Omega\theta)$$

$$\psi' = v_s(I)$$

- Vlasov eq. becomes an integral eq. for $f_m(I)$:

[illegible]

where I_b=circulating current and

$$C_m(q) = \frac{q\frac{2}{\pi}\phi_{\max}\begin{bmatrix} i\cos(q\phi_{\max}) \\ \sin(q\phi_{\max}) \end{bmatrix}}{m^2 - \left(q\frac{2}{\pi}\phi_{\max}\right)^2}$$

- The integral eq. for unknown $f_m(I)$ can be solved by expanding $f_m(I)$ with a set of orthogonal polynomials.
- For a Gaussian energy distribution $f_0(I)$, the best choice is the Laguerre polynomials $L_k(x)$.
- Finally, we get a matrix eigenvalue eq. for Ω:

$$\mathbf{\Omega \cdot a - N \cdot a = M \cdot a}$$

where

$$N_{nl}^{mk} = -m \frac{\pi\eta}{\sqrt{2}\phi_{\max}\beta^2} \left(\frac{\Delta E}{E_0}\right)_{rms} \delta_{mn} L_{kl}$$

$$L_{kl} = \int_0^{\infty} \sqrt{x} e^{-x} L_k(x) L_l(x) dx$$

[illegible]

182

Numerical examples

Main parameters of JHF 50 GeV proton synchrotron at injection

Injection energy, E_i	3GeV
Circumference, C	1442m
Design circulating current, I_b	6.65A
Slippage factor, η	-0.05
Half bunch length in angle, ϕ_{max}	150 degree
RMS energy spread, $(\Delta E/E_0)_{rms}$	0.212%
RMS synchrotron frequency, $\Omega_0/2\pi$	16.97Hz
Impedance of the ring, R_s	10kΩ
Resonant frequency, f_r	3.4MHz
Q-value	1

- Two impedance cases to be studied by the theory and simulations:
  - Resonator impedance
  - Pure inductive impedance
    - the strength chosen to be equal to that of the resonator impedance at low frequency

Resonator impedance

Analytical result

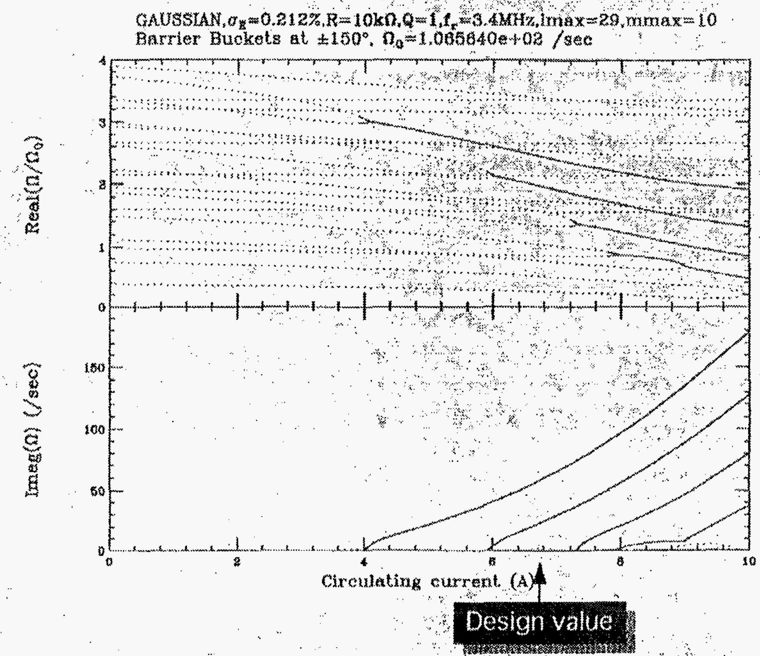

Fig.1: Coherent synchrotron mode frequencies (/ Ω_0) and the growth rate as a function of circulating current.

Simulation result

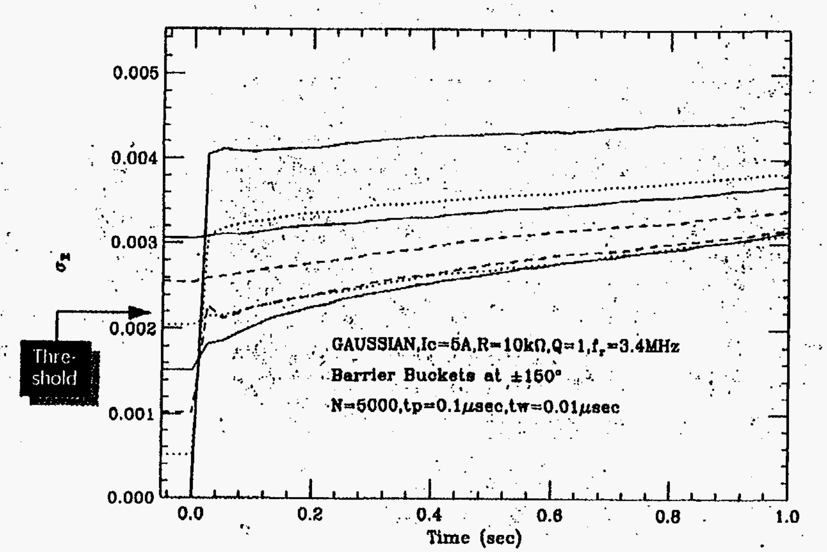

Fig.2: Time evolution of the rms energy spread at 5A for various initial energy spreads.

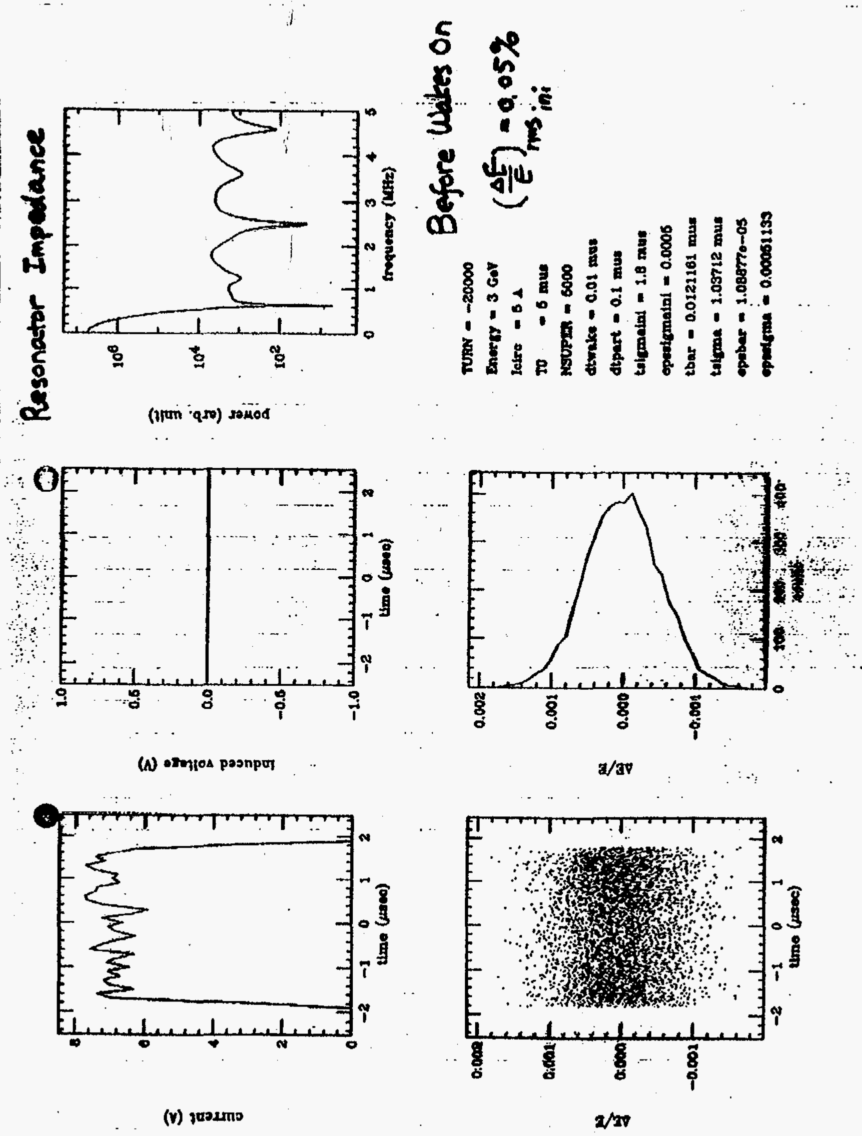

Resonator Impedance

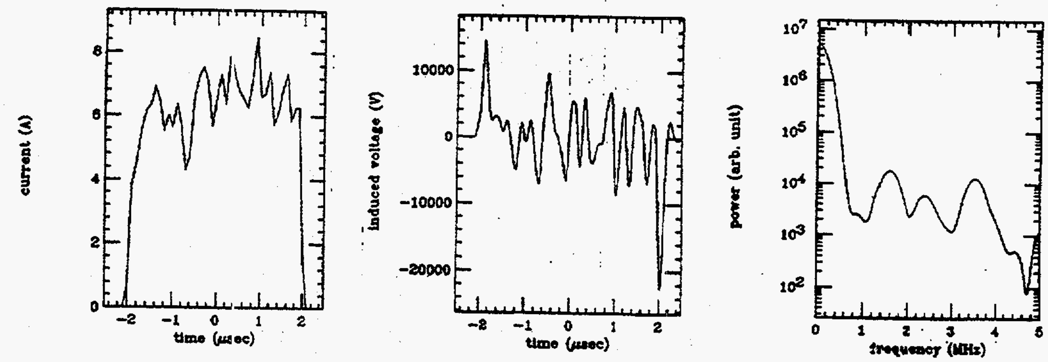

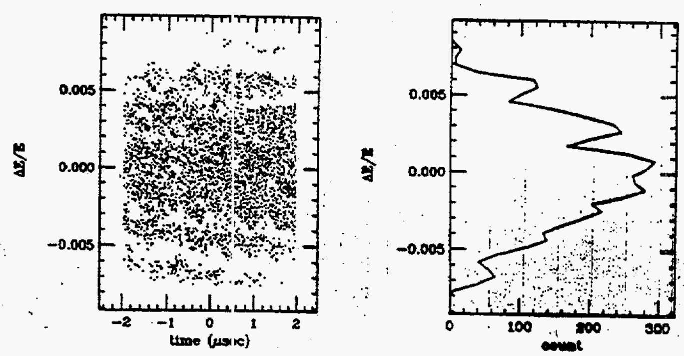

75msec ($\frac{5}{4}\nu_s$)

Afer Wakes On

TURN = 15000
Energy = 3 GeV
Icirc = 6 A
T0 = 5 mus
NSUPER = 5000
dtwake = 0.01 mus
dtpart = 0.1 mus
tsigmaini = 1.8 mus
epssigmaini = 0.0005
tbar = 0.07[illegible] mus
tsigma = 1.10414 mus
epsbar = 0.000209616
epssigma = 0.00[illegible]

Resonator Impedance

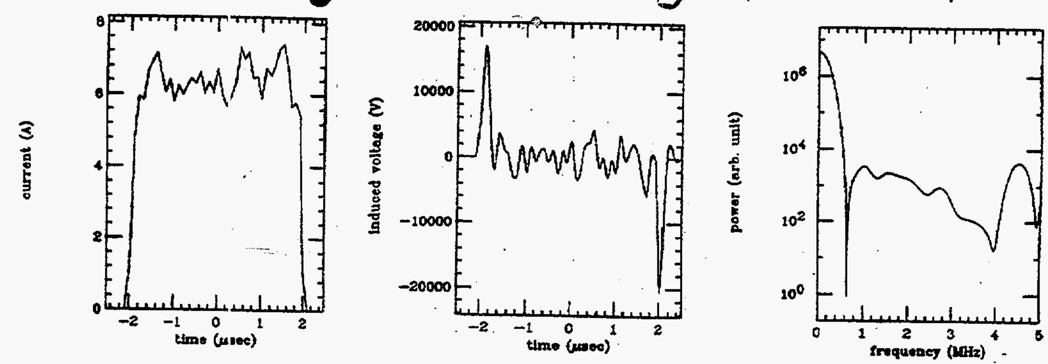

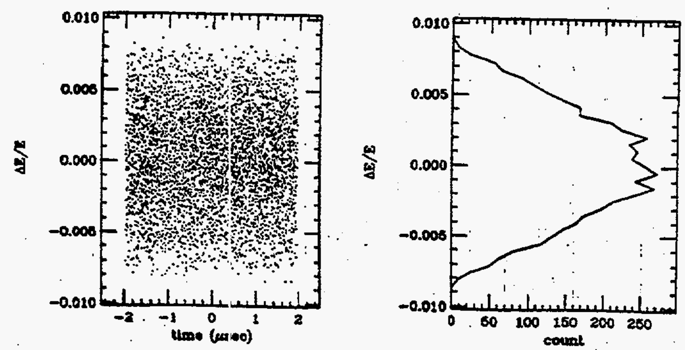

500msec (8.3ν_s)

After Wakes On

TURN = 100000
Energy = 3 GeV
Icirc = 5 A
T0 = 5 mus
NSUPER = 5000
dtwake = 0.01 mus
dtpert = 0.1 mus
tsigmaini = 1.8 mus
epssigmaini = 0.0005
tbar = 0.019706 mus
tsigma = 1.12515 mus
epsbar = 8.40349e-05
epssigma = 0.00351361

- The simulation for 5A shows that the energy distribution stops to blow up at the initial spread of about 0.20%, in good agreement with the analytical result.
- The phase space plots show a uniform particle density after the blow-up the energy spread.

A signature of the microwave instability

Inductive Impedance

- The coasting beam theory predicts the excitation of the negative mass instability.

Analytical result

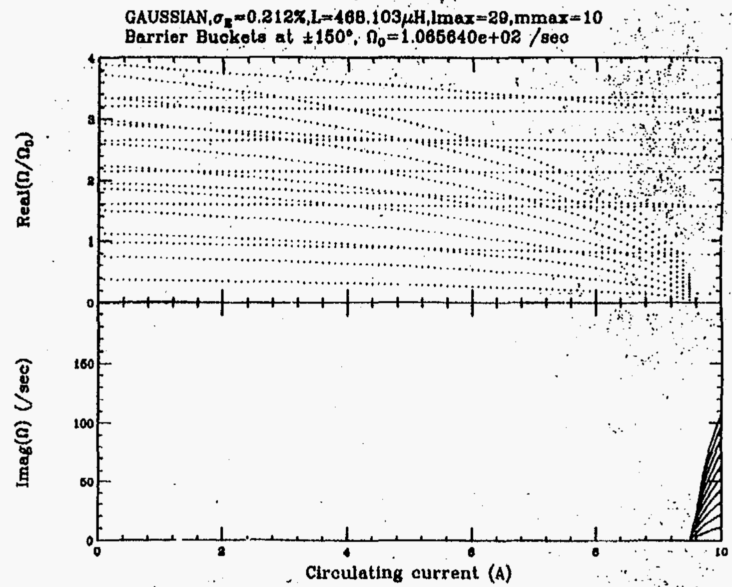

Fig.4: Coherent synchrotron mode frequencies ($/\ \Omega_0$) and the growth rate as a function of circulating current.

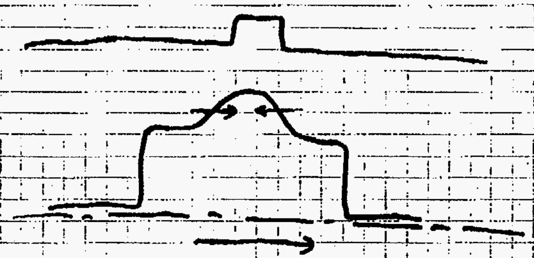

Negative Mass Instability

Simulation result

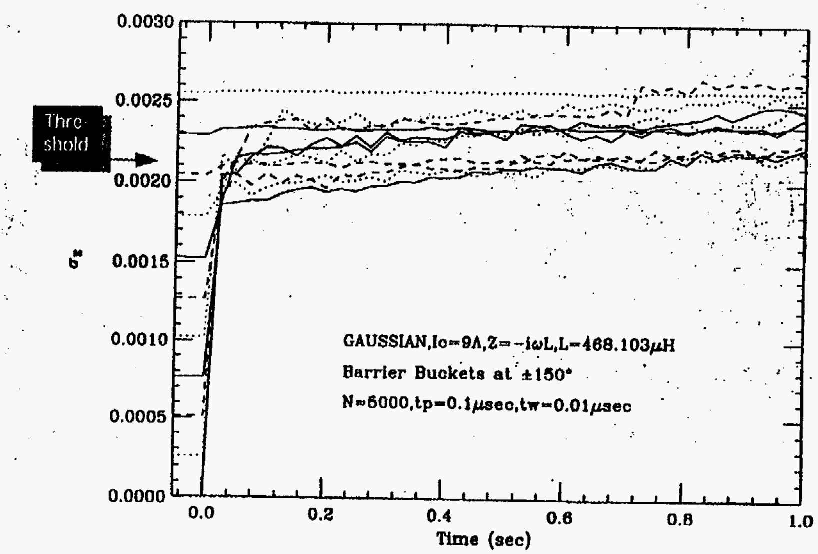

Fig.5: Time evolution of the rms energy spread at 9A for various initial energy spreads.

Simulation result

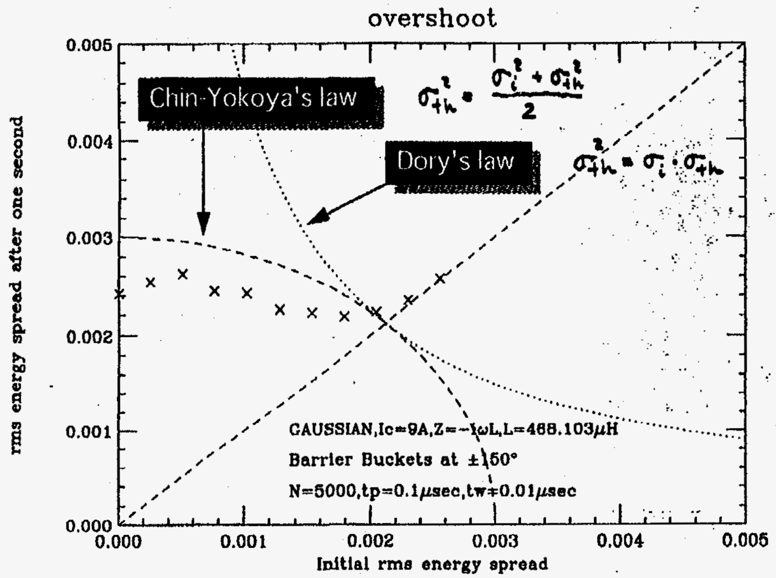

Fig.7: Overshooting of the energy spread. The final spread versus the initial spread.

Simulation result

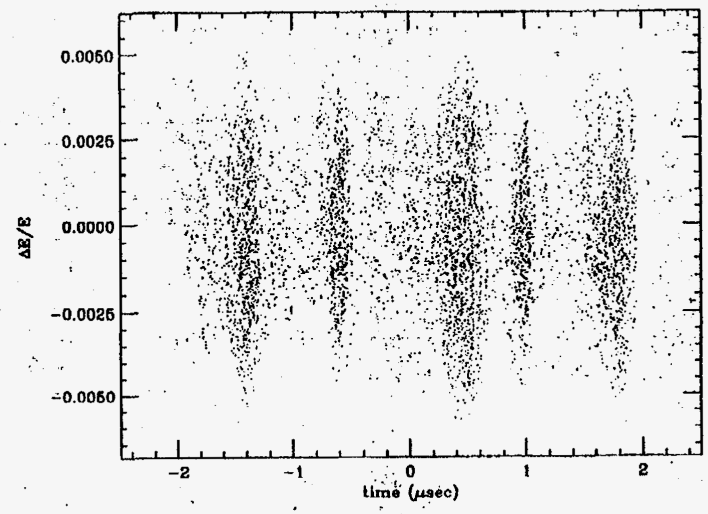

Fig.6: Phase space distribution after the instability ceased for the initial energy spread of 0.05%.

Inductive Impedance

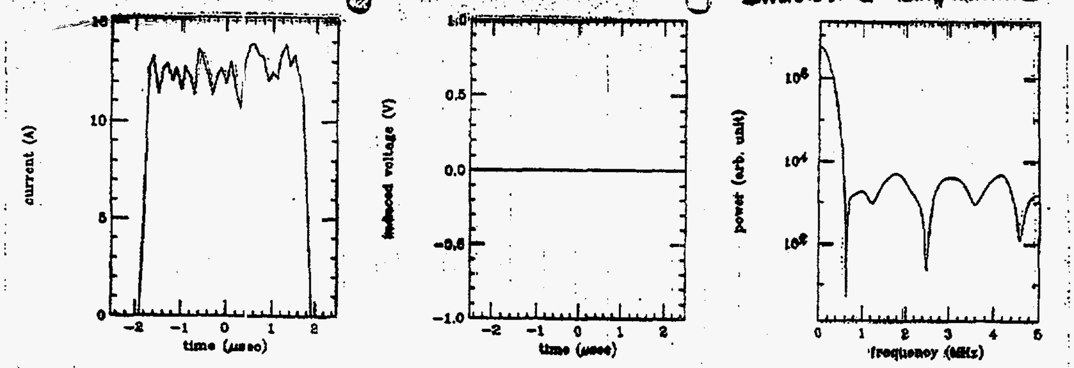

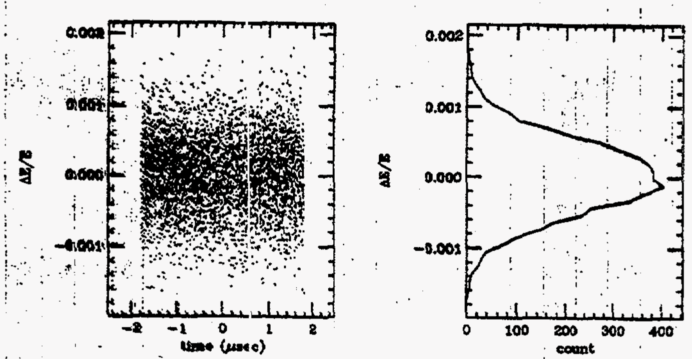

Before Wakes On

TURN = -20000
Energy = 3 GeV
Icirc = 9 A
T0 = 5 mus
NSUPER = 5000
dtwake = 0.01 mus
dtpart = 0.1 mus
tsigmaini = 1.8 mus
epssigmaini = 0.0005
tbar = 0.0121161 mus
tsigma = 1.03712 mus
epsbar = 1.08877e-05
epssigma = 0.00051133

Inductive Impedance

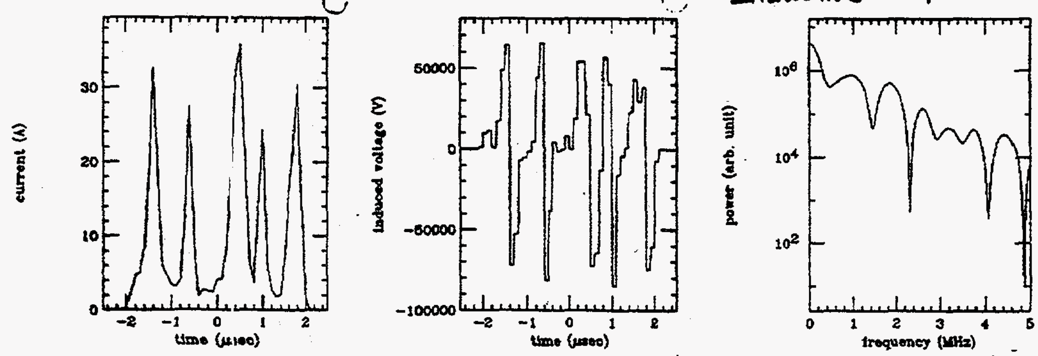

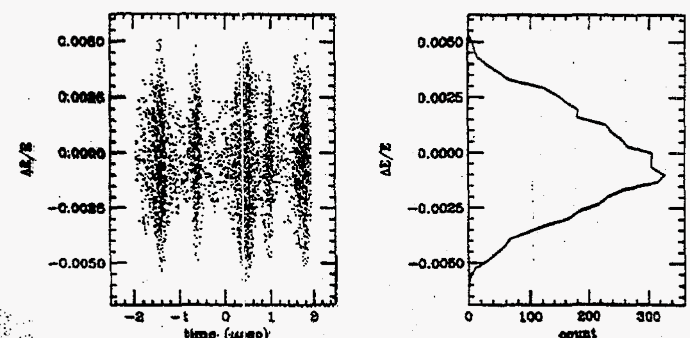

25 msec (0.4 V_s)
After Wakes On

TURN = 5000
Energy = 3 GeV
Icirc = 9 A
T0 = 5 mus
NSUPER = 5000
dtwake = 0.01 mus
dtpart = 0.1 mus
tsigmaini = 1.8 mus
epssigmaini = 0.0005
tbar = 0.16608 mus
tsigma = 1.14167 mus
epsbar = -0.000372246
epssigma = 0.0019937

- The simulation at 9A shows that the energy distribution stops to blow up at the initial spread of about 0.21%, in good agreement with the analytical result again.
- Strong concentration of particles can be observed in the phase space after the instability ceased.

An evidence of the negative mass instability

- The negative mass instability has the same threshold for all coasting beam mode "n" for an inductive impedance:

$$\left|\frac{Z_L}{n}\right| \leq \frac{E\beta^2|\eta|}{eI_p}\left(\frac{\Delta p}{p}\right)^2_{FWHH} \quad \text{(Keil-Schnell-Boussard criterion)}$$

This behavior agrees with the simultaneous onset of mode-coupling instabilities of all synchrotron modes.

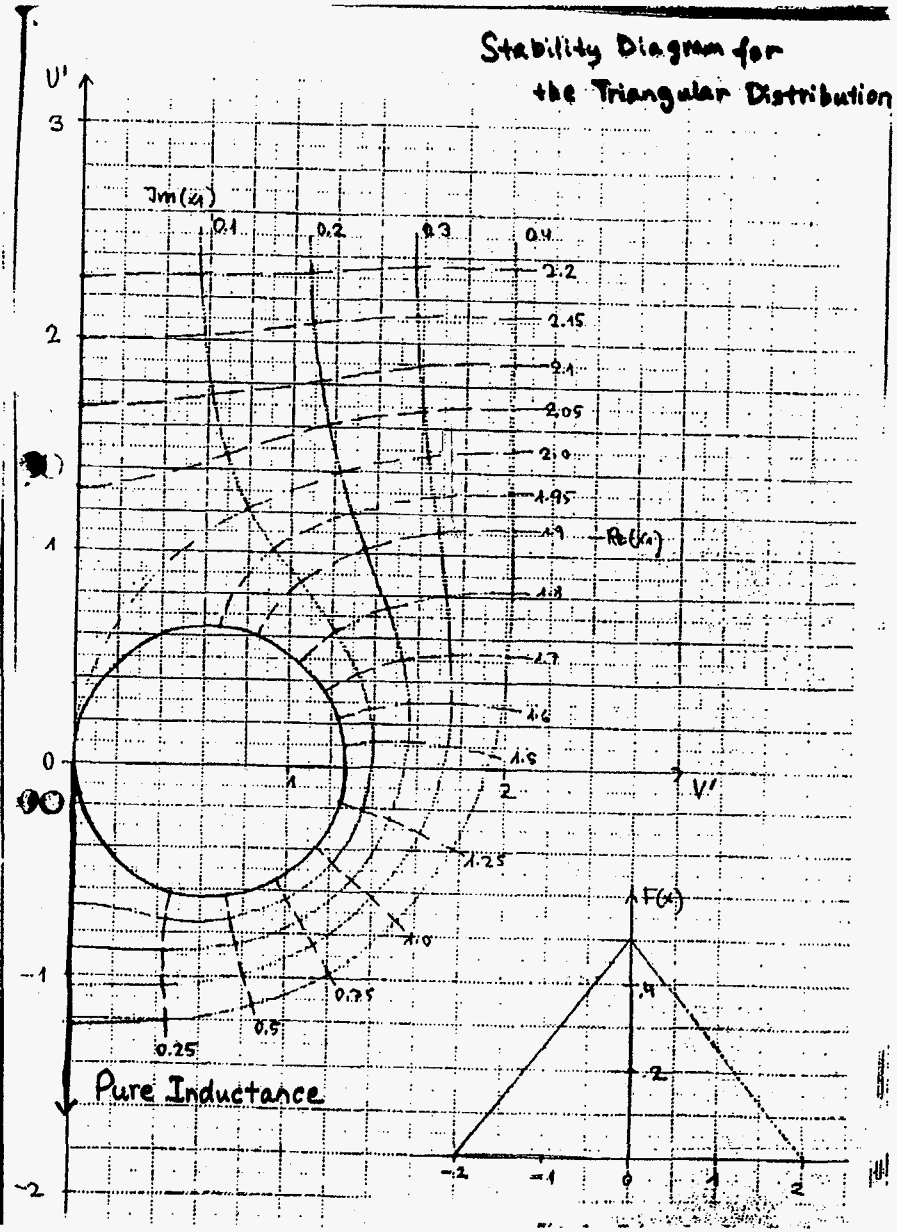

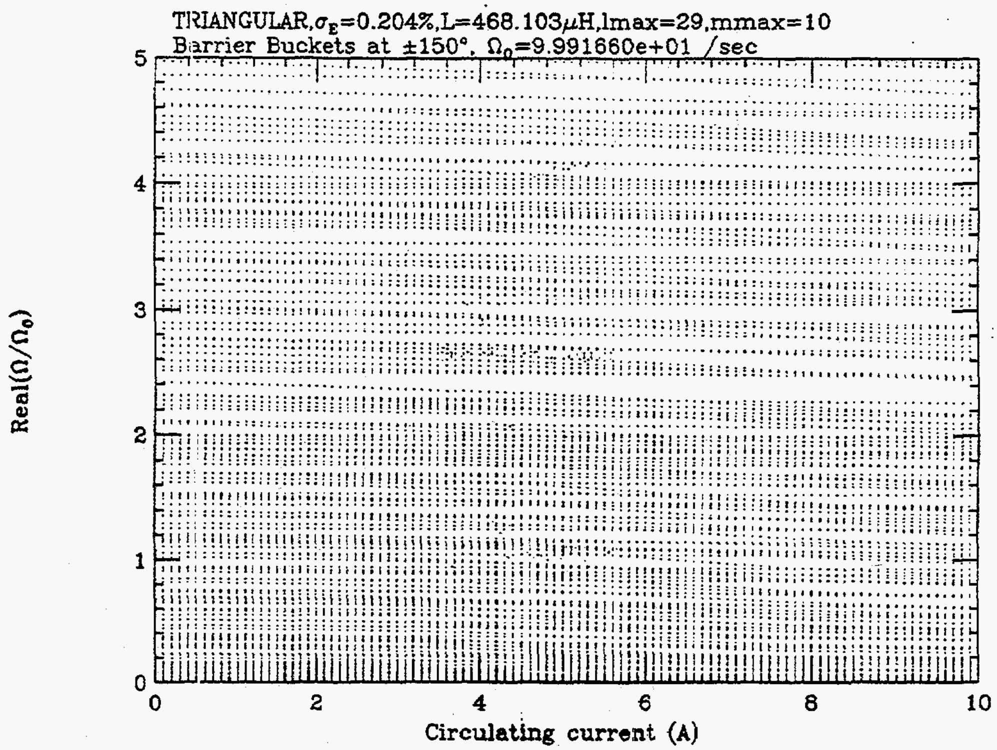
TRIANGULAR,σ_E=0.204%,L=468.103μH,lmax=29,mmax=10
Barrier Buckets at ±150°, Ω_0=9.991660e+01 /sec
Real(Ω/Ω_0)
Circulating current (A)

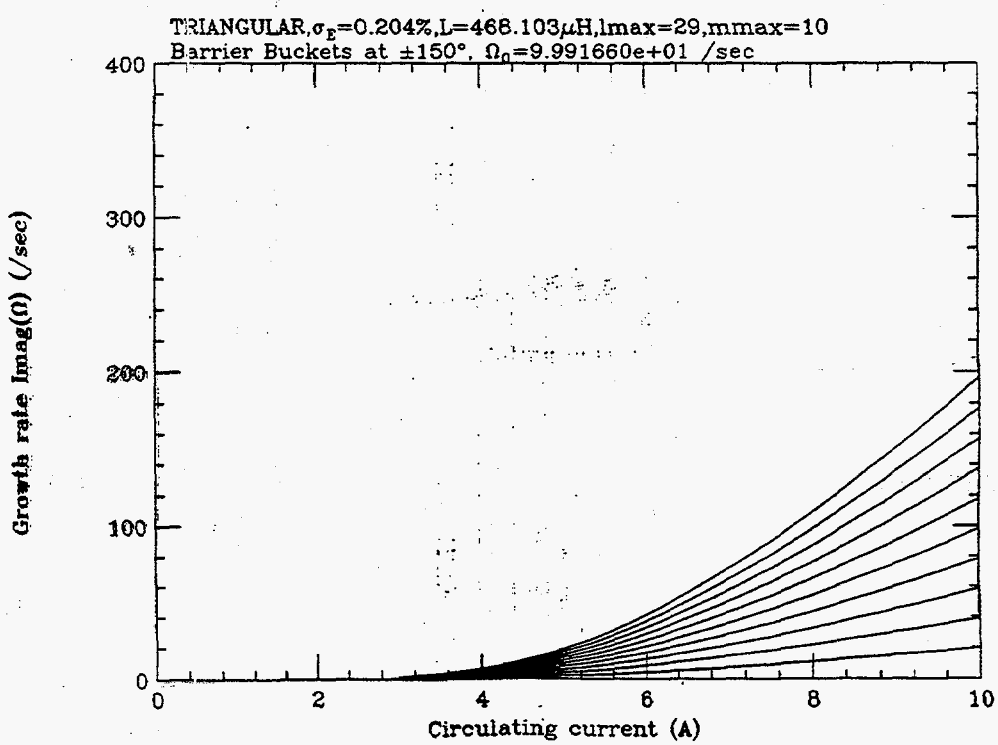
TRIANGULAR,σ_E=0.204%,L=468.103μH,lmax=29,mmax=10
Barrier Buckets at ±150°, Ω_0=9.991660e+01 /sec
Growth rate Imag(Ω) (/sec)
Circulating current (A)

1

Fast P-P Update Schemes

M. Blaskiewicz

Motivation: Allows for smooth symplectic modeling of the space charge force in reasonable time

τ_k = arrival time of particle k

$k = 1, 2, \ldots N$

δ_k = momentum deviation

$$\hat{V}(\underset{\sim}{\delta}, \underset{\sim}{\bar{\tau}}) = \frac{K}{2}\sum_{j,k} \lambda(\bar{\tau}_j - \bar{\tau}_k)$$

$$F = -\sum_k \bar{\tau}_k \delta_k + \hat{V}(\underset{\sim}{\delta}, \underset{\sim}{\bar{\tau}})$$

$$\tau_i = -\frac{\partial F}{\partial \delta_i} = \bar{\tau}_i$$

$$\bar{\delta}_i = -\frac{\partial F}{\partial \bar{\tau}_i} = \delta_i - \frac{\partial \hat{V}}{\partial \bar{\tau}_i}$$

Canonical Transformation, Goldstein # 3

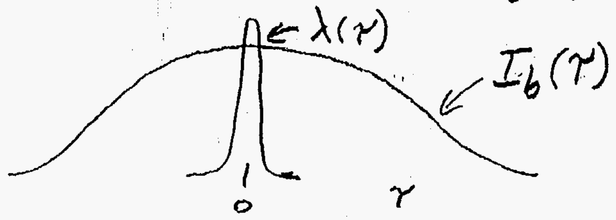

2

so

$$\bar{\delta}_k = \delta_k - K\sum_{j=1}^{N} \lambda'(\tau_k - \tau_j)$$

The pairwise sum for all N particles can be done in $O(N \log N)$ operations for appropriate $\lambda(\tau)$.

$$\lambda(\tau) = (1 + \alpha|\tau|)\, e^{-\alpha|\tau|}$$

continuous with continuous 1st and 2nd derivatives

$$\lambda'(\tau) = -\alpha^2 \tau\, e^{-\alpha|\tau|}$$

$$\bar{\delta}_k = \delta_k + K\alpha^2 \sum_j (\tau_k - \tau_j)\, e^{-\alpha|\tau_k - \tau_j|}$$

$$= \delta_k + \alpha^2 K F_k$$

$\left[\delta \to P_x, \ (\tau_k - \tau_j) \to (X_k - X_j) \right.$

$$F_k = \sum_{j=1}^{N} (\gamma_k - \gamma_j) e^{-\alpha|\gamma_k - \gamma_j|}$$

The Trick:

Sort $\gamma_j \leq \gamma_{j+1}$ which is $O(N \log N)$ with Heapsort or Quicksort

$$F_k = \sum_{j=1}^{k} (\gamma_k - \gamma_j) e^{-\alpha(\gamma_k - \gamma_j)} + \sum_{j=k+1}^{N} (\gamma_k - \gamma_j) e^{\alpha(\gamma_k - \gamma_j)}$$

$$= \gamma_k (S1_k^- + S1_k^+) - (S2_k^- + S2_k^+)$$

$$S2_k^- = \sum_{j=1}^{k} \gamma_j e^{\alpha(\gamma_j - \gamma_k)}$$

$$= \gamma_k + \sum_{j=1}^{k-1} \gamma_j e^{\alpha(\gamma_j - \gamma_k + \gamma_{k-1} - \gamma_{k-1})}$$

$$= \gamma_k + e^{\alpha(\gamma_{k-1} - \gamma_k)} S1_{k-1}^-$$

Since $\gamma_k \geq \gamma_{k-1}$, $e^{\alpha(\gamma_{k-1} - \gamma_k)} \leq 1$

and the recurrence relation is stable

$$S2_k^+ = \sum_{j=k+1}^{N} \gamma_j e^{-\alpha(\gamma_k - \gamma_j)}$$

$$= (S2_{k+1}^+ + \gamma_{k+1}) e^{\alpha(\gamma_j - \gamma_{j+1})}$$

again stable

So, start with

$S_0^- = 0$, $S_N^+ = 0$

and use

$$S1_{n+1}^- = 1 + e^{\alpha(\gamma_n - \gamma_{n+1})} S1_n^-$$

$$S2_{n+1}^- = \gamma_n + e^{\alpha(\gamma_n - \gamma_{n+1})} S2_n^-$$

$$S1_{n-1}^+ = (1 + S1_n^+) e^{\alpha(\gamma_{n-1} - \gamma_n)}$$

$$S2_{n-1}^+ = (\gamma_n + S2_n^+) e^{\alpha(\gamma_{n-1} - \gamma_n)}$$

recurrence is $O(N)$ so $O(N \log N)$ total

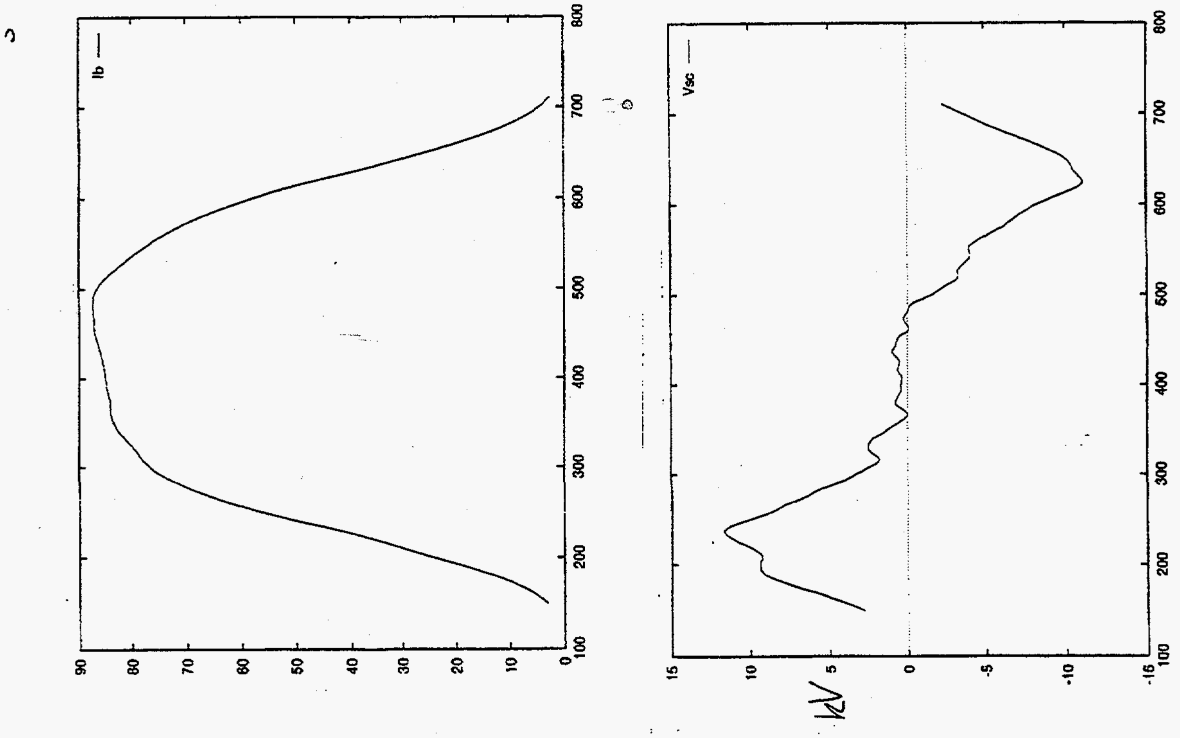
Ib
Vsc
kV
0
10
20
30
40
50
60
70
80
90
100
200
300
400
500
600
700
800
15
5
-5
-10
-15

HOM Dampers for RHIC 28.1 MHz Accelerating Cavity:

Stability in RHIC?

RF Workshop @BNL
May 8, 1997

Jim Rose, RHIC rf

SUPERFISH Output for 28 MHz Cavity (150 kHz low to allow final tuning after manufacture)

```
1SUPERFISH DTL summary                   11/19/95        11:27:39
 Problem name =FINAL 28.15 MHz Cavity- 14 Sep 1
 Mesh problem length [L]  =  200.0000 cm
 Stored energy [U] for mesh problem only =                       7179.22754 mJ
 Power dissipation [P] for mesh problem only =                     77675.50 W
 Q (2.0*pi*f(Hz)*U(J)/P(W)) =                                        16200
 Transit time factor [T] =                                          0.92430
 Shunt impedance [Z] mesh problem only, ((Eo*L)**2/2*P) =            1.030 Mohm
 Shunt impedance per unit length [Z/L] =                             1.030 Mohm/m
 Magnetic field on outer wall =                                       2748 A/m
 Hmax for wall and stem segments at z=214.43,r= 13.49 cm =            8554 A/m
 Emax for wall and stem segments at z= 29.69,r= 13.07 cm =          10.776 MV/m
```

Beta	T	Tp	S	Sp	g/L	Z/L
0.37221783	0.92430	0.02374	0.37410	0.05623	0.007191	1.029926

ISEG	zbeg (cm)	rbeg (cm)	zend (cm)	rend (cm)	Emax*epsrel (MV/m)	Power (W)	df/dz (MHz/mm)	df/dr (MHz/mm)
Wall								Wall
2	0.0000	6.1900	20.9500	6.1900	4.4639	0.0395	0.0000	0.0006
3	20.9500	6.1900	21.4500	6.6900	7.9438	0.0542	0.0011	0.0011
4	21.4500	6.6900	21.4500	9.4800	8.5137	1.0077	0.0061	0.0000
5	21.4500	9.4800	17.4500	13.4800	6.7360	9.0926	0.0056	0.0023
6	17.4500	13.4800	1.5600	13.4900	0.4071	31.2894	0.0000	0.0000
7	1.5600	13.4900	1.5600	20.0000	0.0185	10.5454	0.0000	0.0000
8	1.5600	20.0000	62.7000	20.0000	8.2558	1329.1914	0.0000	0.0958
9	62.7000	20.0000	63.3350	20.6350	8.4820	87.3094	0.0049	0.0049
10	63.3350	20.6350	63.3350	41.9989	6.2291	1738.2368	0.0044	0.0000
11	63.3350	41.9989	216.9305	41.9989	0.6321	16276.6230	0.0000	-0.0229
12	216.9305	41.9989	216.9305	15.3988	0.1076	5750.1382	-0.0103	0.0000
13	216.9305	15.3988	215.0255	13.4938	0.1962	1206.7163	-0.0013	-0.0014
14	215.0255	13.4938	31.4597	13.4938	8.9394	51211.0625	0.0000	0.0777
15	31.4597	13.4938	27.4465	9.4806	10.7765	22.9688	0.0253	0.0291
16	27.4465	9.4806	27.4465	6.6980	9.1560	1.1670	0.0079	0.0000
17	27.4465	6.6980	27.9545	6.1900	8.2337	0.0596	0.0012	0.0012
Wall					Total =	77675.5078		Wall

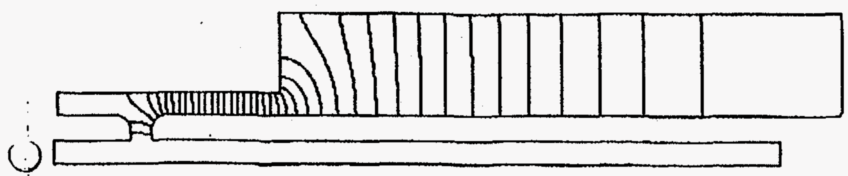

FINAL 28.15 MHz Cavity- 14 Sep 1FREQ= 27.897

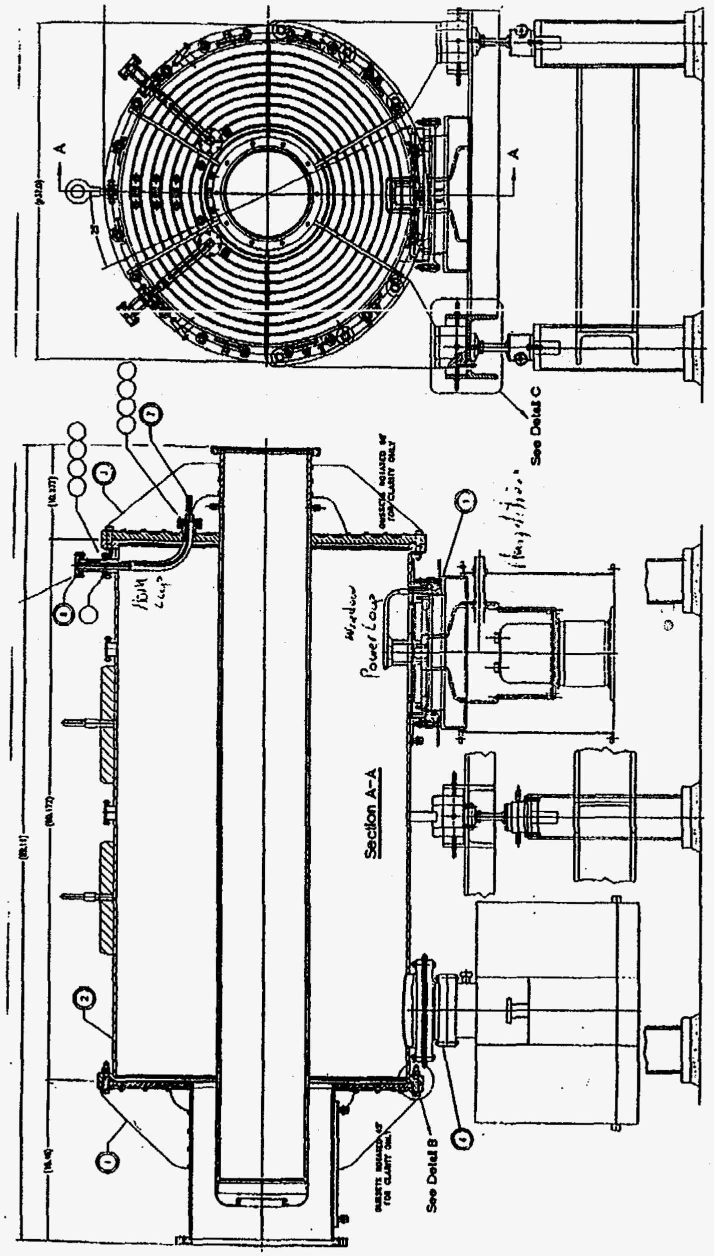

28 MHz Production Cavity

Longitudinal Coupled Bunch Instabilities

Higher Order Modes (HOM's) in the rf cavities havebeen calculated with the code URMEL and agree with measured values of shunt impedance and Q.

Growth rates have been calculated both with the code ZAP and analyticaly with the expression

$$\frac{1}{\tau} = \frac{\omega_s}{r_\phi}\frac{I_0 R}{V_{rf}\cos\phi_s}F_m$$

Where F_m is a form factor less than 0.6 and which falls off as the inverse of both the HOM frequency and the square of the bunch length. Because of the long bunch length in RHIC, only the first few HOM's contribute to instabilities.

Longitudinal Growth Rates (Without Damping)		
HOM Frequency	Growth Rate (sec $^{-1}$)	Stable?
103 MHz	12	U
192 MHz	3.7	U

Modest amounts of passive damping (factor of 10) will bring these within the range of the injection damper rate of 10 sec^{-1}. Damping experiments have confirmed this de-Qing on the Proof of Principle (PoP) 26.7 MHz cavity.

Form Factors for Degenerate case (Σ azimuthal modes)

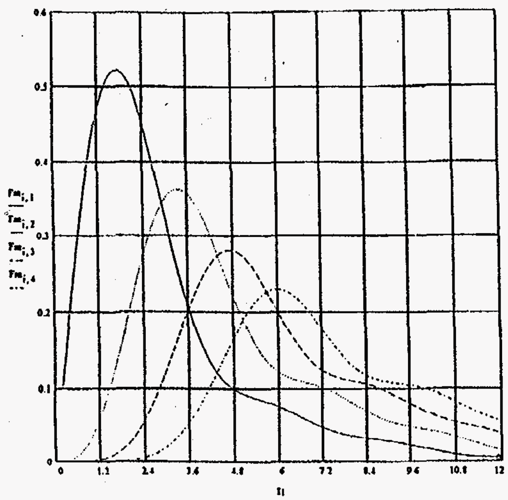

Impedance limit for growth rates of 2 sec^{-1} with undamped (lines) and damped (x's) HOM impedances superimposed

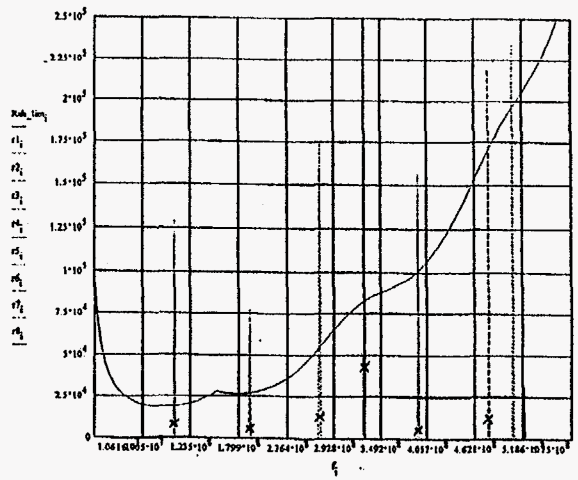

Form Factors for the degenerate case of the radial modes summed over k= 1..4:, m=1(dipole) m=2 (quadrupole)

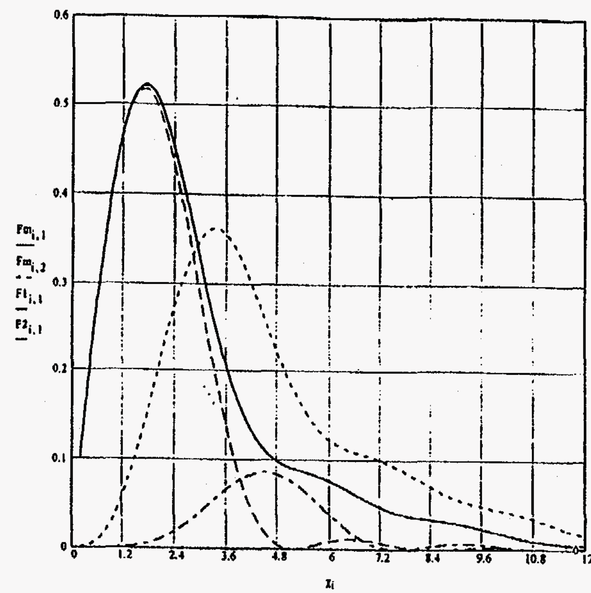

$$F1_{(l,n)} := \left[m_n \cdot \mu \cdot (\mu + 2) \cdot \left(\frac{2}{\chi_l}\right)^{2(2\mu+1)} \cdot \frac{(m_n + 2 \cdot k + \mu) \cdot \Gamma(k+\mu) \cdot \Gamma(m_n + k + \mu)}{(k! \cdot (m_n + k)!)} \cdot Jn(n_n, \chi_l)^2 \right]$$

Distribution $\varphi(r) = K\left[1 - \left(\frac{r}{r_\varphi}\right)^2\right]^\mu \quad \mu = 1$

Impedance limit for $\frac{1}{\tau} = 2\ s^{-1}$ and various bunch lengths and gap volts

$$\chi = \frac{\omega_{res}}{\omega_{rf}} \hat{r}_\phi \quad ; \quad \hat{r}_\phi = \text{bunch half length in radians rf}$$

$$\frac{1}{\tau} = \frac{\omega_\phi}{\hat{r}_\phi} \frac{I_o R_{SH}}{V_\tau \cos\phi_\tau} F$$

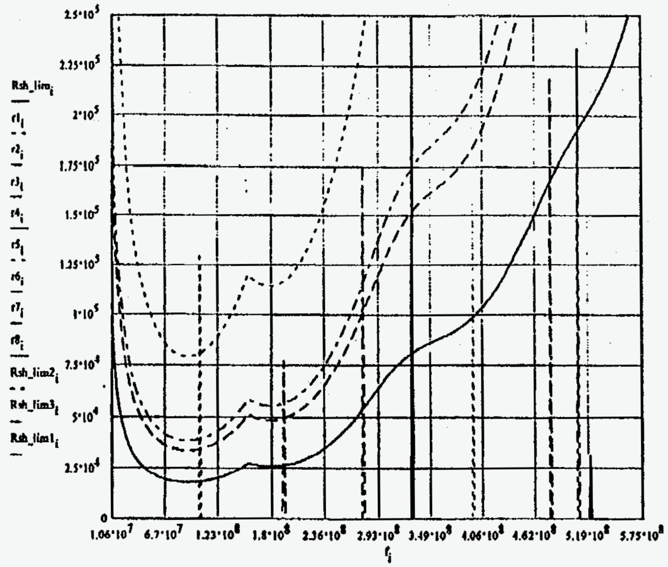

$$R_{sh\_lim} = \frac{\tau\ \hat{r}_\phi\ V_\tau \cos\phi_\tau}{\omega_s\ I_o\ F}$$

HOM dampers performances (two damping loop-longitudinal modes only). MAFIA results.

NO HOM INSTALLED					2 DAMPERS INSTALLED	DAMPING FACTOR
Nr.	F[MHz]	R_{sh}[kΩ]	Q[-]	R/Q[Ω]	R_{sh}'[kΩ]	R_{sh}/R_{sh}'
1	27.7	1120	17900	62.6	1120	1
2	104.7	166	29250	5.7	1.3	128
3	197.9	54	22800	2.4	1.4	38.6
4	269.2	86.3	21400	4.0	7.0	12.3
5	279.0	105.0	20400	5.2	10.1	10.4
6	324.3	342.5	31400	10.3	14.5	23.6

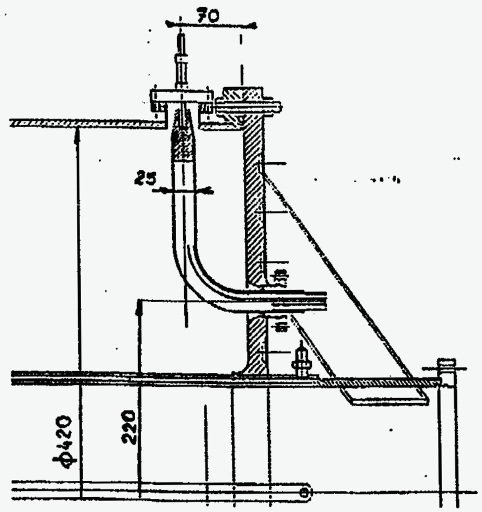

HOM DAMPER (COUPLING LOOP)

Prototype HOM Damper Notch Filter

"Folded" Quarter wave resonator creates open circuit at fundamental rf frequency; similiar to parallel L-C notch filter

Dimensions of 370 mm long by 150mm diameter

Bench test:
Notch depth of -49 dB, 2nd notch at 368 MHz, 3rd at 422 MHz

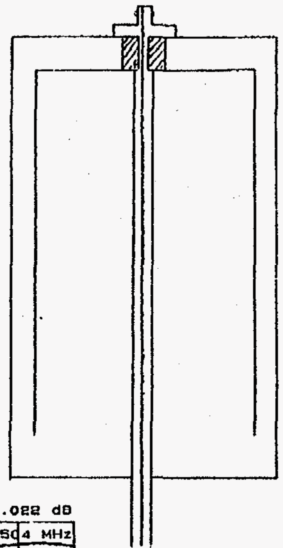

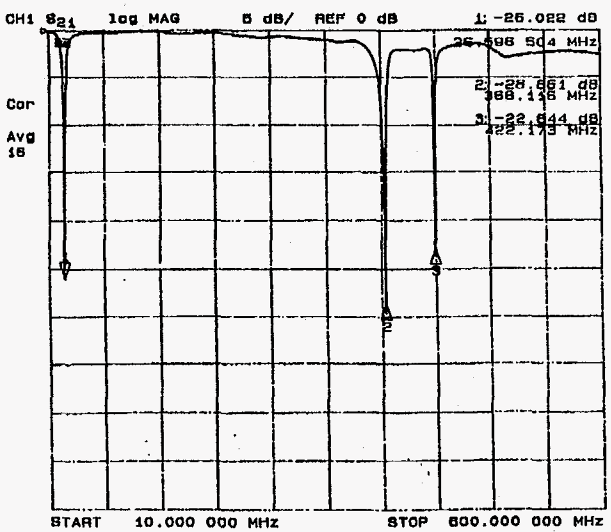


```
sHOMdamp.dat    HOM notch Jan 03, 1995
$reg  dx=0.1, xmax=32.48, ymax=15.24,
      freq=27., xdri=30.48, ydri=15.24,
$po x=0.0, y=0.0 $
$po x=0.0, y=15.24 $
$po x=30.48, y=15.24 $
$po x=30.48, y=2.064 $
$po x=1.635, y=2.064 $
$po x=1.635, y=13.9225 $
$po x=28.48, y=13.9225 $
$po x=28.48, y=14.24 $
$po x=1.0, y=14.24 $
$po x=1.0, y=1.939 $
$po x=32.48, y=1.939 $
$po x=32.48, y=0.0 $
$po x=0.0, y=0.0 $
```

sHOMdamp.dat   HOM notch Jan 03, 1995 Freq = 27.000

V_{in} = 10.7 kV at 400kV gap volts

R_{shunt} = 81 kΩ, Power dissipated = 700 Watts

~325 mm long x 300 mm diameter

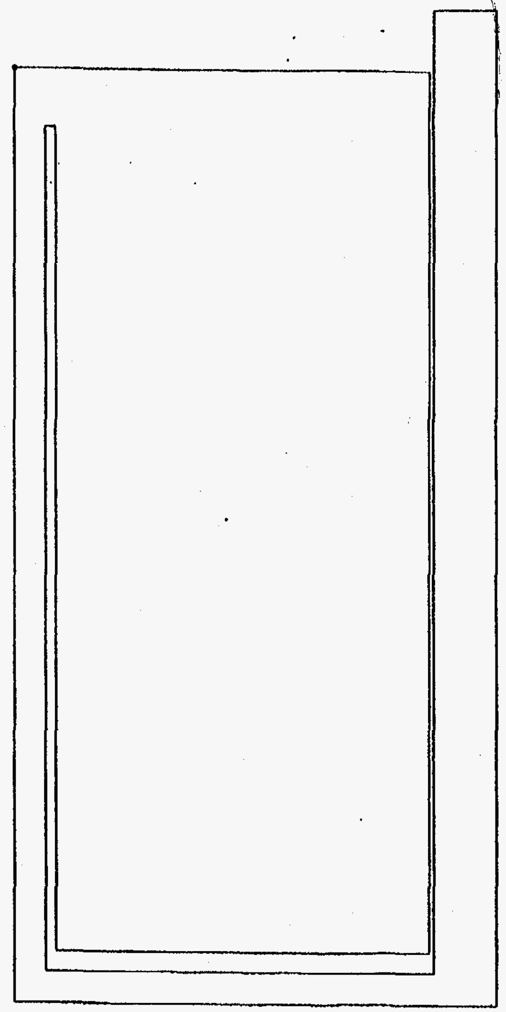

5-Element Chebyshev High Pass Filter. Resistive losses-less than 40W for Ug=400kV. Fundamental frequency attenuation>60dB.

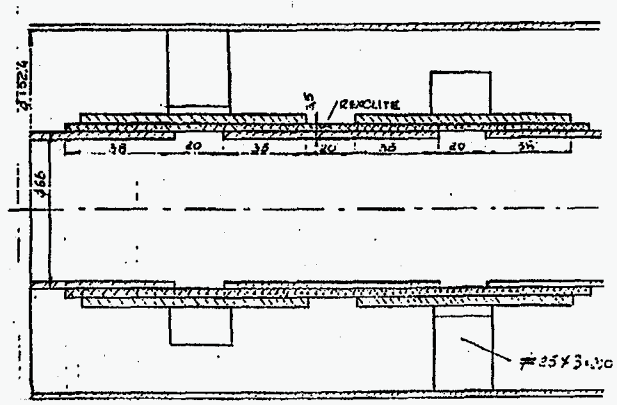

High-Pass 5 element Chebyshev filter

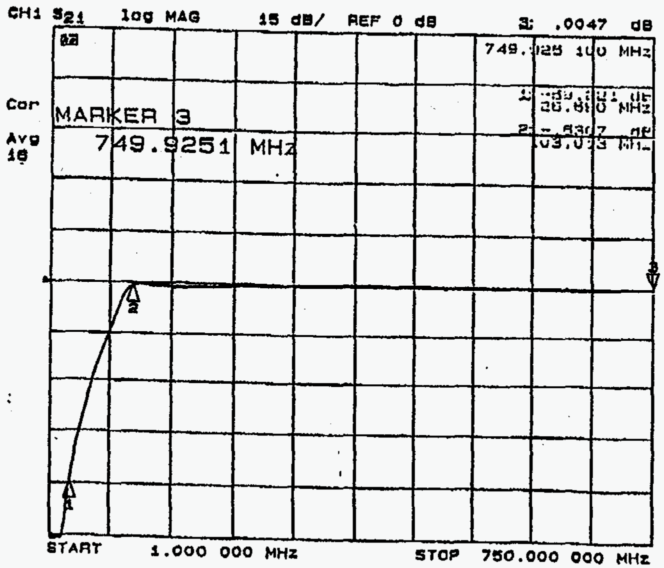

HIGH PASS FILTER MODE DAMPER ASSEMBLY

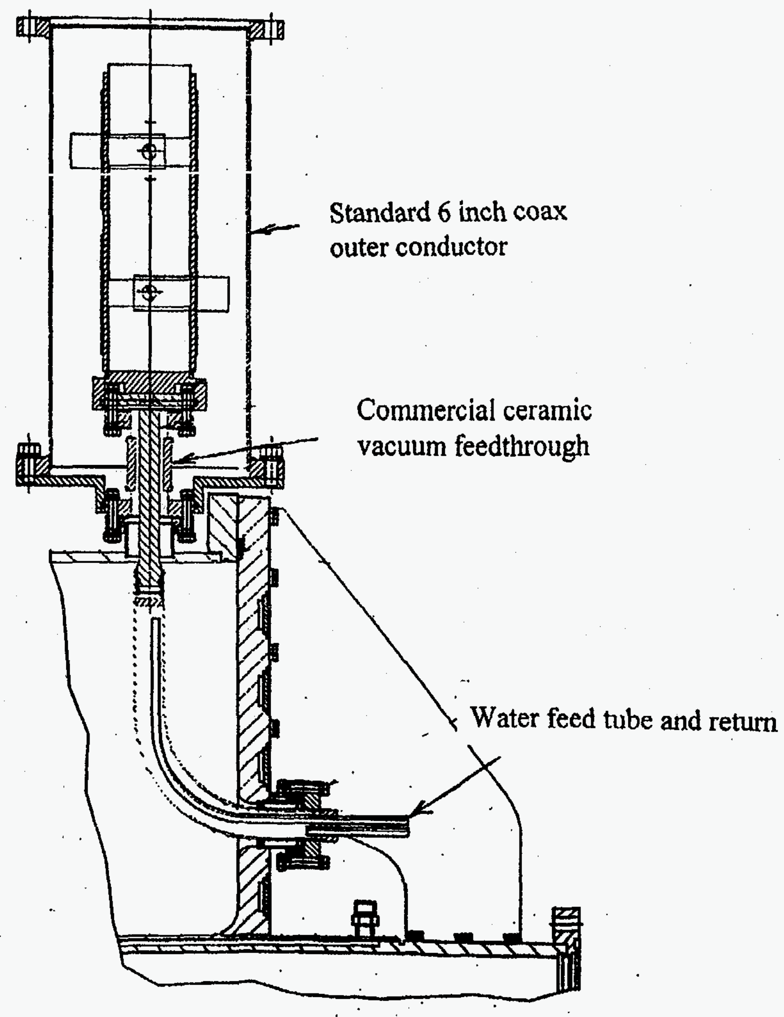

MAFIA RESULTS(NO HOM INSTALLED)						2 Dampers Installed	Damping factor	Loop reactance	Loop voltage
Nr	F[MHz]	Rsh[kΩ]	Q[-]	R/Q[Ω]		Rsh'[kΩ]	Rsh/Rsh'	Xl[Ω]	Ut[kV]
1	26.3	1060	17900	59.4		1060	1	+j16.8	10.4
2	103.2	133	29500	4.5		4.7 (1.3)	28.3	+j92	123
3	192.2	88	37000	2.4		1.4 (1.4)	63	+j950	1250
4	275.1	236	28100	8.4		8.6 (11.6)	27.4	-j134	64
5	313.3	58	16700	3.5		52.5	1.1	-j95	5.9
6	322.7	270	22400	12.1		23 (14.4)	26.2	-j92	26.2
7	377.5	20	46300	0.4		4	11.7	-j70	50.1
8	390.6	165	46700	3.5		6.6 (3.5)	25	-j61	40.3
9	453.6	223	20800	10.7		112 (236)	2	-j42	5.9
10	492.7	24	35500	0.7		12.4 (9.2)	1.9	-j33	15

2 DAMPERS WITH CAVITY BUILDUP

Table 2

POP CAVITY - MAFIA RESULTS								TEST RESULTS			
MODE NR	F[MHz]	Rsh[kΩ]	Q[-] *1000	Rsh/Q	Rsh' [kΩ]	Rsh/Rsh'		F[MHz]	Q[-] *1000	Q'[-] *1000	Q/Q'
1	26. 7	1110	16.4	67.7	76	14.6		26.88	17.3	1.1	15.7
2	99.1	72.1	25.5	2.8	0.8	90		98.8	19.8	0.19	102
3	157.9	5.8	30.8	0.19	0.03	193		157.7	22.3	0.11	203
4	215.7	4.4	38.2	0.12	0.07	63		216.3	29.0	0.46	63
5	286.4	98	27.6	3.6	9.0	10.9		287.4	8.0	1.5	5.3
6	343.4	180	19.2	9.4	32.0	5.6		342.2	8.7	2.1	4.2
7	406.0	112	40.5	2.8	4.7	23.8		402.2	2.3	1.1	2.1

TABLE 3.

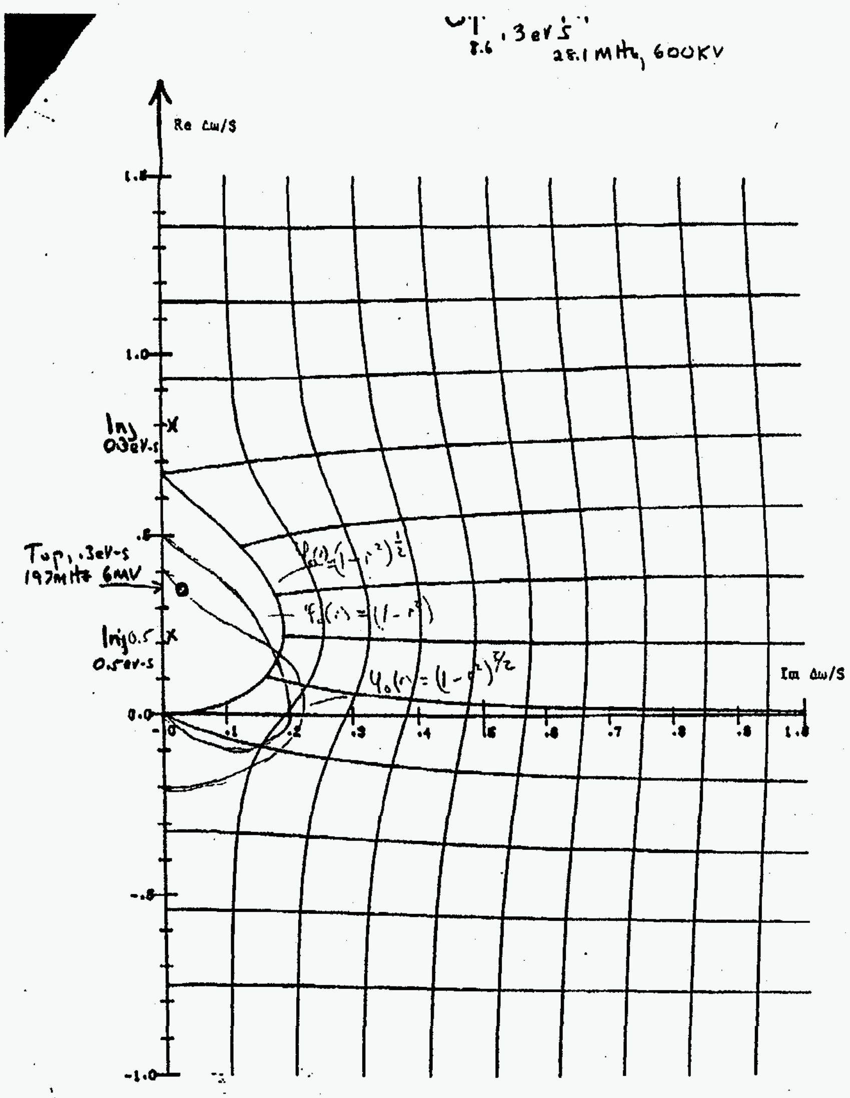

Fig. 1 Stability diagram for beams with parabolic line density.

Session on Beam Loading and rf System Stability

J.M. Brennan

Emmanuel Onillon of Brookhaven gave a lecture on state variable techniques for feedback system analysis and design. He presented a pedagogical summary of the state variable formulation of the analysis of dynamical systems, with frequent references to the classical transfer function technique. For feedback systems used in accelerator applications the state variable technique is attractive because it provides a means for optimizing the performance of complex systems where many loops operate simultaneously. Two techniques were described which allow the designer to find the best set of settings of loop parameters in multi-loop feedback systems such as frequently occur in rf systems.

The two techniques, pole placement and LQR (linear quadratic regulator) were developed in some detail and shown to be complementary. Pole placement is a convenient technique when one wants to obtain analytic formulae for feedback gains in the presence of a changing system parameter, such as, synchrotron frequency or beam energy. LQR is a technique that obtains the optimum set of gains that maximize some performance criterion. Typically the criterion is a weighted sum of output accuracy plus a measure of the control effort.

Onillon showed that in the design of the RHIC beam control system the two techniques were used together. First LQR was used to produce a set of feedback gains and the system poles were obtained. Then analytic relations were found for the gains as functions of beam and rf parameters by pole placement. These analytic relations will be imbedded in the digital signal processing (DSP) algorithms for the RHIC rf beam control system. The benefit is that the system dynamics, bandwidth and tracking error, for example, will be independent of beam energy or rf voltage.

M. Blaskiewicz of Brookhaven presented a description of the rf system for the US National Spallation Neutron Source (NSNS) project. Although the rf system does not accelerate the beam because the ring in only an accumulator it is a high power system because of very high beam loading. At 2×10^{14} protons in the ring the rf beam current will approach 80 A. Making the assumption that the cavity will be essentially uncompensated because the injection period (¡1ms) is shorter than ferrite response time requires full reactive beam current from the power amplifier. The system employs high power tetrodes (600 kW) which are capable of 300 A peak current. Results of a detailed analysis of the tetrodes capabilities based on the constant-current characteristics published by the manufacturer were presented.

Results from particle tracking calculations which included space charge were presented that showed the benefit of tailoring the rf waveform to increase the bunching factor. Addition of a second harmonic voltage improved the bunching factor by 25%, while using a isolated sinewave for a barrier bucket could give an even greater improvement of 35intensity will ultimately be limited by space charge driven tune spread any improvement in bunching factor will likely translate into increased intensity.

System stability was analyzed according to the conventional considerations used for synchrotrons even though the NSNS ring will not accelerate. Blaskiewicz pointed out that although these consideration are sufficient they may not be necessary and that further work is called for in analyzing the accumulator problem.

Roland Garoby of CERN/PS presented a brief description of a newly commissioned diagnostic system at the PS that measures the phase turn-by-turn of each bunch in the PS. The system is based on a commercial DSP board and commercial constant-fraction timing discriminators. Some typical results were shown that showed how the system can reveal coherent dipole oscillations from injection phase errors from one ring of the PS Booster. The main role of the new system will be in detecting and analyzing longitudinal coherent instabilities in the PS.

STATE VARIABLE ANALYSIS

E. Onillon

Concept introduced in control science in the 50's.

Powerful method, can be used for the study of numerous systems, linear or not, stationary or not, continuous or discrete.

Naturally leads to the idea of optimum control.

Associated with the idea of a prescribed trajectory the system has to follow with a minimum error and at a minimum cost (power for instance).

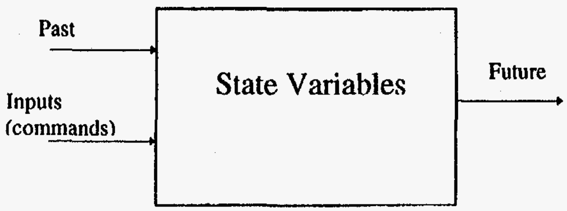

State vector $\vec{X}(t)$ = minimum set of variables (information on the past) sufficient to calculate the future evolution of the system when we know for $t \geq t_0$ the inputs and its internal physical laws

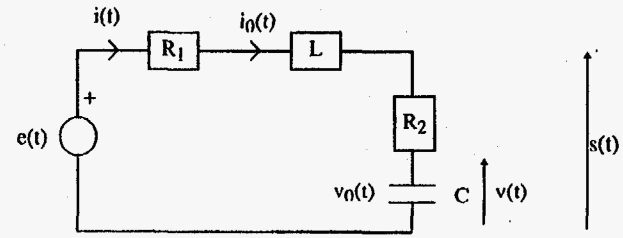

i(0), v(0)

i(t), v(t)

$$\frac{d}{dt}\begin{pmatrix} i \\ v \end{pmatrix} = \begin{bmatrix} \frac{-(R_1+R_2)}{L} & -\frac{1}{L} \\ \frac{1}{C} & 0 \end{bmatrix}\begin{bmatrix} i \\ v \end{bmatrix} + \begin{bmatrix} \frac{1}{L} \\ 0 \end{bmatrix} e$$

$$s = [R_2 \quad 1]\begin{bmatrix} i \\ v \end{bmatrix}$$

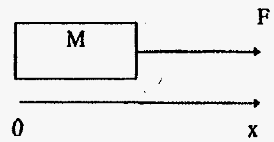

$F = M\ddot{x}$

x(0), v(0)

x(t), v(t)

State vector $\vec{X}(t) = [x_i(t)]^T{}_{1 \le i \le n}$ n order of the system

Input vector $\vec{U}(t) = [u_j(t)]^T{}_{1 \le j \le m}$

Output vector $\vec{Y}(t) = [y_k(t)]^T{}_{1 \le k \le l}$

STATE AND OBSERVATION EQUATIONS

Linear and stationary system: $\begin{cases} \dot{X}(t) = AX(t) + BU(t) & \text{state} \\ Y(t) = CX(t) + DU(t) & \text{observation} \end{cases}$

For a discrete system: $\begin{cases} X_{n+1} = A_d X_n + B_d U_n \\ Y_n = C_d X_n + D_d U_n \end{cases}$

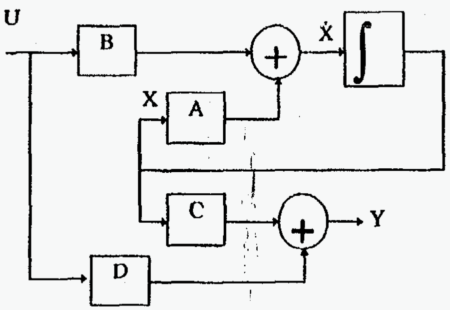

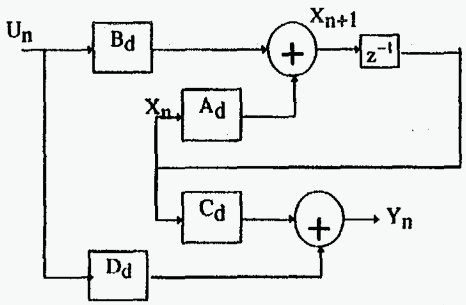

Resolution of the state space equation:

Look for a linear solution

$$X(t_0) \longrightarrow \boxed{\Phi(t, t_0) = e^{A(t-t_0)}} \longrightarrow X(t)$$

State space representation / Transfer function:

$$\begin{cases} \dot{X}(t) = AX(t) + BU(t) \\ Y(t) = CX(t) + DU(t) \end{cases} \Rightarrow \begin{cases} sX(s) - X(0) = AX(s) + BU(s) \\ Y(s) = CX(s) + DU(s) \end{cases} \Rightarrow$$

$$Y(s) = C(sI - A)^{-1} X(0) + \left(D + C(sI - A)^{-1} B\right) U(s)$$

$$\boxed{H(s) = \frac{Y(s)}{U(s)} = D + C(sI - A)^{-1} B}$$

Poles = eigenvalues of A

Example

$$A = \begin{bmatrix} -7 & -12 \\ 1 & 0 \end{bmatrix},\ B = \begin{bmatrix} 1 \\ 0 \end{bmatrix},\ C = [1 \quad 2],\ D = 0$$

$$(sI - A) = \begin{bmatrix} s+7 & 12 \\ 1 & s \end{bmatrix},\ (sI - A)^{-1} = \frac{\begin{bmatrix} s & -12 \\ 1 & s+7 \end{bmatrix}}{s(s+7)+12},\ H(s) = \frac{s+2}{s^2 + 7s + 12}$$

Passage transfer function / state: introduce a new variable

$$\frac{Y(s)}{U(s)} = \frac{Y}{X_1}\frac{X_1}{U} = \frac{s+2}{s^2 + 7s + 12} \Rightarrow$$

$Y = sX_1 + 2X_1$ and $s^2X_1 + 7sX_1 + 12X_1 = U$

or with $X_2 = \dot{X}_1$, (successive derivative)

$Y = X_2 + 2X_1$ and $\dot{X}_2 = -7X_2 - 12X_1 + U$

$$\dot{X} = \begin{pmatrix} \dot{X}_1 \\ \dot{X}_2 \end{pmatrix} = \begin{bmatrix} 0 & 1 \\ -12 & -7 \end{bmatrix} \begin{pmatrix} X_1 \\ X_2 \end{pmatrix} + \begin{bmatrix} 0 \\ 1 \end{bmatrix} U \text{ and } Y = [2 \quad 1] \begin{pmatrix} X_1 \\ X_2 \end{pmatrix}$$

Discrete state space representation

$$\begin{cases} \dot{X}(t) = AX(t) + BU(t) \\ Y(t) = CX(t) + DU(t) \end{cases} \Rightarrow \quad X_{k+1} = e^{At}X_k + \int_{t_k}^{t_{k+1}} e^{A(t_{k+1}-\tau)}BU(\tau)d\tau$$

$$\boxed{\begin{aligned} X_{k+1} &= e^{AT}X_k + \int_0^T e^{A\theta}Bd\theta U_k \\ Y_k &= CX_k + DU_k \end{aligned}}$$

POLE PLACEMENT, LQR

$$\text{System: } \begin{cases} \dot{X} = AX + BU \\ Y = CX + DU \end{cases}$$

Commandability

$$X(t_0) \xrightarrow{U(\tau)\ \tau \geq t_0} X_f \quad ?$$

$\text{rank}\left[B \quad AB \quad \dots \quad A^{n-1}B\right]$ = number of commandable states

Observability

$$Y(t) \xrightarrow{t \geq t_0} X(t_0) \ ?$$

$\text{rank}\left[C^T \quad A^TC^T \quad \dots \quad A^{T^{n-1}}C^T\right]$ = how many states we can reconstruct

POLE PLACEMENT

Specify the poles you want the system to have

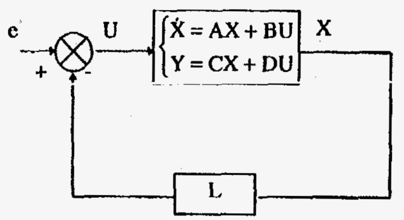

$$U = -LX + e \Rightarrow \dot{X} = \underbrace{(A - BL)}_{\substack{\text{eigenvalues } \lambda_i \\ \text{eigenvectors } v_i}} X + Be$$

(A,B) has to be commandable

Choice of the eigenvalues (poles of the system)

$Re(\lambda_i) < 0$ and if λ_i, $\bar{\lambda}_i$

The further the λ_i are from the eigenvalues of A, the bigger the command effort is.

If $\lambda_i = a_i + jb_i \rightarrow e^{a_i t} \sin b_i t$, $e^{a_i t} \cos b_i t$ The bigger $|a|$, the faster the system is.

With $|\lambda_i| = \omega_0$ and $\lambda_i + \bar{\lambda}_i = \xi\omega_0 = |\sin\theta|\omega_0$

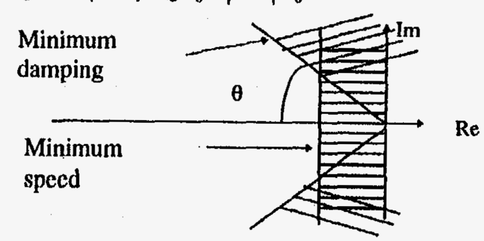

Determination of L

$$\det(\lambda I - (A - BL)) = (\lambda - \lambda_1)\ldots(\lambda - \lambda_n)$$

Discrete Systems

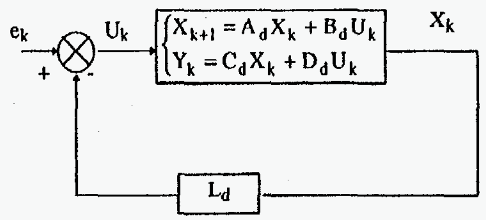

$$\boxed{U_k = -L_d X_k + e_k \Rightarrow X_{k+1} = (A_d - B_d L_d) X_k + B_d e_k}$$

$$\det(\lambda I - (A_d - B_d L_d)) = (\lambda - \lambda_1)\ldots(\lambda - \lambda_n)$$

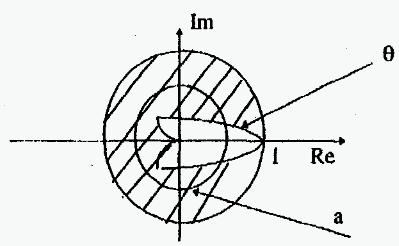

discrete pole = $e^{\text{continuous pole}*\tau_d}$

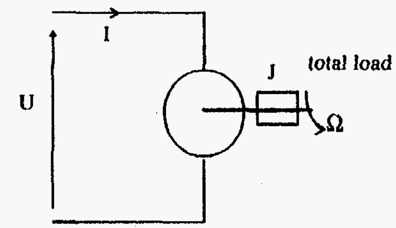

$$\begin{cases} U(t) = RI(t) + L\dfrac{dI}{dt} + \phi_0 I(t) \\ \Gamma(t) = J\dfrac{d\Omega}{dt} = \phi_0 I(t) \end{cases} \Rightarrow \frac{d}{dt}\begin{pmatrix}\Omega(t) \\ I(t)\end{pmatrix} = \begin{bmatrix} 0 & \dfrac{\Phi_0}{J} \\ -\dfrac{\Phi_0}{L} & -\dfrac{R}{L} \end{bmatrix}\begin{pmatrix}\Omega(t) \\ I(t)\end{pmatrix} + \begin{bmatrix} 0 \\ \dfrac{1}{L} \end{bmatrix} U(t)$$

$$\frac{d\Omega}{dt} = \left[-\frac{\Phi^2{}_0}{RJ}\right]\Omega(t) + \left[\frac{\Phi_0}{RJ}\right]U(t)$$

Numerically, R=10Ω, J=5 10^{-5} kg m^2, $\Phi_0 = 0.1$ USI, T=5ms

$$\frac{d\Omega}{dt} = -20\Omega(t) + 200U(t)$$

$$\Omega(k+1) = -0.905\Omega(k) + 0.952U(k)$$

Continuous system: eigenvalue -20 (50ms)

Divide it by 2

$e^{-40T} = 0.819$

$$\Omega(k+1) = (-0.905 - 0.952L)\Omega(k) \qquad L=0.090$$

LINEAR QUADRATIC REGULATOR (L.Q.R.)

Linear system

$$\begin{cases} \dot{X}(t) = AX(t) + BU(t) \\ X(0) = X_0 \end{cases}$$

Goal: bring the state back to zero (regulator) while minimizing

$$J = \frac{1}{2}\int_0^\infty \left(\underbrace{X^T(t)QX(t)}_{\text{GOAL}} + \underbrace{U^T(t)RU(t)}_{\text{COST}} \right) dt$$

$U_{opt}(t) = -LX(t) = -R^{-1}B^TPX(t)$ where P satisfies the algebraic Ricatti equation: $PA + A^TP - PBR^{-1}B^TP + Q = 0$ Optimal cost $J_{opt} = X_0^TPX_0$

To find an optimal command
- -choose Q and R
- -solve the Ricatti equation to find L
- -command=linear combination of the state variables, the new poles being the eigenvalues of A-B*L

(A,B) has to be commandable

Choice of Q and R:

Choose diagonal matrices

$$J = \frac{1}{2}\int_0^\infty \left(Y^TQ_yY + U^TRU\right)dt \text{ with } Y = CX$$

$$Q_y = \begin{bmatrix} q_1 & 0 & 0 \\ 0 & \dots & 0 \\ 0 & 0 & q_p \end{bmatrix}, R = \begin{bmatrix} r_1 & 0 & 0 \\ 0 & \dots & 0 \\ 0 & 0 & r_l \end{bmatrix}$$

In that case: $J = \frac{1}{2}\int_0^\infty \left(\sum\left(q_i y_i^2\right) + \sum\left(r_j u_j^2\right)\right)dt$

q_i and r_j represent the relative importance of the variables toward each other

$Q_y = \begin{bmatrix} 1 & 0 & 0 \\ 0 & a^2 & 0 \\ 0 & 0 & \dots \end{bmatrix}$ the bigger a^2, the bigger the priority of y_2 is compare to y_1.

If R→kR with k>1, the command will be less strong, the closed system will be slower.
If $Q_y \to kQ_y$ with k>1, closed loop faster, stonger command

RHIC CASE

Choice of Q and R

done at injection

requirement: loop response time

modify Q and R to reach that target

limit the phase excursion by having a stronger coefficient on the phase
Command frequency error sent to a DDS: limit the input by minimizing R

Compromise between speed/amplitude of the command and phase excursion

Several iterations before finding Q and R

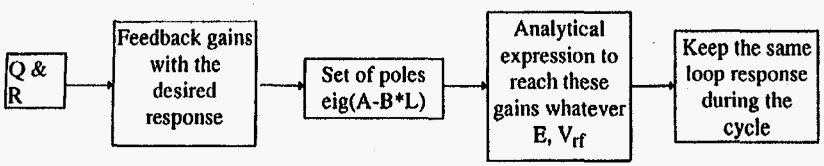

Just a set of gains could not do it (compromize loop response/stability)

Discrete systems

$$\begin{cases} X_{k+1} = A_d X_k + B_d Y_k \\ X_{k=0} = X_0 \end{cases}$$

$$J = \frac{1}{2}\sum_{k=0}^{\infty}\left(X_{k+1}^T Q X_{k+1} + U_k^T R U_k\right)$$

Solution:

$U_k = -LX_k$ with $L = B_d^T P^{-1} B_d + R^{-1}$ where P satisfies the discrete Ricatti equation:

$P = A_d{}^T P A_d - A_d{}^T P B_d \left(B_d{}^T P B_d + R\right)^{-1} B_d{}^T P A_d + Q A_d$

Example:

$\ddot{x}(t) + 2\xi\omega_n \dot{x}(t) + \omega^2{}_n x(t) = Ku(t)$

$\omega_n = (2\pi),\ \xi = 0.1,\ K = \frac{1}{(2\pi)^2}$

$x_1 = x$ and $x_2 = \dot{x}_1$

$\gamma = 2\xi\omega_n$

$T_s = \frac{T_n}{6}$

$A = \begin{bmatrix} 0 & 1 \\ -\omega_n^2 & -\gamma \end{bmatrix},\ B = \begin{bmatrix} 0 \\ 1 \end{bmatrix},\ C = K[1 \quad 0],\ D = 0$

$A_d = \begin{bmatrix} 0.5325 & 0.7815 \\ -0.7815 & 0.3762 \end{bmatrix},\ B_d = \begin{bmatrix} 0.4675 \\ 0.7815 \end{bmatrix}, C_d = C,\ D_d = D$

Integral action

If one wants $y = y_0$

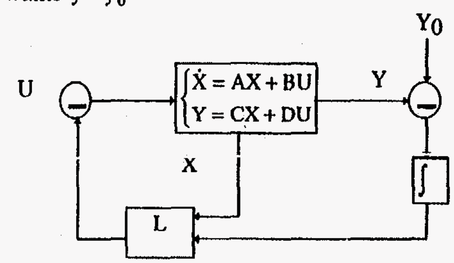

New state variable $z = \int_0^t (y(\tau) - y_0) d\tau$

$$\frac{d}{dt}\begin{pmatrix} X \\ z \end{pmatrix} = \begin{bmatrix} A & 0 \\ C & 0 \end{bmatrix}\begin{pmatrix} X \\ z \end{pmatrix} + \begin{bmatrix} B \\ 0 \end{bmatrix} U + \begin{pmatrix} 0 \\ -y_0 \end{pmatrix}$$

Discrete case

$$z_{k+1} = z_k + (y_k - y_0)$$

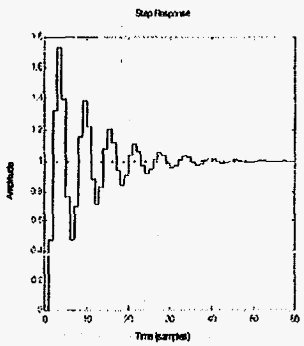

$$Q_d = \begin{bmatrix} 1 & 0 \\ 0 & 0 \end{bmatrix},\ R_d = 1 \Rightarrow L_d = [-0.020 \quad 0.5246]$$

$$A_d - B_d * L_d = \begin{bmatrix} 0.5381 & 0.5362 \\ -0.7721 & -0.0337 \end{bmatrix}$$

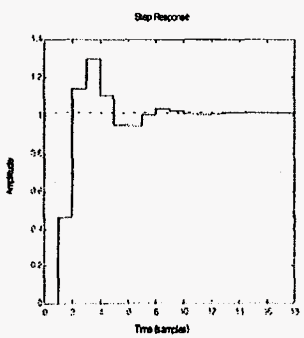

Variables

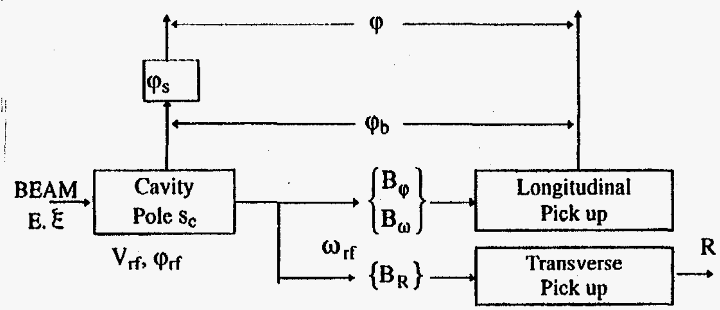

Beam transfer functions

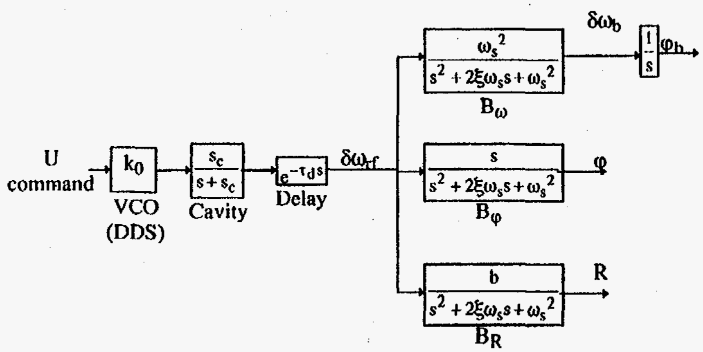

$$b = \frac{ceV_{rf}\cos\varphi_s}{2\pi\beta\gamma_{tr}E} \text{ and } \omega_s = f_\infty\sqrt{\frac{2\pi eV_{rf}\cos\varphi_s h|\eta|}{E}}.$$

THE PHASE AND RADIAL LOOP

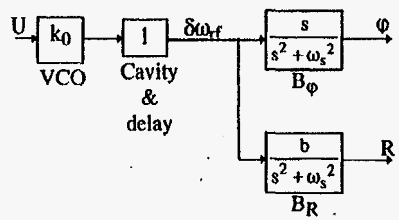

Two state variables: $\begin{cases} x_1 = \dfrac{R}{b} = \dfrac{k_0}{s^2 + \omega_s^2} U \\ x_2 = \dot{x}_1 = \varphi \end{cases}$

$$\begin{pmatrix} \dot{x}_1 \\ \dot{x}_2 \end{pmatrix} = \begin{pmatrix} 0 & 1 \\ -\omega_s^2 & 0 \end{pmatrix} \begin{pmatrix} x_1 \\ x_2 \end{pmatrix} + \begin{pmatrix} 0 \\ k_0 \end{pmatrix} U$$

$$\begin{pmatrix} \varphi \\ R \end{pmatrix} = \begin{pmatrix} 0 & 1 \\ b & 0 \end{pmatrix} \begin{pmatrix} x_1 \\ x_2 \end{pmatrix}$$

Third state variable: $x_3 = z = \int (R - R_0)dt. \Rightarrow \dot{x}_3 = R - R_0 = \frac{1}{b}x_1 - R_0.$

Final state space representation:

$$\begin{cases}\begin{pmatrix}\dot{x}_1\\ \dot{x}_2\\ \dot{x}_3\end{pmatrix}=\underbrace{\begin{pmatrix}0 & 1 & 0\\ -\omega_s^2 & 0 & 0\\ b & 0 & 0\end{pmatrix}}_{A_{\varphi R}}\underbrace{\begin{pmatrix}x_1\\ x_2\\ x_3\end{pmatrix}}_{X_{\varphi R}}+\underbrace{\begin{pmatrix}0\\ k_0\\ 0\end{pmatrix}}_{B_{\varphi R}}U+\begin{pmatrix}0\\ 0\\ -R_0\end{pmatrix}\\ \begin{pmatrix}\varphi_b\\ R\end{pmatrix}=\underbrace{\begin{pmatrix}0 & 1 & 0\\ b & 0 & 0\end{pmatrix}}_{C_{\varphi R}}\begin{pmatrix}x_1\\ x_2\\ x_3\end{pmatrix}\end{cases}$$

$\mathrm{rank}\left[B_{\varphi R}\ A_{\varphi R}B_{\varphi R}\ A_{\varphi R}^2B_{\varphi R}\right]=3\Rightarrow$ Feedback using pole placement

$$\begin{cases}k_R = (l_1l_2+l_1l_3+l_2l_3-\omega_s^2)/bk_0\\ k_\varphi = -(l_1+l_2+l_3)/k_0\\ k_\int = -(l_1*l_2*l_3)/(bk_0)\end{cases}$$

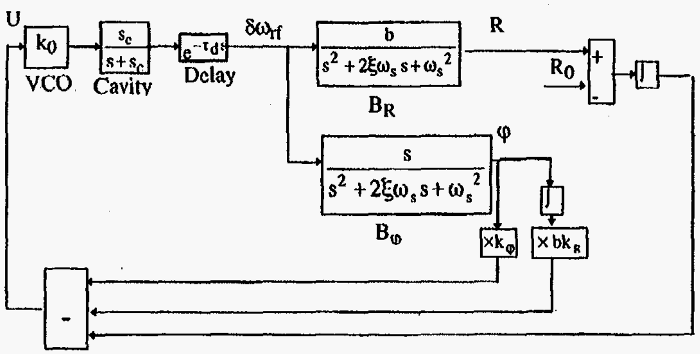

Use of the phase integral: $k_R \to -k_R$ if use of the radius. Transient Simulations: desired poles: $-139+j*139$, $-139-j*139$, -28283. Reference: 1 mm radius step.

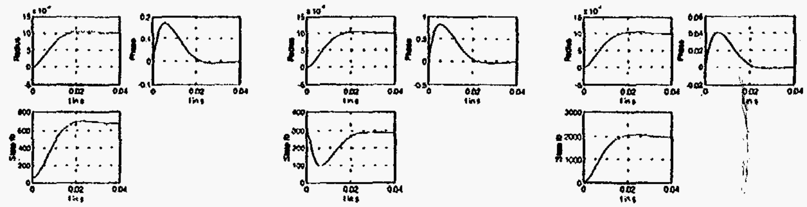

V_{rf}=170 kV, γ=12.6 V_{rf}=300 kV, γ=108.4 V_{rf}=6000kV, γ=108.4

Radius step response

Response time 40 ms

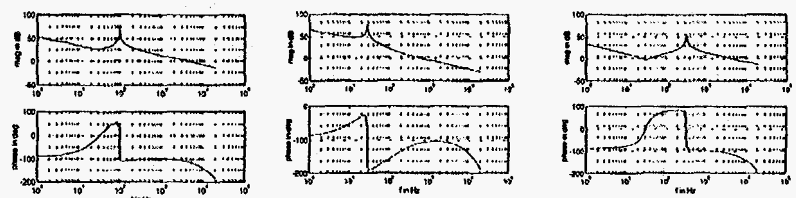

V_{rf}=170 kV, γ=12.6 V_{rf}=300 kV, γ=108.4 V_{rf}=6000kV, γ=108.4

Open loop Bode plots

Phase margin 70°, amplitude margin 15 dB, cut off frequency approximately 3.2 kHz.

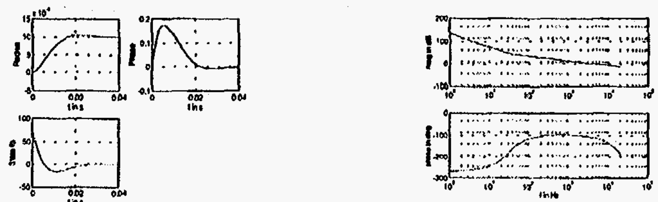

Loop behavior at transition (step response and Bode plot)

phase margin 80°, amplitude margin 10 dB, cut off frequency 3 kHz

Phase: back to zero in less than 100μs.

THE SYNCHRONIZATION LOOP

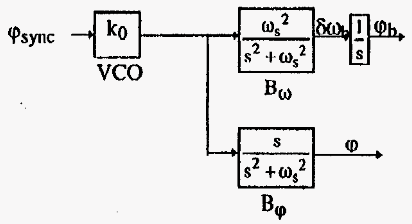

$$X_s = \begin{bmatrix} x_4 = \varphi_b \\ x_5 = \omega_b \\ x_6 = \varphi \end{bmatrix}, \; Y_s = \begin{bmatrix} x_4 = \varphi_b \\ x_5 = \omega_b \\ x_6 = \varphi \end{bmatrix}.$$

Evolution: $\begin{cases} \dot{x}_4 = x_5 \\ \dot{x}_5 = \omega_s^2 x_6 \\ \dot{x}_6 = -\omega_s^2 x_6 + k_0 \varphi_{sync} \end{cases}$

State space representation: $\begin{cases} \dot{X}_s = \underbrace{\begin{pmatrix} 0 & 1 & 0 \\ 0 & 0 & \omega_s^2 \\ 0 & -1 & 0 \end{pmatrix}}_{A_s} X_s + \underbrace{\begin{pmatrix} 0 \\ 0 \\ k_0 \end{pmatrix}}_{B_s} \varphi_{sync} \\ Y_s = \begin{pmatrix} 1 & 0 & 0 \\ 0 & 1 & 0 \\ 0 & 0 & 1 \end{pmatrix} X_s \end{cases}$

$\mathrm{rank}\left[B_s \; A_s B_s \; A_s^2 B_s\right] = 3 \Rightarrow$ Pole placement

$$\begin{cases} k_{\varphi_b} = -\dfrac{l_1 l_2 l_3}{k_0 \omega_s^2} \\ k_{\omega_b} = \dfrac{l_1 l_2 + l_1 l_3 + l_2 l_3}{k_0 \omega_s^2} \\ k_\varphi = \dfrac{l_1 + l_2 + l_3}{k_0} \end{cases}$$

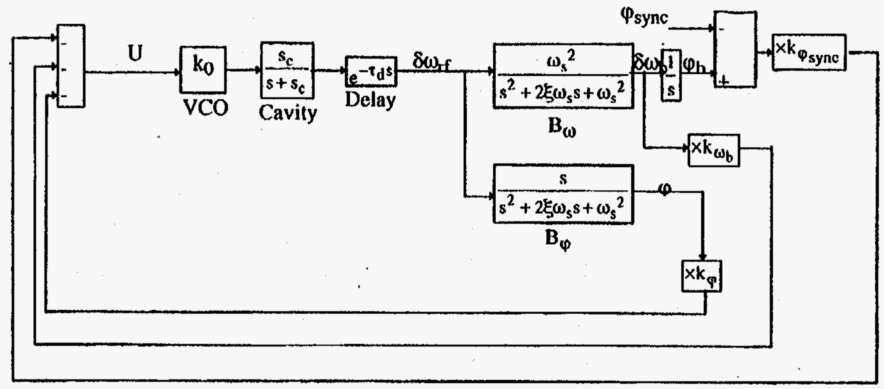

Desired poles: -99638, $-1202 + j*1047$, $-1202 - j*1047$ during acceleration and -220.3, -1469, -9442 during storage.

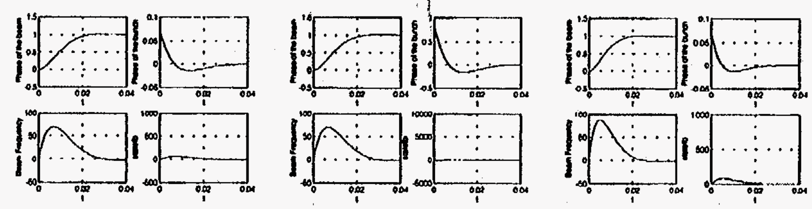

V_{rf}=170 kV, γ=12.6 V_{rf}=300 kV, γ=108.4 V_{rf}=6000kV, γ=108.4

Step response of the synchronization loop

Rise time roughly 20ms. Phase margin 80°, amplitude margin 20 dB and the cut off frequency 1.5 kHz.

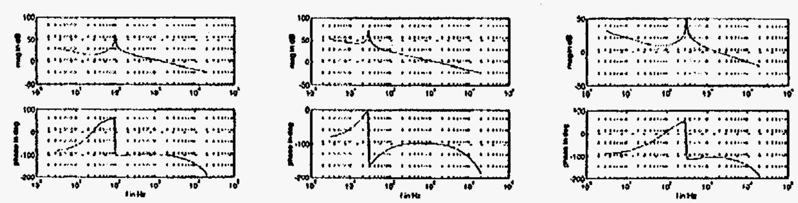

V_{rf}=170 kV, γ=12.6 V_{rf}=300 kV, γ=108.4 V_{rf}=6000kV, γ=108.4

Open loop Bode plots

PHASE ERROR FOR A GIVEN FREQUENCY ERROR

Phase measurements errors

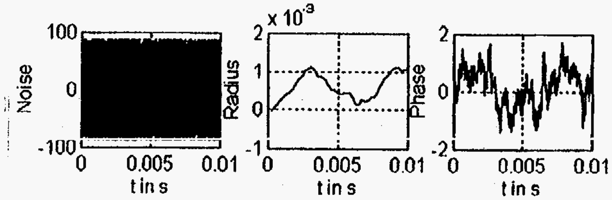

System excited by a white noise (90°amplitude, bandwidth 5000 Hz)

Noise attenuated by a factor of 40.

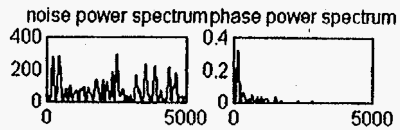

Effects of the tuner on the phase and radial loop.

Tuner effect = rf phase steps.

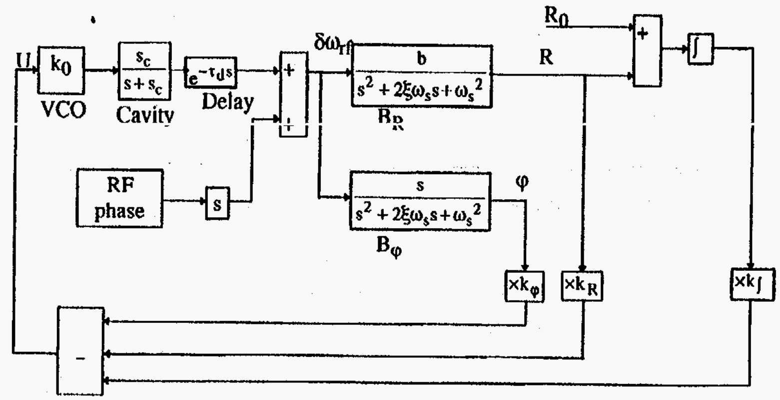

The same simulation has been performed by using real RF phase measurements

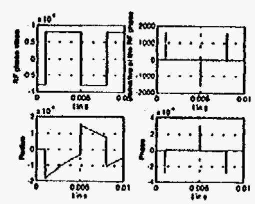

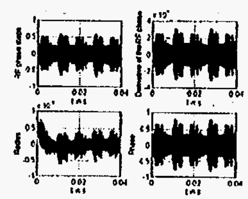

Step on the rf phase ⇒ the feedback tries to bring the phase to zero.
The radius integers the step ⇒ the phase deviates.

$$(\varphi_{rf} \to R) = b\int(\varphi_{rf} \to \varphi) \Rightarrow a(t) = \int_0^t \varphi(u)du = k*R$$

Perturbations due to the tuner can be seen as radius steps.

DISCRETE REALIZATION OF THE LOOPS

Previous analog representation is sampled at the revolution frequency to get a discrete representation which includes the delay.

The phase and radial loop

Original state space-representation with no integral:

$$\begin{cases} x(n+1) = a_d x(n) + b_d U(n) \\ Y(n+1) = c_d x(n) + d_d U(n) \end{cases} \quad \text{where } R(n+1) = C_{d2} x(n)$$

$$x(n) = \begin{pmatrix} \frac{R(n)}{b} \\ \varphi(n) \\ U(n-1) \end{pmatrix}$$

complete state space representation

$$\begin{cases} \underbrace{\begin{pmatrix} x(n+1) \\ z(n+1) \end{pmatrix}}_{X(n+1)} = \begin{pmatrix} a_d & 0 \\ c_{d2} & 1 \end{pmatrix} \underbrace{\begin{pmatrix} x(n) \\ z(n) \end{pmatrix}}_{X(n)} + \begin{pmatrix} b_d \\ 0 \end{pmatrix} U(n) + \begin{pmatrix} 0 \\ -R_0 \end{pmatrix} \\ Y(n+1) = \begin{pmatrix} c_d & 0 \end{pmatrix} X(n) \end{cases}$$

discrete pole $= e^{\text{continuous pole} * \tau_d}$

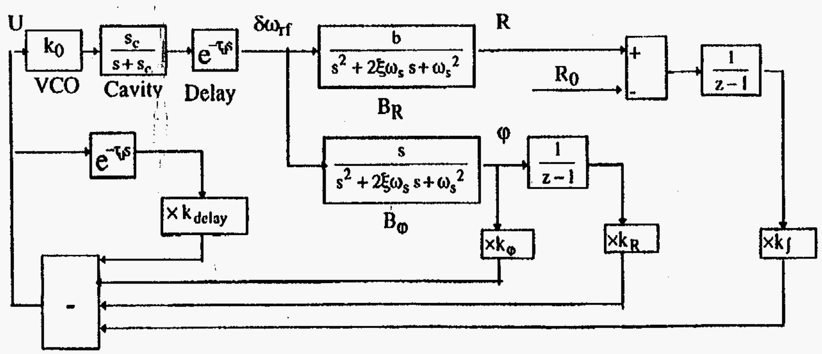

Radius reference: 1mm step.

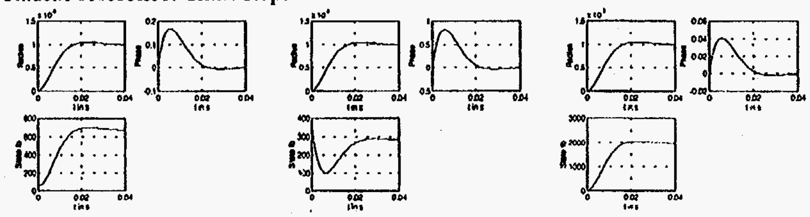

V_{rf}=170 kV, γ=12.6 V_{rf}=300 kV, γ=108.4 V_{rf}=6000kV,γ=108.4

Radius response

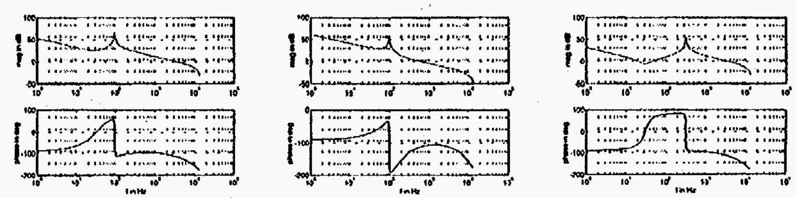

V_{rf}=170 kV, γ=12.6 V_{rf}=300 kV, γ=108.4 V_{rf}=6000kV,γ=108.4

Open loop Bode plots

Phase margin is 70°, amplitude margin 15 dB , cut off frequency 3.2kHz.

Same response at transition (rise time ≅ 20 ms)
phase margin 80°, amplitude margin 10 dB, cut off frequency 3 kHz

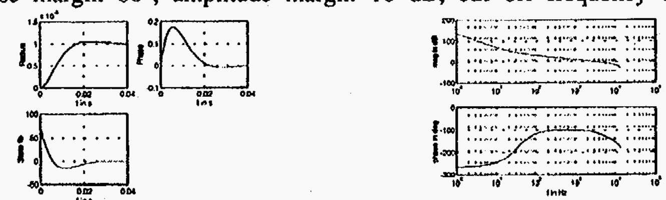

Loop behavior at transition (step response and Bode plot)

Phase comes back to zero in less than 100ms.

The synchronization loop

Discrete state vector: $X(n) = (\varphi_b \quad \omega_b \quad \varphi \quad U(n-1))^T$.

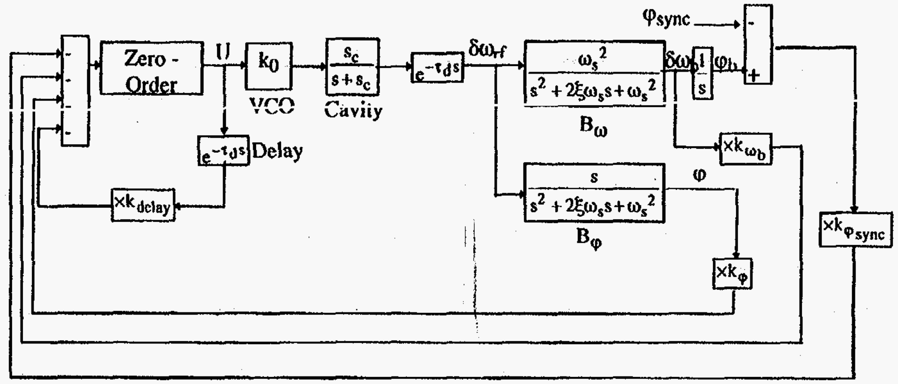

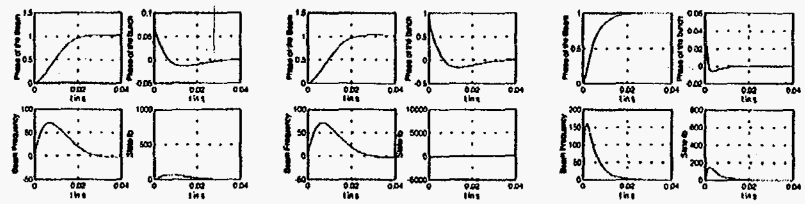

V_{rf}=170 kV, γ=12.6 V_{rf}=300 kV, γ=108.4 V_{rf}=6000kV, γ=108.4

Step response

Rise time 20 ms.

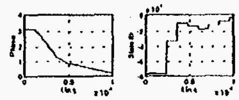

Transition jump

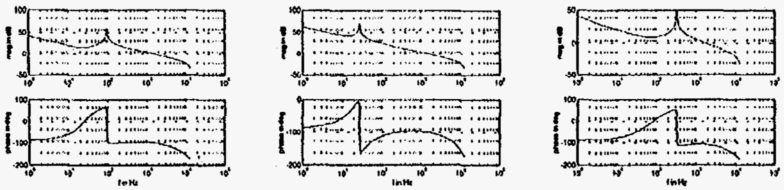

V_{rf}=170 kV, γ=12.6 V_{rf}=300 kV, γ=108.4 V_{rf}=6000 kV, γ=108.4

Open loop Bode plots

Phase margin 80°, amplitude margin 20 dB ,cut off frequency 1.5 kHz.

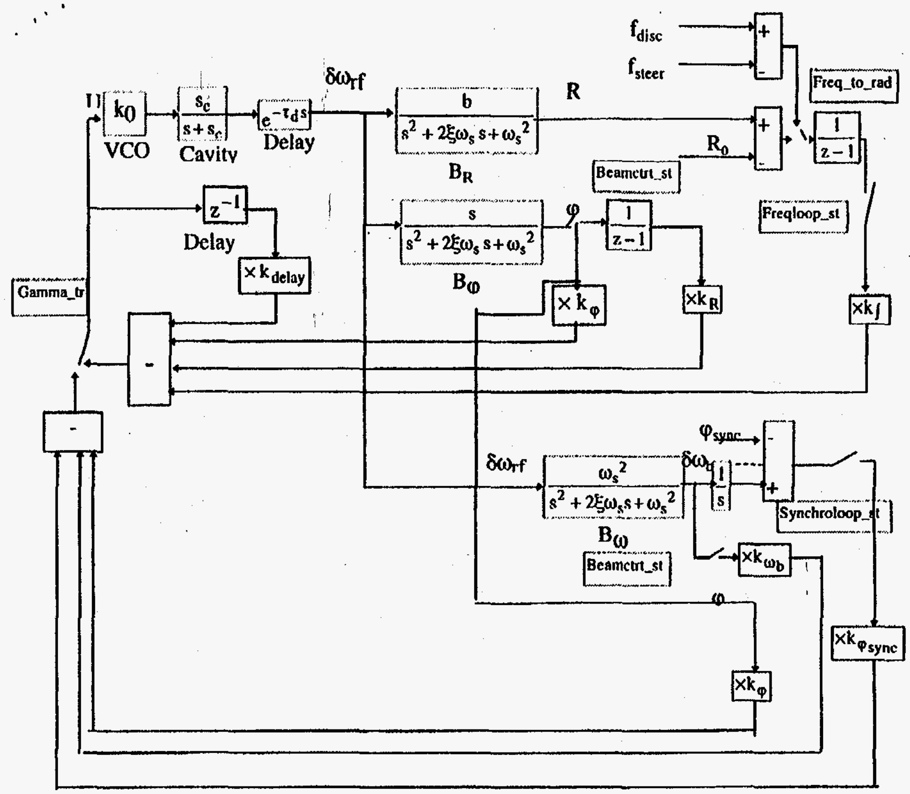

Practical realization

Use of a VME DSP board

Store the feedback gains in a table (RAM), as a function of energy
Access the gain table as a function of the energy

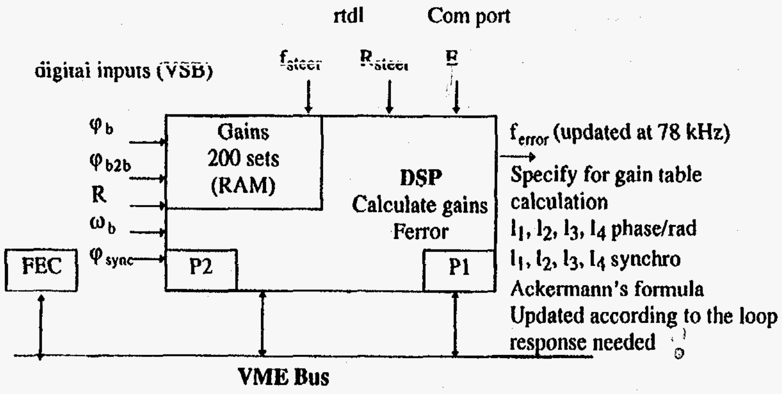

Triggers: VSB interrupts, corresponding to a different part of the DSP code

Gain table

Phase and radial loop

	k_{phase}	$k_{\int phase}$	k_{delay}	$k_{\int radius}$
V_{rf}=170 kV, γ=12.6	0.0242 10^6	6.249 10^6	0.291	0.0208 10^6
V_{rf}=300 kV, γ=108.4	0.0243 10^6	6.671 10^6	0.291	0.1014 10^6
V_{rf}=6000 kV, γ=108.4	0.0242 10^6	1.13 10^6	0.290	0.005 10^6

Only $k_{\int radius}$ changes during acceleration

	$k_{\int radius}$
V_{rf}=170 kV, γ=12.6	0.0208 10^6
V_{rf}=170 kV, γ=108.4	0.1796 10^6
V_{rf}=300 kV, γ=12.6	0.0017 10^6
V_{rf}=300 kV, γ=108.4	0.1014 10^6

Range: 0.0017 10^6 to 0.1796 10^6
200 points: Δgain=1000

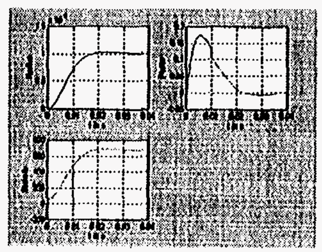
1 mm step: 1° phase jump

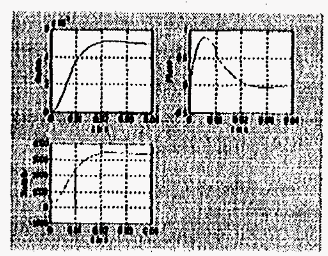
5 mm step: 7° phase jump

Synchronization loop

	$k_{\varphi btb}$	$k_{\varphi b}$	k_{delay}	$k_{\omega b}$
V_{rf}=170 kV, γ=12.6	9.6386 10^3	0.6653 10^3	0.0001 10^3	0.0053 10^3
V_{rf}=300 kV, γ=108.4	9.6447 10^3	7.7186 10^3	0.0001 10^3	0.0728 10^3
V_{rf}=6000 kV, γ=108.4	10.614 10^3	0.6617 10^3	0.0001 10^3	0.0024 10^3

	$k_{\varphi btb}$	$k_{\varphi b}$	$k_{\omega b}$
V_{rf}=170 kV, γ=12.6	9.6386 10^3	0.6653 10^3	0.0053 10^3
V_{rf}=170 kV, γ=108.4	9.6446$10^3$	7.7186 10^3	0.0728 10^3
V_{rf}=300 kV, γ=12.6	9.6386 10^3	0.6653 10^3	0.0052 10^3
V_{rf}=300 kV, γ=108.4	9.6447 10^3	7.7186 10^3	0.0728 10^3

Only $k_{\varphi b}$ and $k_{\omega b}$ change during acceleration

Range:

$k_{\varphi b}$ from 0.6653 10^3 to 7.7186 10^3 20 points Δgain=35

$k_{\omega b}$ from 0.0052 10^3 to 0.0728 10^3 20 points Δgain=0.33

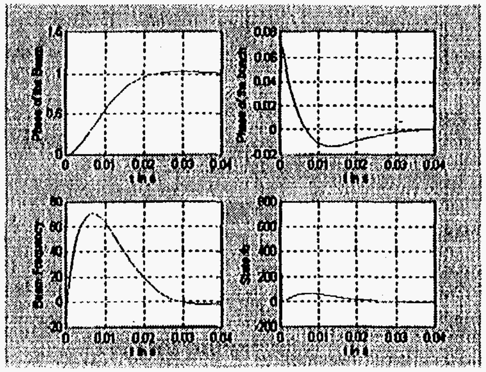

No noticeable effect

The NSNS rf System

M.Blaskiewicz, J.M. Brennan, A. Zaltsman

charge exchange injection for 1ms then extract in one turn
60 Hz repetition rate
2×10^{14} 1 GeV kinetic energy protons at extraction
less than 10^{-4} uncontrolled losses
keep peak current small
Dual Harmonic system:

$$V_{rf}(t) = 40\text{kV}\sin(\omega_0 t) + 20\text{kV}\sin(2\omega_0 t)$$

$$\frac{Z_{sc}}{n} = 120\Omega, \qquad R_{wall} = 20\Omega$$

$$|E - E_0| \le 5.6\text{MeV in Linac}, \qquad 9.4\text{MeV in Ring}$$

$$T_{rev} = 841\text{ns}, \qquad \tau_{chop} = 480\text{ns}$$

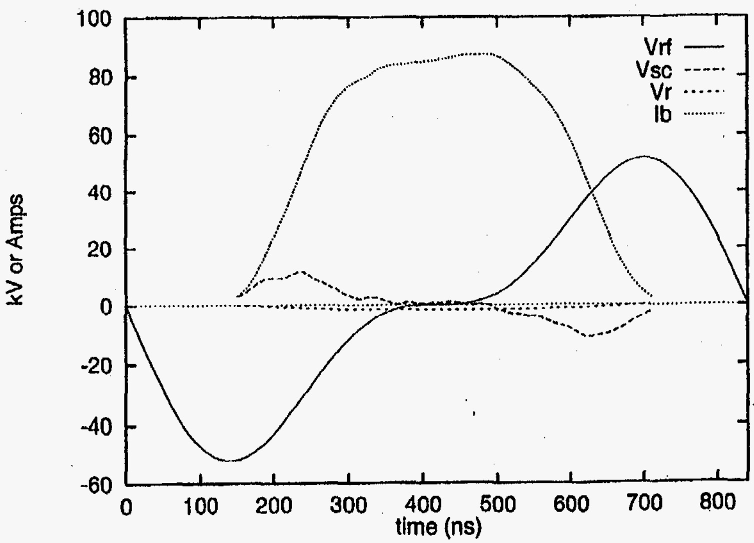

Cavity and Amplifier Design

$$h = 1, \qquad f = 1.26 \text{ MHz}$$

$$h = 2, \qquad f = 2.52 \text{ MHz}$$

$\pm 5\%$ variability built in.
Need 40kV at $h = 1$ and 20kV at $h = 2$
Want to retain the option of zero detuning angle $\omega_r = \omega_0$ so full beam current must be compensated.
$\le$ 10kV per gap. Direct coupling to $\sim$ AGS cavity.
Beam current

$$I_b(t) \approx \bar{I}_b(t)\left[1 + a_1\cos(\omega_0 t) + a_2\cos(2\omega_0 t)\right]$$

$a_1 = 1.3$, $a_2 = .1$, and $\bar{I}_b(t) = 40t$ Amp ms^{-1}.

$$a_1\bar{I}_{max} = 52 \text{ Amps} \gg a_2\bar{I}_{max} = 4 \text{ Amps}$$

Equivalent Circuit

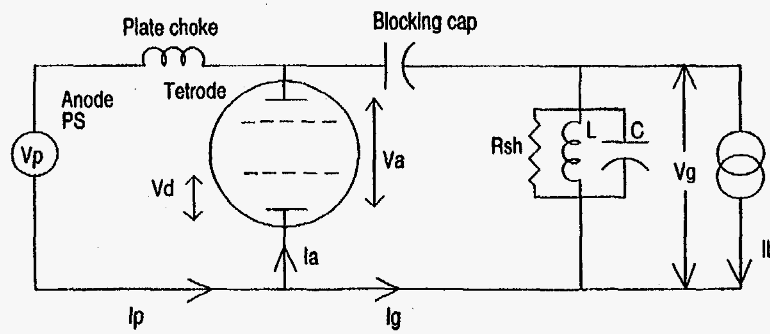

assume blocking capacitor and plate choke are very large
gap voltage

$$V_g(t) = V_a(t) - V_p$$

generator current across gap

$$I_g(t) = -I_a(t) + I_p$$

anode current

$$I_a = I_a(V_a, V_d)$$

$$I_g(t) = -I_a(V_g(t) + V_p, V_d(t)) + I_p$$

power amplifier supplying n_g accelerating gaps in parallel

$$V_g(t) = \int_0^{\infty} W(\tau)(I_b(t-\tau) + I_g(t-\tau)/n_g)d\tau$$

$W(\tau)$ is the wake potential of the *unloaded* cavity

$$W(\tau) = \frac{1}{2\pi}\int d\omega Z(\omega)e^{-i\omega\tau}$$

$$Z(\omega) = \frac{R_{sh}}{1 + iQ(\omega_r/\omega - \omega/\omega_r)}$$

R_{sh} is the shunt impedance per gap of the *unloaded* cavity
ω_r is its resonant frequency
Q is the unloaded quality factor.

Grid drive voltage

$$V_d(t) = \bar{V}_d + \Delta V_d \sin(\omega t + \phi_d)$$

Anode Voltage

$$V_a(t) = \bar{V}_a + \Delta V_a \sin(\omega t)$$

$\Delta V_a = V_g$ for direct coupling Current through tetrode

$$I_a(t) = \bar{I}_a - a\bar{I}\cos(\omega t) + I_0 \sin(\omega t) + \text{higher harmonics}$$

$-a\bar{I}$ compensates the beam current
I_0 drives the cavity
For the $\omega = \omega_r$ case $I_0 = \Delta V_a / R_{sh}$

$$R_{sh} \approx 10\text{k}\Omega \rightarrow I_0 = 1 \text{ Amp}$$

irrelevant compared

$$a_1 \bar{I} = 52 \text{ Amp}$$

. Take

$$n_g = 2 \rightarrow I_g = 104 \text{ Amp}$$

Anode Voltage, 6 gaps at $h = 1$

$$V_a(\omega t) = 9\text{kV} + 7\text{kV}\sin(\omega t)$$

Grid drive voltage

$$V_d(\omega t) = -500V + 450V\cos(\omega t) - 53V\sin(\omega t)$$

Screen grid voltage = 2kV.

Load Line for $h = 1$, TH558 tetrode

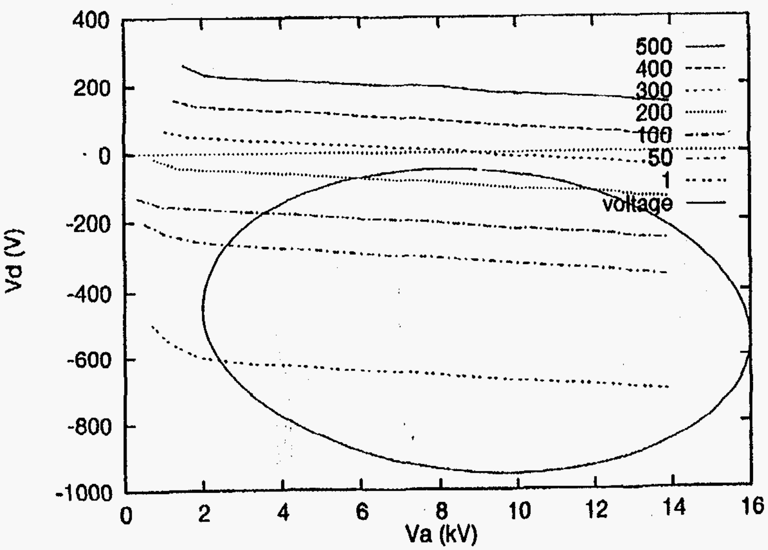

For $V_a > 2\text{kV}$

$$V_a/1000 + (0.132 \pm 0.002)V_d = \text{constant}$$

$$\text{So} \quad I_a = I_a(V_a + 132V_d)$$

in region of interest $\rightarrow$ 1 dimensional interpolation

$$< I_a V_a >= 585 \text{ kW} \leq 600\text{kW manufacturers spec}$$

How far can we push it?

For $h = 2$ two gaps, one tetrode, 20kV/gap, $\approx$ 100kW

Anode Current and its Fourier Reconstruction, $h = 1$

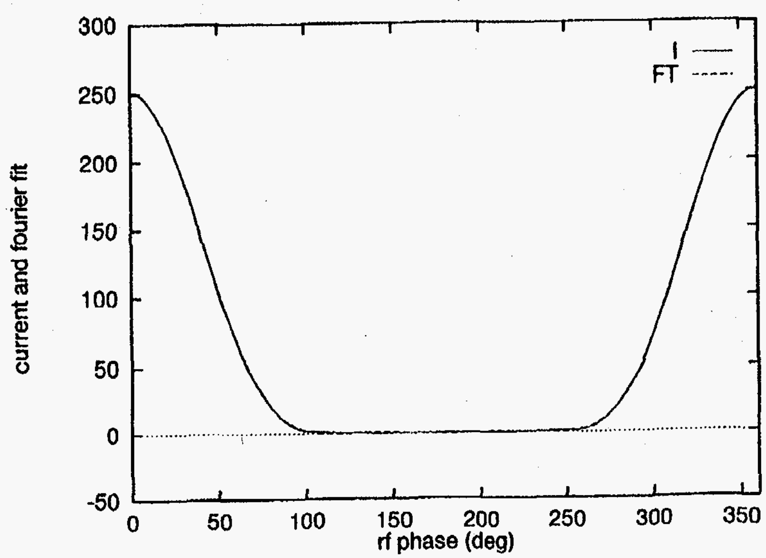

7

Dynamic tuning of the cavity resonant frequency
steady state first

$$\text{gap volts} \qquad V_g(t) = \hat{V}_g \exp(ih\omega_0 t)$$

$$\text{beam current} \qquad I_b(t) = \hat{I}_b \exp(ih\omega_0 t)$$

$$\text{generator current} \qquad I_g(t) = \hat{I}_g \exp(ih\omega_0 t)$$

$$\hat{V}_g = Z_c(\hat{I}_b + \hat{I}_g)$$

relative phase of $\hat{V}_g$ and $\hat{I}_b$ is $\approx 90°$, (R_{wall})

tune the cavity resonant frequency by biasing the ferrite,
for minimum current

$$I_g = V_g/R_{sh}$$

Where $R_{sh} \sim 10\mathrm{k}\Omega$ is the unloaded cavity impedance
Problem is now beam stability (Pederson 1975)
Have Robinson's criteria for single harmonic
Dual harmonic rule of thumb?
took $Y = I_b R_\ell / V_g \lesssim 3$
$R_\ell =$ effective resistance of cavity and tetrode in parallel.

8

Calculating R_ℓ

$$I_g = I_p - I_a(V_d, V_a)$$

$$\delta I_g = -\delta V_a \left.\frac{\partial I_a}{\partial V_a}\right|_{V_d}$$

$$\delta I_g + \delta I_b = \frac{\delta V_g}{R_{sh}} + \frac{1}{L}\int^t \delta V_g(t')dt' + C\frac{d\delta V_g}{dt}$$

$$\delta V_g = \delta V_a$$

$$\delta I_b = \delta V_g \left[\frac{1}{R_{sh}} + Y_a\right] + \frac{1}{L}\int^t \delta V_g(t')dt' + C\frac{d\delta V_g}{dt}$$

where

$$Y_a = \left.\frac{\partial I_a}{\partial V_a}\right|_{V_d} \geq 0$$

So

$$\frac{1}{R_\ell} = \frac{1}{R_{sh}} + \left\langle \left.\frac{\partial I_a}{\partial V_a}\right|_{V_d} \right\rangle_t$$

9

Using $< Y_a >_t = 1/375\Omega$ and 2 gaps per tetrode $R_\ell \approx 750\Omega$

$Y = 5.6$ without rf feedback

Use one turn feedback to reduce R_ℓ by a factor of 3.

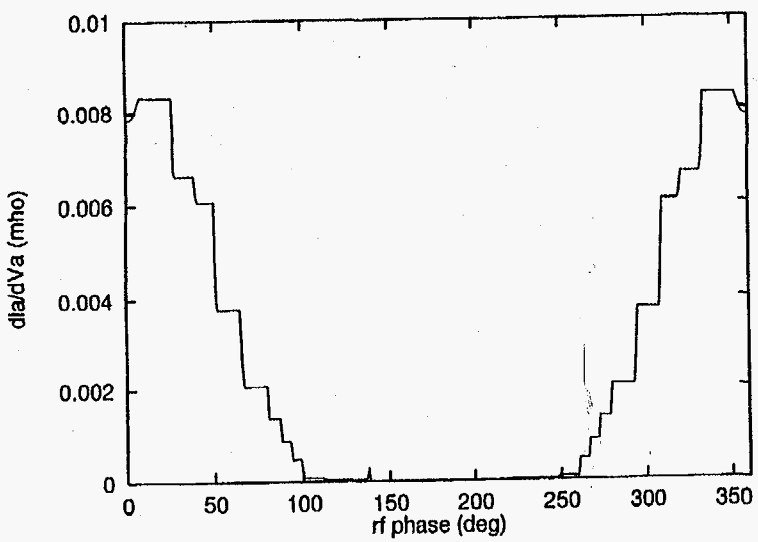

10

Barrier cavity upgrade
Use same tetrodes, but drive with a pulse
reduce gap capacitance
$f_r = 2.33\text{MHz} > 2f_0$ for no debunching
$< I_a V_a > = 1.8\text{MW}$ over one fill
$< I_a V_a > = 220\text{kW}$ over many cycles

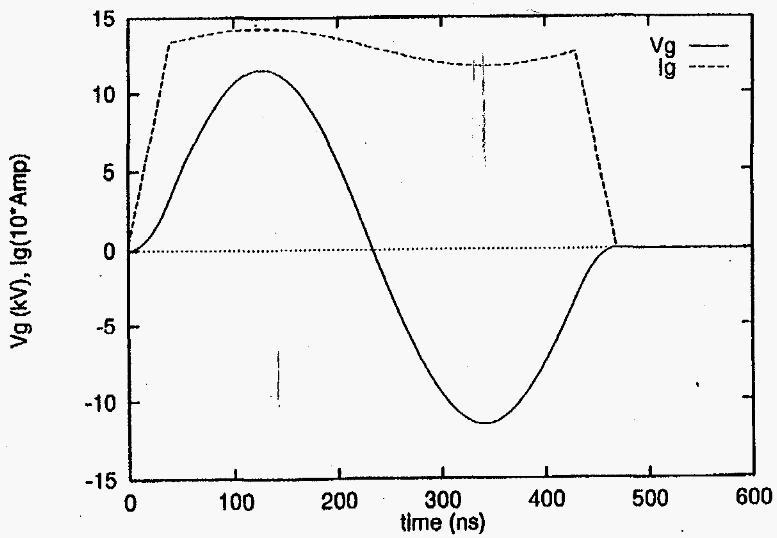

References

[1] M. Blaskiewicz, J.M. Brennan, Y.Y. Lee NSNS tech note # 9, (1996).

[2] Y.Y. Lee NSNS tech note # 26 (1997).

[3] J.M. Brennan, PAC95, pg 1489, (1995).

[4] F. Pederson, IEEE, TNS, Vol. NS-22, No. 3, pg 1906, (1975).

[5] M. Blaskiewicz, J.M. Brennan 5th European Particle Accelerator Conference, pg 2373, 1996.

[6] S. Koscielniak, 5th European Particle Accelerator Conference,pg 1129, 1996.

[7] D. Boussard, CERN 91-04 (1991).

[8] R. Garoby, Fontiers of Particle Beams: Intensity Limitations, US-CERN School on Particle Accelerators, Springer-Verlag, pg 509, (1990).

R. Garoby

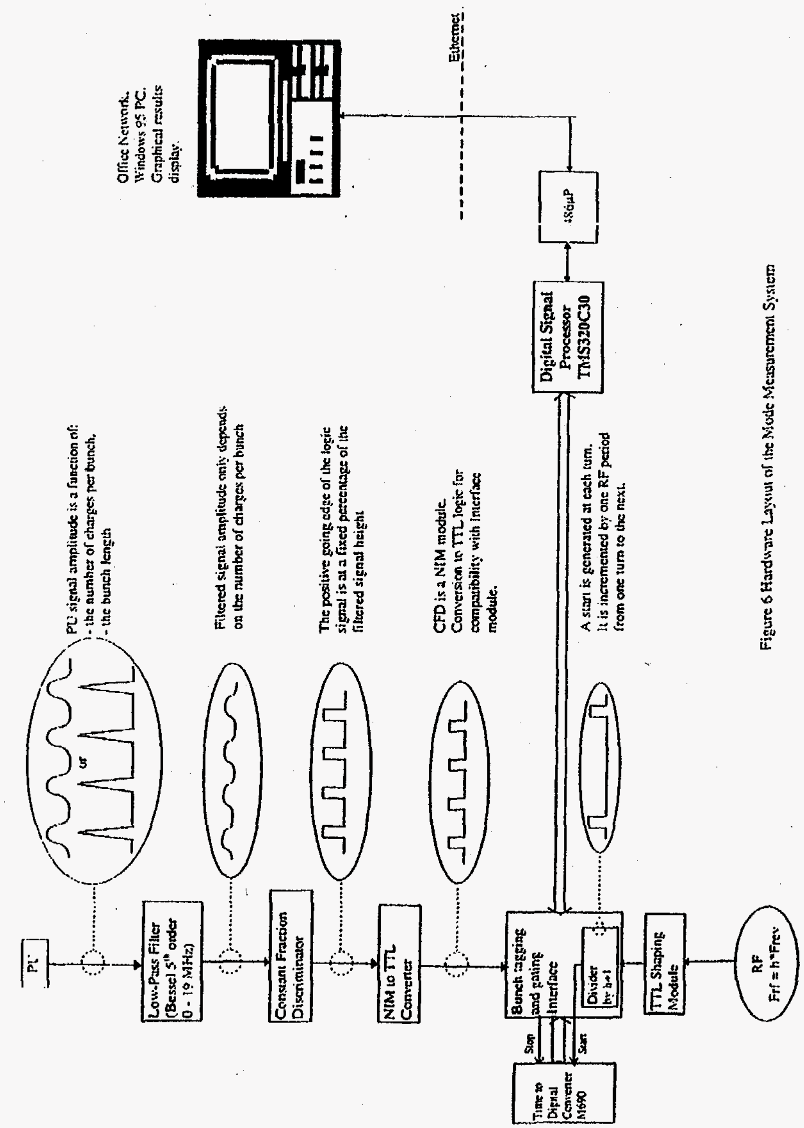

Figure 6 Hardware Layout of the Mode Measurement System

5.1 Sensitivity

The Mode Measurement System must be a highly sensitive tool in order to pin-point the birth and duration of beam instabilities. Proof of the sensitivity can be seen in Figure 33.

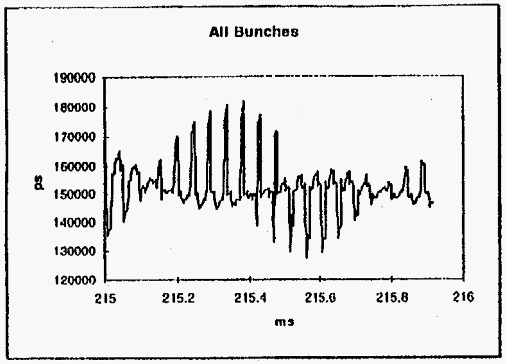

Figure 33 Evidence that bunches are oscillating at f_{s0} proves high sensitivity

This plot was taken at C215 just before injection. Given that the small amplitude synchrotron frequency [5], f_{s0}, is approximately 1.6 kHz on this beam at injection energy, the graph should be able to confirm this statement.

Closer inspection reveals that the period of the signal in Figure 33 is approximately 600 μs. the frequency is thus given by

$$f = 1/T = 1/600E\text{-}06 = 1.67\ \text{kHz} \approx f_{s0}$$

With the knowledge that synchrotron oscillations can successfully be observed, it is true to say that the system sensitivity is of a high quality.

5.2 Analysis of Beam Instabilities

The results of beam instability analysis were the key to completion of the project specification. If coherent longitudinal dipolar instabilities could be identified then RF specialists would be able to better isolate the source(s) of impedance driving the instability.

The first stage in this process - identification of the birth and nature of an instability - was successfully completed during the MD session..

[5] *The small amplitude synchrotron frequency describes the motion of particles which are extremely close to the synchronous point whilst still performing synchrotron oscillations.*

The user then selected a new session following the progress of two chosen bunches, and zooming on the region of instability by selection of new Start, Stop and Step settings (see Figure 36).

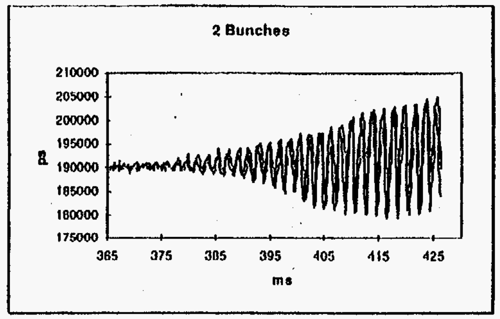

Figure 36 The effect on two bunches due to a growing instability

And inspecting the difference in phase between the two bunches (see Figure 37)

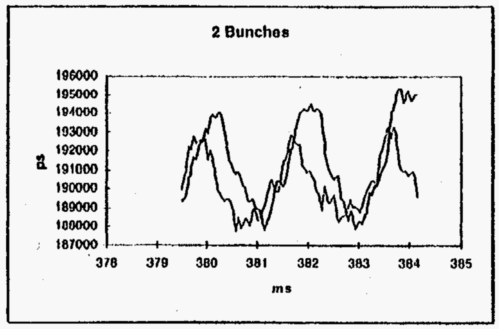

Figure 37 Difference in phase of the two bunches during instability growth

Figures 35 to 37 clearly identify a growing instability. The peak-to-peak magnitude is between 180 and 205 ns which, with an RF period of 110 ns, corresponds to nearly 25 % of one RF turn. The longitudinal movement of the bunches is therefore quite large. The phase difference between two chosen bunches is also quite large. In the ideal case where no instabilities are present, all bunches should remain fixed at the synchronous point with a single phase, φ_s, the synchronous phase.

Increasing the blow-up and hence the longitudinal emittance the situation was restored to that of Figure 34, stable beam.

Participants

Michael Blaskiewicz	BNL
J. Michael Brennan	BNL
Yong Ho Chin	KEK
Weiren Chou	FNAL
Roland Garoby	CERN
Steven B. Hancock	FNAL
Thomas Hayes	BNL
Erk Jensen	CERN
Ioanis Kourbanis	FNAL
Yong Y. Lee	BNL
Trevor Linnecar	CERN
John T.M. Lyles	LANL
King Y. Ng	FNAL
Chihiro Ohmori	KEK
Emmanuel Onillon	BNL
Zubao Qian	FNAL
Jim Rose	FNAL
Thomas Roser	BNL
Shinya Sawada	KEK
Michael J. Syphers	BNL
Arch Thiessen	FNAL
Hiroshi Tsutsui	KEK
Tomonori Uesuigi	KEK
Peter L. Walstron	FNAL
Tai-Sen F. Wang	FNAL
David W. Wildman	FNAL
Masahito Yoshii	KEK
Alex Zaltsman	BNL